In presenting the dissertation as a partial fulfillment of the requirements for an advanced degree from the Georgia Institute of Technology, I agree that the Library of the Institute shall make it available for inspection and circulation in accordance with its regulations governing materials of this type. I agree that permission to copy from, or to publish from, this dissertation may be granted by the professor under whose direction it was written, or, in his absence, by the Dean of the Graduate Division when such copying or publication is solely for scholarly purposes and does not involve potential financial gain. It is understood that any copying from, or publication of, this dissertation which involves potential financial gain will not be allowed without written permission.

3/17/65
b

CONTRIBUTIONS TO THE STUDY OF HOMOGENEOUS NUCLEATION

A THESIS

Presented to

The Faculty of the Graduate Division

by

Alberto Francisco Hidalgo

In Partial Fulfillment

of the Requirements for the Degree

Doctor of Philosophy in the

School of Chemical Engineering

Georgia Institute of Technology

July, 1966

CONTRIBUTIONS TO THE STUDY

OF HOMOGENEOUS NUCLEATION

Approved:

Chairman

Date approved by Chairman: 8-18-66

DEDICATION

To my wife, Matilde,

whose love, patience and devotion have

been dearly tried.

ACKNOWLEDGMENTS

An individual is necessarily a part of the events and people with whom he has become associated. This is especially true of the young professional whose contribution is partly shaped by the contributions of others. The author wishes to acknowledge here the valuable time and talents of the many individuals who contributed to the present work. Special gratitude is expressed to Dr. Clyde Orr, Jr., for the useful research experience acquired while working under his supervision for a number of years. In particular, the author is indebted to him for first suggesting the present topic for doctoral research, and for his continued encouragement and guidance throughout the course of the work. Very valuable assistance was also rendered by Dr. F. Kenneth Hurd and Dr. Julian D. Fleming, Jr., through comments and suggestions as members of the reading committee. The author expresses his appreciation for their conscientious services.

Mr. Edward Y.H. Keng also rendered valuable assistance in sampling the aerosols under study for analysis under the electron microscope. Recognition is also due to Mrs. Jean Doster for her conscientious and efficient services as a typist during the various stages of preparation of this work.

Appreciation is expressed to the Public Health Service of the United States Department of Health, Education and Welfare and to the Engineering Experiment Station of the Georgia Institute of Technology for their support through research grants, employment and facilities.

In his personal life, the author is indebted to his parents, Mrs. Carmen G. Hidalgo and the late Dr. Francisco Hidalgo for their support and inspiration to achieve higher academic goals. Finally, the author expresses his deepest gratitude to his wife, Mrs. Matilde G. Hidalgo, and his children for their continued encouragement and willingness to sacrifice so much of that time which was rightfully theirs so that this work could be made possible.

TABLE OF CONTENTS

TABLE OF CONTENTS (Continued)

TABLE OF CONTENTS (Continued)

APPENDICES

NOMENCLATURE

The numbers in parentheses after description of the symbols refer to the equation in which they are first used or completely defined. Dimensions are given in terms of mass (M), length (L), time (t), temperature (T), and dielectric constant (ϵ). Symbols that appear infrequently or only in one section are not listed.

Symbol	Description	Dimensions
a_o	Activity of solute in a saturated solution (2.11)	- -
a_1	Activity of solute in a supersaturated solution (2.11)	- -
b	Half of separation between ion counter plates (A.1)	L
C	Constant equal to exp $(E_1 - E_L)/RT$ (C.1)	- -
c	Solution molarity, moles of solute per 1000 cm^3 of solution (B.1)	$M\ L^{-3}$
D	Dielectric constant	ϵ
d	Differential operator	- -
E	Electric field strength (A.5)	$\epsilon^{-1/2}\ M^{1/2}\ L^{-1/2}\ t^{-1}$
E_1	Heat of adsorption of a monomolecular layer of gas (C.1)	$M\ L^2\ t^{-2}\ mole^{-1}$
E_L	Heat of liquefaction of adsorbate gas (C.1)	$M\ L^2\ t^{-2}\ mole^{-1}$
e	Electronic charge (C.7)(1.5921 x 10^{-19} abs. Coulombs)	$\epsilon^{1/2}\ M^{1/2}\ L^{3/2}\ t^{-1}$
F	Aerosol flow rate (A.2)	$L^3\ t^{-1}$
$f_{\pm}$	Mean rational activity coefficient (B.3)	- -
G	Gibb's free energy (2.1)	$M\ L^2\ t^{-2}$

Symbol	Description	Dimensions
G^*	Free energy of activation for diffusion (2.16)	$M\ L^2\ t^{-2}$
G_c	Maximum free energy associated with nucleus formation (2.14)	$M\ L^2\ t^{-2}$
G_v	Free energy per unit volume (2.7)	$M\ L^{-1}\ t^{-2}$
H	Relative humidity, per cent (4.1)	- -
h	Planck's constant (2.17)	$M\ L^2\ t^{-1}$
h_c^β	Vertical distance from crystal center of gravity to face β of critical size nucleus (2.22)	L
I	Ion current (A.19)	$\epsilon^{1/2}\ M^{1/2}\ L^{3/2}\ t^{-2}$
i	van't Hoff factor (B.14)	- -
J	Rate of formation of nuclei (2.16)	$t^{-1}\ mole^{-1}$
K	Geometric parameter of ion counter (A.23)	L
K_v	Nucleation rate factor (2.16)	$t^{-1}\ mole^{-1}$
k	Boltzmann's constant (2.16)	$M\ L^2\ t^{-2}\ T^{-1}$
k_l	Davies' slip correction factor (A.26)	- -
L	Characteristic length	L
M	Molar mean molecular weight	$M\ mole^{-1}$
m	Solution molality, moles per 1000 g water (B.2)	$moles\ M^{-1}$
m'	Mass of solute per droplet (C.8)	M
$m_\pm$	Mean ionic molality (B.6)	$moles\ M^{-1}$
N	Number of charged particulates entering ion counter per unit time (A.13)	t^{-1}
N_c	Number of molecules in nucleus of radius r_c (2.15)	- -
N_i	Mole fraction of component i (B.9)	- -
$N_\pm$	Mean ionic mole fraction (B.7)	- -

Symbol	Description	Dimensions
n_e	Number of electronic charges per particulate (A.26)	- -
n_i	Number of ions of mobility ω_i per unit volume (A.13)	L^{-3}
P	Total pressure (2.1)	$M\ L^{-1}\ t^{-2}$
p	Water partial pressure in equilibrium with an aqueous solution (4.1)	$M\ L^{-1}\ t^{-2}$
p_o	Water vapor pressure (4.1)	$M\ L^{-1}\ t^{-2}$
p'_o	Water partial pressure of a saturated solution in equilibrium with large crystals of the solute (C.6)	$M\ L^{-1}\ t^{-2}$
p'_r	Water partial pressure over a droplet of radius r (C.6)	$M\ L^{-1}\ t^{-2}$
R	Gas constant (2.10)	$ML^2\ t^{-2}\ T^{-1}\ mole^{-1}$
R_1	Inner radius of ion counter plate (A.1)	L
R_2	Outer radius of ion counter plate (A.1)	L
r	Radius of a sphere (2.4)	L
r_c	Radius of critical size embryo, or nucleus (2.13)	L
S	Entropy (2.1)	$ML^2\ t^{-2}\ T^{-1}$
T	Absolute temperature (2.1)	T
t	Time	t
U	Internal energy (2.1)	$ML^2\ t^{-2}$
V	Electrical potential (A.5)	$\epsilon^{-1/2}\ M^{1/2}\ L^{1/2}\ t^{-1}$
V_o	Plate potential at which an ion of mobility ω_o will be collected (A.16)	$\epsilon^{-1/2}\ M^{1/2}\ L^{1/2}\ t^{-1}$
v	Volume of gas adsorbed at an equilibrium partial pressure p per unit surface area (C.1)	L
v_m	Volume of gas adsorbed per unit surface area to form a monomolecular layer (C.1)	L

Symbol	Description	Dimensions
v_r	Radial velocity (A.1)	$L\ t^{-1}$
v_z	Particulate settling velocity (A.4)	$L\ t^{-1}$
W_s	Work done by system in creating a surface of discontinuity (2.2)	$ML^2\ t^{-2}$
Z_n	Valence of n-th ion of an electrolyte (B.4)	- -
z	Vertical coordinate (A.1)	L
z_o	Vertical coordinate of ion entering electric field (A.7)	L
α	Degree of solute dissociation in solution (C.5)	
Γ	Ional concentration of electrolyte	moles M^{-1}
$\gamma_{\pm}$	Mean molal activity coefficient (B.6)	- -
Δ	Finite change in a property, positive if an increase	- -
θ	Time required for nucleation (2.23)	t
λ	Mean free path of air molecules at temperature T (A.27)	L
μ	Viscosity (A.1)	$ML^{-1}\ t^{-1}$
μ_i	Chemical potential of component i (2.1)	$ML^2\ t^{-2}\ mole^{-1}$
ν	Number of ions produced per molecule of electrolyte upon complete dissociation (B.5)	- -
ν_o	Molecular jump frequency (2.20)	t^{-1}
ρ	Density of a crystalline phase (2.9)	ML^{-3}
ρ_L	Density of a solution (B.1)	ML^{-3}
ρ_w	Density of water (C.11)	ML^{-3}
$\sum_i$	Summation over i terms	- -
σ	Interfacial free energy per unit surface area (2.4)	Mt^{-2}

Symbol	Description	Dimensions
σ_{LV}	Interfacial surface tension between liquid and vapor phase (C.6)	Mt^{-2}
ϕ	Solution osmotic coefficient (B.13)	- -
ω_i	Mobility of charged particulate (A.4)	$L^{3/2}\ \epsilon^{1/2}\ M^{-1/2}$

LIST OF TABLES

LIST OF ILLUSTRATIONS

LIST OF ILLUSTRATIONS (Continued)

LIST OF ILLUSTRATIONS (Continued)

LIST OF ILLUSTRATIONS (Continued)

LIST OF ILLUSTRATIONS (Continued)

LIST OF ILLUSTRATIONS (Continued)

LIST OF ILLUSTRATIONS (Continued)

SUMMARY

The nucleation of a more stable phase from a metastable phase can be brought about by induced, or heterogeneous nucleation or by spontaneous, or homogeneous nucleation. In the former case, the nucleation of the metastable phase occurs because of foreign particles that serve as nucleation centers for the more stable phase by lowering the free energy of activation required for the phase transition. Special cases of heterogeneous nucleation include those where the process is induced by cavitation in metastable liquid phases due to ultrasonic vibrations or, in the case of vapor phase nucleation, by the presence of free radicals or by ions. In contrast, homogeneous nucleation occurs because of configurational fluctuations in an otherwise homogeneous phase.

The foundations of the theory of homogeneous nucleation have been established for over forty years. More recently, they have been complemented by considering the kinetics of the process of embryo formation. However, verification of the theory has been limited to pure vapor phase nucleation, and to nucleation from pure liquids. There is surprisingly good agreement between theory and experiment in the case of liquid nucleation from the vapor. Progress in the case of condensed phases had been limited because of the difficulty of obtaining conditions where nucleation can be considered spontaneous.

Studies using the so-called droplet technique with some pure condensed systems have given reasonable agreement with the theory. No

published studies have been found in the case of homogeneous nucleation from solutions, however.

In this investigation an aerosol composed of submicroscopic solution droplets of sodium chloride was studied, with particular reference being given to the conditions of droplet supersaturation and the required nucleation time lag. It is estimated that only one in every 10^7 to 10^9 droplets contains a foreign particle capable of inducing nucleation. Therefore, the observed behavior of the supersaturated solution droplets is attributed exclusively to the kinetics of formation of embryos of the more stable phase according to the postulates of the homogeneous nucleation theory.

The choice of sodium chloride as the solute was based upon the fact that this substance is one of the most abundant atmospheric particles, especially in coastal areas where conditions favorable to the formation of fogs are frequent. In addition to this, the atmospheric physics literature reveals that natural fogs, which are constituted of dilute solution droplets, only disappear at lower relative humidities than those at which they originally formed. It had been suggested, therefore, that, in the absence of atmospheric contamination by organic vapors, the phenomenon may be controlled by homogeneous nucleation. The use of sodium chloride as the nucleus material permits comparison to be made with the behavior of some naturally occurring fogs. The present research thus represents an effort to study the behavior of supersaturated solution droplets of sodium chloride formed by moisture adsorption upon submicroscopic crystals in the range of 0.01 to 0.1 micron in radius.

Experimentally an aerosol composed by sodium chloride crystals was first produced; next, the distribution of crystal sizes was sharpened to the limits indicated above; and, finally, the total moisture content of the aerosol cloud was adjusted so that it could be made to reach equilibrium humidity at room temperature from either a dry-crystal or a solution-droplet condition. After this, the aerosol entered a chamber having an adjustable volume so that average residence times from 1 to 40 minutes could be obtained at an aerosol flow rate of 3.79 liters per minute. As the aerosol emerged from this chamber, its dew point was continuously monitored and a size distribution of the particulates was determined from ion mobility data. These experiments were designed to determine the relative humidity at which a given size droplet of known electrolyte content would nucleate after a given residence time. Data were collected for delays between 0 and 20 minutes after the solution-droplet aerosol reached the equilibrium relative humidity.

Since the concentration of the solution droplets at the time of nucleation could not be obtained from the measured droplet size distributions, estimations were made from predictions of droplet size and concentration for a given electrolyte content as a function of equilibrium relative humidity. The procedure made use of a guided extrapolation method for estimating the properties of supersaturated solutions of electrolytes. This permitted calculating the supersaturation ratio of the solute in the droplets at the time of nucleation in terms of solute activity.

The relationship between this supersaturation ratio and the

measured nucleation time lag appears to be in agreement with the classical model of homogeneous nucleation as applied to condensed systems. This finding is considered to be the first evidence of the applicability of the theory to the homogeneous nucleation of supersaturated solutions. Furthermore, the techniques developed appear to be particularly applicable to the study of this problem. Based on the experimental results, estimates can be made of the interfacial free energy between solid nuclei of sodium chloride and the mother liquid phase as well as of the surface free energy of solid sodium chloride. The result, 100 ergs per square centimeter, although somewhat low, is of the same magnitude as obtained by other authors using different experimental procedures. Estimates can also be made of the critical nucleus size as a function of solution supersaturation and of the distribution of particulates which have undergone nucleation as a function of time.

The evidence obtained in this study indicates that the phenomenon of the disappearance of natural fogs at lower relative humidities than those required for their formation is indeed explained by the mechanism of homogeneous nucleation as postulated.

Two computer programs were developed which are considered of general interest. One of these calculates the properties of solutions of monovalent electrolytes and predicts the properties of supersaturated solutions using experimental osmotic coefficient data. The predictions obtained agree very well with fragmentary data available on the vapor pressure of supersaturated solutions of potassium chloride. The second program gives particle size distribution information from microscope particle diameter measurements. This program can process up to 1250

measurements into up to 30 size ranges.

CHAPTER I

INTRODUCTION

Nucleation is a rate phenomenon involving the appearance of more stable molecular aggregates within a metastable mother phase. Under certain conditions of supersaturation of the mother phase, these more stable molecular aggregates, which are called embryos, are able to grow into macroscopic bodies of the more stable phase. An embryo is considered a nucleus when it has grown to the point where it can induce the mother phase to rearrange itself into the structure of the embryo.

Under conditions of supersaturation of the mother phase, which may be brought about by subcooling or by concentration beyond the point of thermodynamic equilibrium with the more organized phase, the embryos exist in a dynamic equilibrium with the metastable mother phase. In turn, the embryos are also metastable intermediate states in the kinetic process until they reach a critical size, i.e., the nucleus size, and possess an excess of surface energy sufficient to induce complete reaggregation of the mother phase or a significant portion of it in order to reestablish the thermodynamic equilibrium between the phases.

The first systematic study of nucleation was carried out two centuries ago by Gabriel Fahrenheit while attempting to obtain the freezing temperature of water as a calibration point in a new system of thermometry. His findings indicated that a certain amount of subcooling was required before a given body of pure water began to freeze. Furthermore, it was also found that this subcooling, although quite constant for

one particular body of water, could be different for another. However, as soon as freezing began, the temperature of all bodies rose to a point which was never higher than a certain value at which both the liquid and the solid phase could coexist in equilibrium. This, in fact could be called the "equilibrium crystallization temperature" and is a function of the chemical species at a given pressure. Above or below this point the interfaces are not stationary.

The apparent capriciousness of the onset of nucleation yet the rough reproducibility of nucleation for one particular sample led investigators to postulate that this could not reflect an intrinsic property of the system. The phenomenon was interpreted as being caused by the presence of minute amount of impurities inadvertently present in the system or on the walls of the container. Hence, the initial points of nucleation would be formed upon particles extrinsic to the system. For each particular system, therefore, the foreign particles would require a different energy of activation for inducing the appearance of nuclei. This form of nucleation is called induced or heterogeneous nucleation. The term homogeneous nucleation is reserved for pure systems absolutely devoid of foreign nuclei.

Turnbull[1] estimates that the single foreign nucleus which may initiate nucleation in a body of a metastable liquid mother phase may not constitute any more than one part in 10^{15} of the volume of that body. It is apparent that no feasible amount of care would produce a macroscopic system devoid of impurities to that high order of magnitude. This means, according to Turnbull, that nucleation occurring in a volume of liquid greater than 10^{-3} cubic centimeters will most

likely be due to induced or heterogeneous nucleation because of the relatively high probability that a body of liquid of such a volume will contain at least one foreign nucleus.

Two techniques have been used by various authors to circumvent the problem of the presence of foreign nuclei. In studies of vapor phases condensing into liquid in a cloud chamber, Wilson[2] developed a technique for eliminating foreign nuclei. In a typical experiment, a volume of inert gas was saturated with water vapor and then expanded. By successive expansions, condensation of moisture on the foreign nuclei present caused these to grow into large drops of water which were allowed to settle from the chamber. Vonnegut[3] first suggested a practical solution to the problem in the case of liquid phases. His procedure consisted of subdividing the bulk liquid into a great many minute droplets isolated from one another either by a second immiscible liquid, as in the case of a colloidal dispersion or an emulsion, or by air or other inert gas, as in the case of an aerosol. In this manner, the more active foreign nuclei would be sequestered in a few of the droplets and their effect could therefore be restricted to a negligible fraction of the total number of droplets constituting the dispersed aerosol. If, for example, a body of liquid is considered which contains 10^{6} foreign nuclei per cubic centimeter, and the liquid were dispersed into droplets of 10^{-8} cubic centimeters of roughly 70 microns in diameter, an average of no more than one droplet in every 100 would contain one of the original foreign nuclei. In such an aggregation of droplets, an independent nucleation event would be required for the crystallization of each individual small droplet. Hence, the vast majority of the droplets would be uninfluenced

by the foreign nuclei and would presumably crystallize by homogeneous nucleation. This has been described as the droplet technique.

Most of the work in the field of homogeneous nucleation has been concerned with crystallization from a pure phase. These studies have been largely in the domain of interest of either atmospheric physicists, in the case of nucleation of water vapor into liquid droplets, or of metallurgists, in the case of crystallization from a pure melt.

The author is not aware of any significant body of published work where the homogeneous nucleation of aqueous solutions was the object of the study. Only suggestions have been made that the time delay in the disappearance of fogs is a problem of homogeneous nucleation.

Atmospheric aerosols, typically fogs, are formed by condensation of moisture upon submicroscopic hygroscopic nuclei--often inorganic salts--that are always present in the atmosphere. Knowledge of these particles is mainly founded on the work of John Aitken[4] from 1884 to 1912. He was able to detect and survey the particle content of the lower atmosphere, especially in the size range of 0.01 to 0.1 micron in radius. It is in recognition of this fact that atmospheric particles in this size range are usually designated Aitken nuclei. That hygroscopic Aitken particles are capable of serving as condensation nuclei for the formation of clouds and fogs is very well established, although it is apparent that particles larger than these are sufficiently numerous in the lower troposphere to condense first the available atmospheric moisture.

Particles that are capable of serving as condensation nuclei come

from several sources according to Byers[5]. Among these are wind erosion of the land, combustion processes, detachment by the wind of a fine spray or bubbles from the sea surface, volcanic eruptions or explosions, extraterrestrial or cosmic sources, and finally, nucleogenic-chemical or photochemical reactions of organic contamination in the atmosphere.

A great number of authors have contributed to the determination of the chemical nature of these atmospheric particles. In general, this depends upon the geography of the region where the samples are collected. Sulphates, chlorides, and nitrates are common either in the acid form or in combination with sodium, potassium, calcium or ammonium. Sulphates and nitrates appear to form largely from combustion processes, whereas chlorides originate both from the sea and the land, and ammonia is contributed by decaying organic matter. Among the easily recognized chemical components, Junge[6] estimates that the continents contribute most of the NH_4^+, NO_3^-, NO_2^-, SO_4^{--}, and Ca^{++} while the oceans are the principal source of Cl^-, Na^+, K^+, and Mg^{++}. Twomey[7] has determined that continental air often contains up to six times as many nuclei as maritime air. Also, Gamble[8] concludes, from the ratios of various cations and anions present in continental rain water, that aerosols of maritime origin contribute only a small proportion of the soluble salts in rain. However, in coastal areas, where fog conditions are especially frequent, atmospheric particles largely originate from the sea. There is agreement among the various investigators that sodium chloride nuclei predominate under these conditions.

Several investigators have been concerned with the ability of atmospheric particles, especially hygroscopic ones, to serve as nuclei

for the formation of fog and rain droplets. The effect of insoluble particles upon the nucleation of ice from supercooled droplets has been studied with regard to the formation of snow and hail.

Comparatively little work has been published regarding the disappearance of fogs and smogs upon a decrease in atmospheric relative humidity. It has been often noticed, although rarely documented[9], that fogs generally only disappear at a lower relative humidity than that at which they formed originally. Dessens[10] was able to verify the form of the curve of the size of solution droplets in equilibrium with the environment relative humidity (see Appendix C) in the case of sodium and zinc chlorides. It was found that solution droplets in the range of 5 to 30 microns in diameter could remain liquid down to equilibrium relative humidities of as low as 40 per cent. A similar effect was found by Junge[11] and by Orr, et.al.[12]. The phenomenon has been interpreted in terms of nucleation kinetics by Corbett[13], and a method was suggested for predicting this behavior in the light of the theory of homogeneous nucleation. The present work is thought to be the first attempt to explain the phenomenon of nucleation of solution droplets in terms of the proposed mechanism.

Definition of the Problem

The research described herein was basically a study of homogeneous nucleation of a solution of sodium chloride at 25°C. The droplet technique was to be employed in order to minimize the effect of foreign nuclei which are always present in solutions. An aerosol composed of sodium chloride crystals in the Aitken range actually was studied. The behavior of the aerosol particulates in equilibrium with the relative

humidity of the environment was to be determined. Special emphasis was to be given the conditions under which the solution droplets formed by moisture condensation upon these crystals can nucleate with subsequent evaporation of the water.

The specific aim of the research was, then, to determine whether or not the behavior of supersaturated solution droplets could be explained in terms of the theory of homogeneous nucleation as applied to condensed phases. Hence, the time necessary for homogeneous nucleation to occur in supersaturated solution droplets of sodium chloride was examined theoretically and experimentally. The choice of sodium chloride as the soluble salt to be studied was based on the expectation that the results of the research might be of value in explaining the behavior of maritime fogs.

Assumptions pertinent to the droplet technique are particularly favorable under the conditions of this study. If, for example, the order-of-magnitude estimation of 10^6 foreign nuclei per cubic centimeter of a carefully prepared solution is accepted, then the probability is that only one in every 10^9 droplets in the aerosols to be studied is likely to have a foreign nucleus. Hence, it is reasonable to attribute the disappearance of the aerosol solution droplets to the homogeneous nucleation of the solute with the subsequent evaporation of the solvent.

The size of the aerosol particulates under study was to be determined from ion mobility data by the use of an ion counter, following the succesful development of this technique by Hurd and Mullins[14].

CHAPTER II

THEORETICAL BACKGROUND

The theory of homogeneous or spontaneous nucleation of a solute in solution will be developed following the principles laid out by Volmer and Weber,[15] and Becker and Döring[16]. The theory is often referred to as the V.W.B.D. Theory. Although it was developed to explain the case of homogeneous nucleation of liquids from supersaturated vapors in one-component systems, the assumptions involved are quite general and may be adapted to the situation concerning nucleation of crystals from a binary solution.

The theory assumes that dense clusters of molecules of the solute exist in a dynamic equilibrium with the solution, and, in the absence of foreign nuclei, some of these clusters, which are called embryos, may become nuclei for the growth of crystals under certain conditions. Because of the nature of the system being studied in this work, i.e., a polydisperse aerosol composed of submicroscopic solution droplets, the theory would apply to conditions involving the crystallization of the solute in a droplet with a subsequent decrease in the size of the particulates upon evaporation of the water. It is further assumed that the standard free energy of the solute in one of these embryos relative to that in a saturated solution at the same conditions of temperature and pressure can be calculated as though the embryos had the same properties with reference to the solute in the liquid phase as those of a macroscopic crystal. In a system maintained at constant

temperature and pressure, the Gibbs free energy of the system is

$$G = U - TS + PV = \sum_i \mu_i N_i \qquad (2.1)$$

where conventional notation is used for designating the various thermodynamic potentials and parameters, i.e., U is the internal energy, T the absolute temperature, S the total entropy of the system, P the pressure, and V the volume of the system. The chemical potential is designated as μ and N denotes number of moles, the subscript i indicating reference to component i of the system.

Hence, when the only form of work involved is that of creating a surface of discontinuity, as is the case in the appearance of an embryo

$$dG = \sum_i \mu_i \, dN_i + dW_s - SdT + VdP \qquad (2.2)$$

Since nucleation is presently being considered under isothermal and isobaric conditions, equation (2.2) may be further simplified to

$$dG = \sum_i \mu_i \, dN_i + dW_s \qquad (2.3)$$

If the system is restricted to that formed by the solute, N_B moles of which are constituting an embryo (phase B) and N_A moles are still in solution (phase A), then the change in free energy of the system as it changes to constitute an embryo, may be described by

$$\Delta G = G_{final} - G_{initial}$$

Hence,

$$\Delta G = (N_A \mu_A + N_B \mu_B + 4\pi r^2 \sigma) - (N_A + N_B) \mu_A \qquad (2.4)$$

where σ is the interfacial free energy per unit surface area which may be a function of the concentration of the solution in equilibrium with the embryo, and r is its radius, assuming a spherical surface of discontinuity.

Simplification of equation (2.4) yields

$$\Delta G = -(\mu_A - \mu_B) N_B + 4\pi r^2 \sigma \qquad (2.5)$$

A prevalent but mistaken concept is that the embryos result from the random simultaneous collisions of all of the molecules composing it. However, in the formation of a nucleus of pure water from saturated air it has been estimated that about 80 molecules of water are involved. The probability of such a simultaneous collision is extremely low. Therefore, another assumption of the V.W.B.D. Theory is that embryos, and ultimately nuclei of crystallization are the result of the stepwise bimolecular addition of molecules. Designating α as a molecule of solute in the liquid phase and β_i a crystalline embryo formed by i molecules, these sequences of bimolecular additions may be represented as follows:

$$\alpha + \alpha \rightleftarrows \beta_2$$

$$\beta_2 + \alpha \rightleftarrows \beta_3$$

$$\text{----}$$

$$\beta_i + \alpha \rightleftarrows \beta_{(i+1)} \qquad (2.6)$$

For spherical embryos of radius r at a given temperature and

external pressure the free energy increase of the solute in an embryo with respect to that in solution may be described by

$$\Delta G = 4\pi r^2 \sigma + (4/3\ \pi r^3)\ \Delta G_v \qquad (2.7)$$

where ΔG_v is the excess free energy per unit volume of the crystalline phase in the embryo over that in solution, or, according to Uhlmann and Chalmers[17]

$$\Delta G = N_r\ v\ \Delta G_v + (36\pi)^{1/3}\ N_r^{2/3}\ \sigma\ v^{2/3} \qquad (2.8)$$

where N_r is the number of molecules in the embryo of radius r and v is the molecular volume of β.

If the reference free energy level is chosen as that of the solute in the saturated solution, ΔG_v is given by

$$\Delta G_v = -(\mu_1 - \mu_o)\ \frac{\rho}{M} \qquad (2.9)$$

where μ_1 is the chemical potential of the solute in the embryo of size r, μ_o the chemical potential of the solute in a saturated solution at the temperature of the system, M the solute molecular weight, and ρ its crystalline density. The activity of the solute in an electrolytic solution, $\underline{a}$, is defined by

$$\mu_1 - \mu_1^o = RT \ln a_1 \qquad (2.10)$$

where the superscript o indicates reference to a particular standard state, in this case the solute at infinite dilution at the same temperature and pressure. Hence, equation (2.9) may be rewritten as

$$\Delta G_v = -\frac{\rho\ RT}{M} \ln \frac{a_1}{a_o} \qquad (2.11)$$

Substitution of equation (2.11) into equation (2.7) yields

$$\Delta G = 4\pi r^2 \sigma - \frac{4\pi r^3 \rho RT}{3M} \ln \frac{a_1}{a_o} \qquad (2.12)$$

where the subscripts 1 and o still refer to the solute in an embryo of radius r and in a saturated solution, respectively.

It can readily be seen that ΔG must go through a maximum as r increases, corresponding to a critical radius r_c, which may be calculated by letting $\partial(\Delta G)/\partial r = 0$. Therefore

$$r_c = \frac{2\sigma M}{\rho RT \ln a_1/a_o} \qquad (2.13)$$

The maximum free energy difference may be calculated by substituting equation (2.13) into equation (2.12), thus

$$\Delta G_c = \frac{16\pi\sigma^3 M^2}{3(\rho RT \ln a_1/a_o)^2} \qquad (2.14)$$

Figure 1 indicates the variation of the free energy ΔG of an embryo as a function of its radius.

Embryos having a radius smaller than r_c will disappear on the average, while those that become larger will grow into crystallization nuclei. Hence an embryo of radius r_c is, by definition, a nucleus. By a similar procedure, the critical number of molecules N_c in a nucleus of radius r_c may be derived. The relation is

$$N_c = \left(\frac{32\pi}{3v}\right)\left(\frac{\sigma}{\Delta G_c}\right)^3 \qquad (2.15)$$

Volmer and Weber[15] developed an expression for the rate of

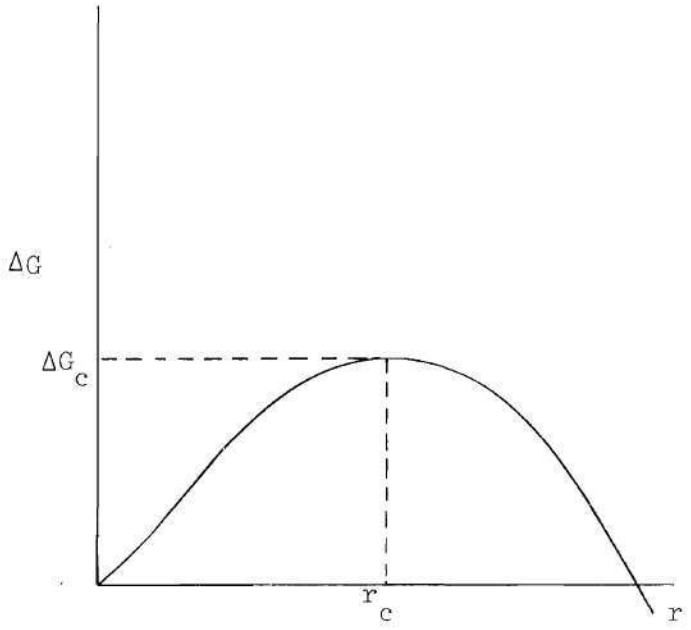

Figure 1. Free Energy of an Embryo as a Function of its Radius.

formation of embryos from a supersaturated vapor phase by considering the kinetics of the forward reaction indicated in equation (2.6). Becker and Döring[16] improved the treatment by considering also the reverse process although the treatment was still restricted to the formation of liquid embryos from a supersaturated vapor phase. Finally, Turnbull and Fisher[18] considered the situation of nucleation in condensed systems and derived an expression for the net rate of embryo formation, J, per unit volume. Following these authors' development, the free energy of $\beta_i + \alpha$, referred to that of α as the standard state, is ΔG_i, while that of β_{i+1} is ΔG_{i+1}. Assuming the intermediate configurations to have greater free energies than ΔG_i or ΔG_{i+1}, there should be one path by which this intermediate configuration should correspond to the lowest free energy maximum. This configuration may be designated as an activated complex. Figure 2 illustrates the variation in free energy resulting in

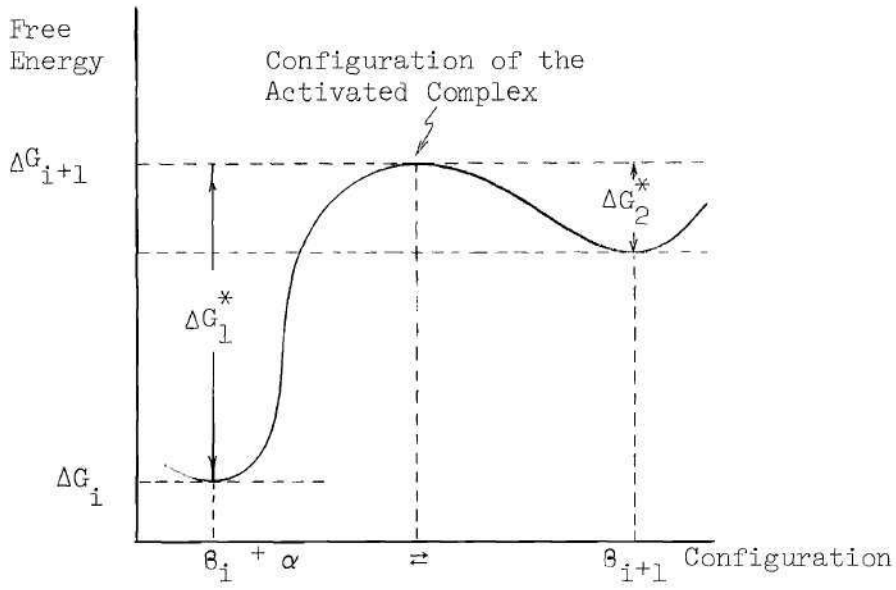

Figure 2. Free Energy Variation with Configuration for Formation of an Embryo.

the association of $\beta_i + \alpha$ to give β_{i+1} or the reverse process as a function of the path followed.

The difference in free energy between the activated complex and the average free energy difference between the end states may be denoted by ΔG^*. This term is the free energy of activation for short range diffusion of molecules moving a fraction of a molecular diameter to join a crystal lattice.

The relation derived by Turnbull and Fisher[18] is

$$J = K_v \exp[-(\Delta G^* + \Delta G_c)/kT] \qquad (2.16)$$

in terms of the number of nuclei per second per mole of untransformed material, where

$$K_v = n_c (A/9\pi)^{1/2} (NkT/h) \qquad (2.17)$$

if n_c is the number of surface atoms in the critical size nucleus, N the number of α atoms in contact with each β nucleus. The A term is proportional to the interfacial free energy per unit area of α - β interface and it may be shown to be given by

$$A = \frac{(36\pi)^{1/3} \sigma v^{2/3}}{kT} \tag{2.18}$$

Furthermore, for most nucleation problems of interest, K_v may be approximated within an order of magnitude by

$$K_v \approx \frac{NkT}{h} \tag{2.19}$$

Using a similar line of reasoning, Uhlmann and Chalmers[17] obtained the expression for K_v

$$K_v = n_c C \upsilon_o r_c^2 \left(\frac{128 \pi^2 v}{9}\right)^{1/2} \tag{2.20}$$

where C is the total number of unassociated molecules per unit volume of mother phase and υ_o the molecular jump frequency (the number of times the activation barrier is attempted). These authors suggest K_v to be taken within an order-of-magnitude as

$$K_v \approx C \upsilon_o \tag{2.21}$$

Where a change of composition is involved, ΔG^* should be considered as the energy of activation for diffusion of the slowest moving component.

A somewhat more general expression for K_v has been developed by Dufour and Defay[19] that does not involve the assumption of spherical embryos. Although developed for application to the nucleation of ice crystals from salt solution droplets, it may be applicable to the nucleation of salt from solution droplets as well. The expression is

$$K_v = Cwv \frac{\Omega_c}{S_c^{\beta} (h_c^{\beta})^2} \left(\frac{S_c^{\beta} \sigma}{\pi k T} \right)^{1/2} \qquad (2.22)$$

where w is the total number of molecules of the precipitating phase won by the nucleus per unit time and unit surface area of the nucleus, Ω_c the surface area of a critical size nucleus, S_c^{β} a shape factor for face β of a nonspherical nucleus, and h_c^{β} the height from the center of a face β of the nucleus. This expression allows for different reaction rate factors for different faces of a nucleus having a crystalline habit such that the distance from a face to the center is not a constant.

The formation of only one nucleus per droplet is sufficient to cause all of the solute to crystallize and the associated moisture to evaporate from the droplet, regenerating the original size crystal. Equation (2.16) may, therefore, be expressed in terms of the time required for nucleation, θ, as follows:

$$\ln \theta = \frac{\Delta G_c + \Delta G^*}{k T} - \ln K_v \qquad (2.23)$$

Substituting Equation (2.14) gives

$$\ln \theta = \frac{16 \pi \sigma^3 M^2}{3 \rho^2 R^2 T^3 k \ln^2 (a_1/a_o)} + \frac{\Delta G^*}{k T} - \ln K_v \qquad (2.24)$$

Equation (2.24) could be used to predict the time required for homogeneous nucleation to occur in a solution droplet as a function of supersaturation ratio. Unfortunately, great uncertainty exists in the estimation of the properties of the molecular clusters that constitute

the embryos. These clusters are too complex to permit meaningful theoretical estimations and they are too small to be subject to direct experimental observation. Certain assumptions may be made which simplify Equation (2.24) so that experimental nucleation data may be studied with respect to the resulting model, however.

If the interfacial free energy of the nucleus is assumed independent of the concentration of the mother liquid phase, a constant K_1 may be defined as

$$K_1 = \frac{16 \pi \sigma^3 M^2}{3 \rho^2 R^2 T^3 k} \tag{2.25}$$

Furthermore, as a rough approximation, the nucleation rate constant K_v may also be taken to be independent of the solution concentration. Under this assumption for isothermal conditions, a constant K_2 is obtained

$$K_2 = \frac{\Delta G^*}{k T} - \ln K_v \tag{2.26}$$

Finally, substituting Equation (2.25) and (2.26) into (2.24) gives

$$\ln \theta = K_1 \left[\ln^{-2} (a_1/a_o) \right] + K_2 \tag{2.27}$$

If the assumptions made in the development of equation (2.27) are acceptable, then a linear relationship should exist between $\ln \theta$ and $\ln^{-2} (a_1/a_o)$.

CHAPTER III

EXPERIMENTAL INVESTIGATIONS

Description of the Apparatus

An apparatus was devised to accomplish three primary functions. With it, it was possible (1) to produce an aerosol composed of an artificial fog of dilute solution droplets of approximately constant particulate concentration in a size range of 0.01 to 0.1 micron in radius, (2) to adjust the moisture content of the fog, and (3) to determine the particulate size distribution after exposure to definite relative humidity levels for given lengths of time. A block diagram of the system is shown in Figure 3. Figure 4 is a photograph of the equipment. The apparatus was designed to operate continuously for long periods of time at very nearly constant conditions. Thus, a detailed study of the size behavior of the aerosol with relative humidity was possible. Special emphasis was placed on the behavior of the aerosol after conditions of supersaturation had been imposed on it but before crystallization and drying of the droplets ensued.

Aerosol Generation Equipment

A Devilbiss No. 180 liquid nebulizer was used to generate an artificial fog from a dilute sodium chloride solution (0.05% by weight). The nebulizer bottle had to be enlarged and redesigned to insure sufficient solution for operation over periods of up to 10 hours without refilling. The nebulizer itself operated on the venturi principle and was provided with an impaction plate in the droplet stream that was capable of

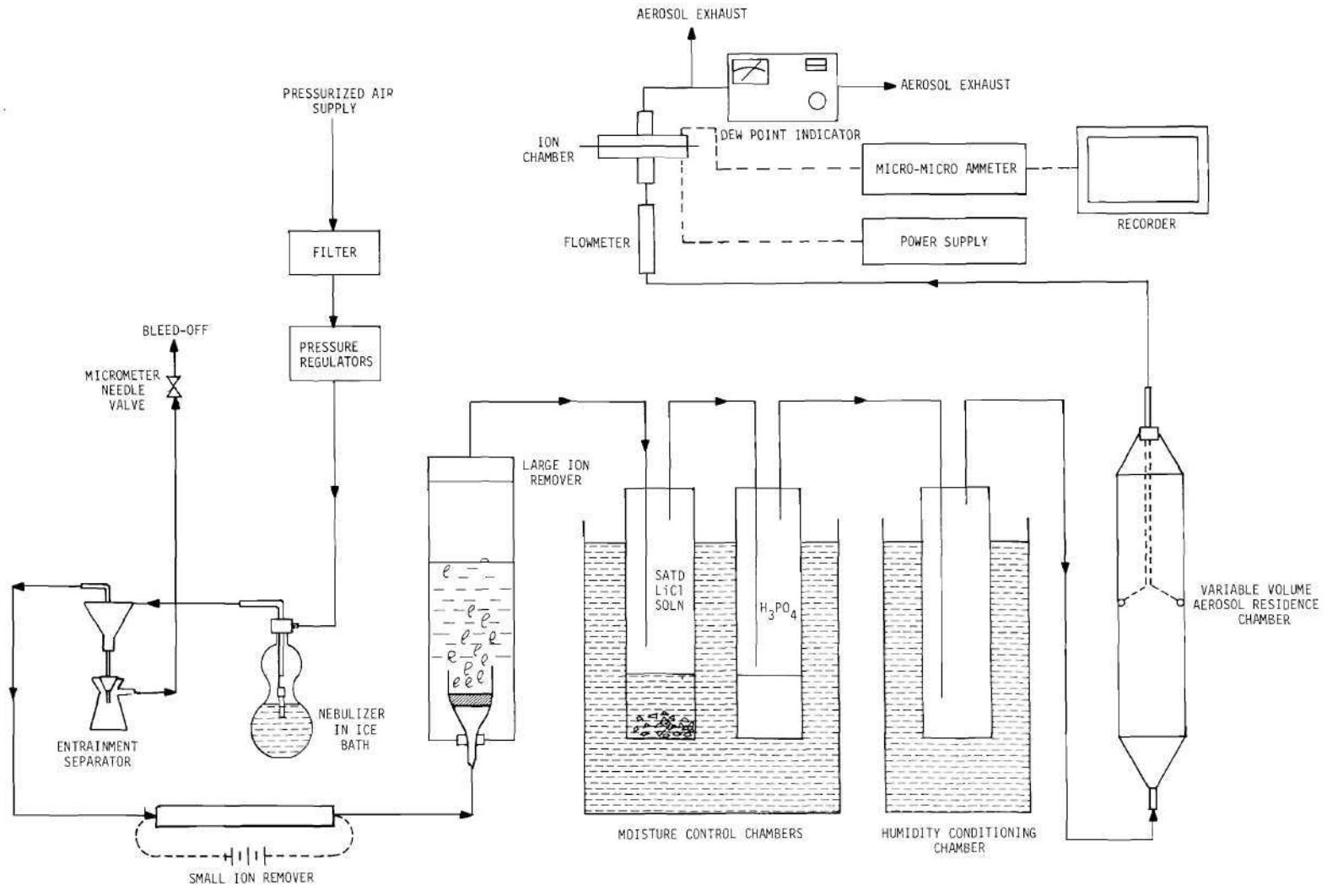

Figure 3. Schematic Diagram of Equipment.

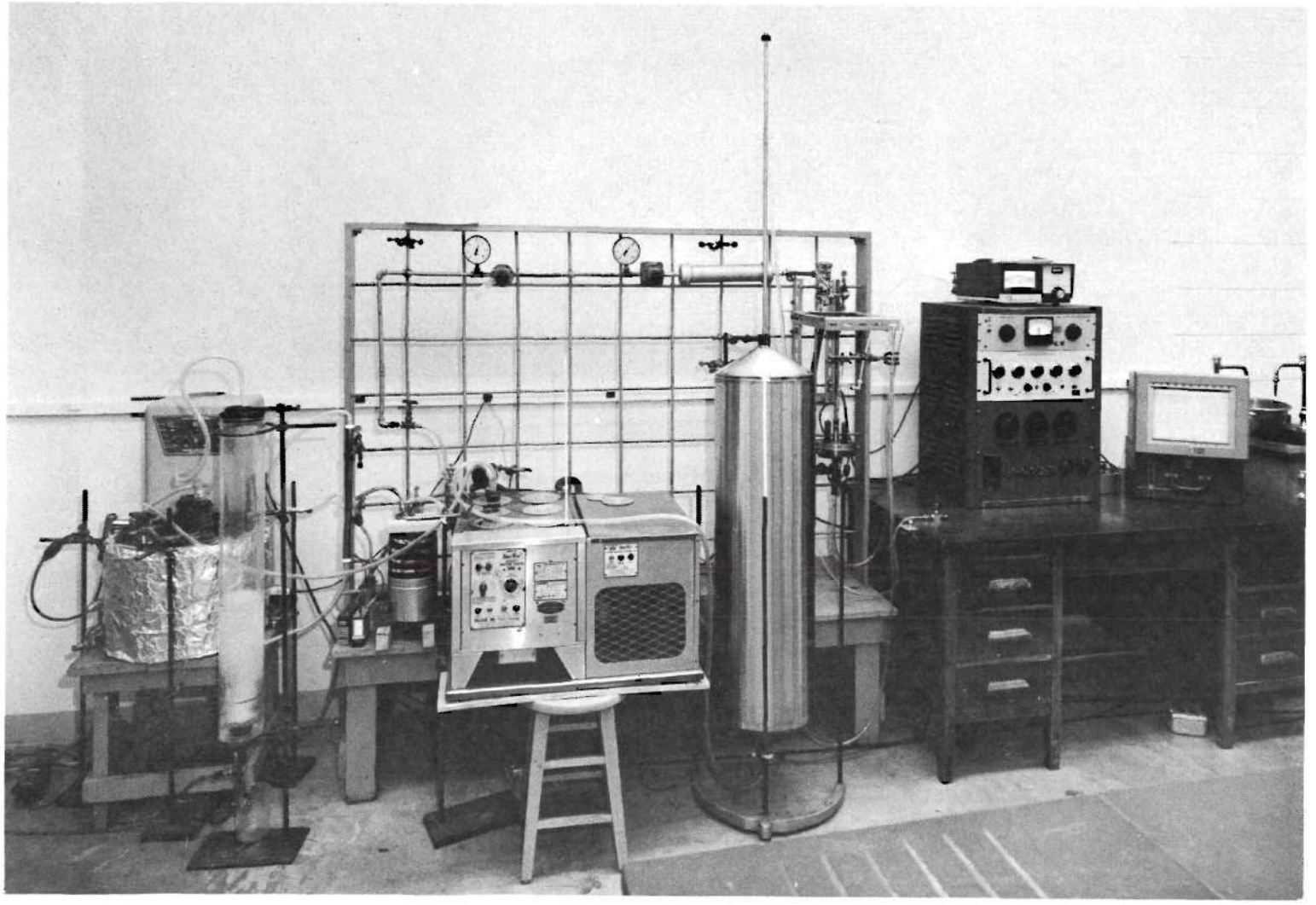

Figure 4. Equipment for Producing and Analyzing Submicroscopic Fog Droplet Behavior with Relative Humidity.

collecting and returning to the main body of solution all droplets larger than about one micron in diameter. Satisfactory performance was obtained by operating the nebulizer with a constant pressure differential of 15 psi. The air was water- and oil-free and was passed prior to use through a filter consisting of 5 inches of firmly packed felt. The nebulizer operating pressure (18 psi) was achieved in two stages using two automatic pressure regulators. Manometers were provided to indicate the pressure in each stage. The nebulizer was immersed in an ice bath during operation in order to reduce solution evaporation. The fog produced had a relative humidity of about 30 per cent at room temperature, hence the aerosol was composed completely of NaCl crystals shortly after generation.

A micrometer needle valve was provided on the downstream side of the nebulizer to bleed off excess aerosol. By careful adjustment of this valve a constant aerosol flow rate was obtained through the rest of the apparatus. An aerosol flow rate of 3790 cm^3 per minute through the ion counter was used since it was found that this yielded the most satisfactory operation of the instrument.

Equipment for Sharpening the Size Distribution of the Aerosol

A small ion remover was designed to precipitate the fraction of aerosol particulates smaller than 0.01 micron in radius. It consisted of a stainless steel tube 15.5 inches long having an internal diameter of 0.800 inch. A brass rod 0.25 inch in diameter and 12.25 inches long was mounted coaxially by means of perforated teflon insulators. The inner rod was installed so that an entrance length of 1.50 inches was provided. The exposed length of the inner rod was 11.75 inches.

By applying a constant electric potential of 90 volts between the inner rod and the outer stainless steel tube an electric field was obtained which collected particulates smaller than 0.01 micron in radius at an aerosol flow rate of 3790 cm^3 per minute.

The aerosol was made to flow from the nebulizer through the small ion remover and then was made to bubble through a water column 15 inches high. A Büchner-type filter funnel of 80 millimeters internal diameter having a coarse-porosity glass support was installed at the bottom of a plexiglass tube 48 inches long and having internal diameter of 4 inches. By passing the aerosol through the glass support, discrete, even sized air bubbles were obtained approximately 0.25 inch in diameter. This bubbling procedure retained particulates larger than about 0.1 micron in radius from the aerosol stream. Figure 5 offers a comparison between the size distributions of the aerosol prior to treatment (Curve A), after passing through the small ion remover only (Curve B), after passing through the bubbling column of water (Curve C), and when both devices were used (Curve D).

This procedure was noted previously by Remy[20] as being an effective means of reducing the particulate concentration of a fog. No evidence was found that there is a discriminating effect due to retention of the larger particulates. Therefore the method was of value in sharpening the size distribution of the aerosol in the size range under consideration.

Moisture Control Chambers

The aerosol moisture content was controlled by circulating the aerosol through two chambers immersed in a temperature-controlled water

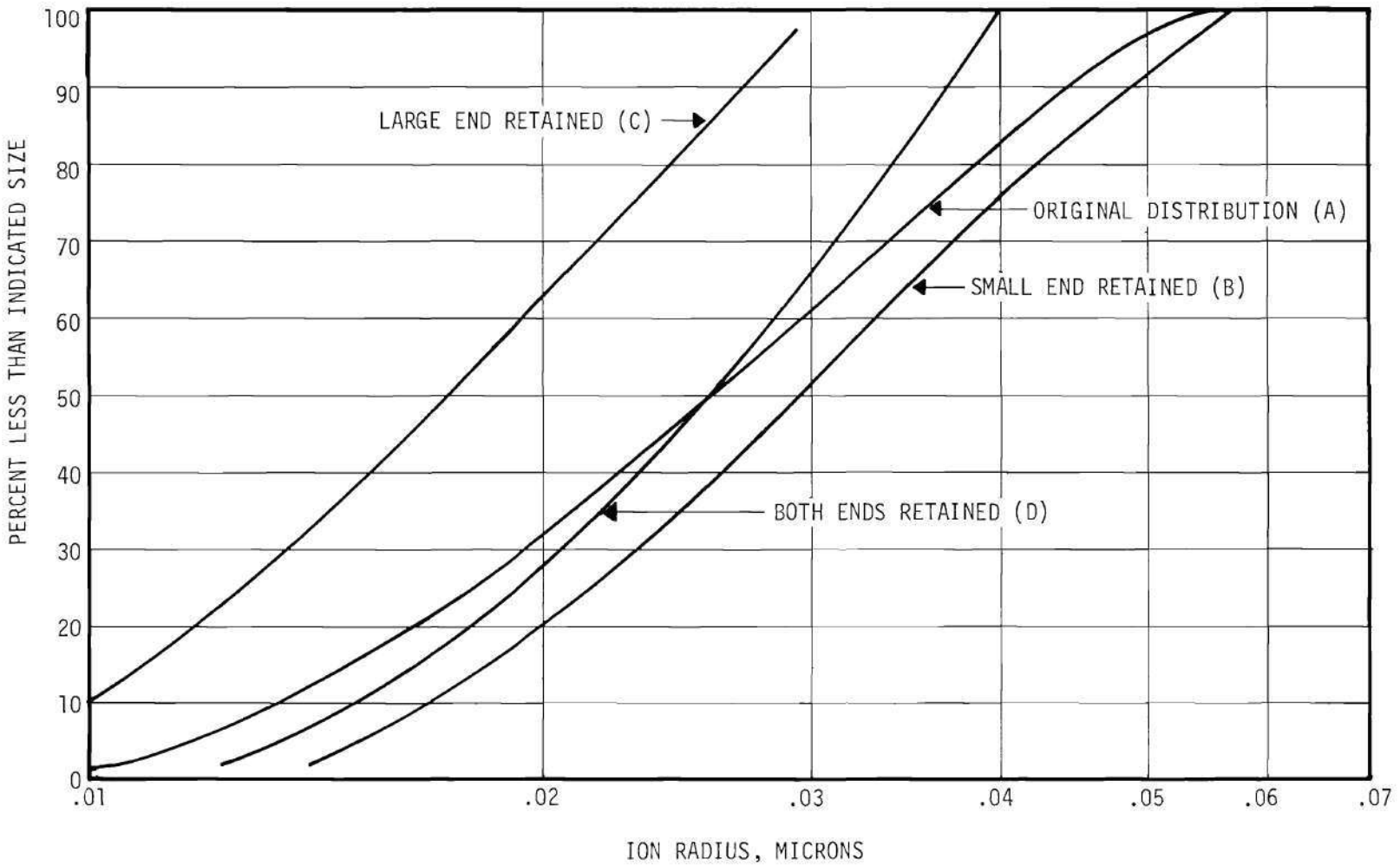

Figure 5. Individual and Combined Effect of Sharpening Devices on the Aerosol Particulate Size Distribution.

bath. The first chamber contained a saturated solution of lithium chloride and the second concentrated phosphoric acid. The water bath was a Hi-Lo Temperature Water Bath, Model No. 832, manufactured by the Wilkens Anderson Company, Chicago, Ill. This instrument used a direct-action mercury thermostat switch which could be adjusted. The range of operation of the unit was from about 0°C to above 50°C and the precision of the temperature control was ± 0.1°C. The moisture content of the aerosol was adjusted by setting the water bath temperature. The aerosol humidity could be regulated from a dew point of approximately -10°C at a bath temperature close to 0°C to a dew point of 25°C at a bath temperature of about 45°C. After thermal equilibrium was established, constant moisture conditions could be maintained for periods of 2 to 3 hours, which was ample time for collection of data.

Humidity Conditioning Chamber

This chamber consisted of an empty reservoir immersed in a constant temperature water bath. The bath used was a Blue M Magni-Whirl Refrigerated Water Bath, Model No. MR-3220-A, manufactured by the Blue M Electric Co., Blue Island, Ill. This instrument had a range of operation of 0°C to 100°C with a control range of ± 0.1°C. The unit was also provided with an automatic, electromagnetically actuated stirring device. It was found, however, that this device introduced a very high level of disturbance on the current readout of the ion counter. Therefore, this stirring mechanism was disconnected and a stirrer operated by an electric motor was used instead.

The purpose of this chamber was to force the aerosol to achieve equilibrium from a high as well as from a low humidity condition.

Therefore, when the temperature of this chamber was much higher than the dew point of the aerosol, a low local relative humidity level was obtained and the solution droplets were forced to evaporate. Conversely, if the temperature was very close to the dew point of the aerosol, a high local relative humidity was obtained and the submicroscopic crystals would adsorb moisture until solution droplets would form. As soon as the aerosol left the chamber and attained room temperature, equilibrium relative humidity conditions would be achieved before entering the residence chamber either from a "dry" or a "wet" aerosol condition as required by the experiment being performed.

Variable Volume Aerosol Residence Chamber

A variable volume chamber was designed to provide residence time for the aerosol before its size distribution was examined. The chamber consisted of two concentric, close-fitting stainless steel cylinders terminated by 30° cones. The outer cylinder cone was welded to a section of 3/8-inch stainless steel tubing and the inner cylinder terminated in a bushing with an O-ring seal to fit over 3/8-inch tubing. An internal sample probe was constructed (see Figure 6) from 3/8-inch stainless steel tubing. It ended in an inverted 30° cone and was movable so that the effective volume of the chamber could be changed from about 4.5 to 140 liters. This represented an average residence time range of from 1.2 to 37 minutes at the aerosol flow rate of 3790 cm^3 per minute used in all of the experiments. The experiments were designed so the entire size distribution of the aerosol was studied at constant residence time. Then the volume of the chamber would be changed to permit study of the aerosol size behavior with relative

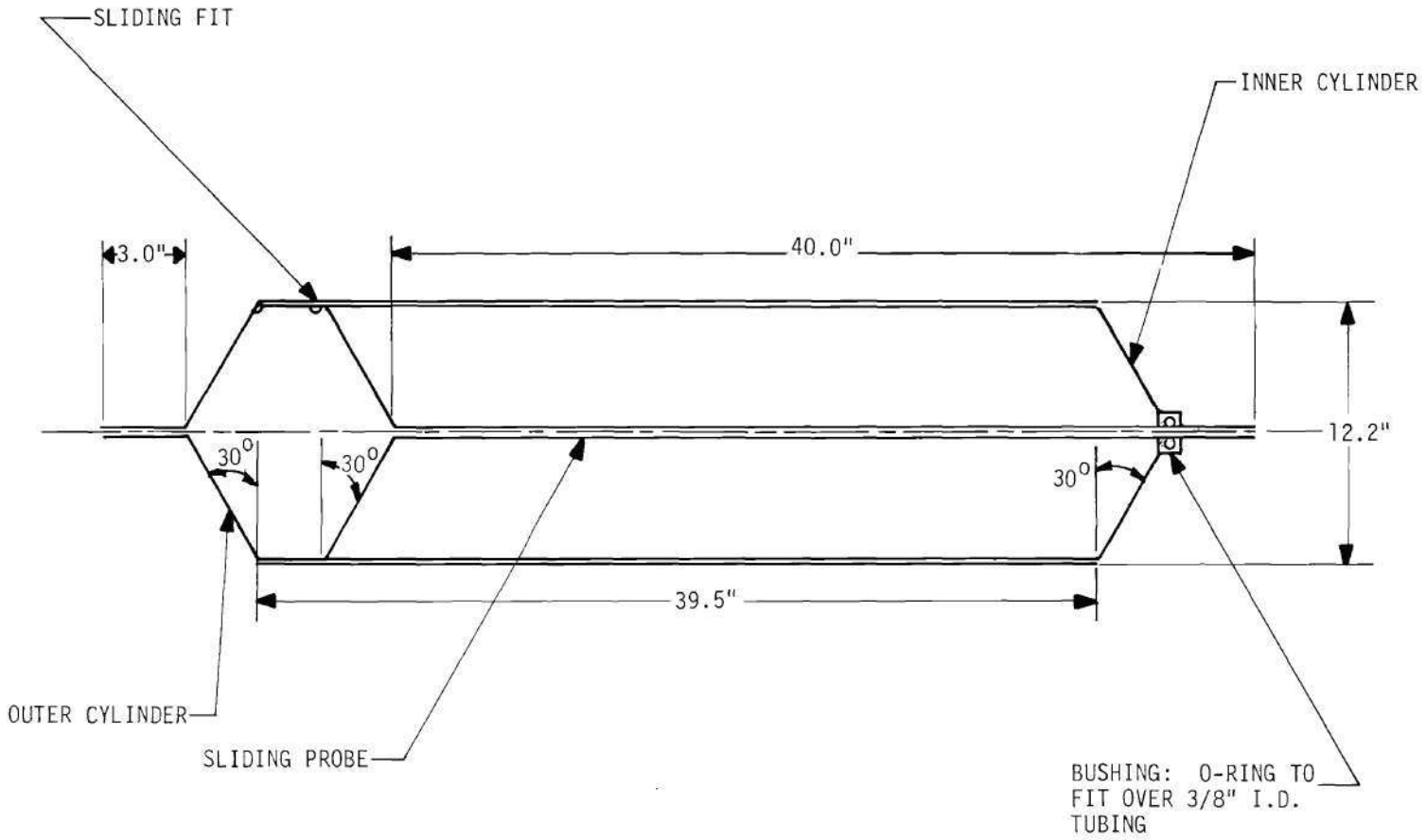

MATERIALS:

SHEET METAL	-	0.040" (Approx.) STAINLESS STEEL
TUBING	-	3/8" I.D. STAINLESS STEEL
BUSHING	-	STAINLESS STEEL

Figure 6. Variable Volume Residence Chamber.

humidity for a longer residence time. Rubber cement was used to coat all movable joints to insure air tightness. The dimensions of the chamber were arrived at by attempting to obtain the highest possible ratio of average linear velocity for the particulates relative to the average random Brownian motion consistent with limitations on the length of the chamber. The final design permited this ratio to be between 18.5 for particulates of 0.01 micron in radius to 184 for particulates of 0.1 micron in radius at a residence time of 30 minutes.

The Ion Counter

The ion counter consisted essentially of two, flat, circular, parallel plates separated by a fixed distance. The plates were mounted inside a metal enclosure and insulated from the surroundings with Teflon insulators. The lower plate was fixed to the lower part of the enclosure and the upper plate was suspended at three points from the upper part of the enclosure. The separation between the plates was adjusted by raising or lowering the upper plate. The aerosol was admitted through the center of the lower plate and was made to flow radially outward. Details of construction are given in Figure 7. The flow rate was adjusted to obtain laminar flow conditions. The plates were maintained at a fixed, but adjustable, potential difference, and, therefore, the charged aerosol particulates when flowing radially outwards between the plates were subjected to an electrical force which tended to move them toward one of the plates according to the nature of their charge. A Keithley Regulated High Voltage Power Supply, Model 241, was used. This instrument had a range of 0-1000 volts at up to 20 milliamperes and its voltage

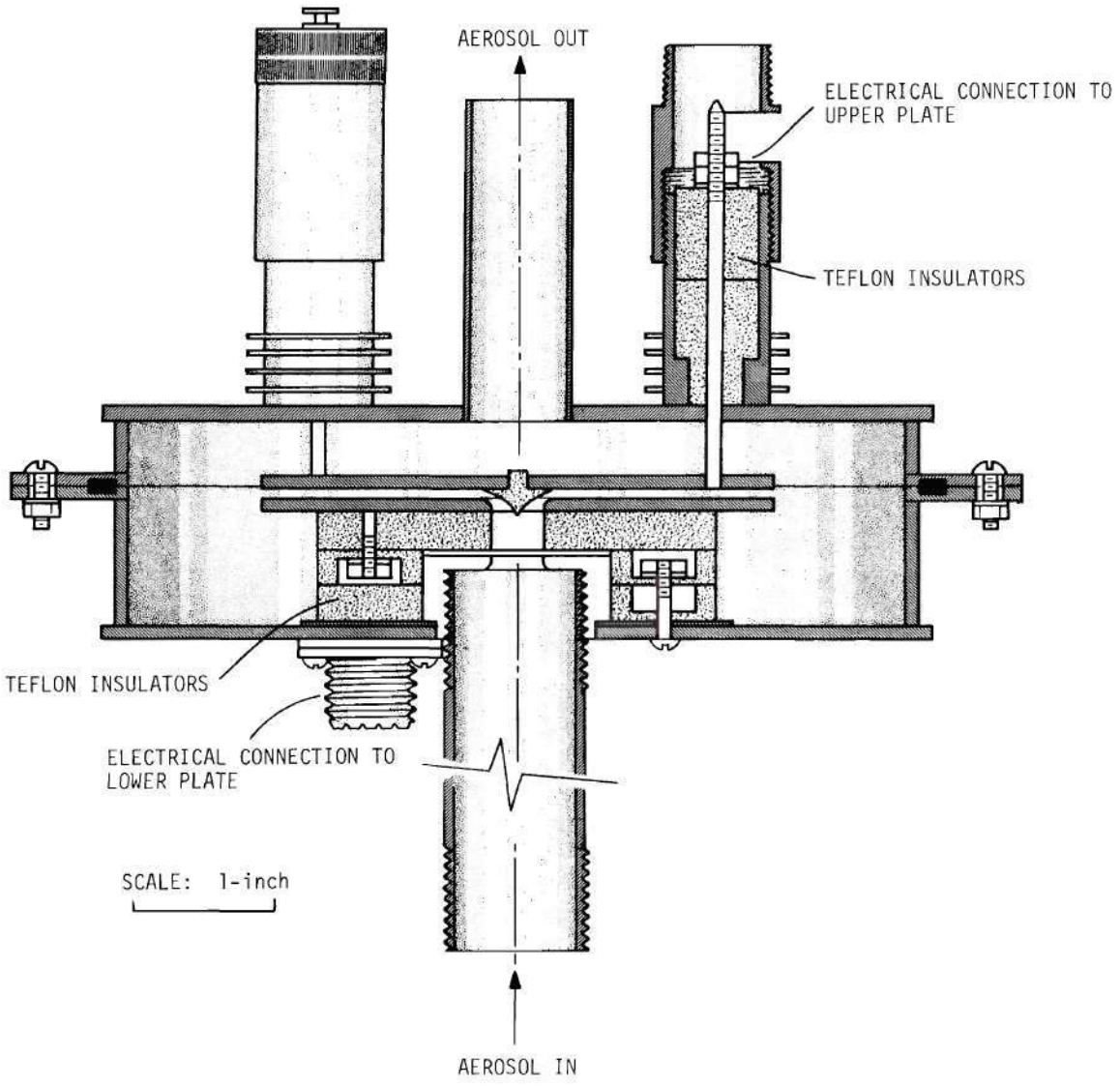

Figure 7. Constructional Details of the Ion Counter.

output could be adjusted in powers of 10 from -2 to +2 with five calibrated panel switches. The accuracy of the output was 0.05 per cent with a stability of 0.005 per cent per hour. The lower plate was operated as the negative electrode so that it collected the positively charged particulates although the polarity could have been reversed. The result was proved to be equivalent, since aerosols generated by nebulizing electrolyte solutions are very nearly electrically neutral and therefore have equal number of positive and negative charges.

A Keithley, Model 410 Micro-Microammeter was used to measure the ion current generated by the deposition of the charged particulates upon the upper plate of the ion chamber. The Micro-Microammeter was a line-operated vacuum tube electrometer designed and constructed to measure currents from 10^{-3} to 3×10^{-13} ampere. It had a zero drift of less than 2 per cent of full scale in eight hours and was provided with an output for driving a 0-1 or 0-5 milliampere recorder at 5 volts for full scale meter deflection. A Speedomax-W Leeds & Northrup recorder was used in connection with an adequate voltage divider to record the current.

For each fixed potential difference a certain fraction of the charged particulates was collected. This fraction increased with the ion chamber plate voltage until all of the charged particulates were collected.

Low-noise, coaxial cable was used to connect both the lower plate of the ion counter to the power supply and the upper plate to the Micro-Microammeter. This was especially important in the second

case since the cable even had to be tied down firmly to avoid vibrations which induce electrostatic effects readily detectable by the micro-micro-ammeter. This electrical noise constituted one of the most difficult problems in all of the experimental operating procedure.

In order to prevent condensation of moisture on the Teflon insulators of the upper plate supports, electrical heaters were built in to keep these components about 10°C above room temperature. A variable transformer supplied power continuously to the heaters at approximately 15 volts. In order to keep the leakage current down to an acceptable low value, the resistance between the plates of the ion counters had to be kept at or above 10^{16} ohms. After several weeks in use it was found necessary to disassemble the ion counter and clean the various components, especially the Teflon insulators. A final rinsing with absolute ethanol and drying in a laboratory oven for several hours at 80°C generally proved adequate. Warm potassium dichromate-sulphuric acid cleaning solution was used on the Teflon insulators for a few minutes in order to dissolve stubborn contamination.

Dew Point Measurement

A continuous reading of the aerosol dew point was made by sampling a fraction of the aerosol stream as it emerged from the ion counter. A Cambridge Systems Thermoelectric Dew Point Hygrometer, Model 990-B, was used for this purpose. This instrument operated by determining the temperature at which condensation begins to form (dew point) upon a rhodium-plated, thermoelectrically cooled silver mirror by detecting a sudden change in reflectivity. The instrument detected and automatically controlled the temperature of the mirror at the dew point of the aerosol

with an approximate accuracy of $\pm$ 0.4°C by using a special solid-state optical system. The mirror was provided with an imbedded, aged, precision thermistor temperature sensor which allowed direct dew point temperature readout on a wide-scale, taut-band meter calibrated in both Fahrenheit and Centigrade scales. The operating range of the instrument was from a frost point of -40°C to a dew point of 25°C. This range permitted measurement of relative humidities from 3 to 100 per cent at an ambient temperature of 25°C. The applicability of this instrument to the aerosols under study was especially useful since the instrument was quite insensitive to deposition of particles on the mirror surface. It was sensitive instead to sudden changes in the reflectivity of the mirror surface. It was found that the instrument could be used over a period of several weeks without cleaning the mirror surface. It was found also that, if the mirror surface was cleaned after such a period of usage, the new reading would be closer to the previous one than the quoted accuracy of the instrument.

Operating Procedure

Equipment Start-up and Operation

Initially, the moisture-control chambers were filled with a saturated solution of lithium chloride (with an ample excess of crystals) and concentrated phosphoric acid, respectively. Both the micro-micro-ammeter and the regulated power supply were kept on (on standby status) at all times to insure operation without drift. The dew point indicator, being all solid state, could be turned off after a run was completed without affecting its stable operation.

The nebulizer container was next filled to the proper level with

a sodium chloride solution of 0.05 per cent by weight concentration and installed in an ice bath inside a Dewar flask. Then, the main air valve was opened and a pressure of 40 psig was set as the primary stage. The secondary air regulator was then adjusted so the nebulizer operating pressure was 18 psig. With the aerosol flowing, water was let into the bubbling column (large ion remover) up to a level of 15 inches. By controlling the micrometer needle valve, the desired aerosol flow rate of 3790 cm^3 per minute was finally obtained.

Data Collection

A complete size spectrum of the aerosol was studied at a constant aging time in the residence chamber. The procedure here consisted of adjusting the temperature of the moisture control chambers close to 0°C to obtain a very low dew point for the aerosol. The humidity conditioning chamber temperature was set at approximately 45°C. This was sufficiently high to insure a relative humidity of less than that at which the NaCl crystals in the aerosol would dissolve (between 70 and 75 per cent, depending on the size). As the aerosol came from the humidity conditioning chamber, the equilibrium relative humidity was thus achieved (when the dry bulb temperature was equal to the room temperature) from a "dry" crystal condition.

As soon as equilibrium conditions were obtained (i.e., constant aerosol flow rate and constant dew point temperature), a complete size spectrum analysis was carried out from ion mobility measurements. In order to accomplish this, a potential of about 900 volts was applied to the ion counter and the ion current generated was plot on the recorder chart. Then, another, lower voltage was applied and the current noted

and recorded until the complete voltage spectrum was covered. Special care had to be exercised in determining the lowest potential at which the maximum ion current was obtained. Under the conditions of this study, a maximum ion current of about 6.5×10^{-12} ampere was obtained for zero residence time; it decreased gradually to about 3.0×10^{-12} ampere for a residence time of 20 minutes.

The test was discarded if a sudden discontinuity was obtained on the ion current plot at constant voltage or if the value of maximum ion current could not be reproduced within 10 per cent after the complete voltage range was covered.

By successively increasing the temperature of the moisture control chambers, new ion current versus plate potential curves could be obtained at correspondingly higher humidity levels of the aerosol. The determination of the relative humidity at which the crystals dissolved was obtained by bracketing the size shift within one half of one per cent, which is within the uncertainty in the calculation of the relative humidity. From this point, the moisture content was increased until data on ion current versus plate potential was obtained for relative humidities of 90 per cent or higher. The information so obtained yielded the size changes of dry crystals in equilibrium with relative humidity when this equilibrium was achieved from a "dry crystal condition."

In order to study the size behavior of the ions when the equilibrium was achieved from a "droplet condition," the temperature of the humidity conditioning chamber was adjusted to be slightly above the dew point of the aerosol. The aerosol crystals thus formed solution droplets

inside the chamber in equilibrium with a relative humidity of 90-95 per cent. Then the reverse process was followed, that is, new ion current versus plate voltage data were obtained for successively decreasing levels of humidity until the shift in size to the original condition of a "dry crystal aerosol" was obtained.

Since maximum ion current variations are present within the set limits of 10 per cent, the ion current data was normalized so that the data from different runs could be referred to a common basis. This normalizing procedure consisted of expressing the ion current data for each run in terms of per cent of the maximum ion current. When this is done, the spectrum of normalized ion current versus plate potential with relative humidity as a parameter may be presented in the much more useful form of normalized ion current versus relative humidity with plate potential as a parameter. This form of presentation of the data can be readily converted into aerosol size distribution at any value of relative humidity, or, in other words, the behavior of a specific size particle can be studied with respect to relative humidity.

CHAPTER IV

RESULTS AND DISCUSSION

The equilibrium relative humidity at which supersaturated solution droplets nucleate, causing a sudden decrease in the size of the particulate as the solute crystallizes and the moisture evaporates, was determined from the experimental plots (presented in Appendix E) of relative humidity versus ion current generated at constant plate potential. A compilation is presented there of all the experimental results. The data represent the complete behavior of aerosols composed by submicroscopic sodium chloride crystals in the range of 0.01 to 0.1 micron in radius as a function of equilibrium relative humidity for various values of residence time after equilibrium had been established. For each value of aerosol residence time, a set of figures is presented illustrating the variation of normalized ion current resulting from the deposition of charged aerosol particulates upon the ion counter plates at various constant plate voltages as a function of equilibrium relative humidity. Nucleation data is represented by the portion of the curves indicated by shaded dots. The data must be converted into normalized ion current at various values of equilibrium relative humidity and previous aerosol history as a function of precipitator plate potential in order to obtain size distribution information according to the theory of operation of the ion counter (Appendix A). An analysis of these curves indicates the aerosol size distribution with equilibrium relative humidity and previous history (i.e., whether equilibrium is

achieved from either "dry" crystals of solute or from supersaturated solution droplets). From the aerosol size distribution curves the behavior of any size particulate near the mean can be studied. A figure is presented also showing the relationship between the equilibrium humidity and the size of the mean aerosol particulates.

In this chapter is presented an analysis of the data pertinent to the nucleation of the supersaturated aerosol solution droplets as obtained from the experimental data compiled in Appendix E.

The nature of the phenomenon studied and the theory of operation of the ion counter is such that during the shift from a dry crystal to a solution droplet, the relative percentile positions of the distribution of particulates is preserved[21]. The same is also true when considering the shift from a solution droplet to a dry crystal. This is apparent from the constant concentration lines of Figures 33 through 36 in Appendix C which represent the solution droplet behavior with relative humidity as predicted by various methods. These figures indicate that smaller droplets will reach a certain supersaturation at a given relative humidity sooner than larger droplets. Hence, even during the shift, smaller droplets will remain as smaller particulates. Therefore, the assumption is made that the relative percentiles are preserved during the crystallization process. Experimental results indicate that the shift is not sudden due to the fact that the nucleation process that controls the phenomenon is time dependent, that is, there is a distribution in the nucleation time of droplets of the same size and electrolyte content. However, the relative humidity at which the shift occurs may be determined within $\pm$ 0.6 per cent by observing the behavior of the

relative humidity versus ion current plots at constant plate potential. Table 1 indicates the average relative humidity at which the nucleation of the aerosol occurred at a given mean residence time as well as the mean of the aerosol size distribution when entirely composed of dry sodium chloride crystals.

Table 1. Relative Humidity Required at a Given Residence Time for the Aerosol Solution Droplets to Nucleate, Regenerating the Indicated Dry Crystal Aerosol.

Mean Dry Solute Crystal Radius (microns) Contained in a Droplet	Average Residence Time θ, Minutes	Relative Humidity at Nucleation, %
0.0231	0.25	56.0
0.0240	2.45	58.0
0.0230	3.85	66.0
0.0260	7.44	69.0
0.0261	14.6	70.5
0.0260	20.5	~ 73

In order to evaluate the data in the light of the theory of homogeneous nucleation, a plot was made of the size behavior with relative humidity of a crystal of sodium chloride equivalent in mass to a sphere of 0.025 micron radius. Unfortunately, the measured size of the solution droplets resulting from the dissolution of such a crystal did not agree well with the prediction obtained using the Kelvin equation (C.14) as applied to solution droplets. However, the reasonably good experimental agreement obtained by Orr, et al.,[21] using

an essentially equivalent expression and the fact that the latter expression was indeed a very good approximation to a thermodynamically correct equation (see Section C, Appendix C) lended confidence to the usefulness of the former equation in predicting the solution droplet properties. To substantiate further the advisability of using equation (C.14) rather than an experimental measurement of droplet size to determine its concentration, an estimate of the maximum possible uncertainty was made assuming an error of 10 per cent in the determination of the particulate size. In the case of a solution droplet of 0.040 micron radius formed by dissolution of a sodium chloride crystal equivalent in mass to a sphere of 0.025 micron in radius, the maximum possible uncertainty in determining the mass of the solute crystal and the molarity of the resulting solution droplet is approximately 30 per cent. The errors compound themselves so that the uncertainties in the calculation of the mole fraction and the molality of the solution droplet are 53 and 63 per cent, respectively. These uncertainties have been calculated by the method discussed by Mickley, et al.,[22].

This method, however, overestimates the uncertainty because it fails to account for compensating errors since it considers the simultaneous occurrence of error extremes. It has been found useful, nevertheless, as an estimation of the maximum limits of uncertainty. The probability of this being the true error is indeed small. An analysis of error probability is not feasible due to the nature of the data of this study.

A prediction was made of the resulting droplet concentration in equilibrium with a given relative humidity using the Kelvin equation

[Equation (C.14)]. These results are presented in Figure 8. Also, a relationship was derived by the procedure indicated in Appendix B between $\ln^{-2}(a_1/a_o)$ and supersaturated solution concentration. This is presented in Figure 9. Then, Figure 10 was constructed, which represents the relationship between the experimental data expressed in terms of $\ln \theta$ and the value of the function $\ln^{-2}(a_1/a_o)$ calculated by using the experimental values of relative humidity at nucleation from Table 1 and the estimated value of the function $\ln^{-2}(a_1/a_o)$ obtained from Figures 8 and 9. The results obtained for the experiments carried out at 2.45, 3.85, 7.44, and 14.6 minutes plot very nearly a linear relationship in agreement with equation (2.27). Figure 10 indicates also the upper and lower limits of uncertainty in the determination of the value $\ln^{-2}(a_1/a_o)$ from an average scattering of the experimental relative humidity for nucleation of $\pm$ 0.6 per cent. The maximum possible uncertainty as determined by the experimental procedure itself is also indicated. This analysis was made in the following manner.

The relative humidity of the aerosol was computed as the vapor pressure of water expressed in per cent of the saturation pressure at a constant room temperature of 25°C. The water vapor pressure was obtained from the Smithsonian Meteorological Tables[23] and measurements of the aerosol dew point using the Cambridge Model 990 Thermoelectric Hygrometer. According to the manufacturer's analysis of errors in this instrument[24], the maximum possible instrumental error is from + 0.453 to -0.556°C. The dry bulb temperature of the aerosol (which was identical to the room temperature) was measured by using a mercury-in-

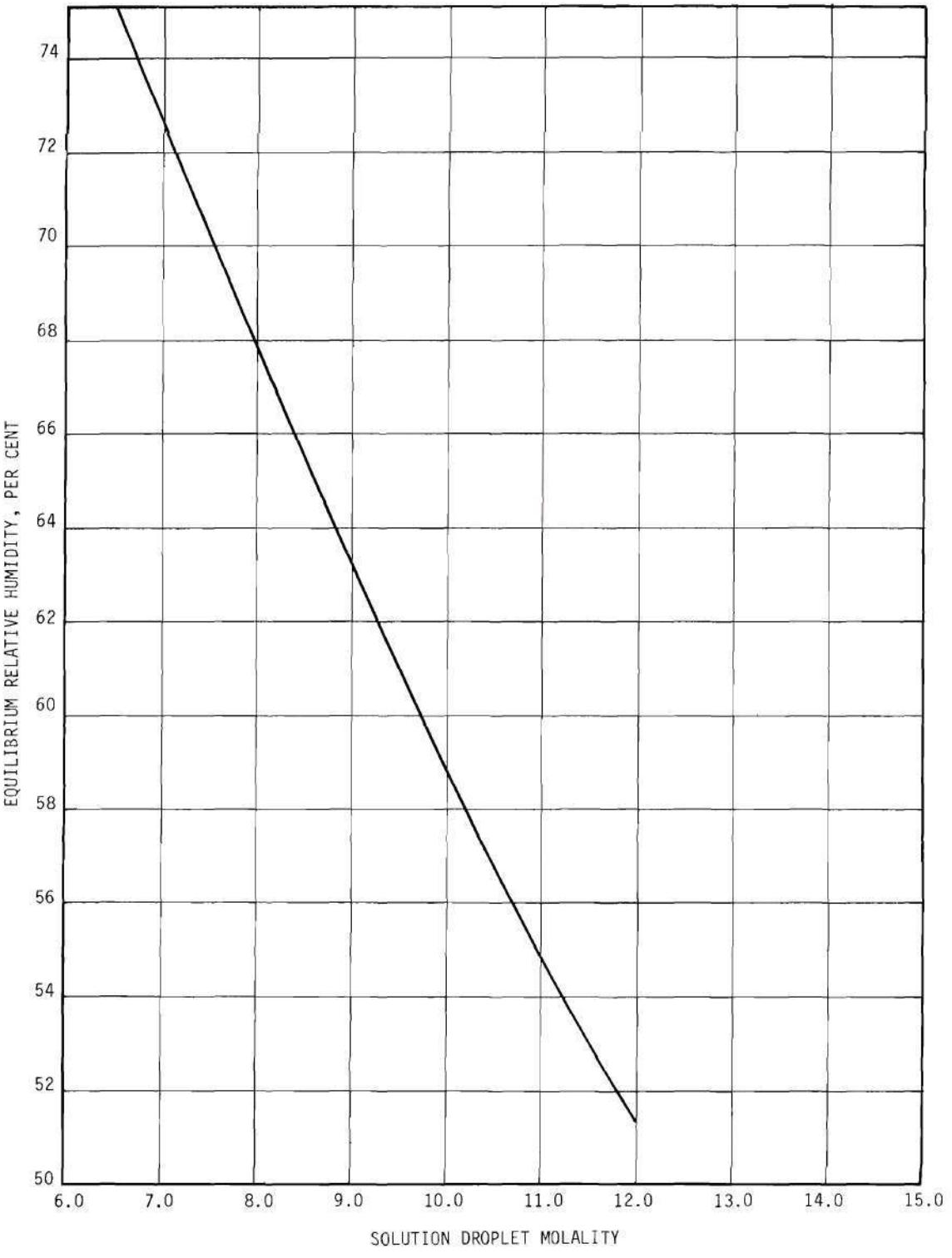

Figure 8. Solution Concentration of a Droplet Formed upon Dissolution of a 0.025 Micron Radius NaCl Crystal in Equilibrium with a Given Relative Humidity.

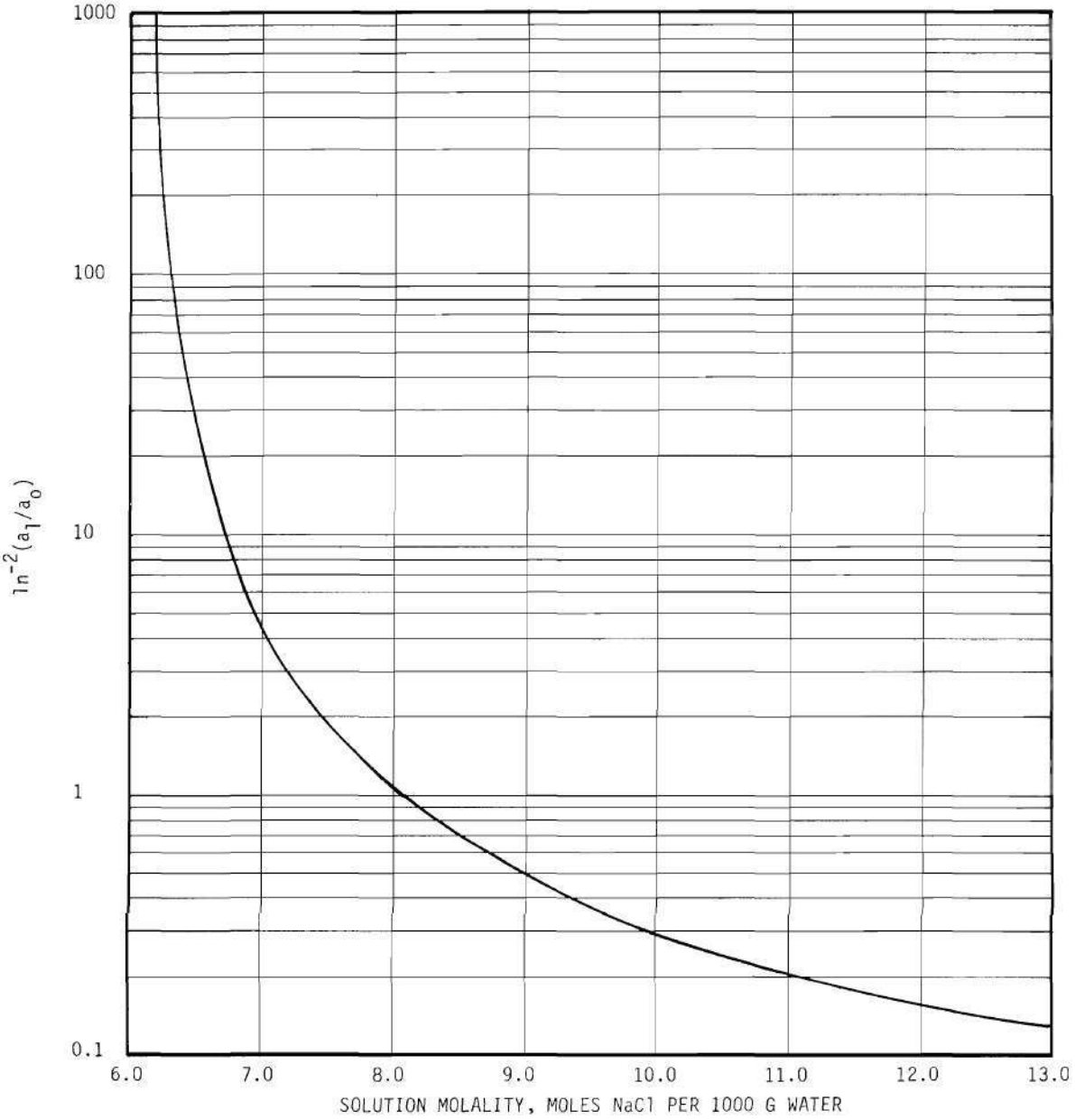

Figure 9. Variation of $\ln^{-2}(a_1/a_o)$ with Concentration for Sodium Chloride Aqueous Solutions at 25°C.

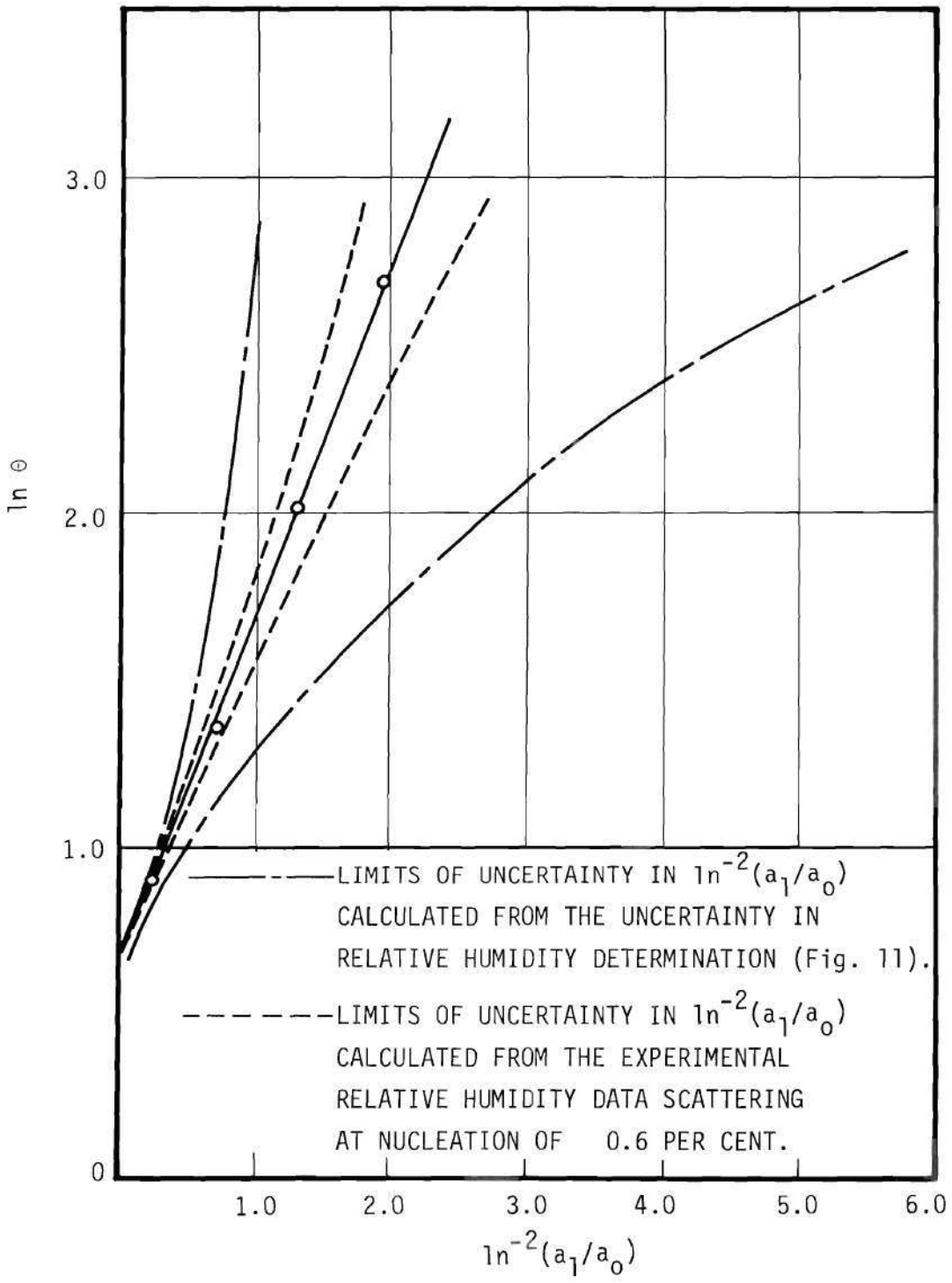

Figure 10. Experimental Data on ln θ versus $\ln^{-2}(a_1/a_o)$ from the Behavior of a 0.025 Micron Radius Sodium Chloride Crystal with Relative Humidity After Various Residence Time Values.

glass thermometer with a maximum error of $\pm$ 0.1°C. In the light of these uncertainties in the primary measurable quantities, an estimation of the maximum possible error in the calculation of the aerosol relative humidity can be obtained by the procedure indicated by Mickley, et al.[22]

The relative humidity of the aerosol was calculated from

$$H = 100. \frac{p}{p_o} \qquad (4.1)$$

where H is the relative humidity, p the vapor pressure in equilibrium with water at the dew point of the aerosol or in equilibrium with ice at the frost point, and p_o the saturation vapor pressure at the temperature of the system.

Figure 11 illustrates the uncertainty in relative humidity values to be very nearly linear with relative humidity in the range from 10 to 90 per cent. In particular, in the range from 56 to 71 per cent where nucleation data were obtained the maximum possible uncertainty is not greater than 2.6 per cent. Values from this plot were used to estimate the upper and lower limits of maximum uncertainty in the calculations of the function $\ln^{-2} (a_1/a_o)$ as shown on Figure 10. It should be recalled, however, that errors estimated by this procedure represent not the most probable but the worst possible situation; the errors compound themselves rather than cancel one another. The seemingly great uncertainty indicated in Figure 10 is also due to the dependence of the function $\ln^{-2} (a_1/a_o)$ on supersaturated solution concentration, i.e., $\ln^{-2} (a_1/a_o)$ approaches infinity very quickly as the supersaturated solution concentration at nucleation decreases, approaching the value at saturation (6.145 molal at 25°C). It is estimated that the uncertainty calculated

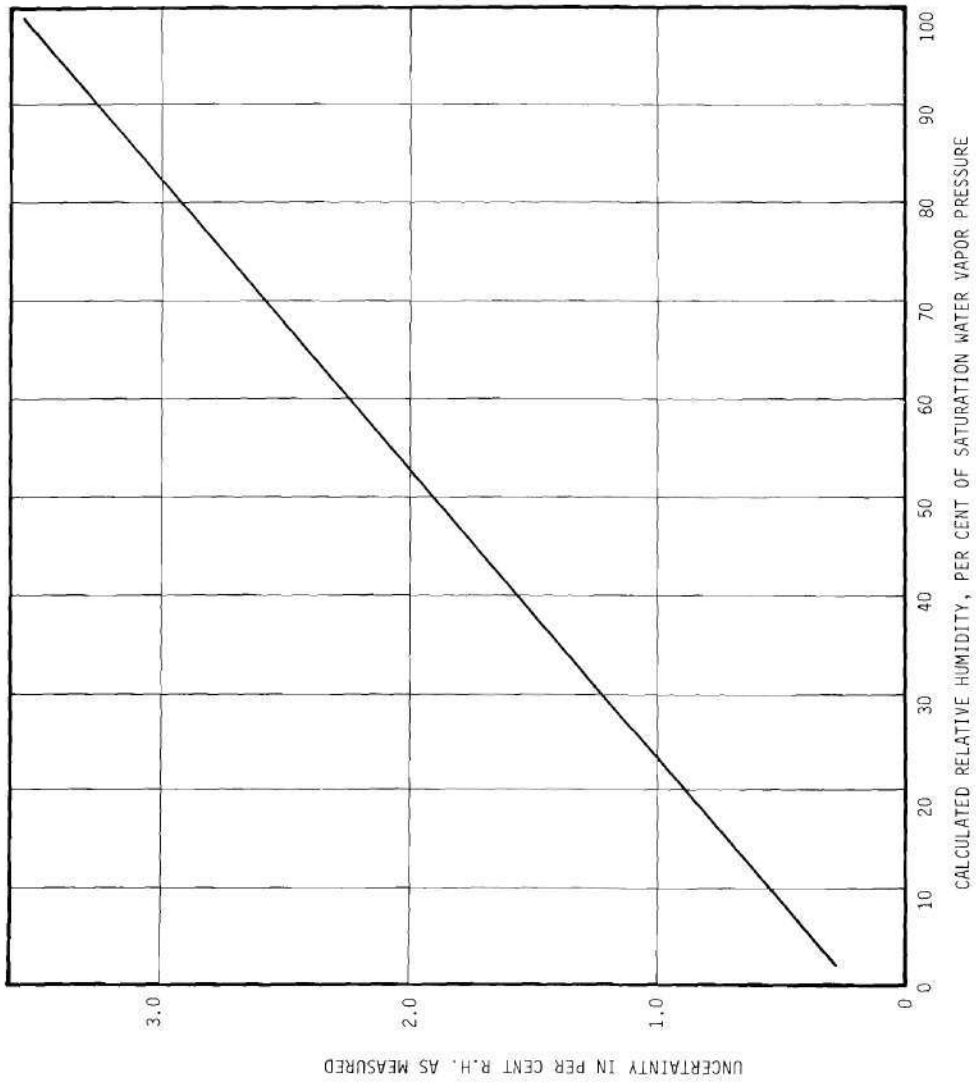

Figure 11. Error in the Measurement of Relative Humidity Using the Cambridge Model 990 Hygrometer.

from the experimental scattering of relative humidity measurements represents the most probable value of uncertainty.

It should be noted that plots of ln θ versus $\ln^{-2} (a_1/a_o)$ were also drawn from data predicted by the Mason, Wright and modified-Wright equations[Equations (C.12), (C.9), and (C.10)]. These plots did not yield a linear relationship. This is interpreted as further confirmation that the Kelvin equation yields by far the best estimation of the concentration and size of solution droplets of a given solute content as a function of the equilibrium relative humidity.

An attempt was made to estimate the distribution of time of nucleation for droplets formed upon dissolution of a sodium chloride crystal equivalent in mass to a spherical particle of 0.025 micron in radius. Figures 12, 13, 14, and 15 illustrate the experimental data obtained on the behavior of such a size particulate with relative humidity. A dashed-line curve represents the predicted size of the resulting solution droplet as calculated from the Kelvin equation. The fact that the data collected from the ion counter do not correlate better with this predicted droplet size was not given much importance, since the main objective of this research was to detect the shift from a solution droplet to a dry crystal. The instrument was quite adequate for detecting this shift. However, the shape of the portion of the experimental curve indicating the shift is interpreted as being an indication of the number distribution of droplets nucleating.

The procedure followed was to read various values of equilibrium relative humidity along this S-shaped curve, starting at the point where

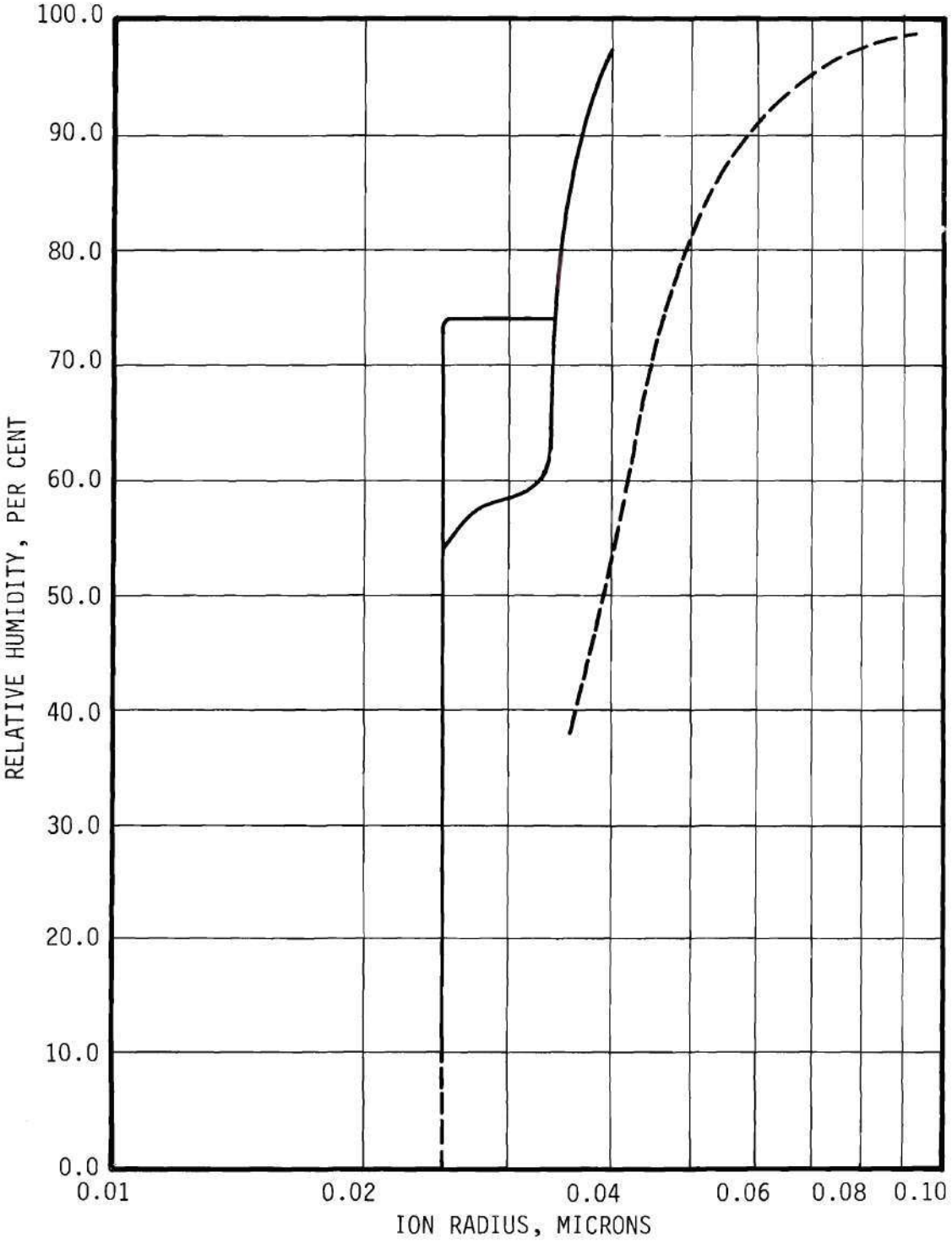

Figure 12. Size Behavior of a 0.025 Micron Radius Sodium Chloride Crystal with Relative Humidity After a Residence Time of 2.45 Minutes and a Comparison with the Predicted Droplet Size Calculated from the Kelvin Equation.

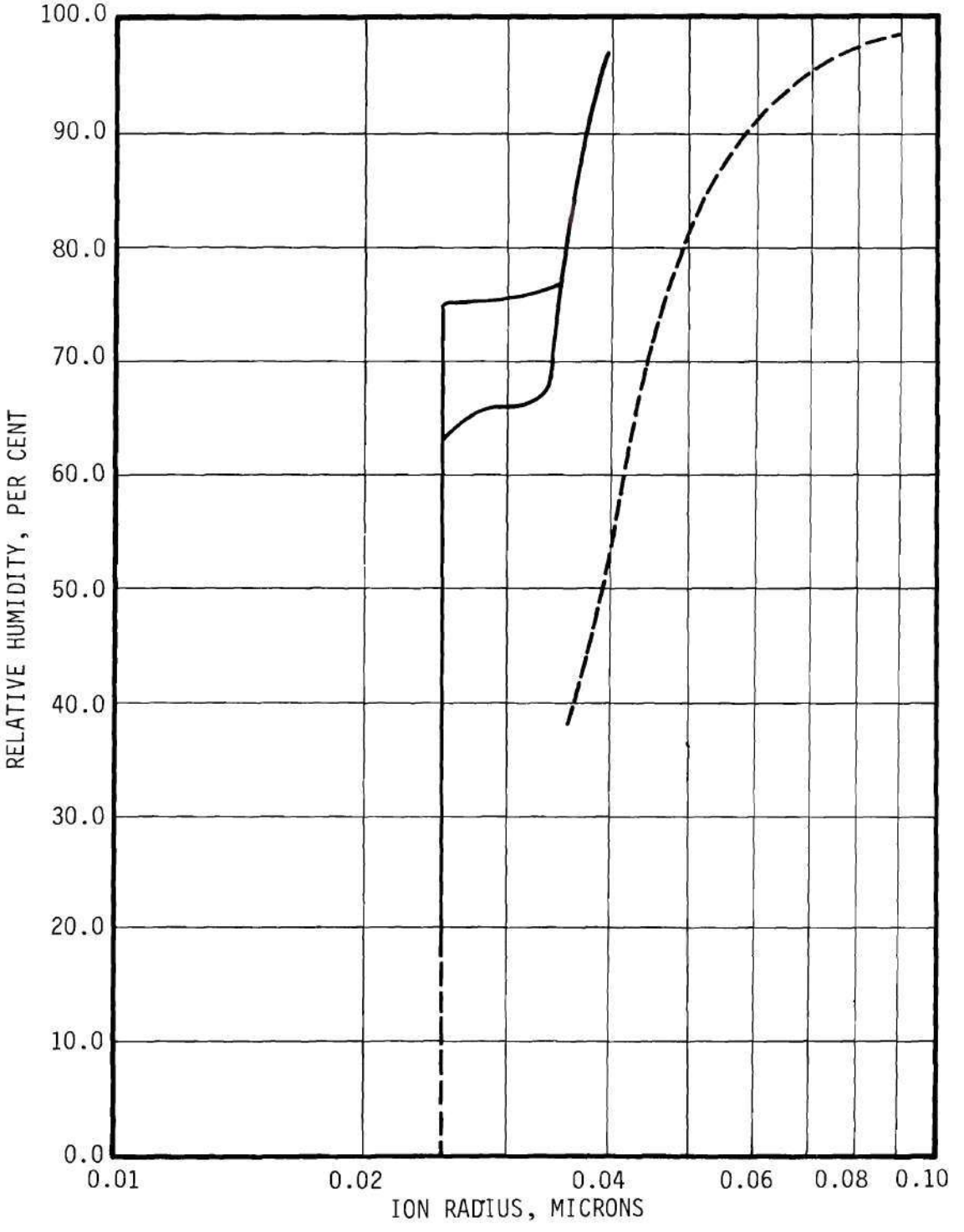

Figure 13. Size Behavior of a 0.025 Micron Radius Sodium Chloride Crystal with Relative Humidity After a Residence Time of 3.85 Minutes and a Comparison with the Predicted Droplet Size Calculated from the Kelvin Equation.

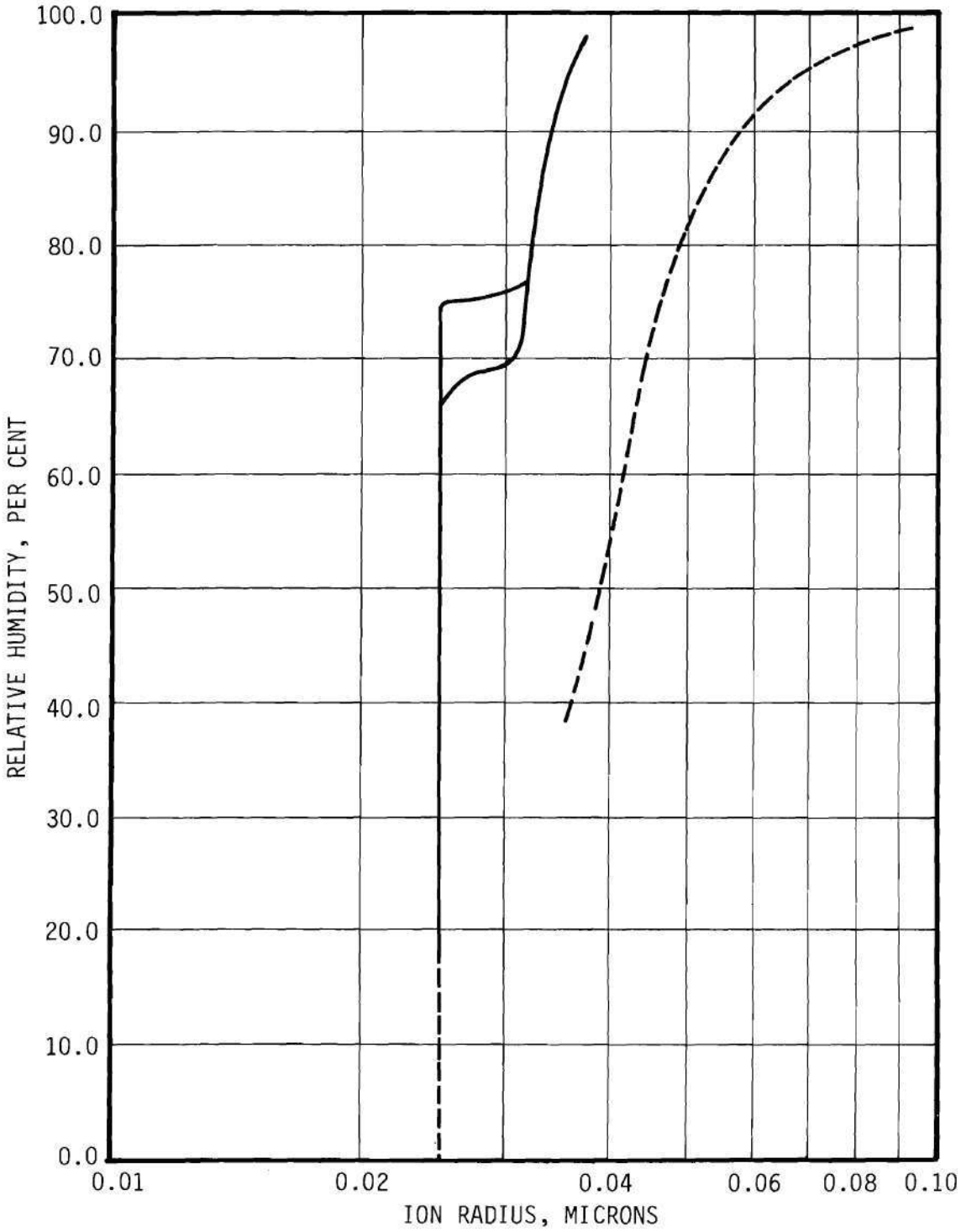

Figure 14. Size Behavior of a 0.025 Micron Radius Sodium Chloride Crystal with Relative Humidity After a Residence Time of 7.44 Minutes and a Comparison with the Predicted Droplet Size Calculated from the Kelvin Equation.

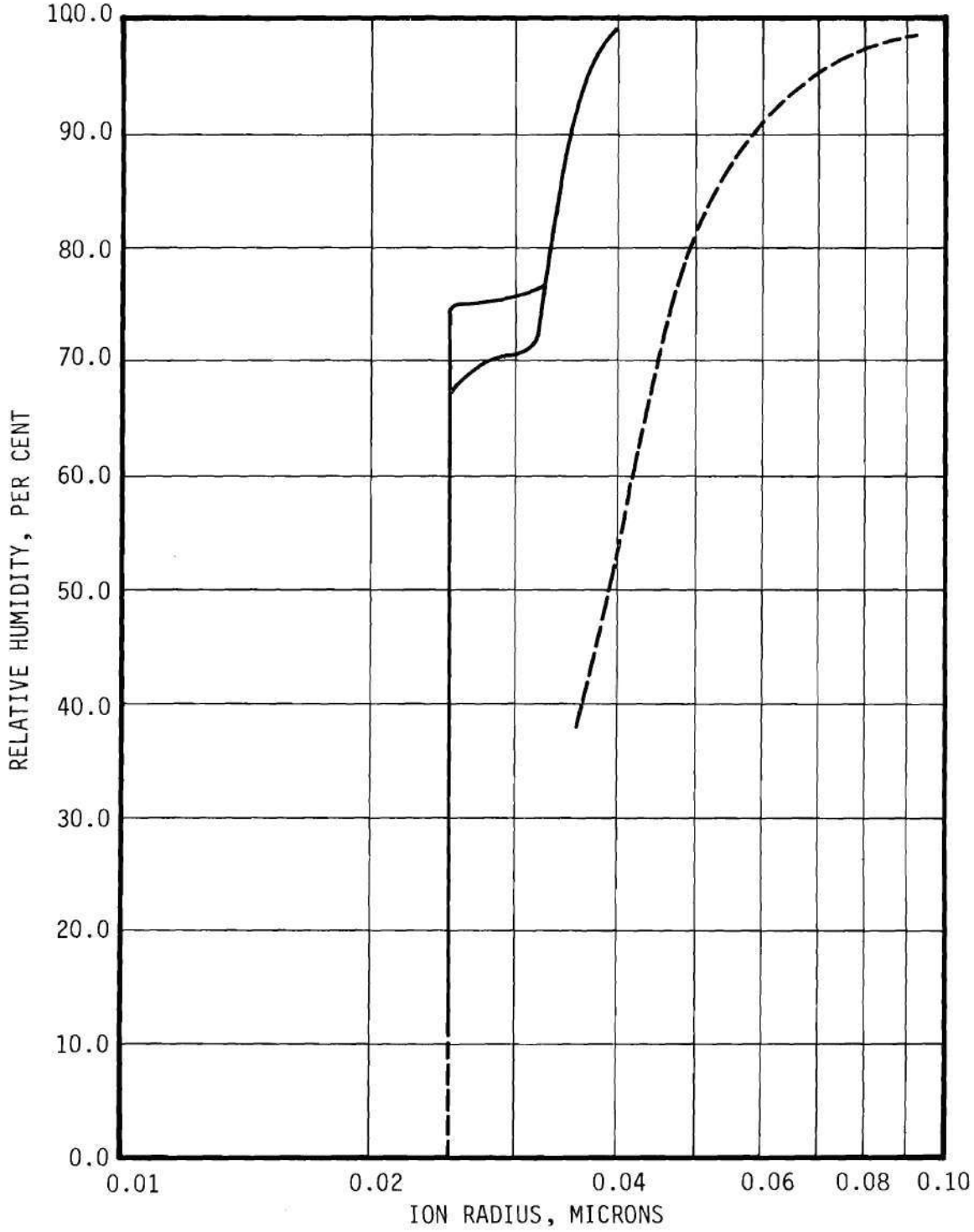

Figure 15. Size Behavior of a 0.025 Micron Radius Sodium Chloride Crystal with Relative Humidity After a Residence Time of 14.6 Minutes and a Comparison with the Predicted Droplet Size Calculated from the Kelvin Equation.

the shift begins and ending at the point where the curve joins the original straight-line for the 0.025 micron radius dry crystal. If it is assumed that at the point where the shift begins no droplets have nucleated and where the shift ends all droplets have nucleated, the concentration of the droplets that are just nucleating at the given humidity may be estimated from Figure 8. Then Figure 9 can be used to obtain the value of the function $\ln^{-2}(a_1/a_o)$ for these droplets just before nucleation begins. Figure 10 may then be used to calculate the nucleation time, θ, at which these droplets are nucleating. An estimation of the nucleation time distribution can be obtained if the assumption is made that a linear relationship remains with the measured particulate sizes during the shift. If G denotes the per cent of droplets that have crystallized

$$G = 100 \frac{R(H) - 0.0250}{R(H_o) - 0.0250} \qquad (4.2)$$

where $R(H_o)$ is the measured radius of the particulates at the relative humidity H_o, when the shift is just beginning, and $R(H)$ is the measured radius of the particulates during the shift that are in equilibrium with a relative humidity, H, such that $0.025 < R(H) < R(H_o)$. Figures 16, 17, 18, and 19 indicate the number distribution of droplets generated by dissolution of a sodium chloride crystal of equivalent spherical radius of 0.025 micron that have nucleated as a function of nucleating time. Table 2 presents the values of the standard deviation, σ_g, calculated at the 84.13 and 15.87 precentiles[25] as well as the ratio of $(\theta_{70} - \theta_{30})/\theta_{50}$, where the subscripts denote the nucleation time at the indicated percentile.

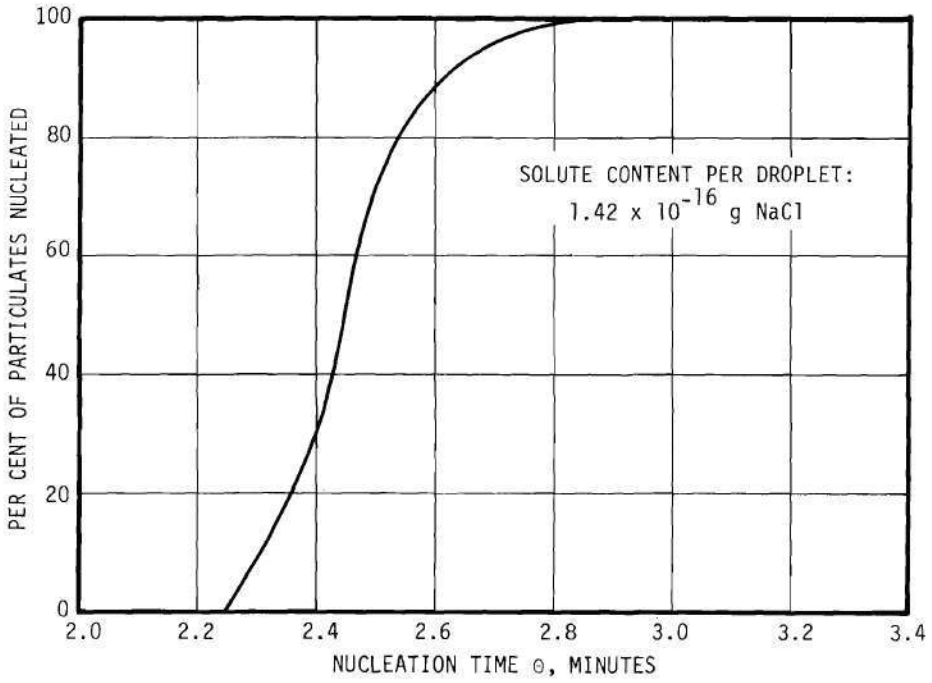

Figure 16. Distribution of NaCl Solution Droplets Which Have Undergone Nucleation at 58.0 Per Cent Relative Humidity.

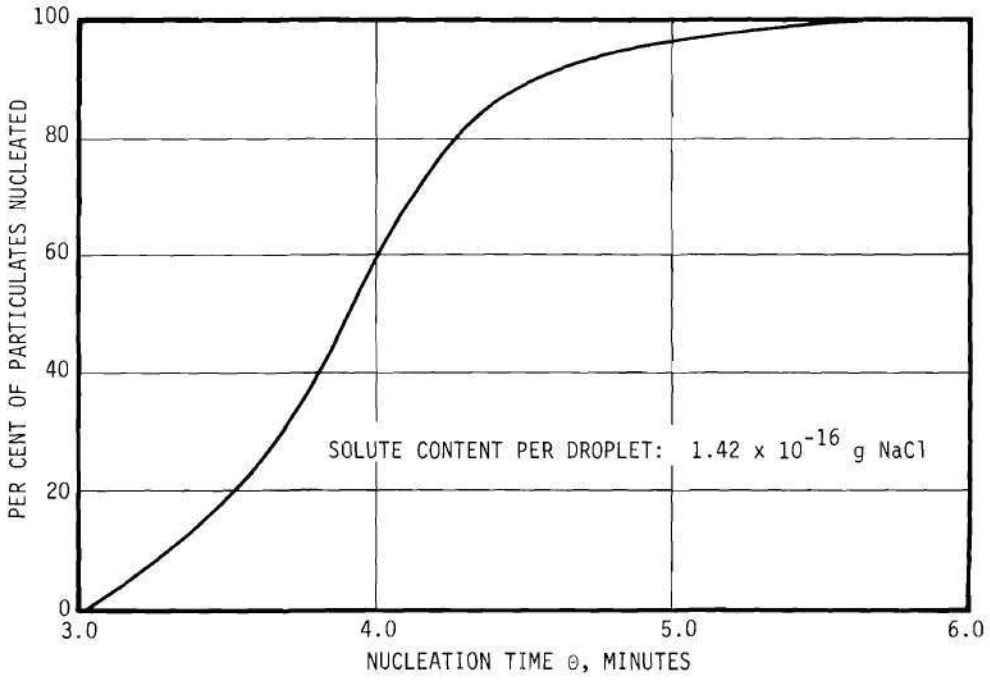

Figure 17. Distribution of NaCl Solution Droplets Which Have Undergone Nucleation at 66.0 Per Cent Relative Humidity.

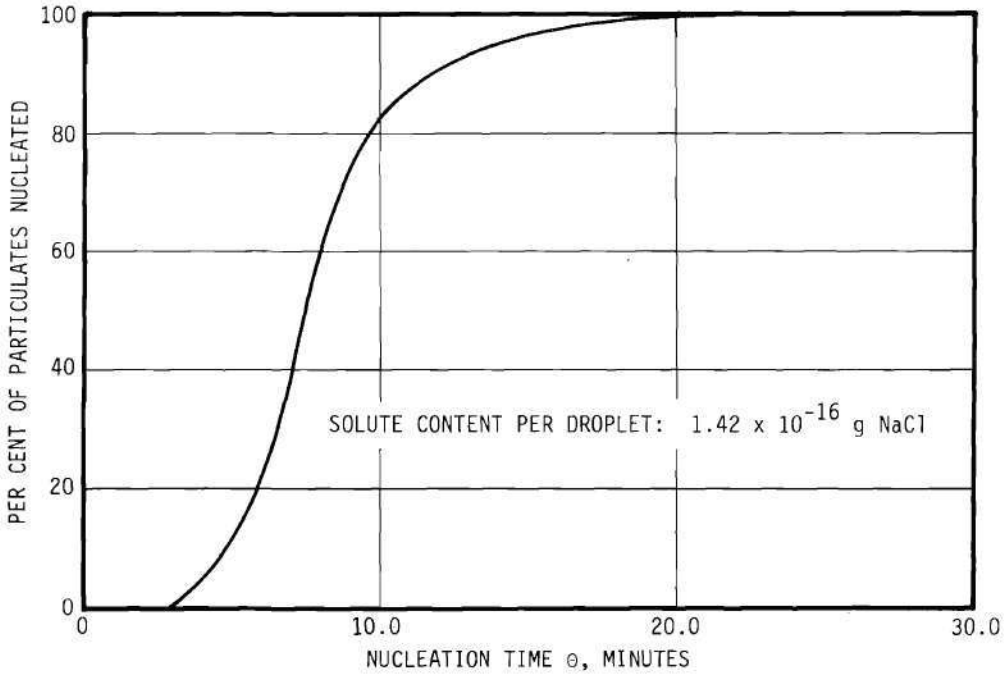

Figure 18. Distribution of NaCl Solution Droplets Which Have Undergone Nucleation at 69.0 Per Cent Relative Humidity.

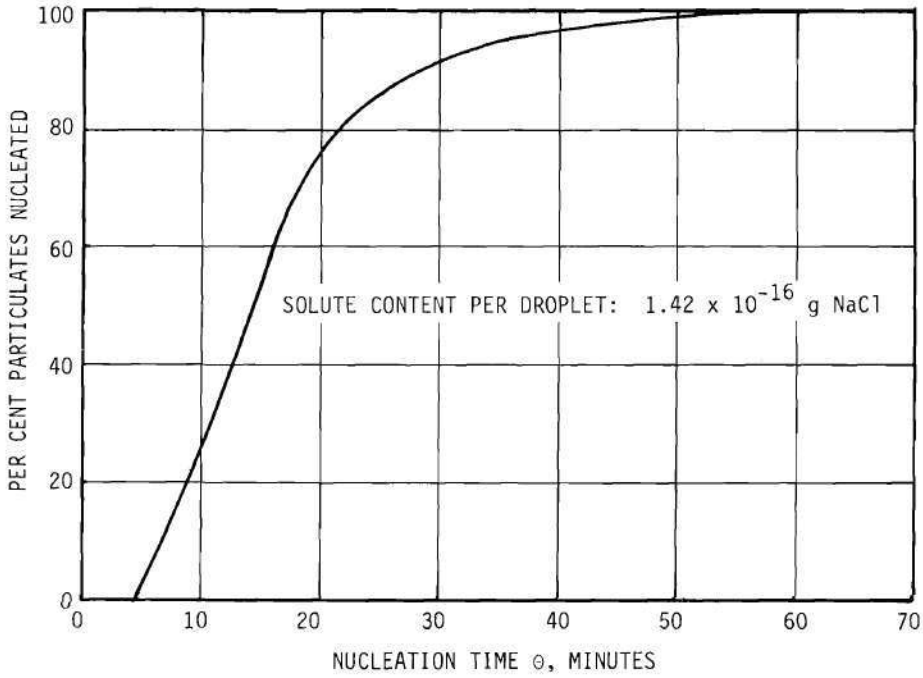

Figure 19. Distribution of NaCl Solution Droplets Which Have Undergone Nucleation at 70.5 Per Cent Relative Humidity.

Table 2. Standard Deviation and Spread of the Nucleation Time Distribution Curves with Average Nucleation Time.

Average θ, minutes	Standard Deviation $\sigma_g=\left(\theta_{84.13}/\theta_{50}\right)$	Standard Deviation $\sigma_g=\left(\theta_{50}/\theta_{15.87}\right)$	Frequency Spread $\left(\theta_{70}-\theta_{30}\right)/\theta_{50}$
2.45	1.05	1.05	0.038
3.85	1.13	1.12	0.11
7.44	1.37	1.36	0.27
14.6	1.62	1.82	0.52

It is to be noted that the standard deviation calculated from both the 84.13 and the 15.87 percentiles are very nearly the same for each distribution, as they should be for a log-normal distribution. Both the standard deviation and the frequency spread, as defined, seem to increase with average nucleation time, θ_{av}. There is really no basis for evaluating these results and the nucleation distributions obtained really should be taken as indicative of the order of magnitude only.

An estimation can be made also of the interfacial tension of a sodium chloride nucleus and the solution in equilibrium with it using Equation (2.25) and the slope of the curve of Figure 10. The possibility of making an estimation of this quantity was suggested by Pound,[26] among other investigators. A value of 12.9 ergs per cm^2 is obtained upon solving for σ in the equation mentioned above. Since σ may change with the supersaturated solution concentration, the value obtained may be taken to be an average for the concentration considered, approximately 9.0 molal. The air-solution interfacial surface energy

at this concentration is estimated from Equation (B.2) to be 86.7 ergs per cm^2. Hence, it is estimated by this method that the surface free energy of a sodium chloride nucleus is approximately 100 ergs per cm^2. This is somewhat lower than the values reported by Corbett[27] in a summary review of the work of various authors, but it is within the acceptable range. Implied in this calculation is the assumption that, σ, the interfacial surface tension between the nucleus and the solution is equivalent to the interfacial surface energy. This assumption can only hold true if the solid nucleus surface is an equilibrium surface. The surface tension, as defined by Gibbs, is the amount of work expended in stretching a surface, whereas the Gibb's surface free energy is the amount of work involved in the formation of an equilibrium surface. In the case of liquids, both terms are numerically equal because of the mobility of the liquid molecules and the subsequent inability of the surface molecules to sustain stress. When solids are concerned it is quite possible that they possess a surface tension that may be different from the equilibrium specific surface Gibbs free energy. This is particularly the case if, during the process of crystallization of a solid from a melt, the melt is subjected to constraints which may impose the formation of a polycrystalline structure. Corbett[27] studied in considerable detail the thermodynamics of formation of equilibrium and non-equilibrium solid surfaces and suggested specifically the use of atomization of very dilute solutions of sodium chloride as an acceptable technique for producing high surface area samples with equilibrium surfaces. In view of this, the assumption of equilibrium surfaces is not unrealistic for the crystallization nuclei of this work

since they are pure microcrystals of solute containing on the order of 100 molecules or less. It might be expected under these conditions that a purely crystalline structure should prevail which would be free of lattice imperfections.

Using the value of 12.9 ergs per cm^2 calculated for the interfacial tension between a sodium chloride nucleus and the solution in equilibrium with it, an estimation was made of the critical nucleus size as a function of concentration using Equation (2.13). This yielded values for a cubic nucleus of about 31 Å on a side at a solution concentration of 6.5 molal decreasing to about 5 Å at 8.5 molal. The latter figure is obviously quite low since it is approximately the size of the sodium chloride molecule. It was interesting to note, however, that, if the supersaturation ratio in terms of mole fractions had been used (which essentially would imply the untenable assumption of ideal solution behavior), the values obtained for the size of a cubic nucleus would be more reasonable and would range from about 50 Å at 6.5 molal to 11 Å at 10.5 molal. This was the procedure employed by Preckshot and Brown[28] in analyzing their data on the nucleation of bulk solutions of potassium chloride. Their estimations of critical nucleus size would also have been unreasonably low if they had not assumed ideal solution behavior (implied in their derivation of the rate equation).

This latter result, presumably, is an indication of some of the weaknesses in the assumption that bulk crystalline solute properties can be attributed to a small cluster of molecules constituting an embryo. Also, the concept of interfacial tension between these small clusters of molecules and the solution is open to question. In light of these

uncertainties the values obtained for σ and r_c may be considered valid to an order of magnitude only.

CHAPTER V

CONCLUSIONS

The most important conclusions derived from this research can be summarized as follows:

(1) An ion counter as applied here affords a satisfactory technique for studying the homogeneous nucleation of solutions.

(2) Hysteresis as encountered in the disappearance of an aerosol of sodium chloride solution droplets is a function clearly dependent on the residence time of the aerosol after achieving equilibrium relative humidity conditions.

(3) The relationship between the time required for supersaturated solution droplets to nucleate and the relative humidity at which nucleation ensues is in agreement with the classical model of the V.W.B.D. theory of homogeneous nucleation as applied to condensed phases.

(4) The interfacial tension between a sodium chloride nucleus of crystallization and the mother liquid phase is estimated to be 12.9 ergs per cm^2 at a solution concentration 9.0 molal.

(5) The surface free energy of a sodium chloride crystal, based upon the previous estimation, is 100 ergs per cm^2, well within the acceptable range of accuracy of values obtained by various other methods.

(6) Estimations of the embryo critical size range from 31 $\mathring{A}$ at a solution concentration 6.5 molal to 5 $\mathring{A}$ at 8.5 molal. These sizes appear to be low, although the values are of the correct order of magnitude.

(7) Droplets of a given size and concentration undergo nucleation in accordance with a log-normal function of time.

(8) Results obtained support the position that hysteresis in the disappearance of natural fogs, especially in the absence of organic atmospheric contamination, is controlled by homogeneous nucleation.

(9) Estimations of the properties of supersaturated solutions of potassium chloride by means of a guided extrapolation of experimental osmotic coefficients give results that agree very well with the available fragmentary vapor pressure data.

CHAPTER VI

RECOMMENDATIONS

Several areas needing further research and development have become apparent as a result of this application of the ion counter to the study of homogeneous nucleation. They are:

(1) An improved ion counter should be designed to give direct and accurate measurements of droplet size distribution. This would permit a calculation of the droplet concentration as a function of relative humidity that then might be compared with the theoretical prediction.

(2) Data should be collected after short residence periods where the distribution of nucleation time is the narrowest and the estimation of the function $\ln^{-2}(a_1/a_o)$ involves the least uncertainty. It is expected that data collected in this manner would permit ascertaining whether or not σ, the interfacial tension, is, as suspected, a function of concentration. If this is the case, the technique might be adequate for determining the surface free energy of various water-soluble salts, the free energy of formation of nuclei, and the free energy of activation for diffusion.

(3) Experiments similar to those described here should be carried out for other atmospheric particles as found by Twomey[29]. The dependence of pertinent phenomenon on temperature should also be considered.

(4) The effect of the presence of small proportions of organic vapors should be studied in order to predict the effect on the behavior of natural fogs.

(5) Basic research should be encouraged in the area of supersaturated solution properties.

(6) Finally, the possibility of extending the range of application of the ion counter should be explored. This would entail the development of a particulate charging device to impose an electrostatic charge as a known function of particulate size. This might extend the present upper limit of application of the instrument into the micron diameter range.

APPENDICES

APPENDIX A

ASSESSMENT OF AEROSOLS BY ION MOBILITY MEASUREMENT

APPENDIX A

ASSESSMENT OF AEROSOLS BY ION MOBILITY MEASUREMENT

A number of techniques for evaluating the size distribution of submicroscopic aerosol particulates in the range of interest of this work, namely 0.01 to 0.1 micron in radius, have been described in the technical literature. The most valuable are those of Hurd and Mullins[14] and Whitby, et al.,[30]. The technique of Hurd and Mullins was employed here because it was specifically applicable to the range of particulate sizes studied.

An ion chamber was used that consisted of two stainless steel, electrically insulated plates upon which a known electrical potential was established (Figure 20). The aerosol was made to flow radially outward between the plates. Since aerosols of electrolytic solutions are found to contain approximately equal numbers of positively and negatively charged particulates, the negatively charged fraction was collected and the resulting ion current on the precipitator plates was measured. Particulates in the range of 0.01 micron in radius have a very low probability of being multiply charged[30], hence their electrical mobility is a direct function of particle size. The mobility distribution function is obtained by analyzing the ion-current versus plate-voltage curve.

The development of the theory of the radial ion counter is largely due to Hurd and Mullins. The presentation here will be theirs with minor modifications.

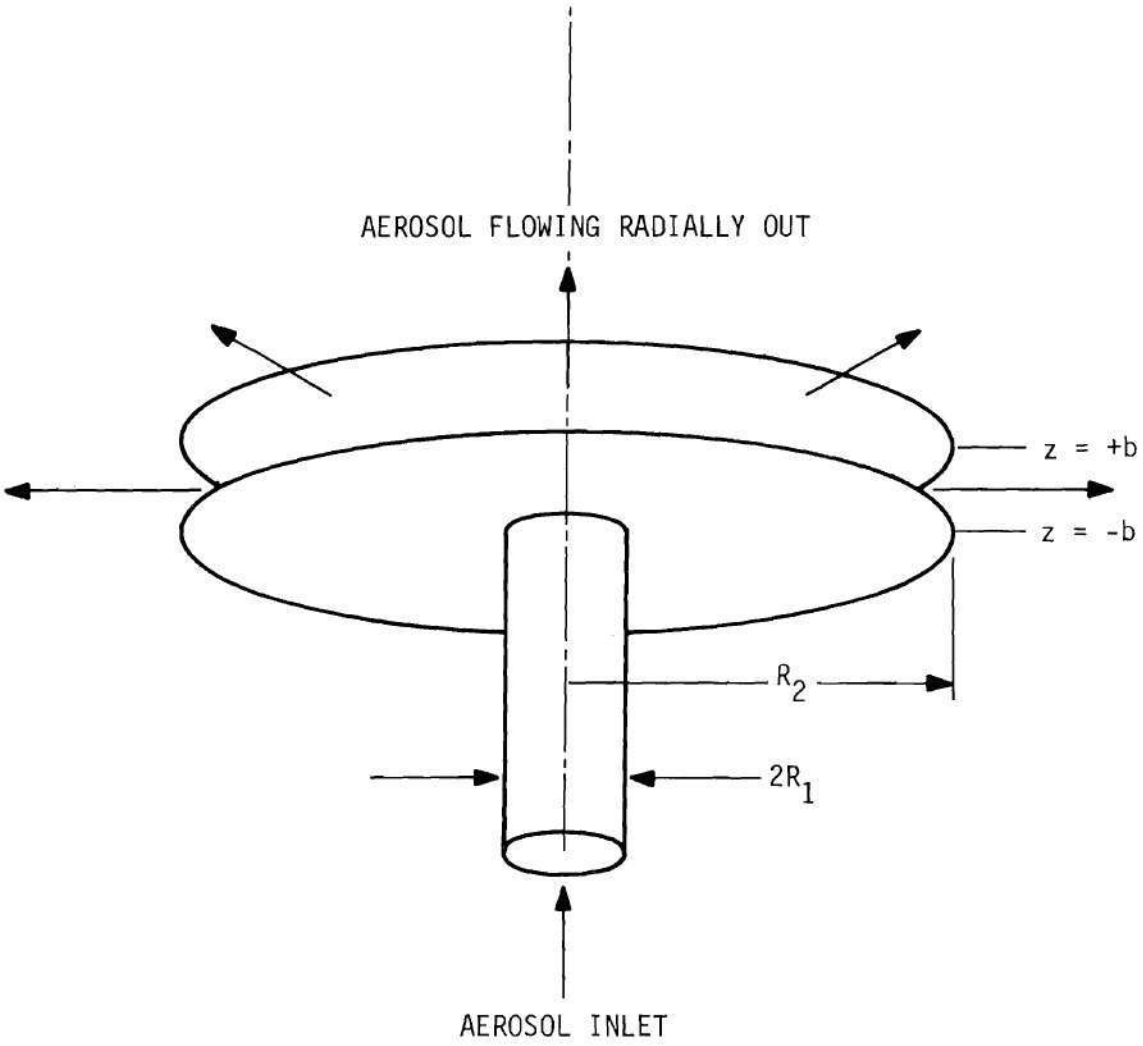

Figure 20. Schematic Diagram of the Ion Counter.

When the flow of the aerosol through the counter is properly adjusted, creeping flow conditions are established between the plates. Under this situation the velocity profile of the air flow in cylindrical coordinates is described by

$$v_r = \frac{b^2 \Delta P}{2R\,\mu\,\ln\,(R_2/R_1)} \left[1 - \left(\frac{z}{b}\right)^2\right] \qquad (A.1)$$

where v_r is the radial velocity of flow; R the distance from the center; 2b the separation between the plates; R_1 and R_2 the inner and outer radii of the plates, respectively; ΔP the pressure drop across the system; μ the viscosity of the air; and z the vertical displacement relative to the origin located midway between the plates.

It can also be established that the flow rate of the aerosol F is given by

$$F = \frac{4\pi\, b^3\, \Delta P}{3\mu\,\ln\,(R_2/R_1)} \qquad (A.2)$$

Combining equations (A.1) and (A.2), the velocity profile is expressed in terms of the aerosol flow rate by

$$v_r = \frac{3F}{8b\,\pi\,R}\left[1 - \left(\frac{z}{b}\right)^2\right] \qquad (A.3)$$

The mobility of a charged particulate in an electric field is defined as the settling velocity per unit field strength. If a cloud of charged particulates (ions) with a single discrete mobility ω_i is considered

$$\omega_i = \frac{v_z}{E} \qquad (A.4)$$

where v_z is the settling velocity in the z- direction and E is the field strength, given by

$$E = \frac{V}{2b} \qquad (A.5)$$

where V is the applied potential difference between the plates.

Combining equations (A.4) and (A.5) gives

$$\omega_i = \frac{2 v_z b}{V} \qquad (A.6)$$

The vertical position of an ion with mobility ω_i entering the chamber at R_1 and z_o is given at time t by

$$z = v_z t + z_o \qquad (A.7)$$

Substituting equation (A.7) into equation (A.3) and integrating with respect to R and t, and assuming v_z independent of t, gives

$$\frac{(R_c^2 - R_1^2)}{2} = \frac{3F}{8b\pi}\left[t_F - \frac{v_z^2}{3b^2} t_F^3 - \frac{z_o v_z}{b^2} t_F^2 - \frac{z_o}{b^2} t_F\right] \qquad (A.8)$$

where R_c is the radial coordinate of the point at which the ion is collected and t_F is the "time of flight" of the ion through the electric field. From equation (A.7), the "time of flight" of a particulate is

$$t_F = \frac{b - z_o}{v_z} \qquad (A.9)$$

and substituting equation (A.9) into equation (A.8) gives

$$\frac{(R_c^2 - R_1^2)}{2} = \frac{F}{8b^3 \pi v_z} \left[z_o^3 + 2b^3 - 3z_o b^2 \right] \qquad (A.10)$$

This latter equation permits calculating the radius R_c at which a particulate that entered the ion counter with coordinates (R_1, z_o) will be collected. Hence, for a particulate collected at the outer radius, i.e. at $R_c = R_2$, the minimum settling velocity for collection is

$$v_z = \frac{F}{4\pi b^3} \left[\frac{z_o^3 + 2b^3 - 3z_o b^2}{R_2^2 - R_1^2} \right] \qquad (A.11)$$

Therefore, combining equations (A.6) and (A.11), the minimum plate voltage required for collecting an ion of mobility ω_i entering the ion counter with coordinates (R_1, z_o) may be calculated from

$$V = \frac{F}{2\pi b^2 \omega_i} \left[\frac{z_o^3 + 2b^3 - 3z_o b^2}{R_2^2 - R_1^2} \right] \qquad (A.12)$$

It is to be noted here that all ions entering the chamber at R_1 with $z > z_o$ will also be collected.

The number of ions entering the chamber at R_1 with $z > z_o$ is given by

$$N = 2\pi R_1 n_i \int_{z_o}^{+b} v_r \, dz \qquad (A.13)$$

where n_i is the concentration of ions of mobility ω_i per unit volume.

Therefore, substituting equation (A.3) into equation (A.13) and integrating, gives

$$N = \frac{F\, n_i}{4\, b^3}\left[2b^3 - 3\, z_o b^2 + z_o^3\right] \tag{A.14}$$

Combining equations (A.12) and (A.14) gives

$$N = \frac{V\, \omega_i n_i\, \pi}{2b}\left[R_2^2 - R_1^2\right] \tag{A.15}$$

This latter relationship indicates that for a discrete mobility, the number of ions collected is a linear function of the applied voltage.

The specific voltage V_o which will collect all particles of mobility ω_o may be obtained from equation (A.12) by setting $z_o = -b$, hence

$$V_o = \frac{2\, b\, F}{\pi\, \omega_o\, (R_2^2 - R_1^2)} \tag{A.16}$$

and combining with equation (A.15), by letting $V_o = V$, gives

$$\frac{N}{F\, n_i} = \frac{\omega_i}{\omega_o} \tag{A.17}$$

where Fn_i represents the total number of ions of mobility ω_i entering the ion counter. Thus, for $\omega_i < \omega_o$, the ratio ω_i/ω_o is the fraction of ions of mobility ω_i which will be collected at a voltage V_o.

Under the assumption that each particulate carries a number of electronic charges n_e which is only a function of particulate radius r, i.e., $n_e = n_e(r)$, an ion current versus voltage curve may be interpreted in terms of mobility and size distribution.

The frequency curve $f(\omega)$ of a continuous ion mobility distribution is defined by

$$\int_0^\infty f(\omega)\, d\omega = 1 \qquad (A.18)$$

The relationship between $f(\omega)$ and the current-voltage curve must be established before mobility can be related to particulate size. At the voltage V_o all ions of mobility $\omega \geq \omega_o$ are collected, producing a current

$$I_1 = I_{max} \int_{\omega_o}^\infty f(\omega)\, d\omega \qquad (A.19)$$

where I_{max} is the ion current obtained when the entire distribution is collected.

For ions of mobility $\omega < \omega_o$, the fraction ω/ω_o of the ions of mobility ω which is collected produces a current given by

$$I_2 = \frac{I_{max}}{\omega_o} \int_0^{\omega_o} \omega\, f(\omega)\, d\omega \qquad (A.20)$$

Hence, the total current I_o obtained at the voltage V_o is defined by

$$I_o = I_{max} \left[\frac{1}{\omega_o} \int_0^{\omega_o} \omega\, f(\omega)\, d\omega + \int_{\omega_o}^{\omega} f(\omega)\, d\omega \right] \qquad (A.21)$$

from which, by differentiating with respect to ω, is obtained

$$\frac{dI_o}{dV_o} = - \frac{I_{max}}{\omega_o^2} \int_0^{\omega_o} \omega \, f(\omega) \, d\omega \qquad (A.22)$$

Differentiating equation (A.16) with respect to V_o, gives

$$\frac{d\omega_o}{dV_o} = - \frac{K \, \omega_o^2}{F} \qquad (A.23)$$

where $K = (R_2^2 - R_1^2)/2b$ is a constant having a value that depends only upon the geometry of the ion counter and, for a given instrument, upon only the separation between the plates.

Combining equations (A.22) and (A.23), gives

$$\frac{dI_o}{dV_o} = \frac{I_{max} K}{F} \int_0^{\omega_o} \omega \, f(\omega) \, d\omega \qquad (A.24)$$

Finally, rearranging equation (A.21) and substituting equation (A.24) gives

$$\int_{\omega_o}^{\infty} f(\omega) \, d\omega = \frac{I_o - V_o (dI_o/dV_o)}{I_{max}} \qquad (A.25)$$

It is to be noticed that the left side of equation (A.25) is the fraction of ions with mobility $\omega > \omega_o$, while the right side is the intercept on the current axis of the tangent to the current versus voltage curve at V_o divided by the maximum current.

In order to relate mobility with size for small particulates, Stoke's Law is applied with a correction for slip. Hence,

$$\omega = \frac{n_e(r)\, k_1}{6\pi\mu r} \qquad (A.26)$$

where k_1 is the Davies' correction for slip[31], applicable to particulates comparable in size to the mean free path of air molecules at room temperature, and given by

$$k_1 = 1 + \frac{\lambda}{r}\left[0.882 + 0.281 \exp\left(-1.57r/\lambda\right)\right] \qquad (A.27)$$

where λ is the mean free path of air molecules at the temperature and pressure of the system.

Substituting equation (A.26) into equation (A.25) permits particulate size distribution information to be obtained directly from the ion current versus plate voltage curve, namely by

$$G(r) = \int_{r_o}^{0} g(r)\, dr = \frac{1}{I_{max}}\left[I_o - V_o \frac{dI_o}{dV_o}\right] \qquad (A.28)$$

Figure 21 illustrates the graphical procedure for evaluating the frequency distribution function G(r).

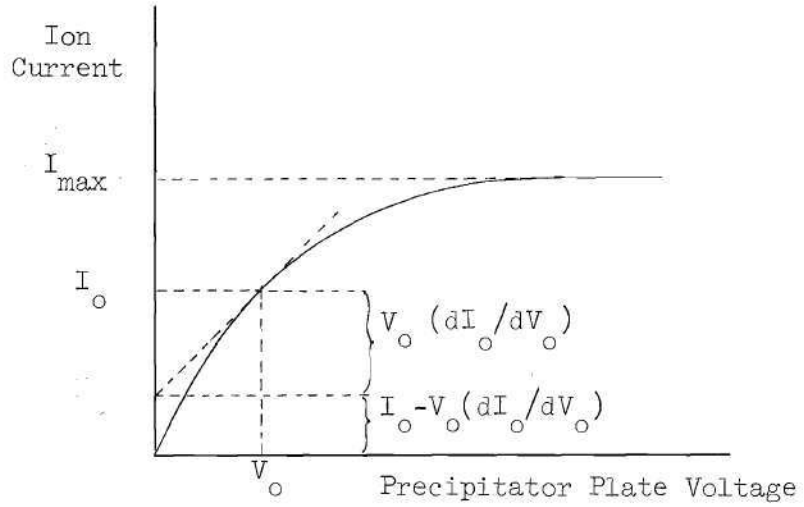

Figure 21. Typical Ion Current-Voltage Curve

Since the charge distribution for particulates having radii from 0.01 to 0.1 micron in radius is expressed simply by $n_e = 1$, combining equations (A.16), (A.26), and (A.27) permits relating the precipitator plate voltage V_o to the maximum size particulate collectible r_o through

$$V_o = \frac{12\mu\, r_o\, b\, F}{(R_2^2 - R_1^2)\left\{1 + \frac{\lambda}{r_o}\left[0.882 + 0.281 \exp\left(-1.57 r_o/\lambda\right)\right]\right\}} \qquad (A.29)$$

Equation (A.29) has been programmed in Algol for the Burroughs 220 Compiler (see Program 5, Appendix F). Figure 22 represents the relationship between V_o and r_o for a precipitator plate separation of 2.0 mm (0.0787 inch) using aerosol flow rate as a parameter.

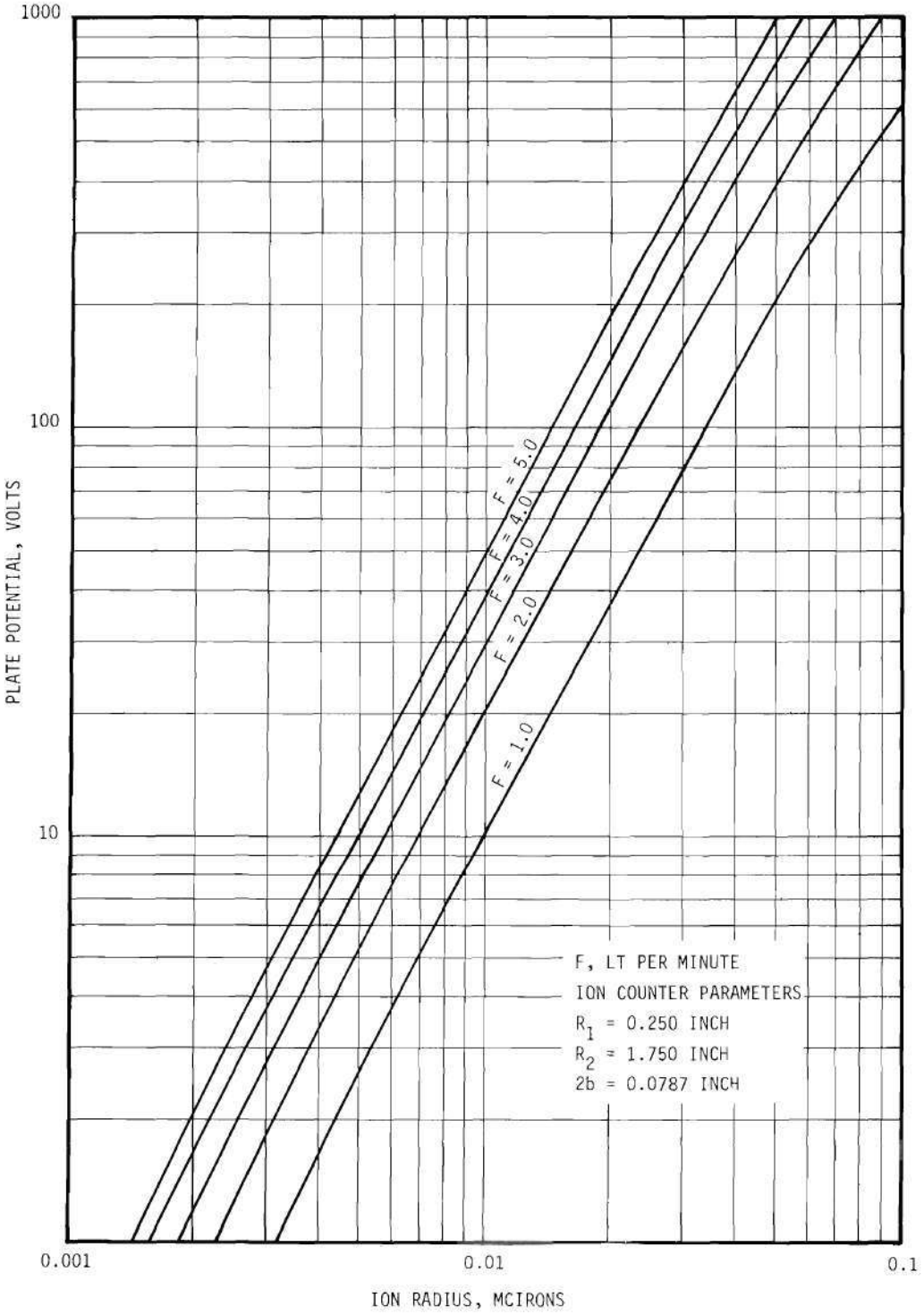

Figure 22. Plate Voltage versus Ion Size with Flow Rate as Parameter for a Plate Separation of 0.0787 Inch.

APPENDIX B

METHODS FOR ESTIMATING THE PROPERTIES OF SUPERSATURATED SOLUTIONS

APPENDIX B

METHODS FOR ESTIMATING THE PROPERTIES OF SUPERSATURATED SOLUTIONS

Generally in studying the behavior of solution droplets just prior to the onset of nucleation, it has been assumed that there is no discontinuity in passing from the unsaturated into the supersaturated region. This assumption is justified on the basis that some data are available for certain electrolyte solutions, especially for potassium chloride and calcium chloride in the supersaturated region. In estimating the properties of supersaturated solutions of sodium chloride, therefore, the approach used has been to extrapolate the properties in the unsaturated region by using the behavior of the various other members of the alkali chloride series as a general guide. In particular, lithium and cesium chloride are used because they are much more soluble than any of the other compounds in the series.

Estimation of Density Data

The density of the alkali chlorides as employed in this study was taken from the International Critical Tables[32]. In the specific case of sodium chloride[33] a third-degree polynomial fits the available experimental data; this gives a very smooth extrapolation into the supersaturated region. In view of this fact, the data for the other alkali chlorides were also fit to a third degree polynomial using a least-squares technique. A computer program (Program No. 1, Appendix F)

was written in Algol for use on the Burrough's 220 Compiler to perform the task.

The polynomial fit obtained is of the form

$$\rho_L = A + Bc + Cc^2 + Dc^3 \qquad (B.1)$$

where ρ_L is the density of the solution at 25°C and c is the solution molarity (moles of solute per 1000 cm^3 of solution). Table 3 gives the values obtained for the constants, A, B, C and D. Figure 23 presents the density data of some of the alkali chlorides as well as the extrapolation (in dashed lines) into the supersaturated region using the third degree polynomial fit. Concentration was expressed in terms of weight per cent. This permits comparison of the extrapolation of the lighter alkali chlorides versus cesium chloride for which experimental data are available up to a concentration of 65 per cent by weight. The fact that a reasonably well related family of curves is obtained using this extrapolation procedure lends confidence to the adequacy of the method.

Estimation of Surface Tension Data

The International Critical Tables[34] presents data on the surface tension increase of sodium chloride solutions relative to that of water (both interfaces in contact with air) at temperatures between 10° and 30°C. The solution-air interface surface tension was calculated using a surface tension value for the water-air interface at 25°C of 71.97 $\pm$ 0.05 dynes/cm[35]. The result is plotted as Figure 24. The data fit a linear equation of the form

Table 3. Constants for Third Degree Polynomial Fit of the Density of Aqueous Solutions of the Alkali Chlorides at 25°C.

Salt	Value of Constant				$\Delta^{(*)}$
	A	B	C	D	
LiCl	0.99758095	0.23532938 (10^{-1})	-0.34358888(10^{-3})	0.13569114 (10^{-4})	0.04
NaCl	0.99710894	0.40791932 (10^{-1})	-0.95848049 (10^{-3})	0.51355065 (10^{-4})	0.002
KCl	0.99713190	0.46861351 (10^{-1})	-0.11857587 (10^{-2})	0.83756631 (10^{-4})	0.005
RbCl	0.99717941	0.87739701 (10^{-1})	-0.92540459 (10^{-3})	0.41109851 (10^{-4})	0.007
CsCl	0.99556700	0.12973410	-0.14425922 (10^{-2})	0.85208636 (10^{-4})	0.08

(*) Δ Represents the maximum deviation in per cent from the experimental data

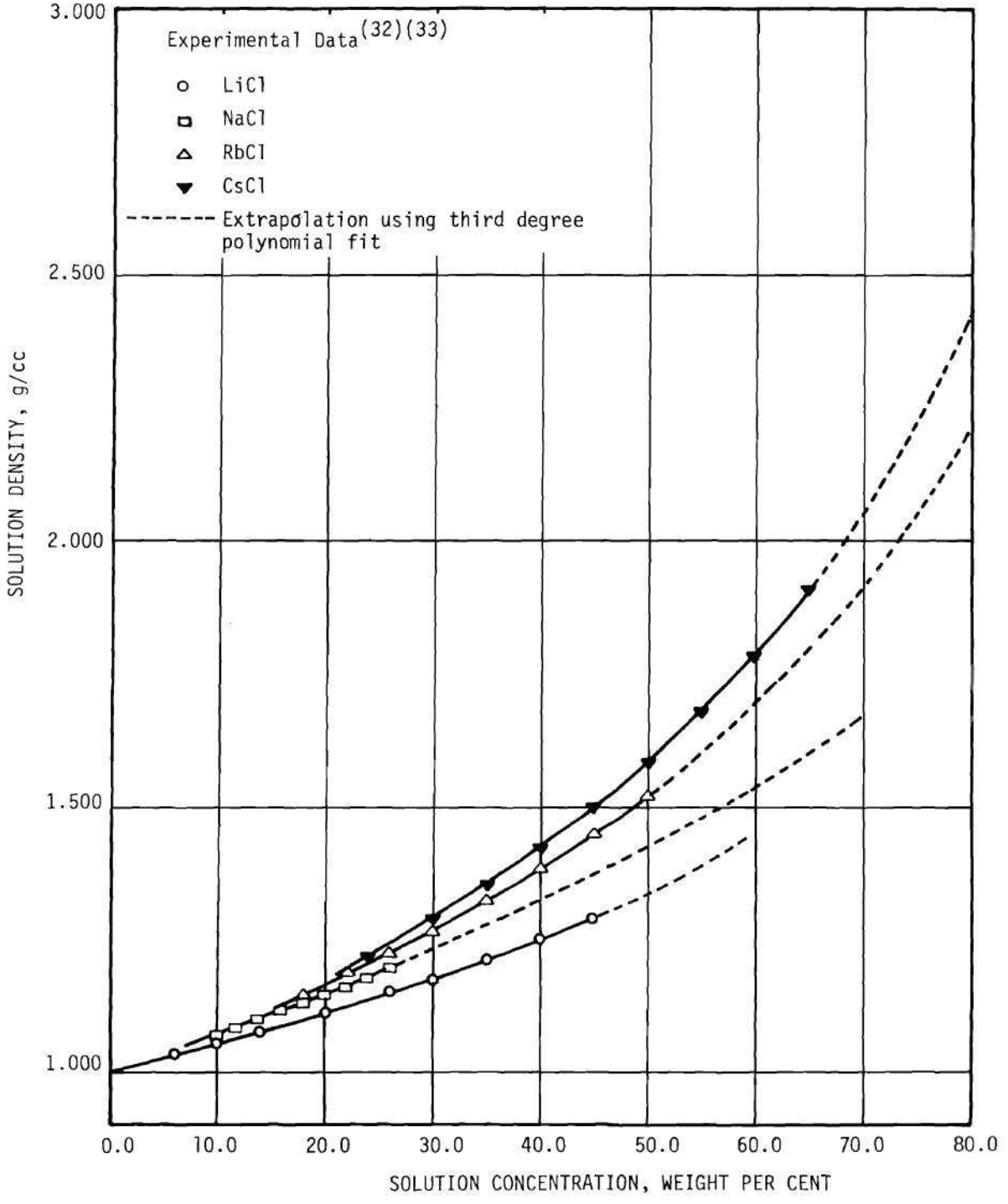

Figure 23. Density of Aqueous Alkali Chloride Solutions at 25°C.

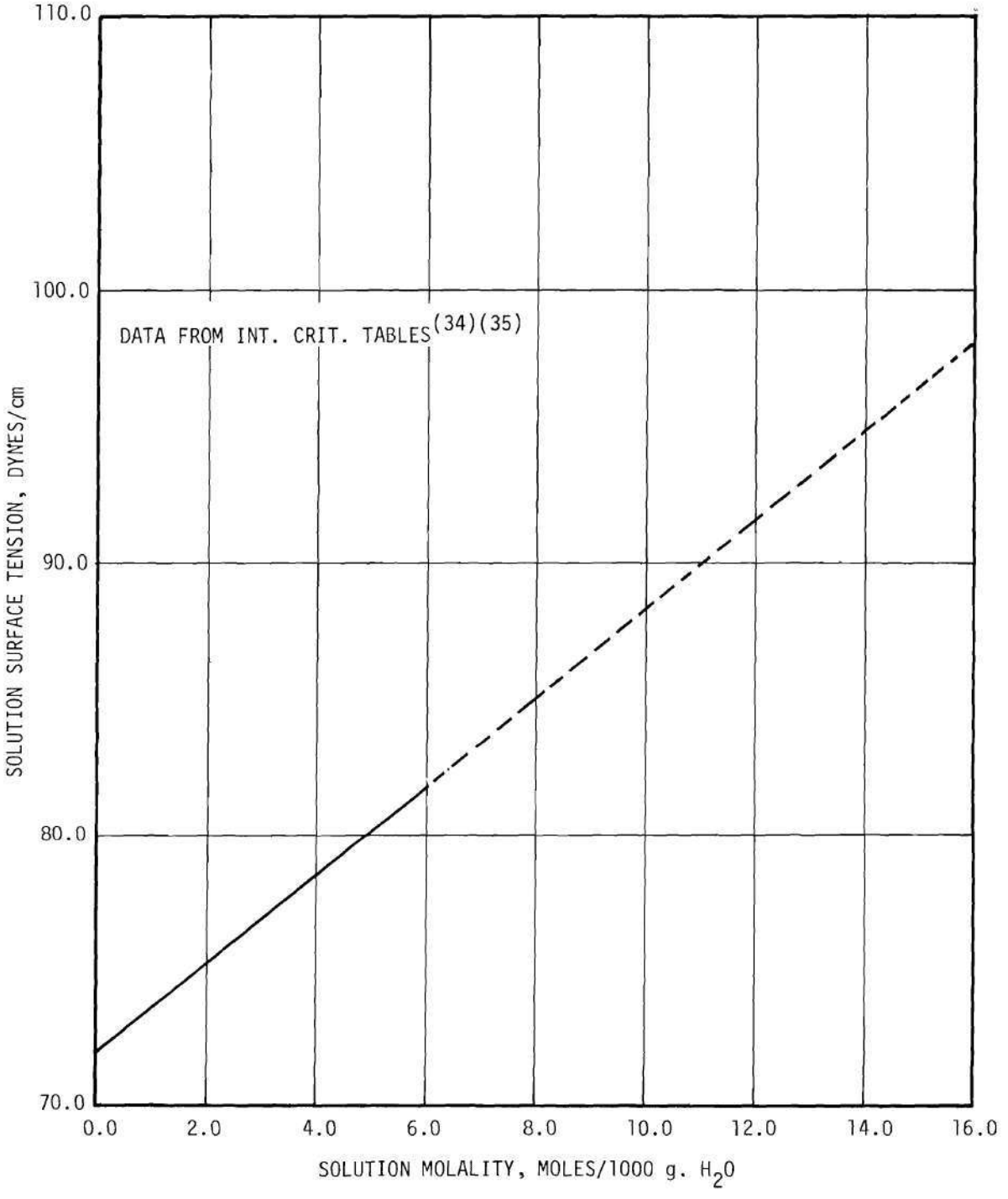

Figure 24. Surface Tension of Sodium Chloride Solutions at 25°C.

$$\sigma = 71.975069 + 1.6329979\ m \qquad (B.2)$$

where σ is the surface tension in ergs/cm^2 and m is the molal concentration (moles of solute per 1000 g of solution.) The deviation between this expression and the data in the region covered by experiment is less than 0.01 per cent. The surface tension of supersaturated solutions was obtained, therefore, by extrapolating Equation (B.2).

Estimation of Activity Coefficients, Activities, van't Hoff Factors and Solution Vapor Pressures

A method was sought here that would involve, at least, a semi-empirically justifiable extrapolation procedure rather than use a rough extrapolation of experimental data on solute activity coefficients as has been done in previous work[12]. The initial approach was to use the semi-empirical equation given by Harned and Owen[36]. This equation represents an extension of the Debye-Hückel "limiting law" for activity coefficients. The equation is

$$\log f_{\pm} = - \frac{S_f \sqrt{\Gamma}}{1 + 35.57\ A\ (DT)^{-1/2} \sqrt{\Gamma}} + Bc + D'\ c^2 \qquad (B.3)$$

where $f_{\pm}$ is the mean rational activity coefficient and A, B, and D' are parameters that are constant for a given electrolyte. Values for the alkali chlorides are presented in Table 4. The quantity S_f represents the limiting slope of the Debye-Hückel theoretical equation for the activity coefficients of electrolytes as derived from considerations of interionic attraction. In the case of the alkali chlorides, the number of ions per molecule is 2 and S_f is then given by

Table 4. Parameters of Equation (B.3)

Compound	Max. Dev. to 4 molal	Constants		
		A	B	D'
LiCl	0.002	4.25	0.111	0.0070
NaCl	0.001	4.2	0.0410	0.0053
KCL	0.001	3.85	0.0187	0.0034
RbCl	0.003	3.2	0.0235	0.0023
CsCl	0.006	2.5	0.0229	0.0024

$$S_f = 1.290 \times 10^6 \, |Z_1 \, Z_2| \, (DT)^{-3/2} \qquad (B.4)$$

where Z_1 and Z_2 represent the valence of the ions, D the dielectric constant of the solvent and T the absolute temperature. In the case of interest $Z_1 = Z_2 = 1$, and for water at 25°C, DT = 23417[37]. The symbol Γ represents the "ional" concentration and is defined by

$$\Gamma = \sum_i^{\nu} c_i \, Z_i^2 \qquad (B.5)$$

where c_i is the molar concentration of the solution (moles of ion i per 1000 cc of solution) and ν the total number of ions produced per molecule.

The mean molal activity coefficient of the electrolyte $\gamma_{\pm}$ (generally designated in the literature simply as the molal activity coefficient) referred to a standard state of the solute at infinite dilution, may be obtained from equation (B.3) using the relationship[38]

$$\gamma_{\pm} = \frac{1000 \, f_{\pm} \, N_{\pm}}{m_{\pm} \, M_1} \qquad (B.6)$$

where $N_{\pm}$ is the mean ionic mole fraction defined by[38]

$$N_{\pm} = \frac{m_{\pm}}{\nu m + 1000/M_1} = \frac{c_{\pm}}{\nu c + (1000\rho_L - cM_2)/M_1} \qquad (B.7)$$

where $m_{\pm}$ is the mean ionic molality, $c_{\pm}$ the mean ionic molarity and M_1 and M_2 the molecular weight of the solvent and the solute, respectively. In the case of the alkali chlorides $m_{\pm} = m$ and $c_{\pm} = c$. The symbol ρ_L stands for the density of the solution.

The activity of the solute may then be computed from

$$a_2 = (\gamma_{\pm}\, m)^{\nu} \qquad (B.8)$$

Using a form of the Gibbs-Duhem equation applicable for conditions of constant temperature and pressure, the activity of water may be calculated in terms of the activity of the solute. The equation is

$$N_1\, d(\ln a_1) + N_2\, d(\ln a_2) = 0 \qquad (B.9)$$

where N represents the mole fraction and $\underline{a}$ the activity while the subscripts 1 and 2 refer, as before, to the solvent (water) and the solute, respectively.

Integration of equation (B.9) gives

$$\ln \frac{a_1}{(a_1)_o} = - \int_{(a_2)_o}^{a_2} \frac{N_2}{(1-N_2)\, a_2}\, da_2 \qquad (B.10)$$

where $(a_1)_o$ is the activity of water when the activity of the solute is $(a_2)_o$.

It may be established from thermodynamic considerations that the activity of the solvent is related to the partial pressure p and the vapor pressure of the solvent p_o [39] by

$$\ln a_1 = \ln \left(\frac{p}{p_o}\right) - \int_{p_o}^{p} \frac{\alpha}{RT}\, dp \qquad (B.11)$$

where α is the coefficient of compressibility of the solution. However, the term containing α is usually neglected as being smaller than the

experimental error in vapor pressure measurements. Therefore, an acceptable approximation of equation (B.11) is

$$a_1 = \frac{p}{p_o} \tag{B.12}$$

where p_o has a value of 23.7560 mm of mercury in the case of water at 25.0°C.

The osmotic coefficient ϕ of the solution was calculated using the relation[40]

$$a_1 = \exp -\left(\frac{\phi \nu m M_1}{1000}\right) \tag{B.13}$$

It was found necessary to obtain data on the van't Hoff factor, since most predictions of the size behavior of solution droplets with relative humidity involve it. In the case of electrolytes, Raoult's law may be extended to concentrated solutions if the van't Hoff factor is introduced. This takes into account the dissociation of the electrolyte in solution. In this modified form Raoult's law is described by the relation

$$\frac{p - p_o}{p_o} = - \frac{i M'}{i M' + M} \tag{B.14}$$

where i is the van't Hoff factor, M' the moles of solute and M the moles of water in the solution.

The factor i varies both with the chemical nature of the electrolyte and with the concentration of the solution. For an infinitely dilute solution, i is equal to the number of ions dissociated from one molecule of the solute, i.e., i = 2 for 1:1 electrolytes, i = 3 for 1:2

electrolytes, etc.

As the concentration increases, the van't Hoff factor first decreases and then, for moderate concentrations, may equal the value at infinite dilution. At high concentrations it may exceed that value considerably. The effect is especially marked in the case of strongly polar electrolytes or in the case of those that form hydrates. This is interpreted as being due to a clustering of the highly polar water molecules around the ions in solution tying up a large proportion of the water molecules. This causes the solution to behave as if there were an apparent ionic concentration larger than the actual value. This explains the sharp decrease in the partial pressure of electrolyte solutions with concentration.

McDonald[41] has computed values for the van't Hoff factor for aqueous sodium chloride solutions at concentrations up to 6.0 molal. Values for concentrations less than 0.1 molal were calculated from the vapor pressure data of Dieterici and Smits[42]. Values at higher concentrations were calculated from the vapor pressure data given in the International Critical Tables[43]. McDonald's results are presented in Table 5.

Equation (B.14) may be rewritten in a more useful form in terms of the water activity a_1 and the mole fraction of the solute N_2. The equation is

$$i = \left[(1/a_1) - 1\right]\left[(1/N_2) - 1\right] \qquad (B.15)$$

A program was written for calculating the mean molal activity coefficient, the solute activity, the solution partial pressure, the

Table 5. Values of the van't Hoff Factor for Sodium Chloride Solutions at 25°C.

Molality	van't Hoff Factor
0.0	2.00
0.044	1.96
0.070	1.90
0.098	1.86
0.1	1.83
0.2	1.82
0.4	1.84
0.6	1.85
0.8	1.87
1.0	1.89
2.0	2.04
2.8	2.19
5.0	2.66
6.00	2.91

van't Hoff factor, and the solution osmotic coefficient using the procedure outlined above. This program (Program No. 2 in Appendix F) was written in Algol 58 for use on the Burrough's 220 compiler. The results indicated, however, that the properties of the solutions of the alkali chloride series were in very poor agreement with experimental data at low concentrations, were in moderate to good agreement for a certain region of intermediate concentration, and that the predicted values exceeded the experimental ones at high concentration. The latter behavior was expected from the limits of applicability indicated in Table 4.

On the basis of these findings a new approach was taken. Using the data on osmotic coefficients reported by Robinson and Stokes[44], the ratio of the osmotic coefficients of the alkali chlorides relative to those of lithium chloride (for which experimental data are available up to 20.0 molal) was plotted giving the solid line segments on Figure 25. Then, making use of the fact that there are experimental data for cesium chloride (the heaviest in the series) up to 11.0 molal, the curves for sodium, potassium, and rubidium chlorides were extrapolated. This extrapolation is indicated by the dashed-line segments of Figure 25.

Using this guided extrapolation, the experimental data on osmotic coefficient were plot as shown on Figure 26 with the extrapolation indicated also by the dashed-line segments.

Then a new computer program was written (Program No. 3, Appendix F) using values for the alkali chlorides from the data of Robinson and Stokes[44] and the extrapolated data calculated from Figure 25. The activity of water in the solution was computed from Equation (B.13) and

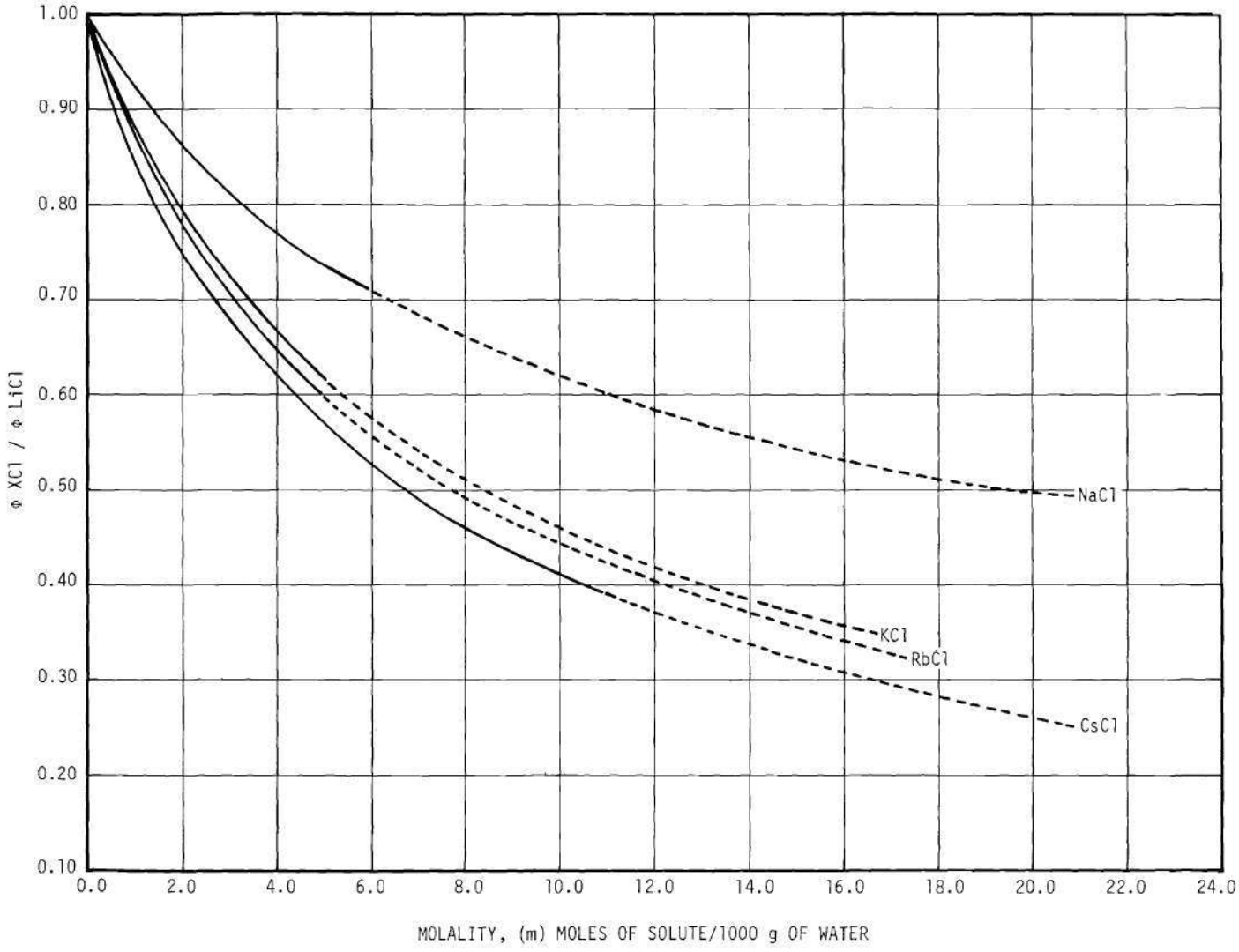

Figure 25. Osmotic Coefficient Ratios of the Alkali Chlorides Relative to Lithium Chloride in Aqueous Solutions at 25°C.

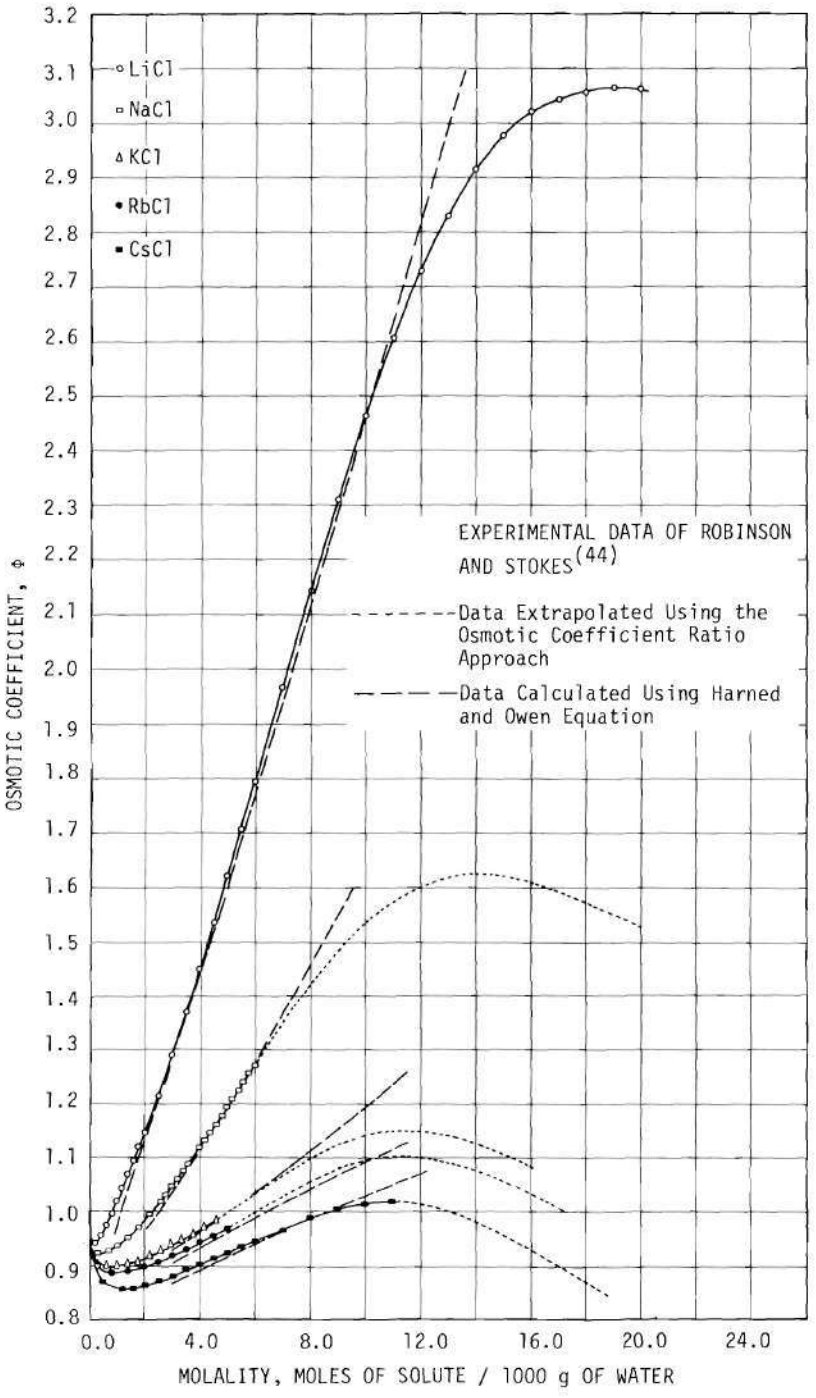

Figure 26. Experimental Osmotic Coefficients for the Alkali Chlorides in Aqueous Solutions at 25°C and Guided Extrapolation Using Osmotic Coefficient Ratios.

the solution vapor pressure from Equation (B.12). The van't Hoff factor was obtained using Equation (B.15).

A numerical integration procedure was employed to calculate the activity coefficient and the activity of the electrolytes using the Gibbs Duhem relation in the form[45]

$$d(\ln \gamma_{\pm}) = -\frac{1}{m} d[m(1-\phi)] \qquad B.16)$$

Rearranging Equation (B.16) and integrating from an initial condition (subscript o) to a final condition, gives

$$\gamma_{\pm} = (\gamma_{\pm})_o \exp\left[\phi - \phi_o - \int_{m_o}^{m} \frac{1-\phi}{m}\, dm\right] \qquad (B.17)$$

whereby the mean molal activity coefficient may be calculated. The value chosen for m_o was 0.1 and the corresponding values for $(\gamma_{\pm})_o$ and ϕ_o were taken from experimental data for each alkali chloride.

The activity a_2 of the solute was calculated using Equation (B.8).

Tables 6 through 10 give the properties of the aqueous solutions of lithium, sodium, potassium, rubidium, and cesium chlorides, respectively, as computed with Program No. 3.

Figure 26 also presents the data on osmotic coefficients computed by the equation of Harned and Owen [Equation (B.3)]. The inability of this equation to predict even the experimental data at high concentrations for LiCl and CsCl is self evident.

Figure 27 presents experimental data for the activity coefficients of the alkali chloride series taken from Robinson and Stokes[44]. The solid line represents the data predicted from the experimental osmotic

TABLE 6.

AQUEOUS LICL SOLUTION PROPERTIES AT 25 DEG C FROM OSMOTIC COEFFICIENT DATA

MOLALITY	WEIGHT PER CENT	MOLE FRACTION	OSMOTIC COEFFICIENT	WATER ACTIVITY	PARTIAL PRESSURE MM HG	VAN'T HOFF FACTOR	SOLUTE MEAN MOLAL ACTIV. COEFFICIENT	SOLUTE ACTIVITY
.20	.840	.00359	.9390	.99325	23.5957	1.8843	.7572	.2293,-01
.40	1.667	.00715	.9540	.98634	23.4315	1.9211	.7399	.8759,-01
.60	2.480	.01069	.9730	.97918	23.2615	1.9666	.7427	.1986, 00
.80	3.280	.01420	.9950	.97172	23.0843	2.0188	.7556	.3654, 00
1.00	4.067	.01769	1.0180	.96398	22.9004	2.0738	.7742	.5995, 00
1.20	4.841	.02116	1.0410	.95598	22.7104	2.1295	.7962	.9130, 00
1.40	5.603	.02460	1.0660	.94764	22.5122	2.1903	.8229	.1327, 01
1.60	6.353	.02801	1.0910	.93903	22.3078	2.2520	.8524	.1860, 01
1.80	7.090	.03141	1.1160	.93017	22.0972	2.3147	.8846	.2535, 01
2.00	7.817	.03477	1.1420	.92099	21.8792	2.3806	.9202	.3387, 01
2.20	8.532	.03812	1.1700	.91142	21.6518	2.4519	.9605	.4465, 01
2.40	9.236	.04144	1.1970	.90166	21.4199	2.5222	1.0027	.5791, 01
3.00	11.284	.05127	1.2860	.87021	20.6729	2.7593	1.1560	.1202, 02
3.50	12.922	.05931	1.3645	.84191	20.0004	2.9778	1.3144	.2116, 02
4.00	14.500	.06721	1.4490	.81152	19.2785	3.2228	1.5098	.3647, 02
4.50	16.022	.07499	1.5315	.78010	18.5322	3.4768	1.7369	.6109, 02
5.00	17.491	.08263	1.6190	.74700	17.7459	3.7596	2.0139	.1013, 03
5.50	18.910	.09015	1.7025	.71362	16.9529	4.0498	2.3312	.1643, 03
6.00	20.280	.09755	1.7910	.67895	16.1292	4.3743	2.7178	.2659, 03
6.50	21.605	.10482	1.8800	.64383	15.2949	4.7239	3.1761	.4262, 03
7.00	22.887	.11198	1.9650	.60919	14.4719	5.0868	3.7024	.6717, 03
7.50	24.127	.11903	2.0520	.57434	13.6440	5.4849	4.3299	.1054, 04
8.00	25.328	.12597	2.1430	.53916	12.8084	5.9302	5.0903	.1658, 04
8.50	26.492	.13279	2.2210	.50650	12.0324	6.3625	5.9120	.2525, 04
9.00	27.620	.13952	2.3100	.47278	11.2315	6.8772	6.9468	.3909, 04
9.50	28.714	.14613	2.3900	.44126	10.4827	7.3981	8.0951	.5914, 04
10.00	29.775	.15265	2.4640	.41154	9.7767	7.9365	9.3787	.8796, 04
10.50	30.805	.15907	2.5390	.38266	9.0905	8.5281	10.8774	.1304, 05
11.00	31.805	.16539	2.6070	.35583	8.4532	9.1347	12.5265	.1898, 05

TABLE 6. (CONTINUED)

AQUEOUS LICL SOLUTION PROPERTIES AT 25 DEG C FROM OSMOTIC COEFFICIENT DATA

MOLALITY	WEIGHT PER CENT	MOLE FRACTION	OSMOTIC COEFFICIENT	WATER ACTIVITY	PARTIAL PRESSURE MM HG	VAN'T HOFF FACTOR	SOLUTE MEAN MOLAL ACTIV. COEFFICIENT	SOLUTE ACTIVITY
11.50	32.777	.17162	2.6700	.33075	7.8575	9.7659	14.3489	.2722, 05
12.00	33.722	.17776	2.7300	.30715	7.2967	10.4337	16.3792	.3863, 05
12.50	34.640	.18380	2.7840	.28538	6.7796	11.1191	18.5734	.5390, 05
13.00	35.533	.18976	2.8300	.26563	6.3105	11.8036	20.8760	.7365, 05
13.50	36.402	.19563	2.8760	.24684	5.8641	12.5446	23.4419	.1001, 06
14.00	37.248	.20142	2.9150	.22981	5.4595	13.2868	26.1136	.1336, 06
14.50	38.072	.20712	2.9500	.21410	5.0863	14.0507	28.9412	.1761, 06
15.00	38.875	.21274	2.9780	.19997	4.7506	14.8037	31.8121	.2277, 06
15.50	39.657	.21829	3.0040	.18679	4.4375	15.5895	34.8527	.2918, 06
16.00	40.419	.22375	3.0220	.17513	4.1604	16.3396	37.8276	.3663, 06
16.50	41.162	.22914	3.0345	.16462	3.9107	17.0705	40.7702	.4525, 06
17.00	41.887	.23446	3.0440	.15496	3.6812	17.8052	43.7435	.5530, 06
17.50	42.594	.23970	3.0510	.14604	3.4694	18.5460	46.7446	.6691, 06
18.00	43.284	.24487	3.0570	.13769	3.2711	19.3109	49.8274	.8044, 06
18.50	43.958	.24997	3.0620	.12988	3.0855	20.0995	52.9842	.9608, 06
19.00	44.616	.25501	3.0660	.12257	2.9119	20.9114	56.2072	.1140, 07
19.50	45.259	.25997	3.0650	.11607	2.7574	21.6768	59.2454	.1334, 07
20.00	45.887	.26487	3.0630	.10999	2.6130	22.4559	62.2993	.1552, 07

TABLE 7.

AQUEOUS NACL SOLUTION PROPERTIES AT 25 DEG C FROM OSMOTIC COEFFICIENT DATA

MOLALITY	WEIGHT PER CENT	MOLE FRACTION	OSMOTIC COEFFICIENT	WATER ACTIVITY	PARTIAL PRESSURE MM HG	VAN,T HOFF FACTOR	SOLUTE MEAN MOLAL ACTIV. COEFFICIENT	SOLUTE ACTIVITY
.20	1.155	.00359	.9245	.99335	23.5982	1.8551	.7347	.2159,-01
.40	2.284	.00715	.9203	.98682	23.4429	1.8528	.6932	.7689,-01
.60	3.388	.01069	.9230	.98024	23.2866	1.8645	.6732	.1631, 00
.80	4.467	.01420	.9288	.97358	23.1284	1.8826	.6628	.2812, 00
1.00	5.522	.01769	.9355	.96685	22.9685	1.9028	.6572	.4319, 00
1.20	6.554	.02116	.9428	.96005	22.8070	1.9245	.6546	.6172, 00
1.40	7.564	.02460	.9513	.95314	22.6429	1.9489	.6548	.8406, 00
1.60	8.552	.02801	.9616	.94607	22.4748	1.9775	.6578	.1107, 01
1.80	9.519	.03141	.9723	.93888	22.3041	2.0072	.6623	.1421, 01
2.00	10.466	.03477	.9833	.93159	22.1308	2.0379	.6680	.1785, 01
2.20	11.393	.03812	.9948	.92417	21.9546	2.0701	.6750	.2205, 01
2.40	12.302	.04144	1.0068	.91661	21.7751	2.1038	.6832	.2689, 01
3.00	14.918	.05127	1.0453	.89315	21.2178	2.2132	.7140	.4589, 01
3.50	16.983	.05931	1.0796	.87271	20.7321	2.3130	.7460	.6818, 01
4.00	18.949	.06721	1.1158	.85144	20.2269	2.4210	.7836	.9826, 01
4.50	20.825	.07499	1.1531	.82947	19.7048	2.5358	.8264	.1382, 02
5.00	22.615	.08263	1.1916	.80680	19.1663	2.6583	.8745	.1912, 02
5.50	24.326	.09015	1.2309	.78353	18.6137	2.7880	.9280	.2605, 02
6.00	25.964	.09755	1.2706	.75980	18.0499	2.9245	.9869	.3506, 02
6.50	27.532	.10482	1.3065	.73639	17.4937	3.0568	1.0468	.4630, 02
7.00	29.035	.11198	1.3440	.71249	16.9259	3.1997	1.1133	.6074, 02
7.50	30.477	.11903	1.3827	.68821	16.3491	3.3529	1.1866	.7921, 02
8.00	31.861	.12597	1.4170	.66467	15.7899	3.5003	1.2601	.1016, 03
8.50	33.191	.13279	1.4505	.64130	15.2348	3.6524	1.3378	.1293, 03
9.00	34.471	.13952	1.4810	.61861	14.6958	3.8022	1.4164	.1625, 03
9.50	35.702	.14613	1.5070	.59699	14.1821	3.9442	1.4930	.2011, 03
10.00	36.888	.15265	1.5300	.57620	13.6883	4.0824	1.5690	.2461, 03
10.50	38.031	.15907	1.5538	.55551	13.1968	4.2297	1.6498	.3000, 03
11.00	39.133	.16539	1.5720	.53629	12.7402	4.3629	1.7247	.3599, 03

TABLE 7. (CONTINUED)

AQUEOUS NACL SOLUTION PROPERTIES AT 25 DEG C FROM OSMOTIC COEFFICIENT DATA

MOLALITY	WEIGHT PER CENT	MOLE FRACTION	OSMOTIC COEFFICIENT	WATER ACTIVITY	PARTIAL PRESSURE MM HG	VAN'T HOFF FACTOR	SOLUTE MEAN MOLAL ACTIV. COEFFICIENT	SOLUTE ACTIVITY
11.50	40.197	.17162	1.5855	.51841	12.3154	4.4837	1.7937	.4255, 03
12.00	41.224	.17776	1.6000	.50066	11.8938	4.6131	1.8664	.5016, 03
12.50	42.217	.18380	1.6084	.48460	11.5122	4.7226	1.9291	.5814, 03
13.00	43.176	.18976	1.6160	.46909	11.1437	4.8323	1.9911	.6700, 03
13.50	44.105	.19563	1.6211	.45450	10.7971	4.9347	2.0485	.7648, 03
14.00	45.003	.20142	1.6222	.44117	10.4805	5.0220	2.0977	.8624, 03
14.50	45.873	.20712	1.6210	.42873	10.1850	5.1005	2.1414	.9641, 03
15.00	46.716	.21274	1.6180	.41707	9.9079	5.1719	2.1803	.1069, 04
15.50	47.533	.21829	1.6121	.40642	9.6550	5.2300	2.2117	.1175, 04
16.00	48.325	.22375	1.6080	.39572	9.4008	5.2973	2.2456	.1291, 04
16.50	49.094	.22914	1.5981	.38669	9.1863	5.3353	2.2652	.1396, 04
17.00	49.840	.23446	1.5900	.37759	8.9700	5.3820	2.2871	.1511, 04
17.50	50.565	.23970	1.5800	.36924	8.7718	5.4180	2.3031	.1624, 04
18.00	51.269	.24487	1.5680	.36169	8.5923	5.4420	2.3127	.1733, 04
18.50	51.953	.24997	1.5577	.35403	8.4105	5.4742	2.3246	.1849, 04
19.00	52.618	.25501	1.5490	.34629	8.2266	5.5146	2.3387	.1974, 04
19.50	53.266	.25997	1.5372	.33957	8.0668	5.5360	2.3441	.2089, 04
20.00	53.895	.26487	1.5260	.33297	7.9100	5.5596	2.3494	.2207, 04

TABLE 8.

AQUEOUS KCL SOLUTION PROPERTIES AT 25 DEG C FROM OSMOTIC COEFFICIENT DATA

MOLALITY	WEIGHT PER CENT	MOLE FRACTION	OSMOTIC COEFFICIENT	WATER ACTIVITY	PARTIAL PRESSURE MM HG	VAN'T HOFF FACTOR	SOLUTE MEAN MOLAL ACTIV. COEFFICIENT	SOLUTE ACTIVITY
.20	1.469	.00359	.9130	.99344	23.6002	1.8320	.7189	.2067,-01
.40	2.896	.00715	.9017	.98708	23.4492	1.8151	.6666	.7111,-01
.60	4.282	.01069	.8976	.98078	23.2994	1.8127	.6374	.1462, 00
.80	5.629	.01420	.8970	.97447	23.1496	1.8173	.6184	.2447, 00
1.00	6.938	.01769	.8974	.96818	23.0001	1.8241	.6046	.3656, 00
1.20	8.212	.02116	.8986	.96189	22.8506	1.8325	.5942	.5084, 00
1.40	9.451	.02460	.9010	.95556	22.7004	1.8435	.5865	.6742, 00
1.60	10.658	.02801	.9042	.94920	22.5493	1.8563	.5808	.8635, 00
1.80	11.832	.03141	.9081	.94280	22.3972	1.8707	.5766	.1077, 01
2.00	12.976	.03477	.9124	.93636	22.2442	1.8861	.5736	.1316, 01
2.20	14.091	.03812	.9168	.92990	22.0907	1.9018	.5715	.1581, 01
2.40	15.178	.04144	.9214	.92341	21.9365	1.9182	.5701	.1872, 01
3.00	18.279	.05127	.9367	.90370	21.4683	1.9715	.5698	.2922, 01
3.50	20.695	.05931	.9504	.88704	21.0726	2.0194	.5726	.4017, 01
4.00	22.972	.06721	.9647	.87019	20.6723	2.0699	.5775	.5337, 01
4.50	25.122	.07499	.9795	.85314	20.2674	2.1231	.5842	.6912, 01
5.00	27.156	.08263	.9950	.83588	19.8573	2.1795	.5925	.8778, 01
5.50	29.082	.09015	1.0110	.81843	19.4428	2.2387	.6022	.1097, 02
6.00	30.908	.09755	1.0270	.80089	19.0259	2.2998	.6130	.1352, 02
6.50	32.643	.10482	1.0445	.78299	18.6008	2.3666	.6256	.1653, 02
7.00	34.293	.11198	1.0610	.76520	18.1782	2.4330	.6385	.1997, 02
7.50	35.864	.11903	1.0785	.74717	17.7499	2.5042	.6529	.2397, 02
8.00	37.362	.12597	1.0955	.72921	17.3232	2.5764	.6678	.2854, 02
8.50	38.791	.13279	1.1095	.71190	16.9120	2.6426	.6814	.3355, 02
9.00	40.157	.13952	1.1210	.69522	16.5156	2.7037	.6939	.3900, 02
9.50	41.462	.14613	1.1315	.67887	16.1273	2.7637	.7060	.4499, 02
10.00	42.713	.15265	1.1390	.66338	15.7593	2.8165	.7163	.5131, 02
10.50	43.910	.15907	1.1433	.64883	15.4138	2.8610	.7244	.5785, 02
11.00	45.059	.16539	1.1455	.63506	15.0867	2.8996	.7308	.6463, 02

TABLE 8. (CONTINUED)

AQUEOUS KCL SOLUTION PROPERTIES AT 25 DEG C FROM OSMOTIC COEFFICIENT DATA

MOLALITY	WEIGHT PER CENT	MOLE FRACTION	OSMOTIC COEFFICIENT	WATER ACTIVITY	PARTIAL PRESSURE MM HG	VAN'T HOFF FACTOR	SOLUTE MEAN MOLAL ACTIV. COEFFICIENT	SOLUTE ACTIVITY
11.50	46.162	.17162	1.1457	.62204	14.7773	2.9326	.7357	.7159, 02
12.00	47.221	.17776	1.1450	.60952	14.4798	2.9632	.7398	.7881, 02
12.50	48.240	.18380	1.1429	.59764	14.1976	2.9895	.7426	.8617, 02
13.00	49.220	.18976	1.1380	.58680	13.9402	3.0064	.7431	.9332, 02
13.50	50.163	.19563	1.1320	.57658	13.6972	3.0193	.7424	.1004, 03
14.00	51.072	.20142	1.1235	.56736	13.4783	3.0232	.7395	.1072, 03
14.50	51.948	.20712	1.1145	.55861	13.2705	3.0246	.7360	.1138, 03
15.00	52.794	.21274	1.1040	.55063	13.0807	3.0198	.7310	.1202, 03
15.50	53.610	.21829	1.0920	.54341	12.9094	3.0088	.7246	.1261, 03
16.00	54.399	.22375	1.0800	.53652	12.7458	2.9967	.7179	.1319, 03

TABLE 9.

AQUEOUS RBCL SOLUTION PROPERTIES AT 25 DEG C FROM OSMOTIC COEFFICIENT DATA

MOLALITY	WEIGHT PER CENT	MOLE FRACTION	OSMOTIC COEFFICIENT	WATER ACTIVITY	PARTIAL PRESSURE MM HG	VAN'T HOFF FACTOR	SOLUTE MEAN MOLAL ACTIV. COEFFICIENT	SOLUTE ACTIVITY
.20	2.361	.00359	.9070	.99348	23.6012	1.8199	.7092	.2012,-01
.40	4.614	.00715	.8930	.98721	23.4522	1.7975	.6525	.6812,-01
.60	6.765	.01069	.8870	.98100	23.3047	1.7911	.6202	.1384, 00
.80	8.821	.01420	.8860	.97478	23.1569	1.7948	.5996	.2301, 00
1.00	10.789	.01769	.8850	.96861	23.0104	1.7985	.5839	.3409, 00
1.20	12.673	.02116	.8860	.96241	22.8631	1.8063	.5724	.4718, 00
1.40	14.479	.02460	.8880	.95619	22.7153	1.8163	.5636	.6227, 00
1.60	16.213	.02801	.8900	.94998	22.5678	1.8264	.5564	.7927, 00
1.80	17.877	.03141	.8930	.94372	22.4191	1.8387	.5510	.9839, 00
2.00	19.476	.03477	.8960	.93747	22.2705	1.8511	.5466	.1195, 01
2.20	21.015	.03812	.9000	.93114	22.1202	1.8657	.5435	.1429, 01
2.40	22.496	.04144	.9030	.92488	21.9715	1.8783	.5404	.1682, 01
3.00	26.622	.05127	.9160	.90572	21.5164	1.9257	.5365	.2591, 01
3.50	29.740	.05931	.9280	.88955	21.1323	1.9689	.5365	.3526, 01
4.00	32.603	.06721	.9410	.87317	20.7430	2.0155	.5388	.4645, 01
4.50	35.242	.07499	.9535	.85675	20.3530	2.0623	.5421	.5953, 01
5.00	37.683	.08263	.9660	.84026	19.9614	2.1103	.5466	.7471, 01
5.50	39.946	.09015	.9800	.82348	19.5626	2.1632	.5529	.9249, 01
6.00	42.050	.09755	.9950	.80645	19.1580	2.2202	.5607	.1131, 02
6.50	44.012	.10482	1.0100	.78934	18.7517	2.2789	.5692	.1369, 02
7.00	45.845	.11198	1.0250	.77218	18.3440	2.3393	.5786	.1640, 02
7.50	47.562	.11903	1.0400	.75499	17.9355	2.4017	.5886	.1949, 02
8.00	49.174	.12597	1.0550	.73777	17.5266	2.4659	.5994	.2299, 02
8.50	50.690	.13279	1.0660	.72145	17.1388	2.5212	.6082	.2673, 02
9.00	52.117	.13952	1.0770	.70521	16.7529	2.5780	.6175	.3088, 02
9.50	53.465	.14613	1.0865	.68941	16.3777	2.6322	.6261	.3538, 02
10.00	54.738	.15265	1.0930	.67446	16.0226	2.6789	.6331	.4009, 02
10.50	55.944	.15907	1.0970	.66031	15.6865	2.7193	.6386	.4497, 02
11.00	57.087	.16539	1.1000	.64662	15.3612	2.7575	.6435	.5011, 02

TABLE 9. (CONTINUED)

AQUEOUS RBCL SOLUTION PROPERTIES AT 25 DEG C FROM OSMOTIC COEFFICIENT DATA

MOLALITY	WEIGHT PER CENT	MOLE FRACTION	OSMOTIC COEFFICIENT	WATER ACTIVITY	PARTIAL PRESSURE MM HG	VAN'T HOFF FACTOR	SOLUTE MEAN MOLAL ACTIV. COEFFICIENT	SOLUTE ACTIVITY
11.50	58.173	.17162	1.0995	.63406	15.0629	2.7855	.6460	.5520, 02
12.00	59.204	.17776	1.0970	.62230	14.7834	2.8073	.6471	.6031, 02
12.50	60.187	.18380	1.0930	.61122	14.5203	2.8243	.6470	.6542, 02
13.00	61.123	.18976	1.0870	.60099	14.2772	2.8346	.6454	.7041, 02
13.50	62.016	.19563	1.0810	.59106	14.0412	2.8446	.6436	.7550, 02
14.00	62.868	.20142	1.0730	.58200	13.8261	2.8474	.6403	.8036, 02
14.50	63.684	.20712	1.0650	.57325	13.6182	2.8496	.6367	.8525, 02
15.00	64.464	.21274	1.0550	.56540	13.4318	2.8442	.6317	.8979, 02
15.50	65.212	.21829	1.0450	.55787	13.2527	2.8380	.6264	.9428, 02
16.00	65.928	.22375	1.0310	.55190	13.1109	2.8166	.6185	.9793, 02
16.50	66.616	.22914	1.0200	.54530	12.9541	2.8050	.6122	.1020, 03
17.00	67.277	.23446	1.0060	.53998	12.8278	2.7815	.6039	.1054, 03

TABLE 10.

AQUEOUS CSCL SOLUTION PROPERTIES AT 25 DEG C FROM OSMOTIC COEFFICIENT DATA

MOLALITY	WEIGHT PER CENT	MOLE FRACTION	OSMOTIC COEFFICIENT	WATER ACTIVITY	PARTIAL PRESSURE MM HG	VAN,T HOFF FACTOR	SOLUTE MEAN MOLAL ACTIV. COEFFICIENT	SOLUTE ACTIVITY
.20	3.257	.00359	.8970	.99355	23.6029	1.7998	.6953	.1933,-01
.40	6.309	.00715	.8750	.98746	23.4582	1.7610	.6288	.6326,-01
.60	9.175	.01069	.8640	.98149	23.3163	1.7442	.5899	.1252, 00
.80	11.870	.01420	.8590	.97554	23.1749	1.7394	.5640	.2036, 00
1.00	14.410	.01769	.8570	.96959	23.0336	1.7407	.5453	.2974, 00
1.20	16.808	.02116	.8560	.96366	22.8928	1.7440	.5307	.4056, 00
1.40	19.075	.02460	.8560	.95773	22.7520	1.7495	.5190	.5281, 00
1.60	21.222	.02801	.8570	.95179	22.6108	1.7570	.5097	.6651, 00
1.80	23.257	.03141	.8590	.94581	22.4686	1.7667	.5022	.8174, 00
2.00	25.191	.03477	.8620	.93977	22.3251	1.7786	.4964	.9858, 00
2.20	27.029	.03812	.8650	.93372	22.1816	1.7906	.4915	.1169, 01
2.40	28.779	.04144	.8690	.92760	22.0362	1.8049	.4878	.1370, 01
3.00	33.559	.05127	.8810	.90916	21.5980	1.8486	.4800	.2074, 01
3.50	37.079	.05931	.8910	.89371	21.2311	1.8859	.4764	.2780, 01
4.00	40.244	.06721	.9010	.87821	20.8629	1.9242	.4746	.3603, 01
4.50	43.106	.07499	.9120	.86253	20.4904	1.9657	.4745	.4560, 01
5.00	45.706	.08263	.9220	.84695	20.1202	2.0059	.4751	.5644, 01
5.50	48.079	.09015	.9320	.83135	19.7496	2.0472	.4766	.6872, 01
6.00	50.254	.09755	.9440	.81539	19.3704	2.0944	.4798	.8287, 01
6.50	52.253	.10482	.9550	.79958	18.9948	2.1404	.4831	.9862, 01
7.00	54.098	.11198	.9650	.78396	18.6237	2.1851	.4865	.1159, 02
7.50	55.806	.11903	.9760	.76816	18.2484	2.2336	.4909	.1355, 02
8.00	57.391	.12597	.9880	.75216	17.8684	2.2861	.4962	.1576, 02
8.50	58.867	.13279	.9960	.73708	17.5102	2.3292	.5000	.1806, 02
9.00	60.243	.13952	1.0040	.72210	17.1543	2.3734	.5040	.2057, 02
9.50	61.531	.14613	1.0090	.70794	16.8180	2.4103	.5067	.2317, 02
10.00	62.738	.15265	1.0130	.69419	16.4912	2.4451	.5090	.2591, 02
10.50	63.871	.15907	1.0160	.68086	16.1746	2.4777	.5109	.2878, 02
11.00	64.937	.16539	1.0180	.66798	15.8687	2.5080	.5123	.3176, 02

TABLE 10. (CONTINUED)

AQUEOUS CSCL SOLUTION PROPERTIES AT 25 DEG C FROM OSMOTIC COEFFICIENT DATA

MOLALITY	WEIGHT PER CENT	MOLE FRACTION	OSMOTIC COEFFICIENT	WATER ACTIVITY	PARTIAL PRESSURE MM HG	VAN'T HOFF FACTOR	SOLUTE MEAN MOLAL ACTIV. COEFFICIENT	SOLUTE ACTIVITY
11.50	65.943	.17162	1.0160	.65639	15.5932	2.5266	.5117	.3463, 02
12.00	66.892	.17776	1.0120	.64560	15.3369	2.5391	.5100	.3745, 02
12.50	67.789	.18380	1.0060	.63565	15.1005	2.5452	.5071	.4019, 02
13.00	68.640	.18976	.9990	.62628	14.8780	2.5477	.5036	.4287, 02
13.50	69.446	.19563	.9900	.61781	14.6767	2.5434	.4990	.4539, 02
14.00	70.213	.20142	.9790	.61026	14.4975	2.5319	.4933	.4770, 02
14.50	70.941	.20712	.9675	.60321	14.3299	2.5180	.4872	.4991, 02
15.00	71.635	.21274	.9550	.59680	14.1777	2.4999	.4805	.5196, 02
15.50	72.297	.21829	.9415	.59106	14.0414	2.4775	.4733	.5382, 02

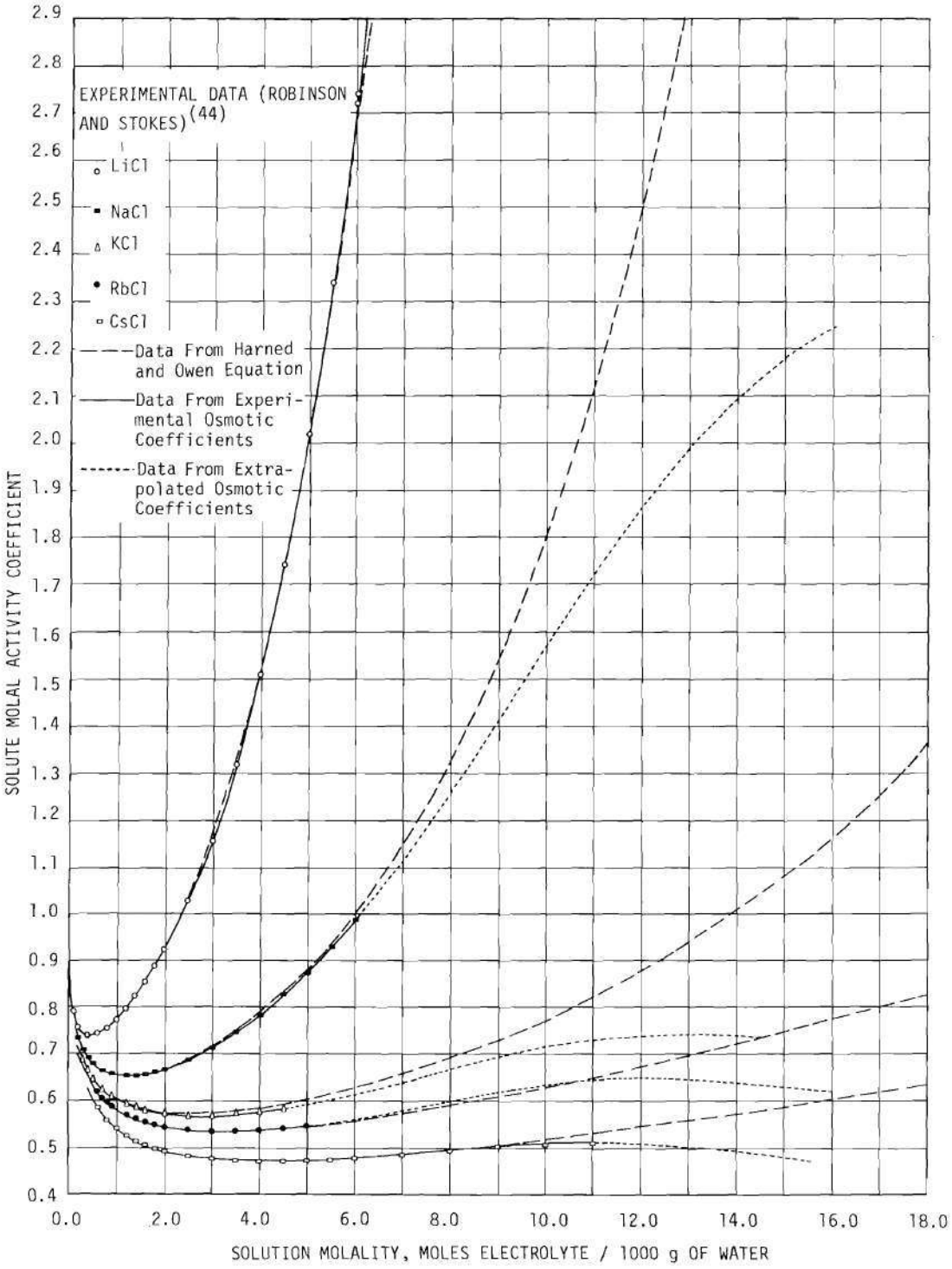

Figure 27. Predicted and Experimental Molal Activity Coefficients of the Alkali Chlorides in Aqueous Solutions at 25°C.

coefficients as calculated by Program No. 3. The results for the supersaturated region using the extrapolated osmotic coefficient data are indicated by the short, dashed lines. Figure 28 is a semilog plot of the same data showing the excellent agreement between the experimental data for the activity coefficients of LiCl over the complete range of the data compared with that calculated from osmotic coefficients. It is very important to note the similarity of the extrapolated curves for NaCl, KCl, and RbCl with those of LiCl and CsCl for which experimental data are available up to 20.0 and 11.0 molal, respectively. The data predicted by the equation of Harned and Owen [Equation (B.3)] are also indicated in both figures by the long dashes.

Figure 29 presents the experimental data reported by McDonald[41] for the van't Hoff factor of aqueous sodium chloride solutions at 25°C. The data calculated from Program No. 3 using the osmotic coefficient ratio approach are also presented as solid lines for the unsaturated region and as short dashed lines for the supersaturated region. The agreement between the experimental data and the computed values is excellent even at very low concentrations.

Finally, Figure 30 presents the experimental data for the vapor pressure of NaCl and KCl[43] [44] as well as the data computed by Program No. 3 using the osmotic coefficient approach and as computed by Program No. 2 using the Harned and Owen equation [Equation (B.3)] for LiCl, NaCl, KCl, and CsCl. It is considered very significant that the data obtained from the extrapolated osmotic coefficients of KCl predict with remarkable accuracy the data for supersaturated KCl solutions reported in the International Critical Tables[43].

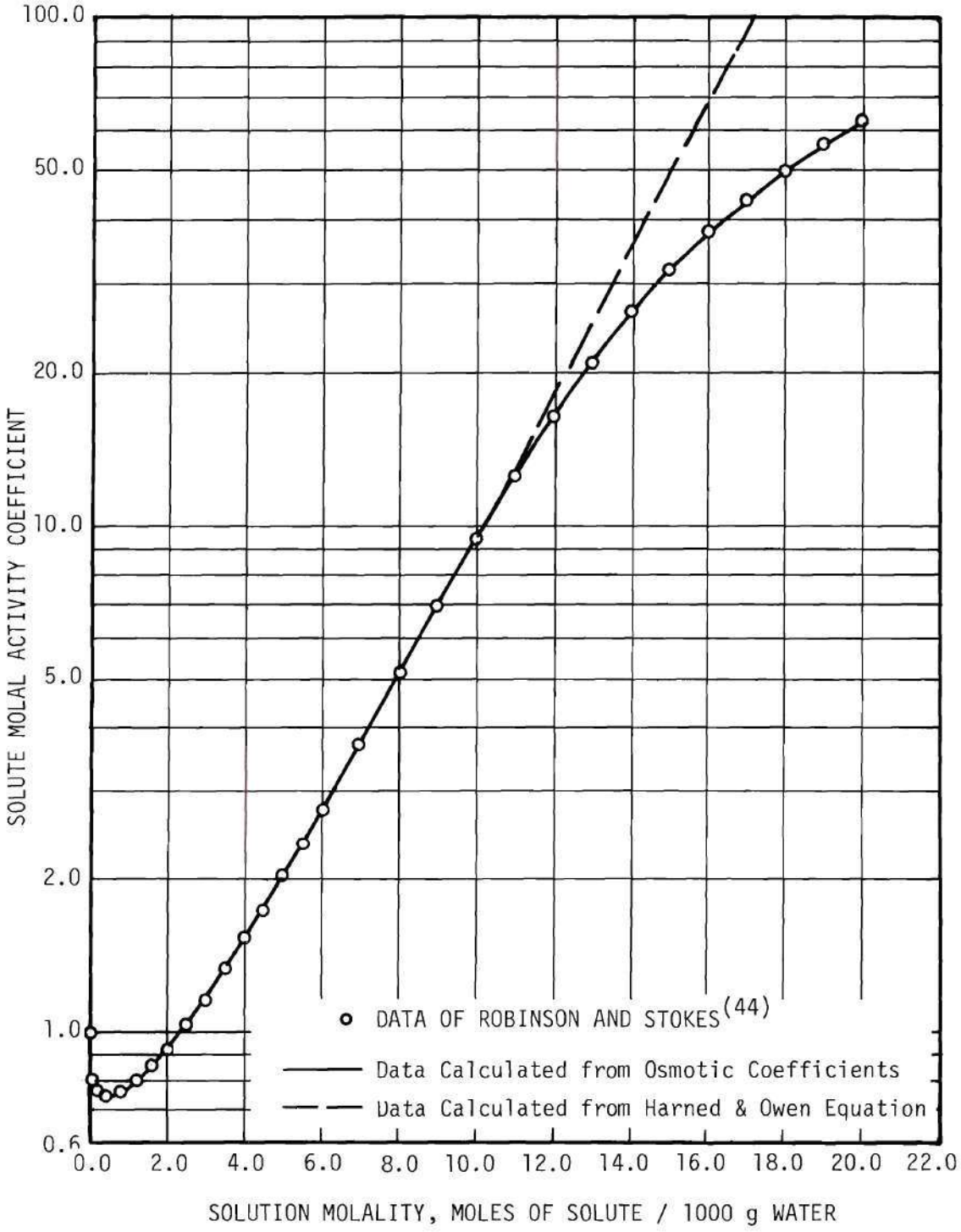

Figure 28. Activity Coefficients of Aqueous LiCl Solutions at 25°C.

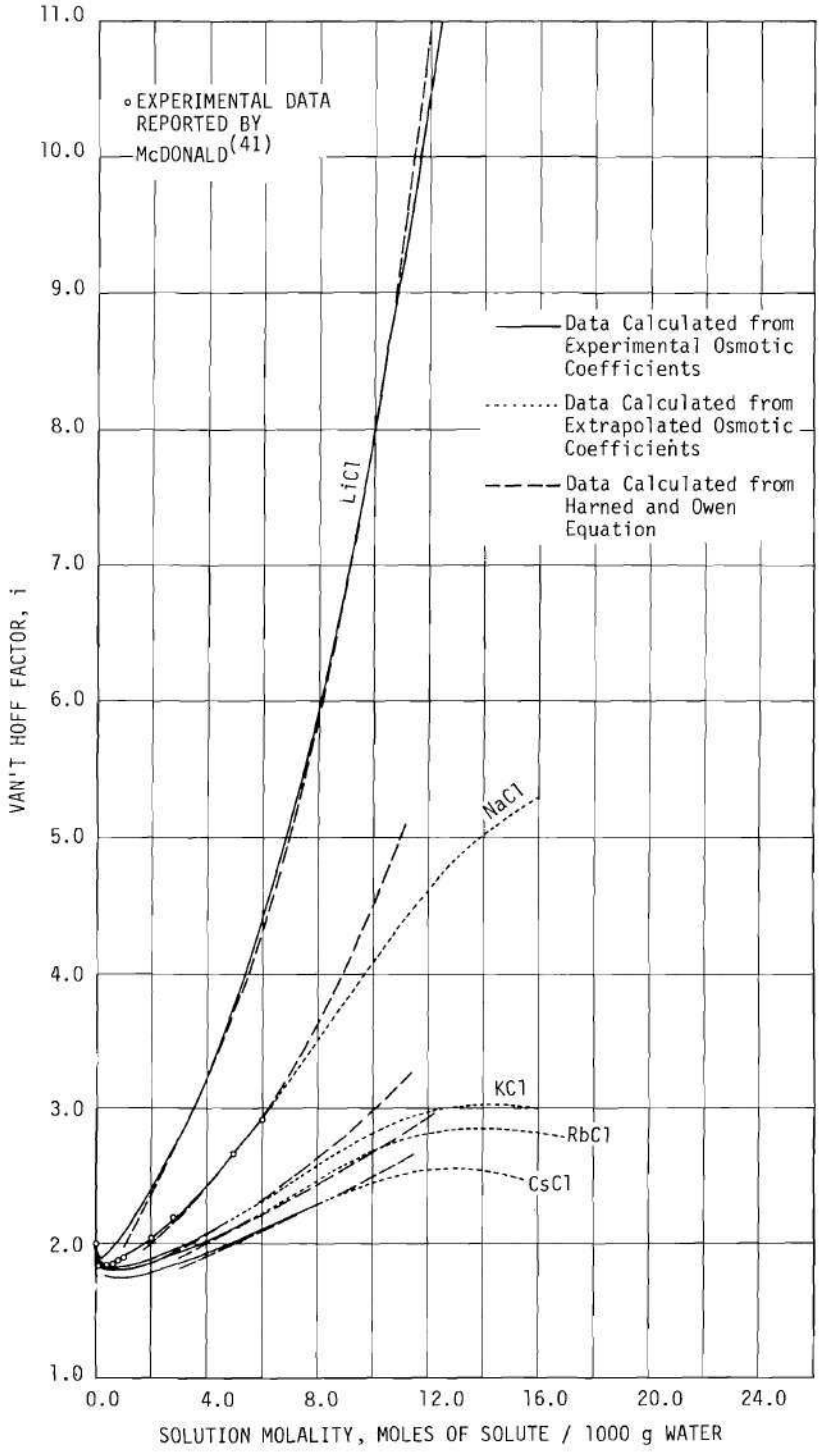

Figure 29. Van't Hoff Factors for Aqueous Solutions of the Alkali Chlorides at 25°C.

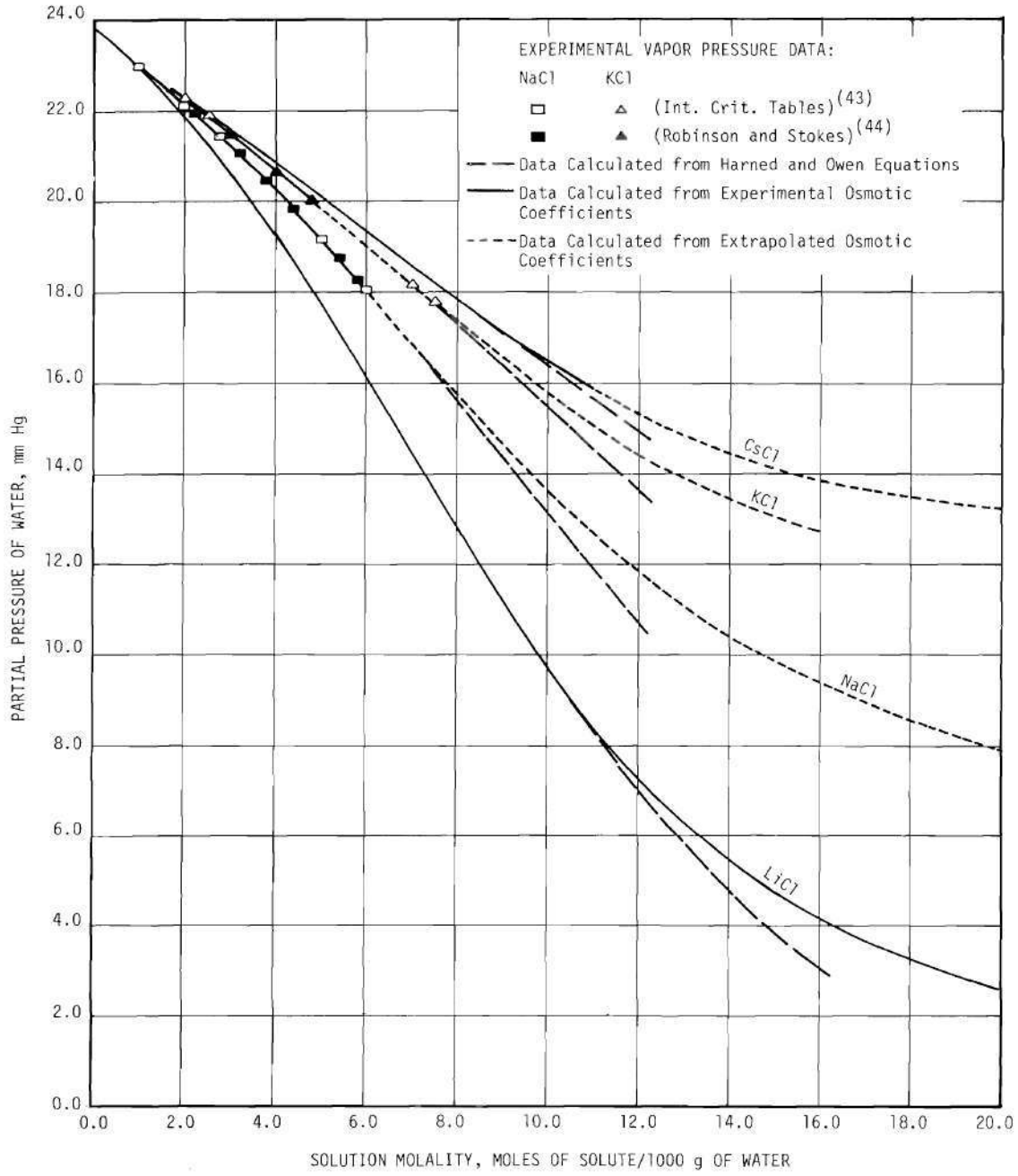

Figure 30. Vapor Pressure of Aqueous Solutions of the Alkali Chlorides at 25°C.

APPENDIX C

PREDICTION OF THE SIZE OF HYDROSCOPIC NUCLEI WITH RELATIVE HUMIDITY

APPENDIX C

PREDICTION OF THE SIZE OF HYGROSCOPIC NUCLEI WITH RELATIVE HUMIDITY

Solid Crystals at Low Relative Humidities

The behavior of solid crystals at low relative humidities can best be explained in terms of gas adsorption theory. It is a well known and documented phenomenon that gas or vapor molecules are adsorbed at the interface between a solid and its gaseous environment, the adsorption being due to the existence of unbalanced intermolecular forces on the surface molecules of the solid. The surface molecules attract other molecules from the environment in order to satisfy these unbalanced surface forces.

The most generally employed theory to describe physical adsorption is that of Brunauer, Emmett and Teller[46], ordinarily designated the BET theory. The basic assumption of this theory is that the same forces responsible for the condensation of vapors are also active in the adsorption of gases in multimolecular layers. In a sense it is a generalization of the earlier theory of Langmuir that was limited to adsorption of gas molecules in a single molecular layer. According to the BET theory, the volume of gas adsorbed up to a partial pressure p is given by the relationship

$$v = \frac{v_m C p}{(p_o - p)[1+(C-1)(p-p_o)]} \qquad (C.1)$$

where p_o is the saturation pressure at the temperature of the system, v

the volume of gas adsorbed at the pressure p, v_m the volume adsorbed to form a monomolecular layer on the surface, and C equal to $\exp(E_1-E_L)/RT$, E_1 being the heat of adsorption of the gas liberated in forming the first layer, E_L the heat of liquefaction, R the gas constant and T the absolute temperature of the system. The quantity (E_1-E_L) can be interpreted, therefore, as the excess of energy liberated upon adsorption of the gas on the solid surface over that liberated by condensation alone. It now seems reasonable to assume, especially in the case of solids that are soluble in the condensed film, that this quantity may be taken approximately equal to the surface energy of the solid.

Unfortunately, an entirely satisfactory theory has not been developed that permits accurate calculations of the surface energy of solids although much effort has been expended toward that goal. A number of investigators have concentrated their efforts on calculating the surface energies of the alkali halides although their results show marked differences. Even experimental determinations offer relatively wide ranges of values for the surface energies of the same solids. The difficulties that cause these inconsistencies are due to the fact that, unlike the case for liquids, the surface energy of solids cannot be determined directly by surface extension, except perhaps in the case of amorphous materials at high temperatures. Therefore, experimental techniques must be based on indirect manifestations of the surface energy. Corbett[27] has pointed out the difficulties inherent in the various experimental approaches as well as given a thorough discussion of the differential heat-of-solution calorimetric method as applied to the determination of the surface energies of sodium and potassium chloride.

This investigator has suggested that all of the experimentally determined values for the surface energy of sodium chloride using the differential heat-of-solution method are high either because the samples studied had been generated by a volatilization technique which did not yield equilibrium surfaces or because of inaccurate methods being employed for the determination of the specific surface area of the material tested. At any rate, the best experimental value for the surface energy of sodium chloride at 25°C has been reported by Benson, et.al.[47] as 276 $\pm$ 5 ergs/cm^2 although this value exceeds the theoretical by 40 to 100 per cent. This value is used in the calculations here, nevertheless, since the increase in radius of a submicroscopic crystal in the size range of interest is almost negligible when gas adsorption is the predominant phenomenon and therefore the uncertainty in this quantity is of little significance.

Assuming a spherical model for the submicroscopic crystal, a circular cross section for an adsorbed water molecule, and using the value of 10.8 $\mathring{A}^2$ for the cross sectional area of the water molecule as reported by Livingstone[48], the radius r in microns of a crystal of original radius r_o at a water vapor pressure p is given, according to Equation (C.1), by the expression

$$r = r_o + \frac{3.71 \times 10^{-4}\, C(p/p_o)}{(1-p/p_o)\,[1+(C-1)(p/p_o)]} \qquad (C.2)$$

or, expressed in terms of the equilibrium relative humidity H in per cent and using the value 1380 for C

$$r = r_o + \frac{0.514\ H}{(100-H)(1+13.79H)} \qquad (C.3)$$

Figure 31 presents the increase in size of a sodium chloride crystal as a function of the equilibrium relative humidity as calculated from Equation (C.3).

Transition From a Crystal to a Saturated Solution Droplet

In the case of a hygroscopic particle, the moisture adsorbed will cause it to dissolve at some relative humidity, which, for a given material at a constant temperature, is only dependent upon the size of the particle. This dissolution will result in an abrupt size increase. If no concentration gradient is assumed across the liquid film adsorbed on the particle, the humidity at which the particle will dissolve may be calculated by assuming the partially dissolved solid nucleus, the adsorbed liquid film of water, and the water vapor in the surroundings to be a three-phase system in equilibrium. The solid particle is assumed in equilibrium with a saturated solution, and the solution, in turn, is assumed to be in equilibrium with the surrounding atmosphere. The liquid film exerts a vapor pressure that is both dependent upon the concentration of the solution and the curvature of the film. The dissolved solid material will lower the vapor pressure while the curvature of the film will tend to increase it. The relation between particle size, surface energy, and equilibrium concentration for ionic solutions is given by the Ostwald-Freundlich equation, which was derived in its most general form by Gibbs[49] from the first law of thermodynamics and the concept of free energy. The result may be written

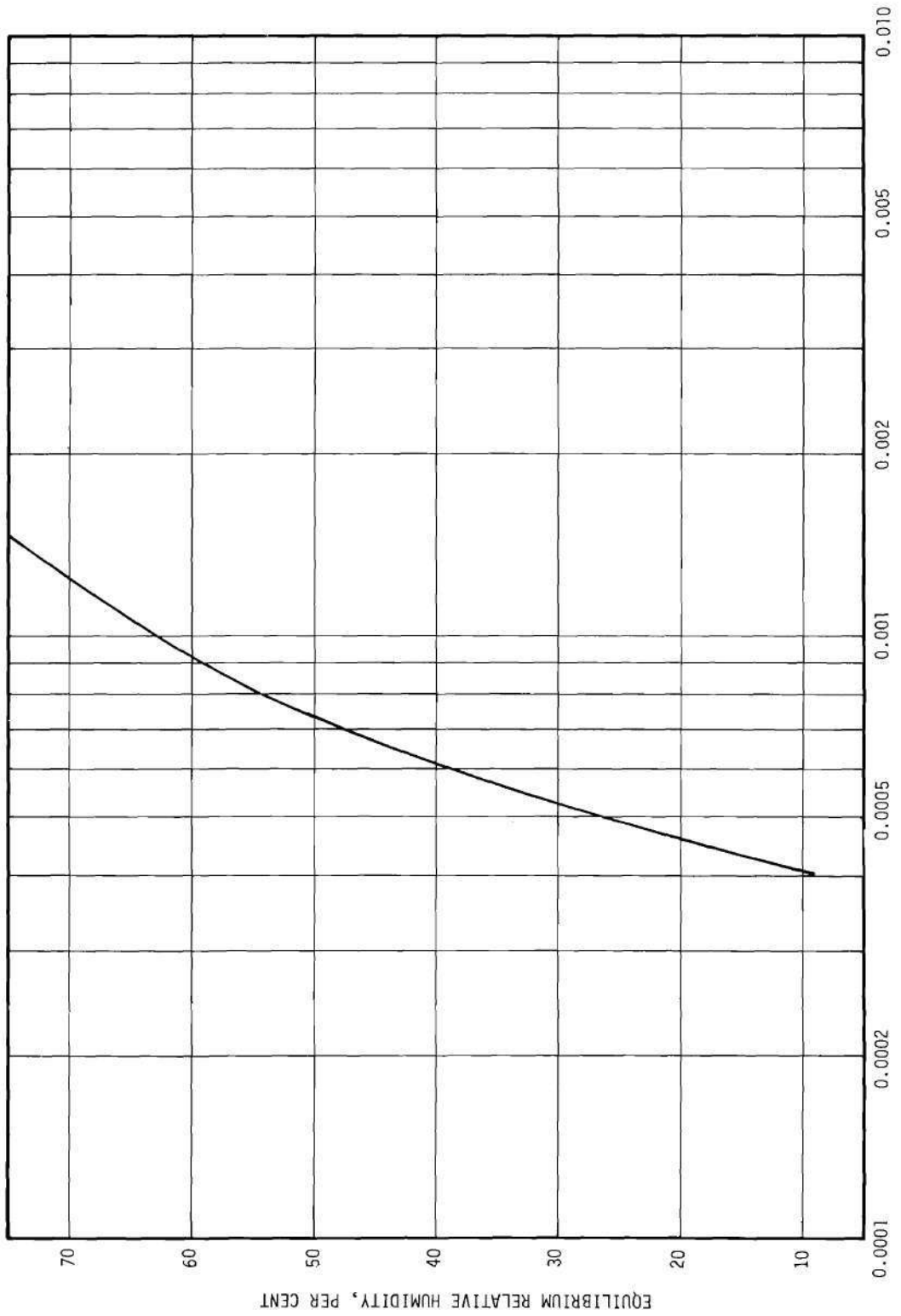

Figure 31. Increase in Size of a Sodium Chloride Crystal with Relative Humidity Due to Water Vapor Adsorption.

$$\ln \frac{a_2}{a_1} = \frac{2\sigma M}{\rho RT}\left[\frac{1}{r_2} - \frac{1}{r_1}\right] \qquad (C.4)$$

where a is the solute activity when the solution is in equilibrium with a particle of radius r, r_2 the radius of a small particle, r_1 the radius of a large crystal (generally taken so that $1/r_2 \gg 1/r_1$), σ the surface free energy of the solid, M the molecular weight of the solid, and ρ the density of the solid.

This general form of the Ostwald-Freundlich relation may be used to predict the activity of the solution in equilibrium with a small crystal provided the necessary data are available. Hence, the activity a_2 of the film of solution adsorbed in equilibrium with a small crystal of radius r_2 may be calculated in terms of the activity a_1 of a saturated solution in equilibrium with large crystals of radius r_1 such that the approximation $1/r_1 = 0$ is tenable. A plot of solution activity versus concentration may be used to determine the concentration of the adsorbed film of solution.

In the absence of activity data, an alternate form of Equation (C.4) may be used which was developed by Dundon and Mack[50] and Dundon[51] in the course of work on the surface free energy of various salts. This equation may be written

$$i \ln \frac{S_2}{S_1} = \frac{2\sigma M}{\rho RT}\left[\frac{1}{r_2} - \frac{1}{r_1}\right] \qquad (C.5)$$

where $i = (1 - \alpha + \nu\alpha)$ is the van't Hoff factor which depends upon the concentration of the solution, α the degree of dissociation of the solute, ν the number of ions formed by the dissociation of one molecule

of the solute, S_2 the solubility of a crystal of radius r_2, and S_1 the solubility of a crystal of radius r_2, and S_1 the solubility of a large crystal of radius r_1.

The partial pressure of water over the liquid solution may be calculated, once the concentration of the adsorbed liquid film of solution is established from either form of the Oswald-Freundlich equation, by using the Kelvin equation which takes into account the curvature of the liquid film, viz., by

$$\ln \frac{p'_r}{p'_o} = \frac{2M_w}{RT} \frac{\sigma_{LV}}{\rho_L} \frac{}{r} \qquad (C.6)$$

where p'_r is the partial pressure of water over a droplet of solution of radius r (which is equal to the vapor pressure of water p_o at the temperature of the system times the relative humidity of air in equilibrium with a liquid droplet of radius r), p'_o the partial pressure of a saturated solution in equilibrium with large crystals, M_w the molecular weight of the solvent (water), σ_{LV} the interfacial surface tension of the droplet of solution, and ρ_L the density of the solution. Actually this result should be designated the Kelvin-Gibbs equation since Kelvin[52] derived a simpler, but essentially equivalent equation in 1869-71* upon which Gibbs generalized and improved (1876-1878).

In the case of electrically charged particles, Thomson[53] has shown that the effect of potential energy due to the presence of electric charges on a droplet reduces the vapor pressure at the surface. This effect may be taken into account by introducing an

---

* Not in 1881 as often stated in texts.

additional term into the Kelvin equation, giving

$$\ln \frac{p'_r}{p'_o} = \frac{M_w}{\rho_L RT}\left[\frac{2\sigma_{LV}}{r} - \frac{n_e^2 e^2}{8\pi r^2}\right] \qquad (C.7)$$

where n_e denotes the number of elementary charges e carried by the particle. However, the effect amounts to less than one per cent in the case of singly charged droplets of radius greater than 2×10^{-3} micron. Since the correction is inversely proportional to r^2, it is taken to be negligible here.

These relations predict that a soluble, small crystal will change rather suddenly into a saturated solution droplet at a certain environmental relative humidity depending only upon the size of the original crystal and its chemical species at a given constant temperature and constant total pressure. As the relative humidity increases, the thickness of the adsorbed layer of water on the surface of the crystal also increases as predicted by gaseous adsorption theory. The additional water adsorbed causes more of the soluble crystal to dissolve. This decrease in the size of the crystal permits the concentration of solution in equilibrium with it to increase, as predicted by the Ostwald-Freundlich relationship. This, in turn, causes a lowering of the vapor pressure exerted by the liquid film whereby more moisture is condensed from the surrounding atmosphere. This also contributes to an increase in the size of the particle and a corresponding decrease in its curvature. As the surface curvature is decreased the vapor pressure exerted by the liquid film is further decreased. At a certain relative humidity the situation becomes unstable and equilibrium is established

only after complete dissolution of the crystal. Hence, the solubility, surface curvature, and other factors establishing the point of dissolution are determined only by the original crystal size. The relative humidity at which a given crystal dissolves increases with size increase up to an asymptotic value that is characteristic of the nature of the chemical species. This phenomenon is illustrated in the case of sodium chloride in Figure 32. These results do not agree precisely with the predictions made by Orr, et.al.[12]. It seems apparent that in using the Ostwald-Freundlich relation,[Equation (C.4)],these authors used the activity coefficient of the solute rather than the activity. This explains the apparent disagreement between their predictions and their experimental findings, which correlate very well with Figure 32.

Solution Droplets and Relative Humidity

The behavior of solution droplets with change in relative humidity was first described quantitatively by Köhler in 1921. A modified derivation was obtained by Wright in 1936[54] by adding a correction to the general equation of Kelvin as applied to pure water for the vapor pressure lowering due to the presence of the solute. In this development Wright assumed the ratio of the vapor pressure depression to the vapor pressure over a plane surface of solution was proportional to the concentration of the solution and that the constant of proportionality, which was called the hygroscopic factor, was independent of the solution concentration and only dependent upon the chemical species of the solute. The expression obtained is

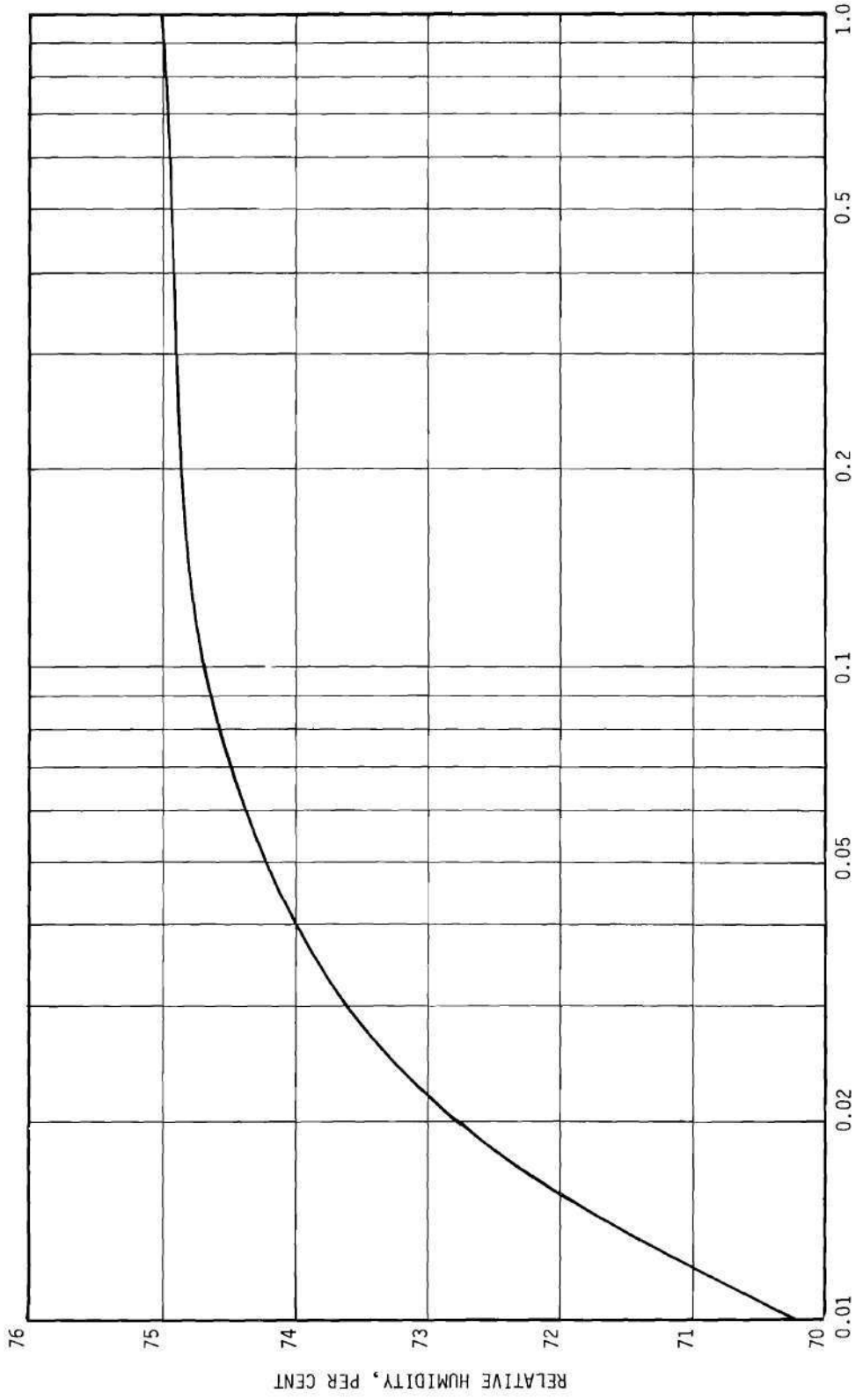

Figure 32. Relative Humidity at Which a Given Size Dry NaCl Crystal Will Dissolve.

$$\frac{p'_r}{p_o} = \exp\left[\frac{2\,\sigma_{LV} M_w}{RT\,\rho_L\, r}\right] - \frac{750\, m'\, C}{\pi\, r^3\, \rho_L\, M} \qquad (C.8)$$

where p'_r is the partial pressure in equilibrium with a solution droplet of radius r, p_o the vapor pressure of bulk water at the temperature T, m' the mass of the solute contained in a droplet of radius r, M the molecular weight of the solute, and C the hygroscopic factor. Using Wright's nomenclature Equation (C.8) is expressed by

$$\frac{H}{100} = \exp \frac{P}{r} - \frac{Q}{r^3} \qquad (C.9)$$

where

$$P = \frac{2\,\sigma_{LV}\, M_w}{RT\,\rho_L}, \text{ and } Q = \frac{750\, m'\, C}{\pi\,\rho_L\, M}$$

Because of the assumptions involved, Wright's equation is only adequate at very low droplet concentrations such as occur at values of relative humidity near saturation. In an attempt to circumvent the assumption of constant hygroscopic factor, Equation (C.8) was rewritten, following Mason[55], as

$$\frac{H}{100} = \exp\left[\frac{2\,\sigma_{LV}\, M_w}{RT\,\rho_L\, r}\right] - \frac{i\, M_w\, m'}{\frac{4}{3}\,\pi\, r^3\, \rho_L\, M} \qquad (C.10)$$

where i is the van't Hoff factor, H the relative humidity in per cent, and $i\, M_w = 1000\, C$.

A somewhat different treatment of the problem was considered by Howell in 1949[56]. Because applicability of Raoult's law was assumed,

the results are limited to high relative humidities for which the behavior of the dilute solution would make the assumption acceptable. Howell's work is discussed in a paper published by McDonald[41] in which a modified form of Raoult's law is suggested for use in Howell's development. This treatment involves the use of the van't Hoff factor to account for the dissociation of the solute.

It was not until 1957, however, that a more satisfactory treatment of the subject was given by Mason[55]. By calculating the decrease in free energy of a solution upon transferring an elemental mass of water from a droplet to a plane water surface, Mason arrived at the expression

$$\frac{p'}{p_o} = \left[\exp\left(\frac{2\ \sigma_{LV}\ M_w}{\rho_L\ RT\ r}\right)\right]\left[1 + \frac{i\ m'\ M_w}{M\left(\frac{4}{3}\ \pi\ r^3\ \rho_L - m'\right)}\right]^{-\left(\frac{\rho_w}{\rho_L}\right)} \qquad (C.11)$$

This equation seems to be sufficiently general to take into account the dissociation of the solute at all concentrations, and, presumably, is also applicable in the supersaturated solution region, provided the corresponding data are available either from experimental measurements or guided extrapolations of concentrated solution properties.

When the solution droplet is in equilibrium with the surrounding atmosphere with its surface temperature equal to that of the air, p must equal the partial pressure of the water vapor and, therefore, Equation (C.11) becomes

$$\frac{H}{100} = \left[\exp\left(\frac{2\ \sigma_{LV}\ M_w}{\rho_L\ RT\ r}\right)\right]\left[1 + \frac{i\ m'\ M_w}{M\left(\frac{4}{3}\ \pi\ r^3\ \rho_L - m'\right)}\right]^{-\left(\frac{\rho_w}{\rho_L}\right)} \qquad (C.12)$$

The Kelvin equation, which has been derived from strict thermodynamical considerations, may be used to predict the partial vapor pressure p_r' in equilibrium with a droplet of a pure liquid of radius r

$$\ln \frac{p_r'}{p_o} = \frac{2\sigma_{LV} M_L}{\rho_L RT r} \qquad (C.13)$$

where M_L and ρ_L represent the molecular weight and the density of the liquid, respectively.

Byers[57] has proved that, to a high degree of approximation, a similar form of the Kelvin equation may be derived, which permits calculation of the partial pressure of water p_r' in equilibrium with a droplet of solution. Following his development, the difference in the chemical potential μ_r' of water in a droplet of solution of radius r over that in a bulk solution of the same concentration μ', is given by

$$\mu_r' - \mu' = \frac{RT}{M_w} \ln \frac{p_r'}{p}$$

where p is the water partial pressure in equilibrium with a bulk solution. If an infinitesimal mass of water $dM = d(\frac{4}{3} \pi r^3 \rho_w)$ is added to the spherical solution droplet, the resulting change in free energy is balanced by the change in surface free energy $d(4 \pi r^2 \sigma_{LV})$, such that

$$d(\tfrac{4}{3} \pi r^3 \rho_L) \frac{RT}{M_w} \ln \frac{p_r'}{p} = d(4 \pi r^2 \sigma_{LV})$$

or, differentiating

$$\left(\rho_L r^2 + \frac{1}{3} r^3 \frac{d \rho_L}{d r}\right) \frac{RT}{M_w} \ln \frac{p_r'}{p} = 2 \sigma_{LV} r + r^2 \frac{d \sigma_{LV}}{d r}$$

In this equation, the second term of each side is at least four orders of magnitude smaller than the first in the droplet size range of 0.01 to 10 microns, hence the equation may be approximated by

$$\ln \frac{p_r'}{p} = \frac{2\,\sigma_{LV}\,M_w}{\rho_L\,RT\,r}$$

or, expressed in terms of the relative humidity $H = 100\ (p_r'/p_o)$

$$\frac{H}{100} = \frac{p}{p_o}\left[\exp\left(\frac{2\,\sigma_{LV}\,M_w}{\rho_L\,RT\,r}\right)\right] \qquad (C.14)$$

An essentially equivalent expression to Equation (C.14) was used by Orr, et al.[21] to predict the size of solution droplets in equilibrium with the environment relative humidity. Their results correlated very closely with experimental measurements obtained from ion mobility.

Program Number 4 in Appendix F was written to calculate from the data on solutions and the extrapolations obtained for supersaturated sodium chloride solutions (Table 7) the relative humidity in equilibrium with a given size droplet and its concentration, given the amount of solute, m', per droplet.

Figure 33 through 36 present in sequence the data calculated from the equation of Wright, Equation (C.9), the modified form of Wright's equation, Equation (C.10), the equation of Mason, Equation (C.12), and the Kelvin equation as applied to solution droplets, Equation (C.14). A family of curves for seven values of electrolyte content per droplet is presented with the dashed lines representing constant droplet molality. The choice of values of m' permits direct comparison with Wright's results.

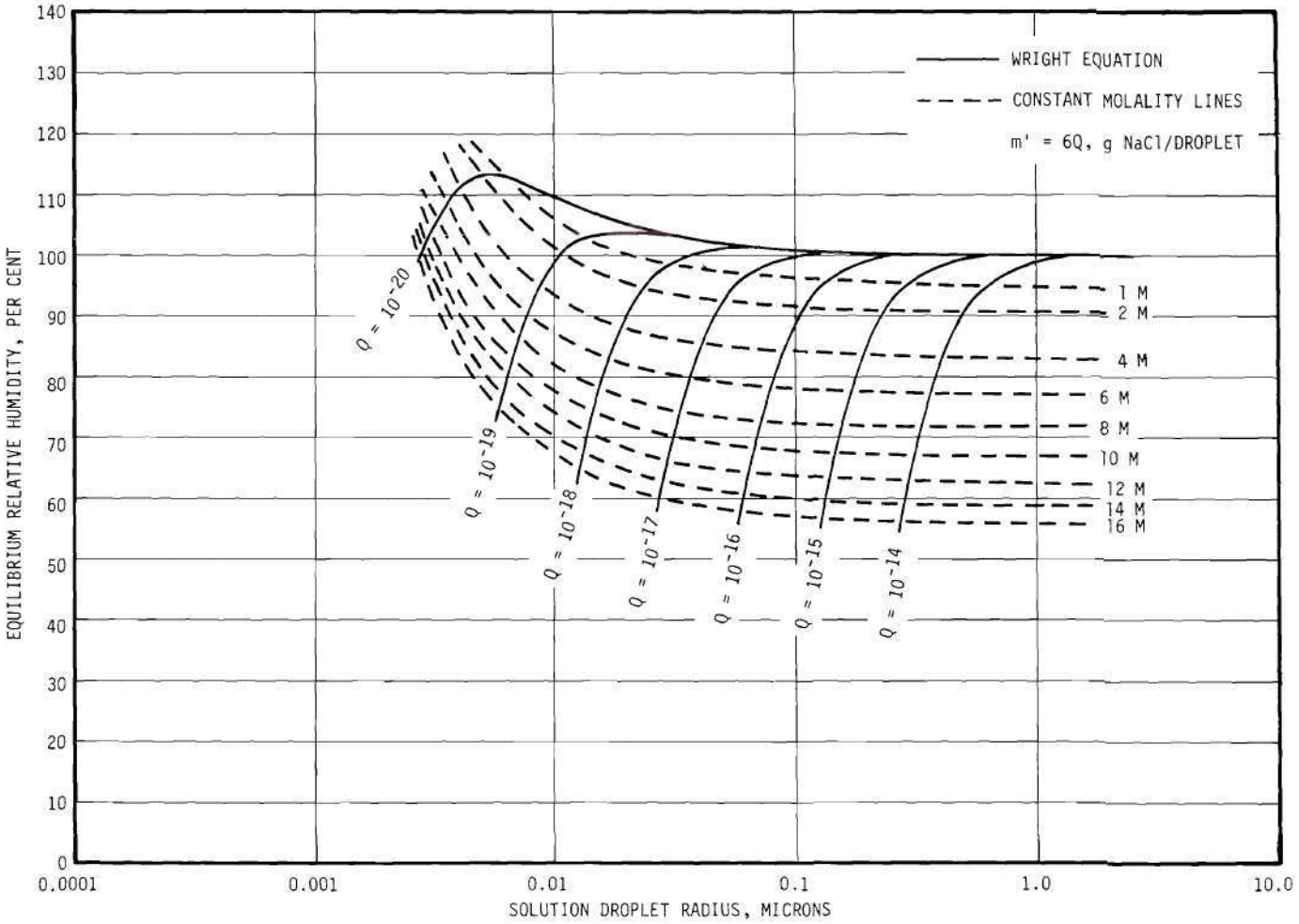

Figure 33. Variation in the Radius of Sodium Chloride Solution Droplets with Relative Humidity at 25°C as Calculated from the Wright Equation.

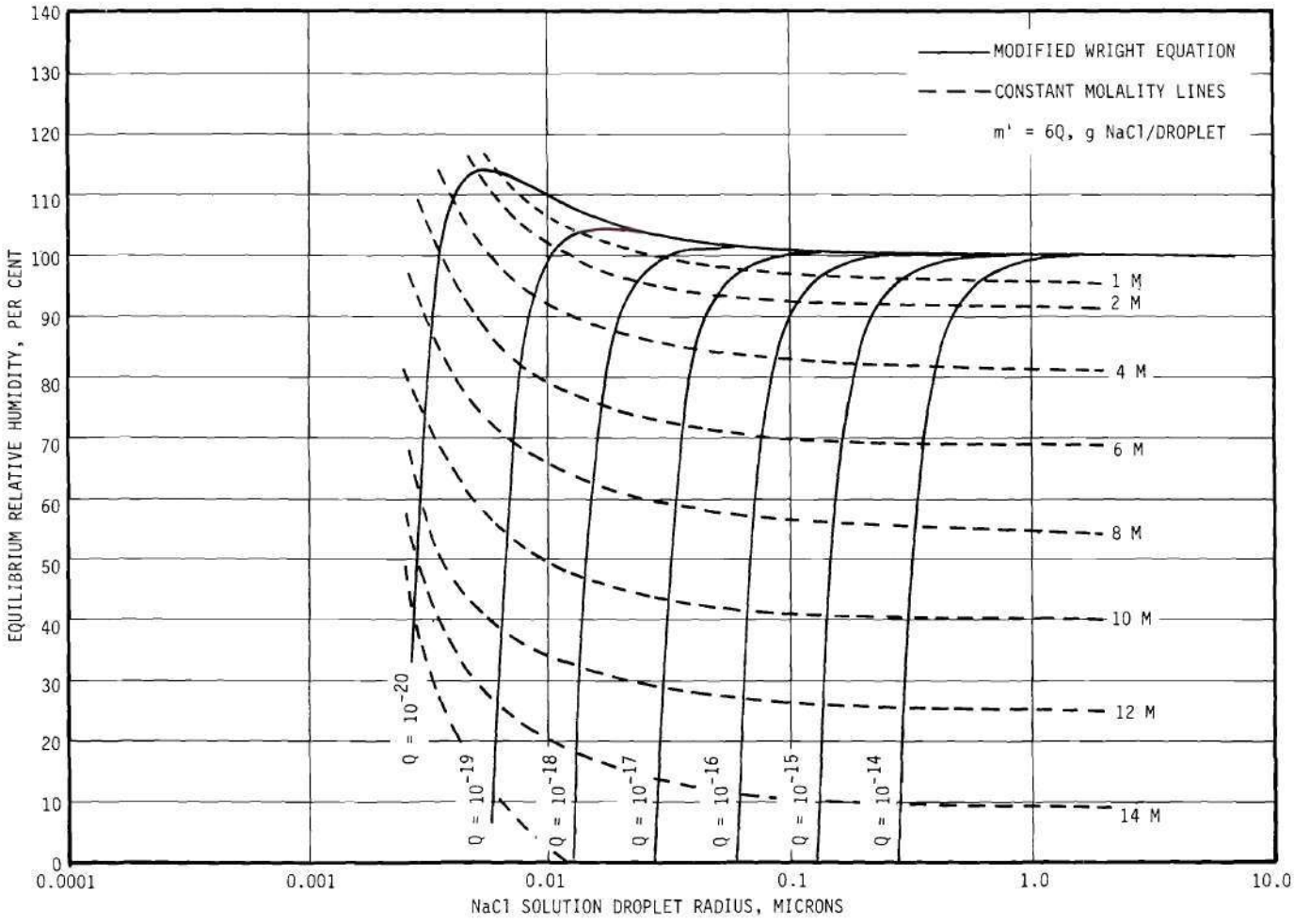

Figure 34. Variation in the Radius of Sodium Chloride Solution Droplets with Relative Humidity at 25°C as Calculated from the Modified Equation of Wright.

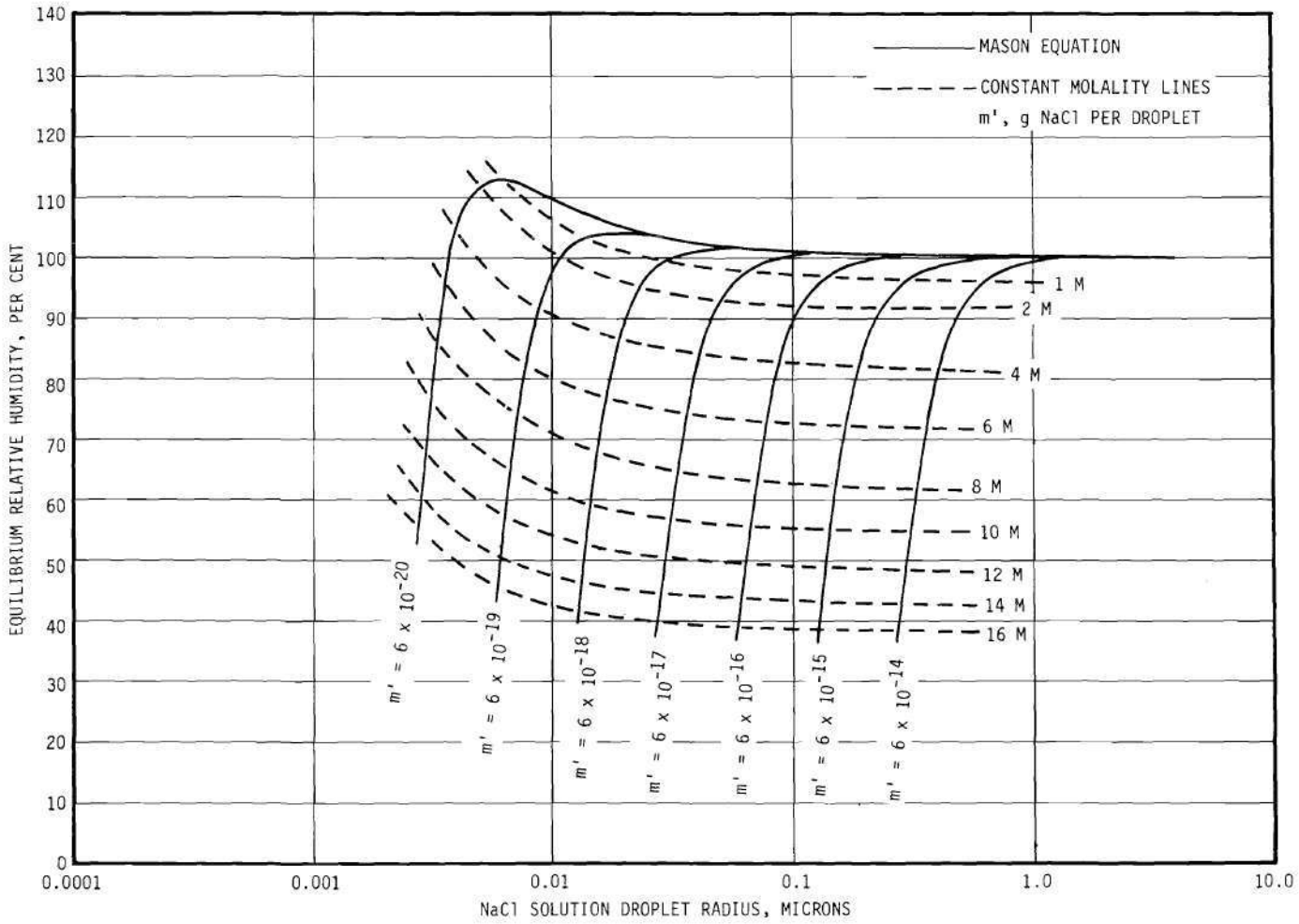

Figure 35. Variation in the Radius of Sodium Chloride Solution Droplets with Relative Humidity at 25°C as Calculated from the Mason Equation.

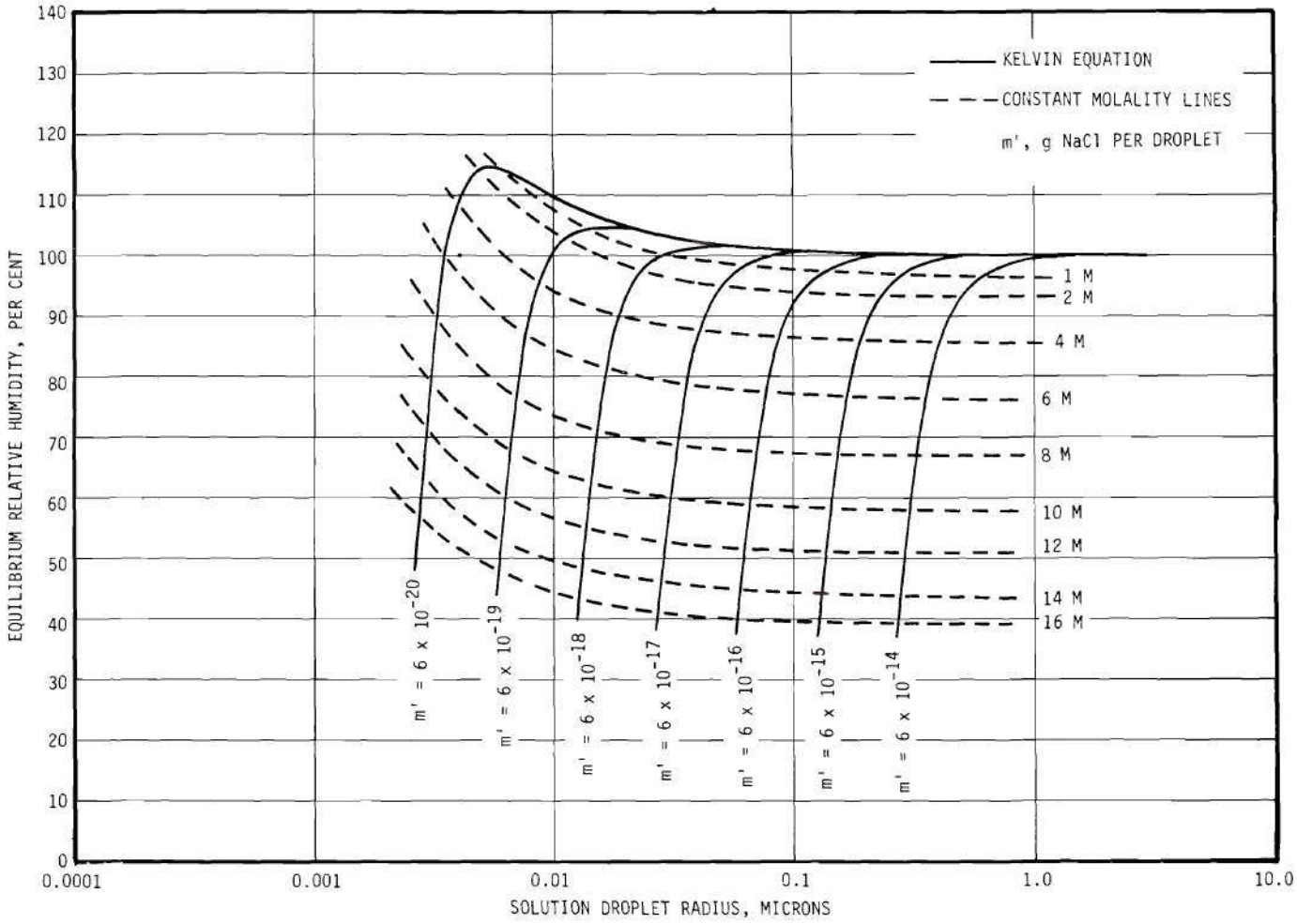

Figure 36. Variation in the Radius of Sodium Chloride Solution Droplets with Relative Humidity at 25°C as Calculated from the Kelvin Equation.

When the actual solution properties are used in Wright's equation, it predicts extremely high droplet concentrations in equilibrium with moderately high relative humidities. In the case of the modified form of Wright's equation, the situation is just the opposite. This is taken as an indication that Wright's model is not applicable for conditions of high droplet concentrations.

In contrast, the results calculated using the equation of Mason and the Kelvin equation agree reasonably well. However, the lines of constant droplet concentration appear to be significantly displaced, comparing both models. The fact that the Kelvin equation as applied to a solution (Equation C.14) has been proved by Byers[57] to be a very good approximation, and the experimental verification of this equation by Orr, et al.,[21] tend to give confidence on the accuracy of these results over those calculated from the Mason equation.

Finally, Figure 37 presents the relationship between sodium chloride solution droplet size in equilibrium with the relative humidity of the environment and the droplet concentration as calculated from the Kelvin equation.

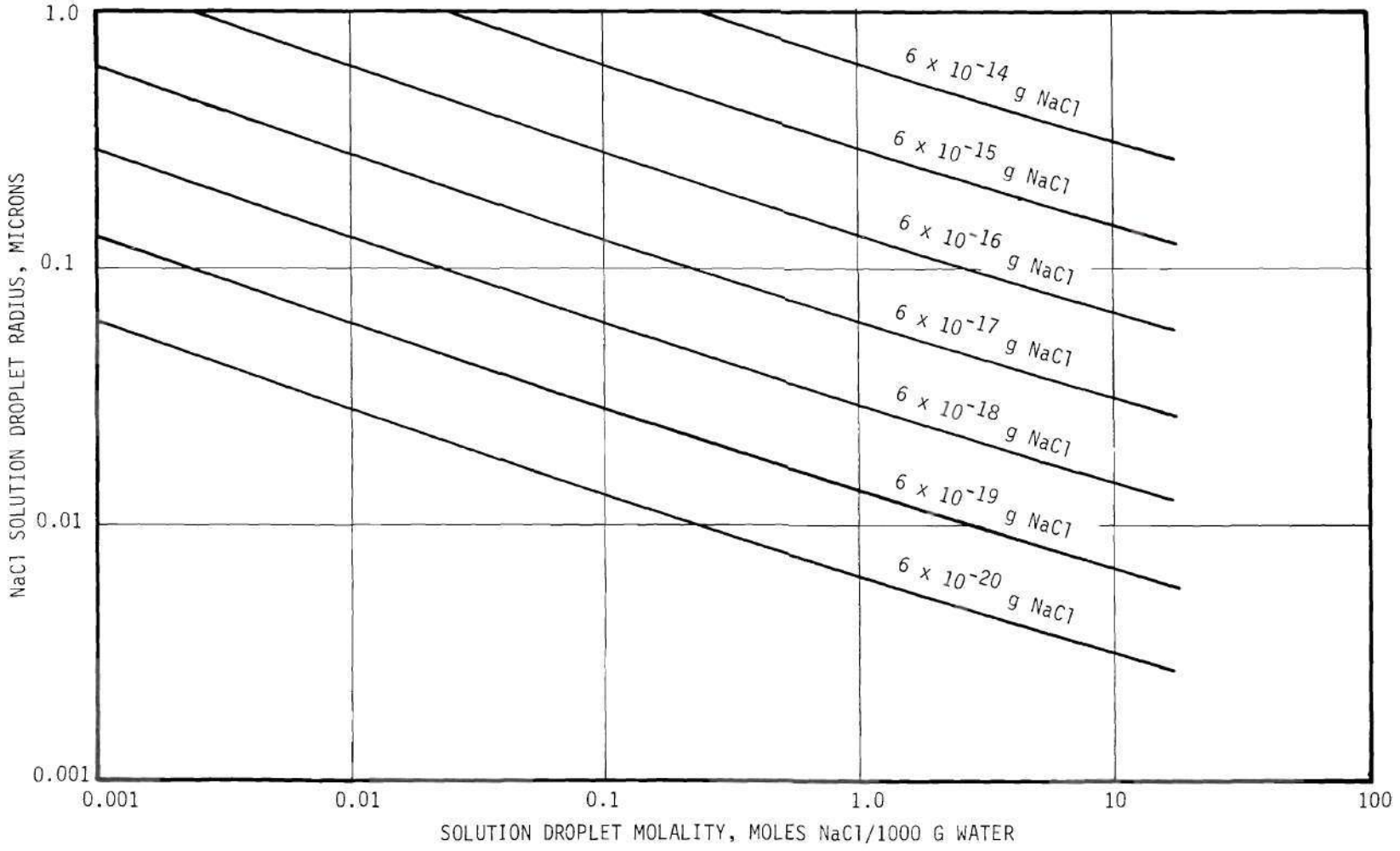

Figure 37. Sodium Chloride Solution Droplet Concentration as a Function of Radius in Equilibrium with Relative Humidity with Solute Content per Droplet as Parameter.

APPENDIX D

CORRELATION BETWEEN ION COUNTER AND ELECTRON MICROGRAPH AEROSOL SIZE DISTRIBUTIONS

APPENDIX D

CORRELATION BETWEEN ION COUNTER AND ELECTRON MICROGRAPH PARTICLE SIZE DISTRIBUTIONS

A comparison was made between particle size distributions obtained using the ion counter and those obtained from particle counts on electron micrographs.

An aerosol was produced entirely of crystals of NaCl in equilibrium with a relative humidity of less than 25 per cent. This aerosol was sampled directly upon coming from the humidity conditioning chamber without any aging and also after aging for 20 minutes in the residence chamber. Experiments had previously indicated a decrease in the concentration of the aerosol with time. This had been interpreted in terms of agglomeration of the aerosol.

The non-aged aerosol was sampled for 30 minutes using a radial thermal precipitator and two electron microscope grids placed at different locations along the radius. A sampling time of 1 hour was used in the case of the aerosol that was aged 20 minutes. Size distributions were made also from ion mobility measurements on the two aerosols.

Upon examination of the electron microscope samples it was determined that there was no statistical difference between the size distributions of the samples collected at the two positions on the plates of the thermal precipitator. There also appeared to be no evidence of *significant particle agglomeration* with aging up to about 20 minutes. Agglomeration should therefore not be a factor of any significance with

an aerosol composed of droplets. Figure 38 presents typical electron micrographs of the aerosol particles.

It was found, following Montgomery[58], that a large particle count was necessary in order to ascertain the size distribution with an acceptable degree of confidence.

In order to accomplish this efficiently, a program was written in Algol 58 for use on the Burrough's 220 Compiler. This program (Program No. 6, Appendix F) made a complete size distribution analysis, given the number of size ranges desired, the conversion factor, the number of particles counted, and the unconverted particle size readings obtained by microscopic measurements using a filar micrometer.

Figure 39 shows the size distribution of the aerosol using 25 size ranges. From the correlations of Montgomery, Table 11 was constructed, which indicates N_1, the number of particles that must be counted to be 99 per cent certain that the mean of the distribution is known within 10 per cent, N_2 the number required to be 99 per cent certain that the complete distribution is known within 10 per cent, and N_o the actual number of particles counted.

Table 11. Number of Particles Counted for Acceptable Levels of Confidence

Condition	N_o	N_1	N_2
Non-aged Aerosol	624	200	600
Aerosol after Aging 20 Minutes	1248	250	750

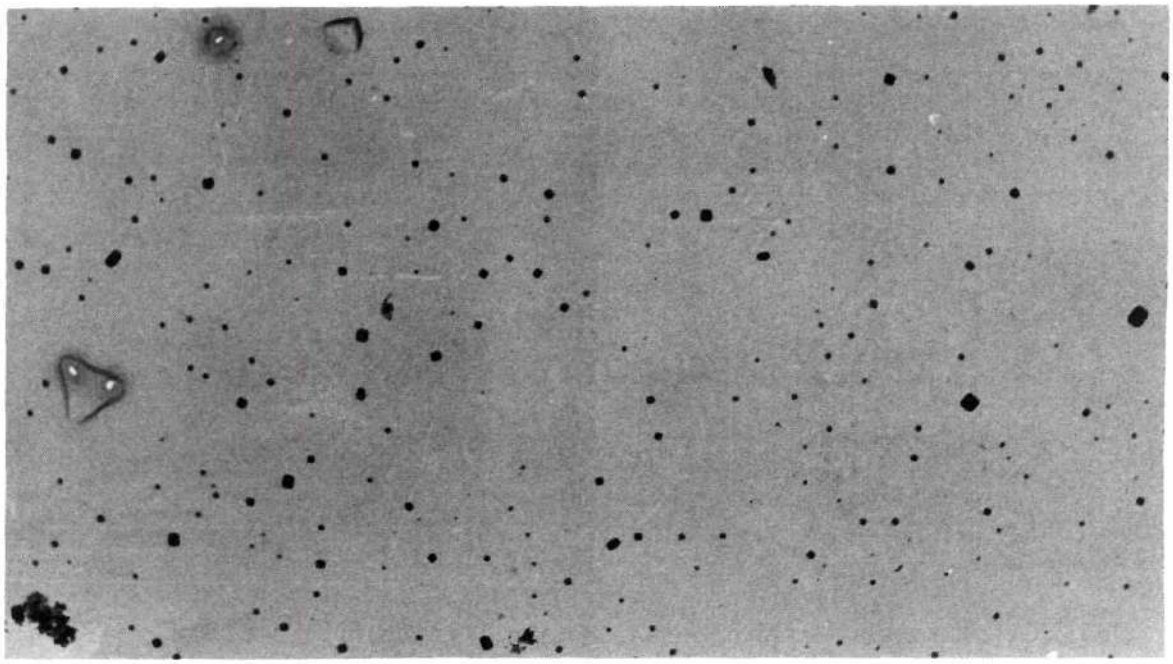

(a) Non aged aerosol (15,000x)

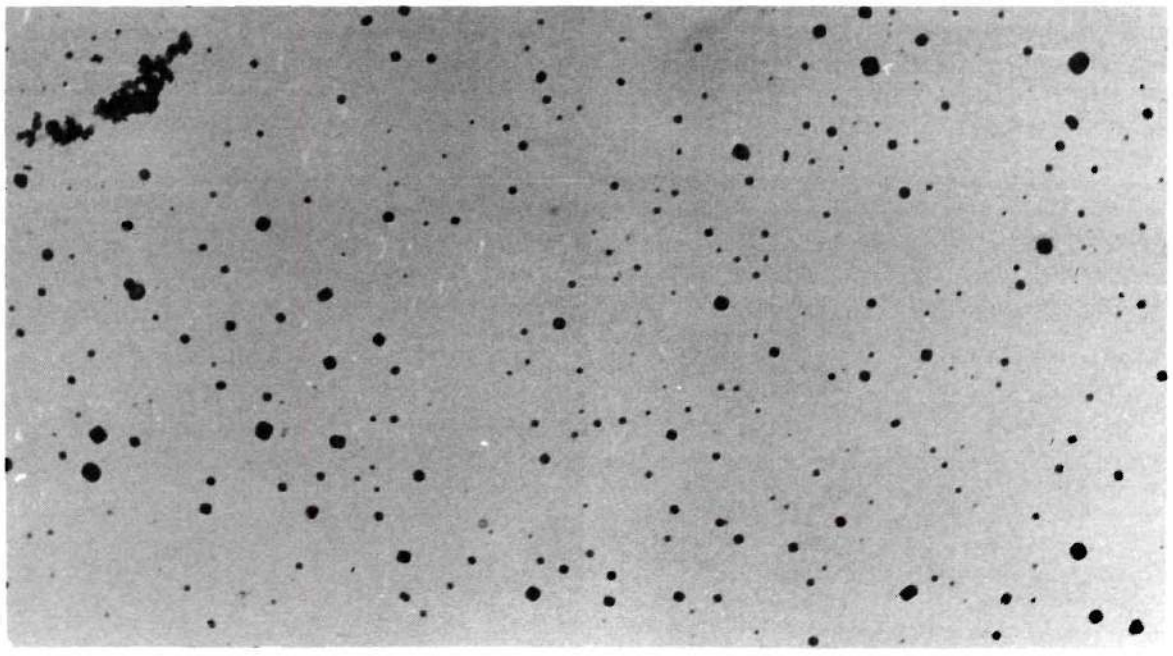

(b) Aerosol after aging 20 minutes (15,000x)

Figure 38. Electron Micrographs of Aerosols of Sodium Chloride Crystals.

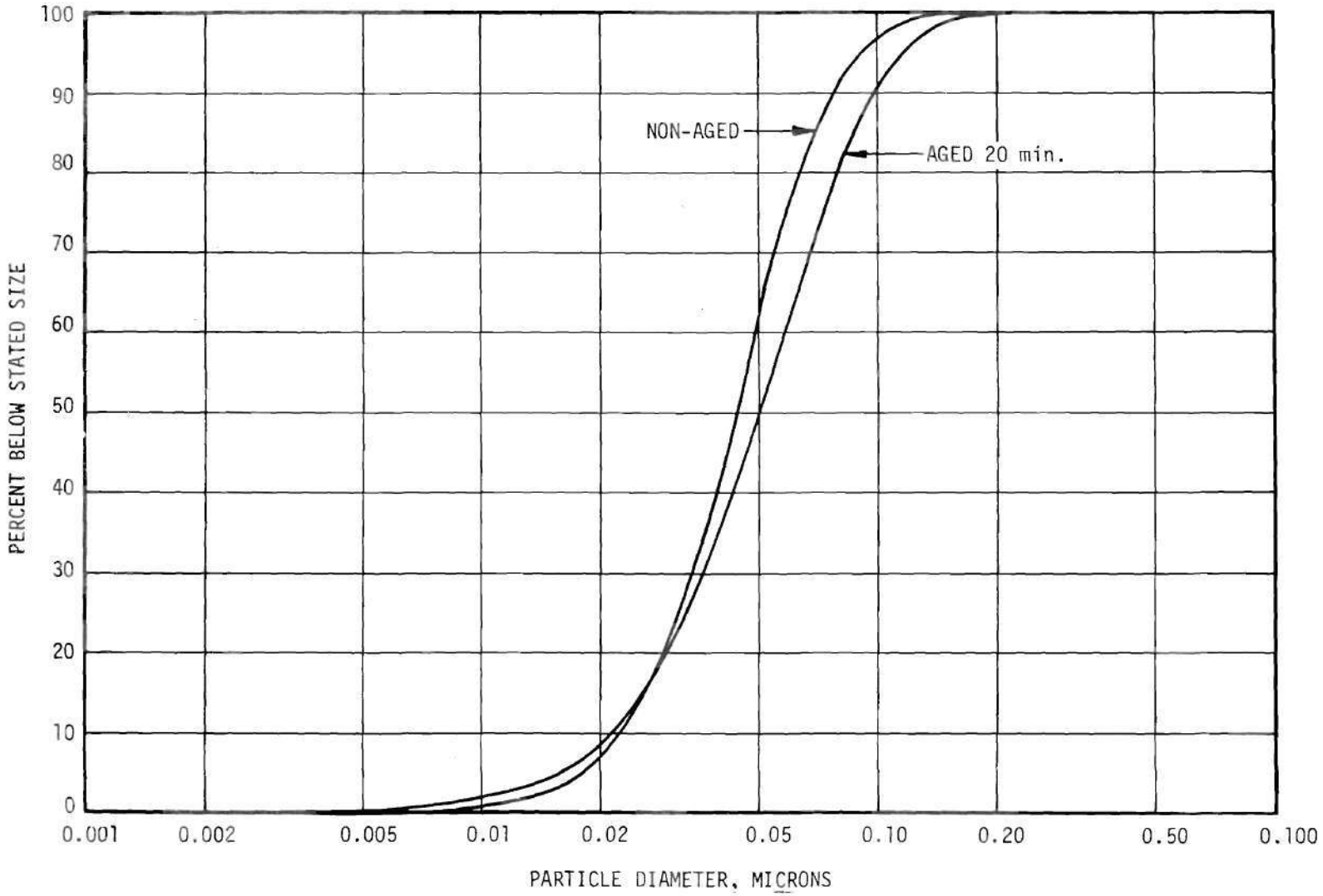

Figure 39. Aerosol Size Distributions from Electron Micrographs.

The number of particles counted, therefore, insures at the 99 per cent confidence level that not only the mean but also the complete distribution of both samples is known within 10 per cent.

The size distribution obtained from ion mobility measurements based on an actual separation between plates of 2.0 mm (0.0787 inch) agreed with the size distributions using electron micrographs and optical microscope counts over the small end of the distributions but departed noticeably over the large end. This was to be expected as a result of the assumption of a single electron charge on the particles. However, due to the construction of the ion counter, the method of calibrating the separation between the plates was not accurate and there was no way of insuring that the plates would be perfectly parallel. On these grounds, therefore, it was decided to change arbitrarily the value of the separation between the plates in the calculations until a value was found that gave an acceptable agreement between the calculated size distribution and that obtained from visual particle counts. It turned out that this was accomplished with a separation between the plates of 1.37 mm (0.054 inch). Figure 40 represents a comparison between the size distribution from electron micrograph counts and those obtained assuming a separation between the plates of 0.054 inch and 0.0787 inch in the case of the non-aged aerosol. Figure 41 presents equivalent data on the aerosol aged 20 minutes.

In the light of this result a value of 0.054 inch was used as the effective separation between the plates of the ion counter in processing all other experimental data.

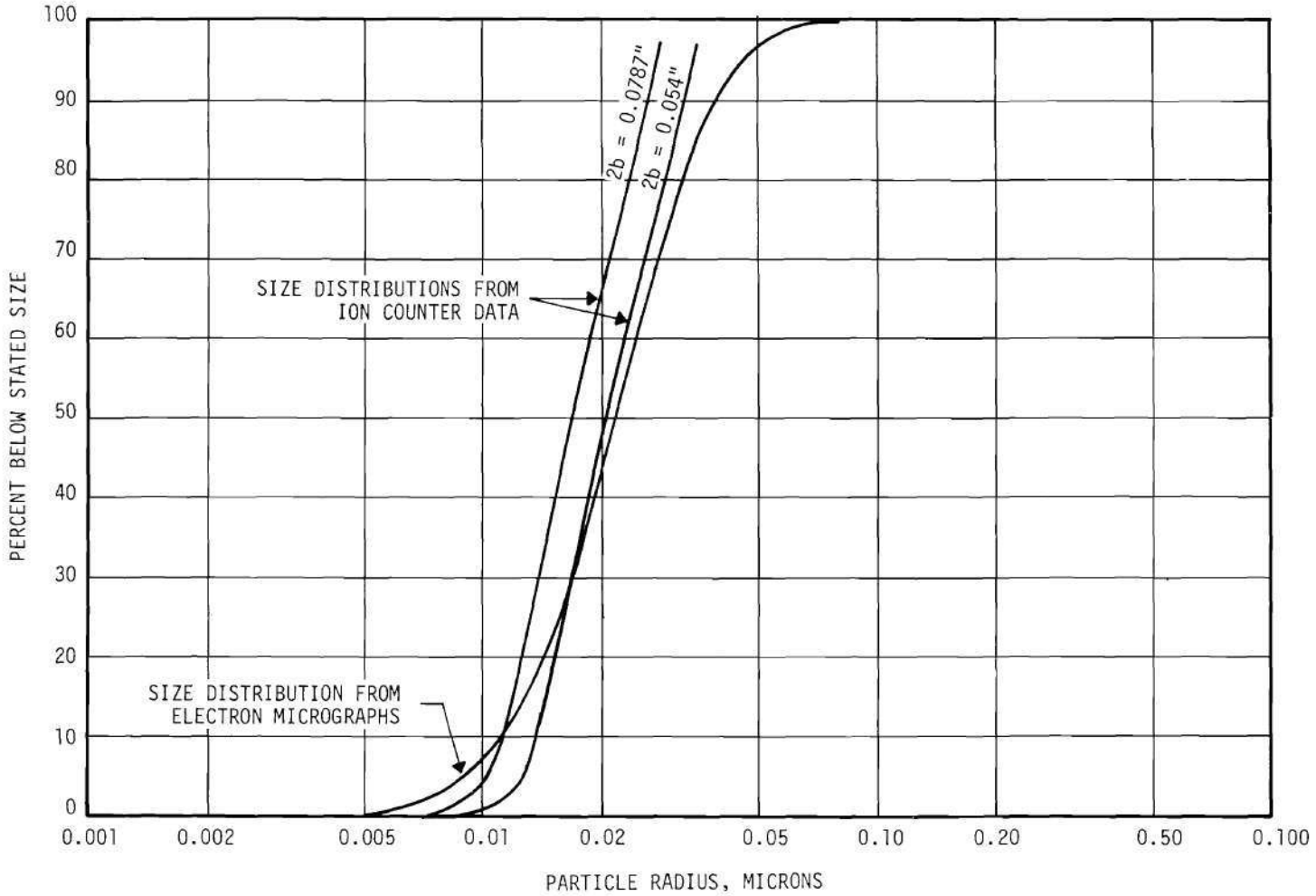

Figure 40. Non Aged Aerosol Size Distribution as Compared to Ion Counter Results.

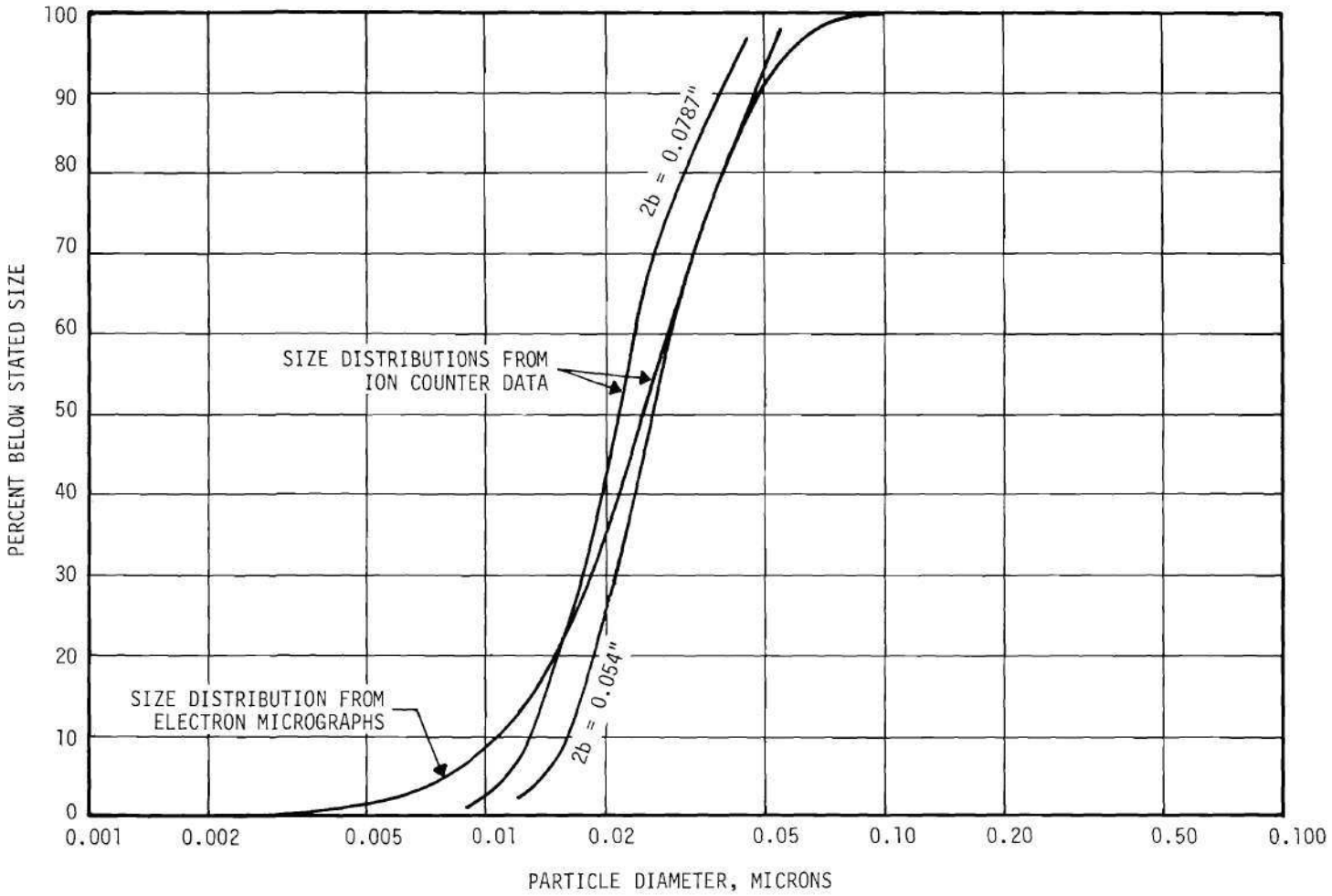

Figure 41. Size Distribution of Aerosol Aged 20 Minutes as Compared to Ion Counter Results.

APPENDIX E

EXPERIMENTAL AND CALCULATED DATA

APPENDIX E

EXPERIMENTAL AND CALCULATED DATA

This section contains in sequential order the experimental and calculated data on the behavior of the sodium chloride aerosols studied with regard to size changes and equilibrium relative humidity. The order in which the data are presented is that of increasing aerosol residence time. For each value of residence time, a figure is presented which illustrates the measured size variation of the mean of the distribution with equilibrium relative humidity. Following this is a figure which indicates the size distribution of the aerosol in equilibrium with increasing levels of relative humidity followed by another which indicates the behavior for decreasing values of equilibrium relative humidity, when equilibrium was approached from an aerosol composed of solution droplets. The following two figures indicate the normalized ion current with ion counter plate potential, one representing the data for increasing relative humidity and the other representing that for decreasing relative humidity, the equilibrium being approached from a solution droplet condition. The following four figures indicate the experimental data on relative humidity versus normalized ion current at various values of ion-counter plate potential. The value of the relative humidity at which nucleation of the solution droplets occurred was obtained from these plots. The open points indicate that the equilibrium condition was attained from a dry-crystal condition. The solid points indicate that equilibrium was approached from a solution droplet. The data

presented here indicate the behavior of the aerosol after average residence times of 0.25, 2.45, 3.85, 7.44, and 14.6 minutes in equilibrium with the environmental relative humidity. Data were also collected at a residence time of 20.5 minutes; essentially no detectable hysteresis was indicated.

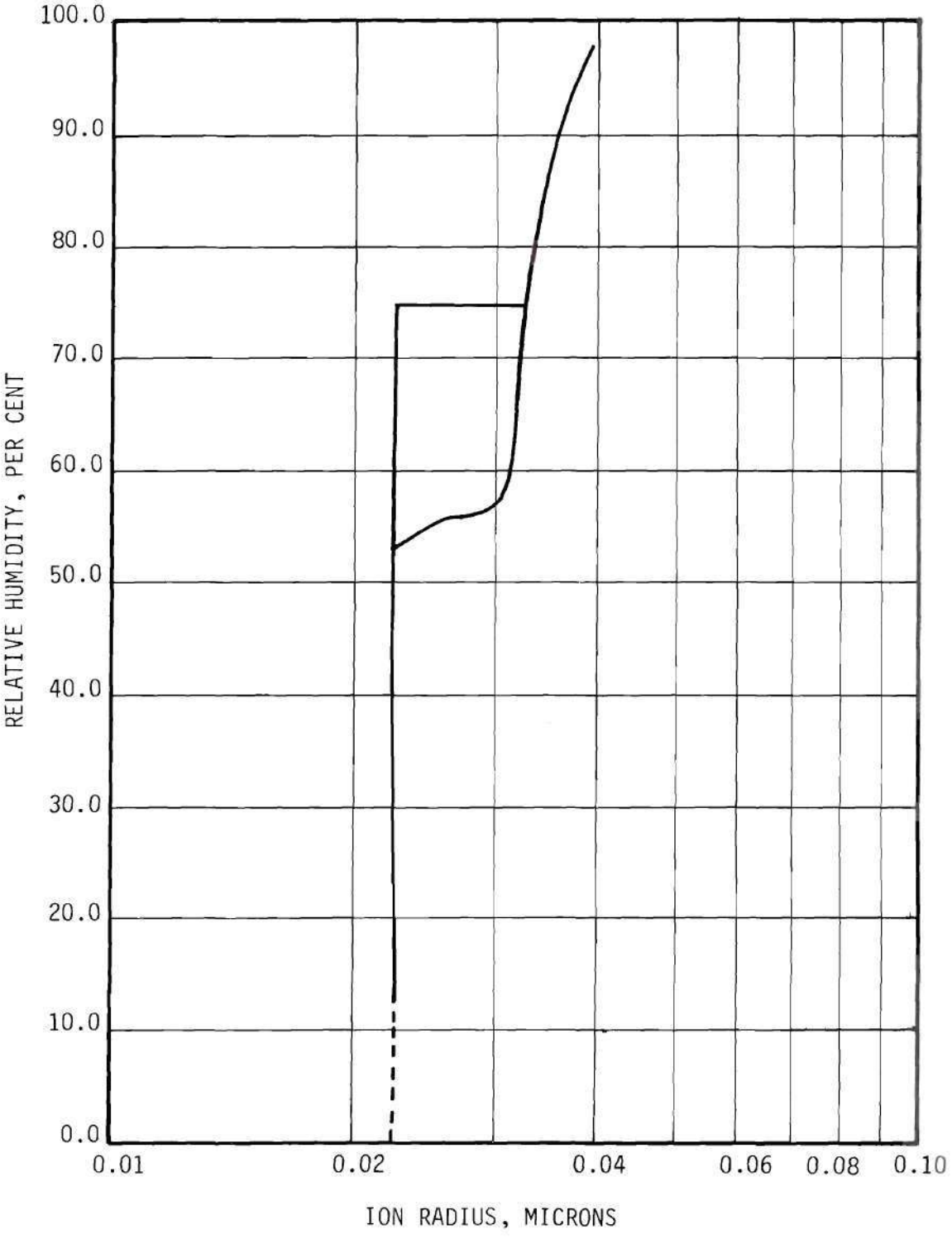

Figure 42. Size Variation of the Mean of the Distribution of a Sodium Chloride Aerosol After a Residence Time of 0.25 Minute at Equilibrium Relative Humidity.

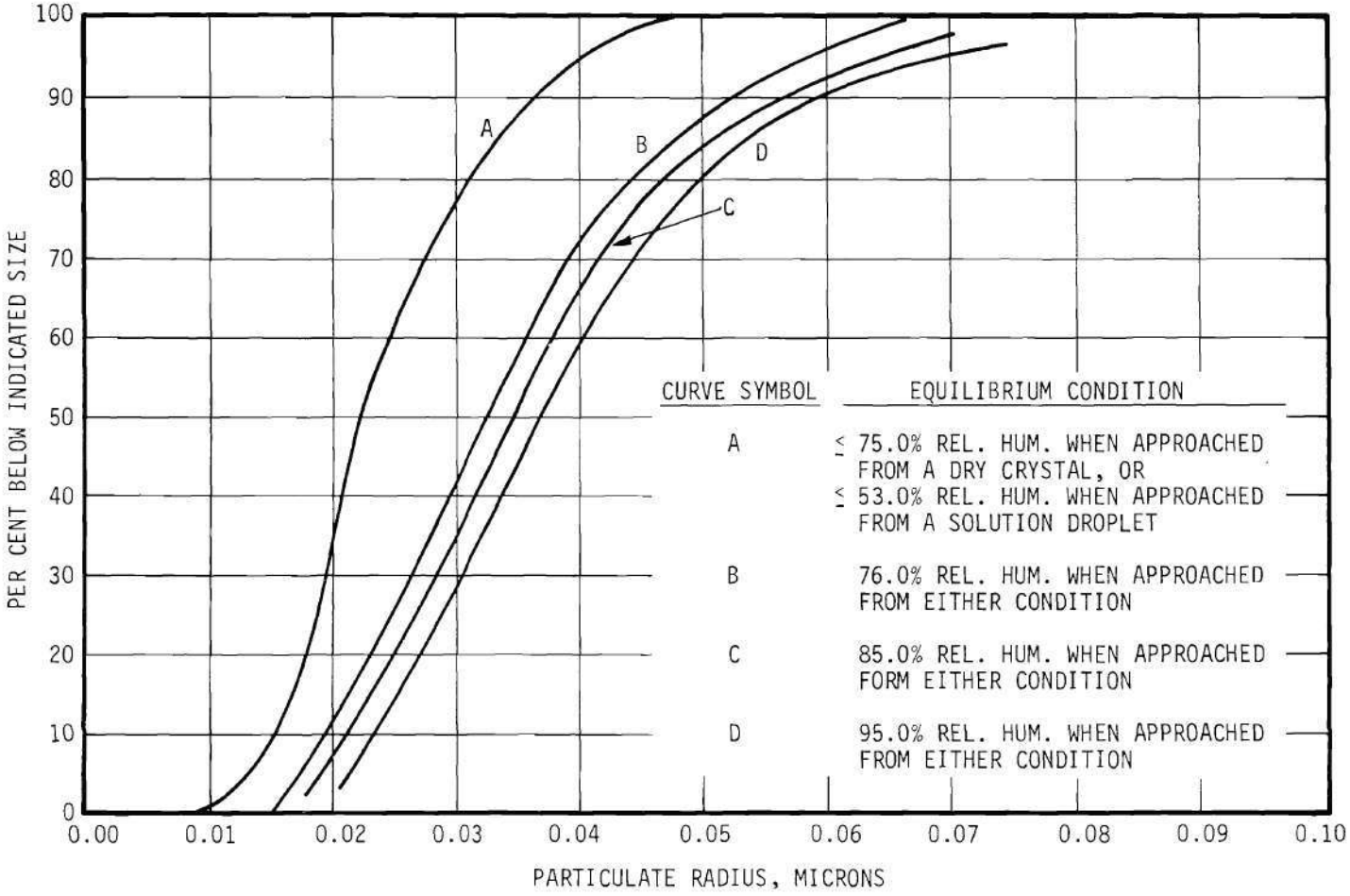

Figure 43. Effect of Increasing Equilibrium Relative Humidity on the Aerosol Size Distribution After a Residence Time of 0.25 Minute.

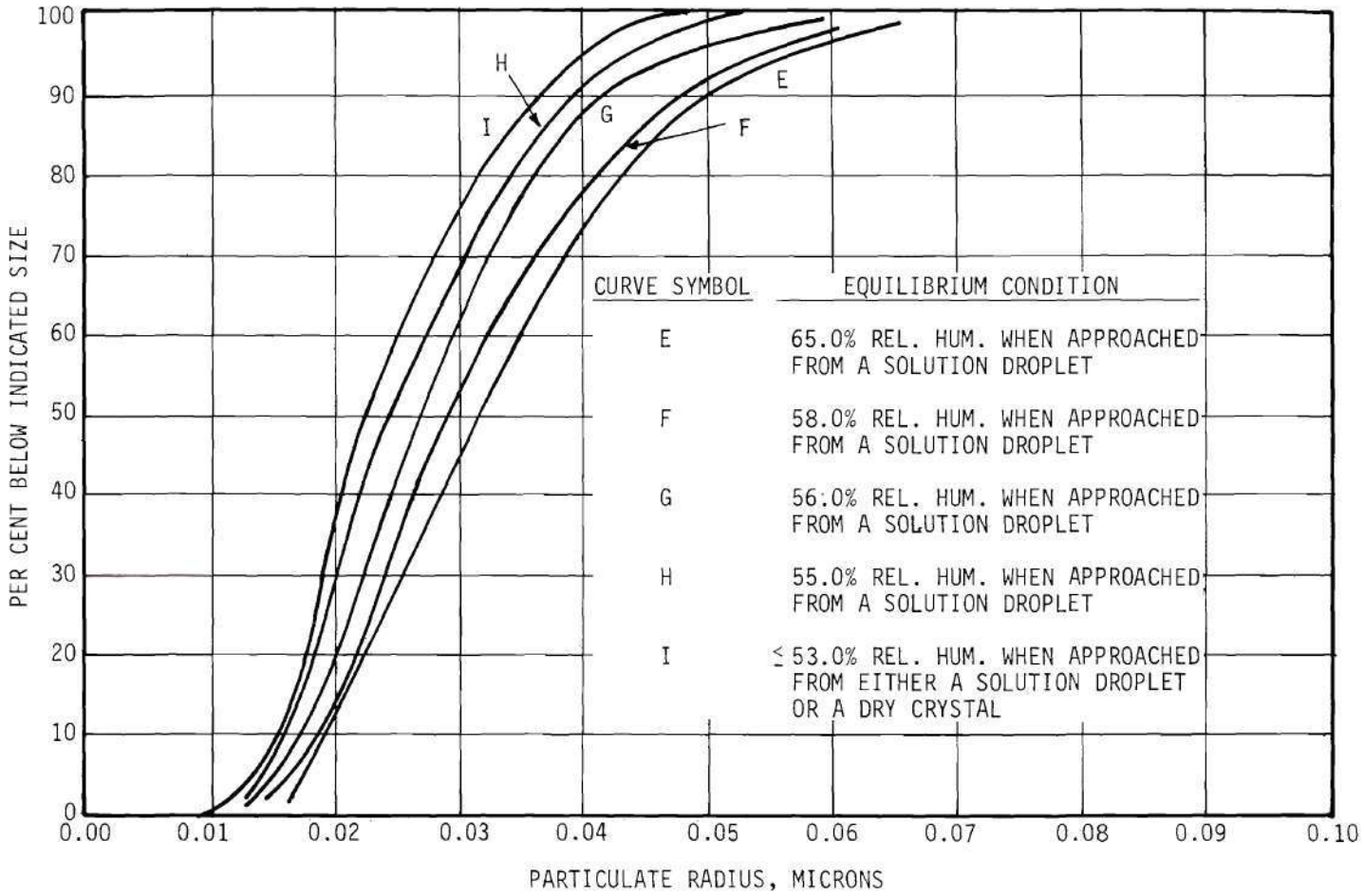

Figure 44. Effect of Decreasing Equilibrium Relative Humidity on the Aerosol Size Distribution After a Residence Time of 0.25 Minute.

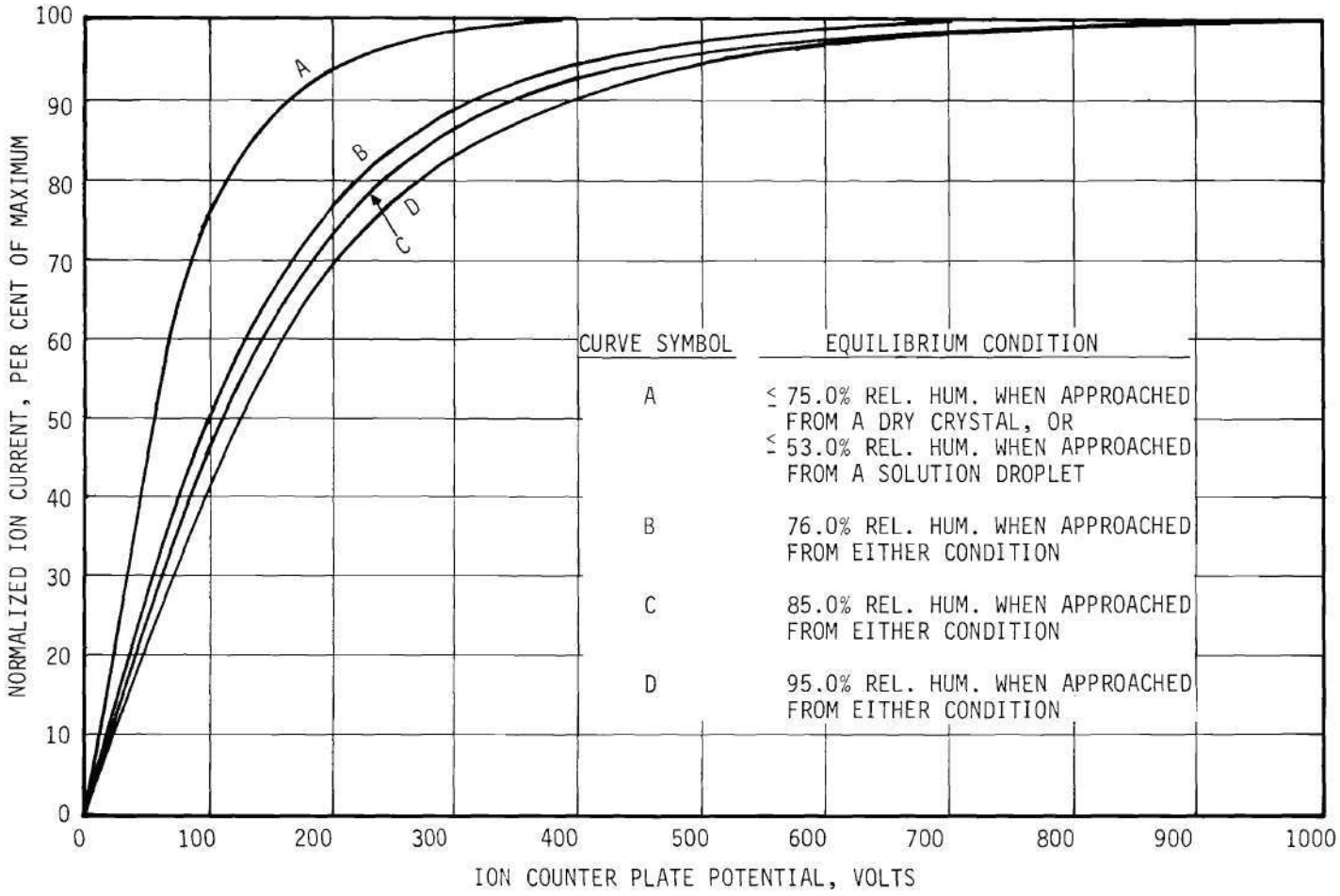

Figure 45. Ion Current Variation with Plate Potential for an Aerosol Residence Time of 0.25 Minute with Increasing Equilibrium Relative Humidity as Parameter.

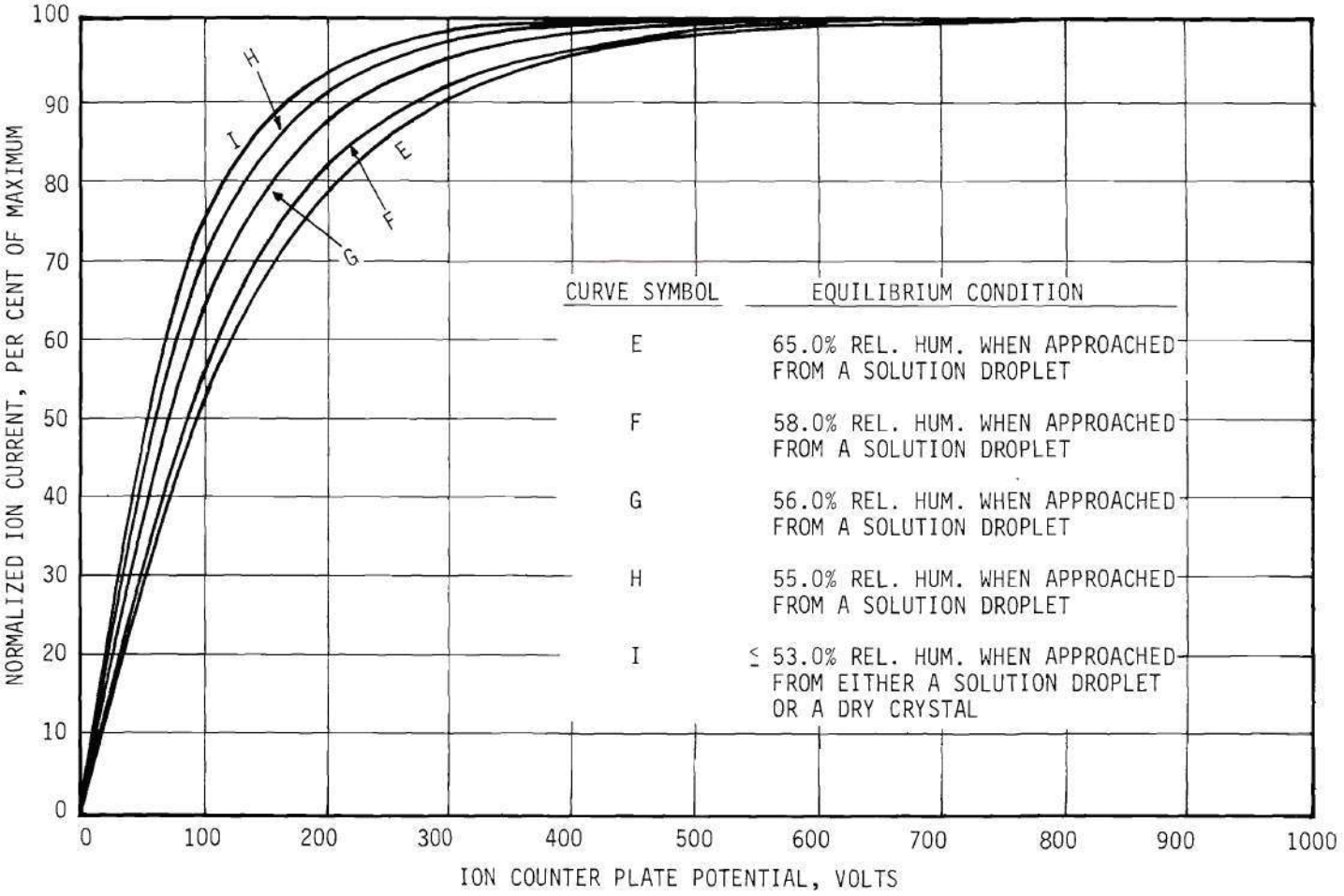

Figure 46. Ion Current Variation with Plate Potential for an Aerosol Residence Time of 0.25 Minute with Decreasing Equilibrium Relative Humidity as Parameter.

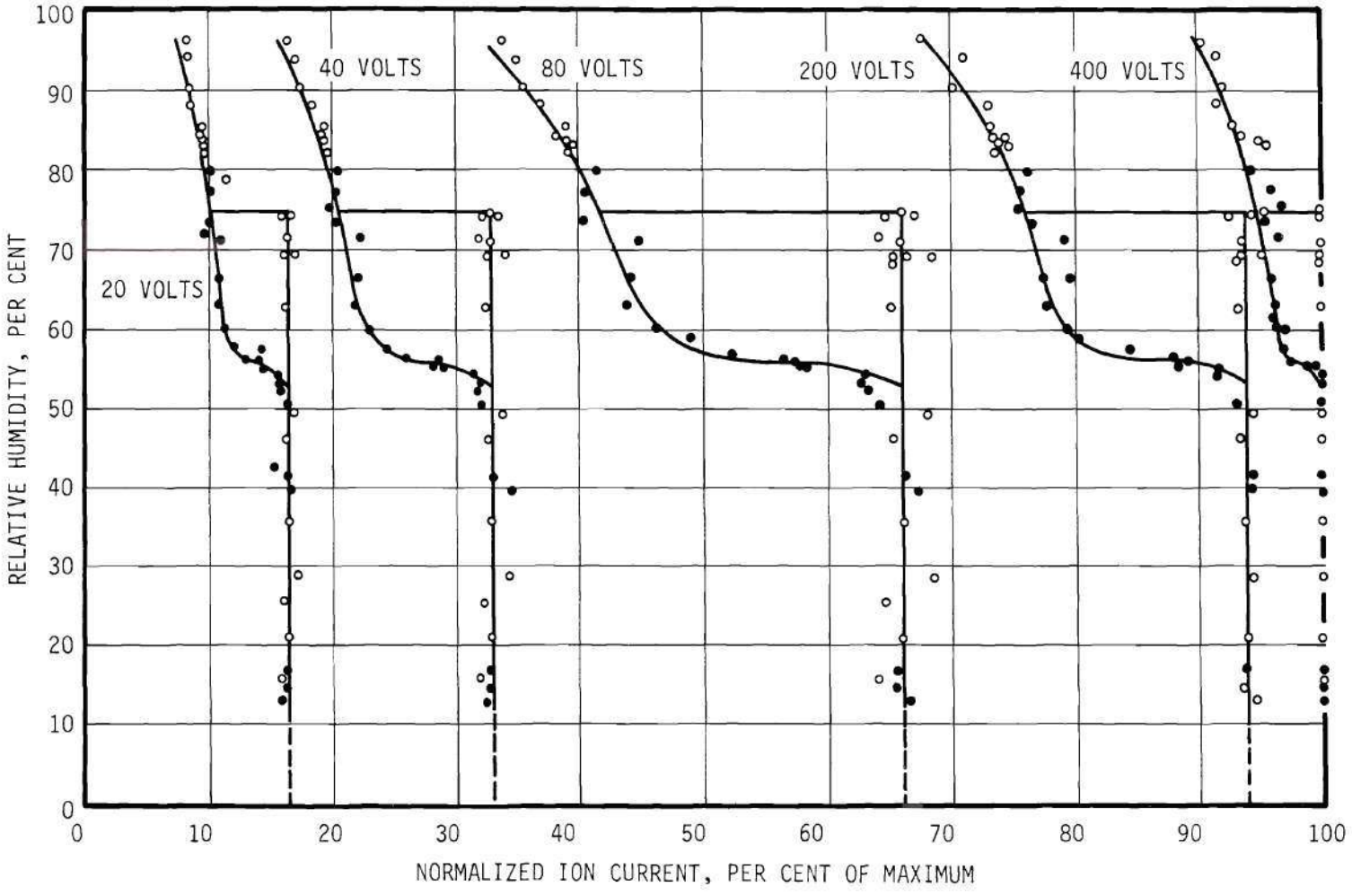

Figure 47. Ion Current Variation with Relative Humidity at a Constant Plate Potential of 20, 40, 80, 200 and 400 Volts for an Aerosol Residence Time of 0.25 Minute.

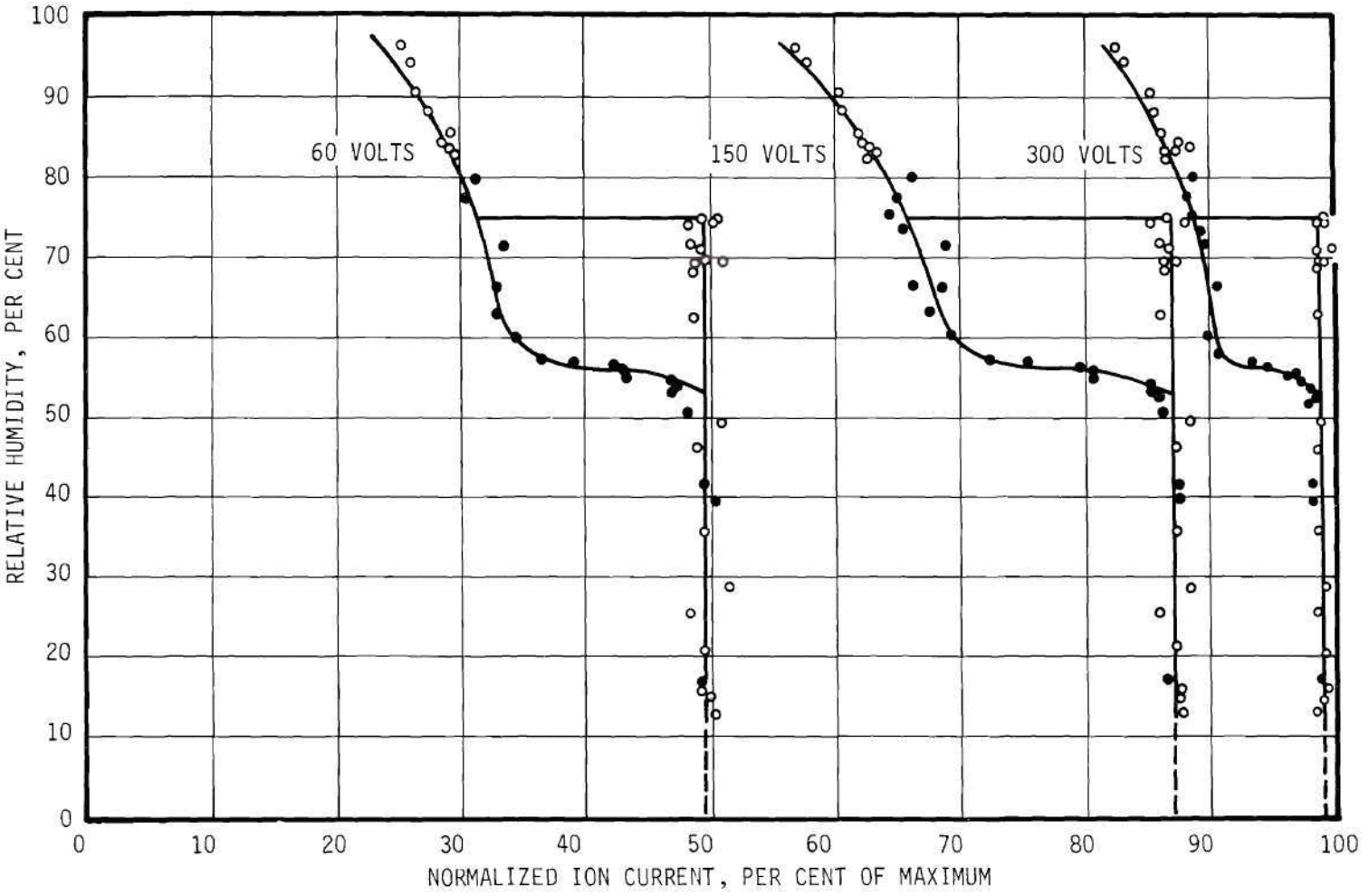

Figure 48. Ion Current Variation with Relative Humidity at a Constant Plate Potential of 60, 150 and 300 Volts for an Aerosol Residence Time of 0.25 Minute.

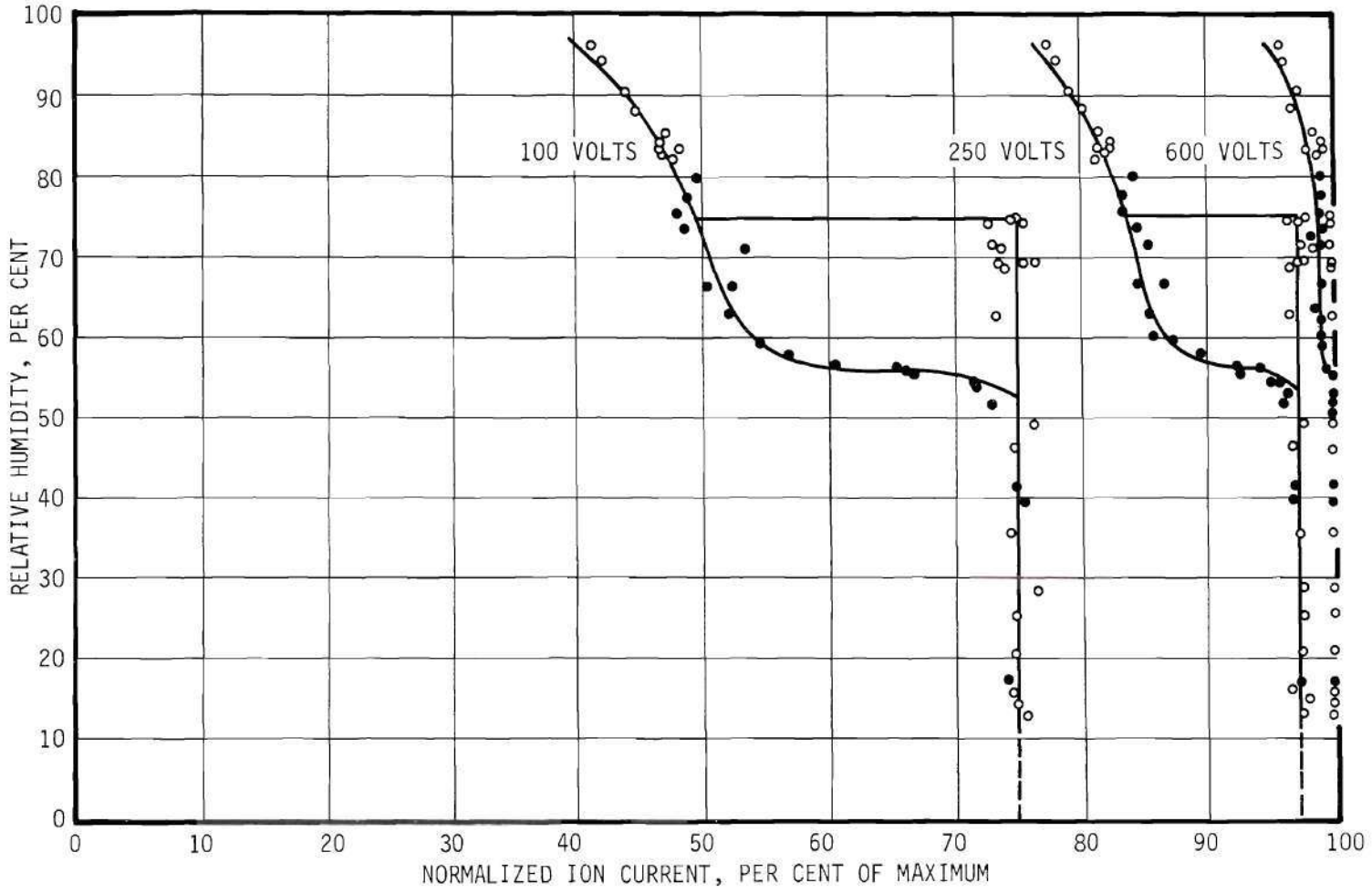

Figure 49. Ion Current Variation with Relative Humidity at a Constant Plate Potential of 100, 250 and 600 Volts for an Aerosol Residence Time of 0.25 Minute.

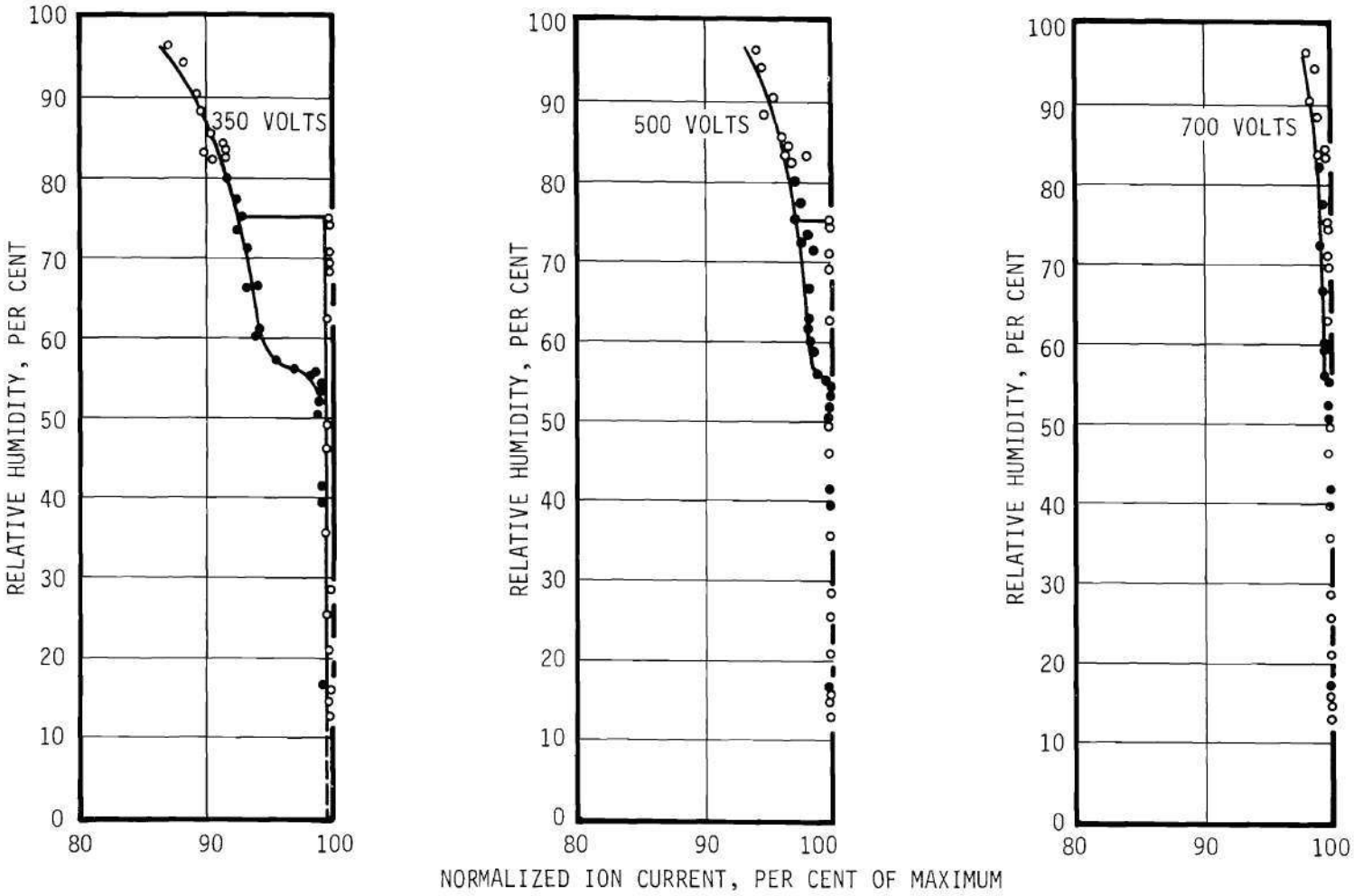

Figure 50. Ion Current Variation with Relative Humidity at a Constant Plate Potential of 350, 500 and 700 Volts for an Aerosol Residence Time of 0.25 Minute.

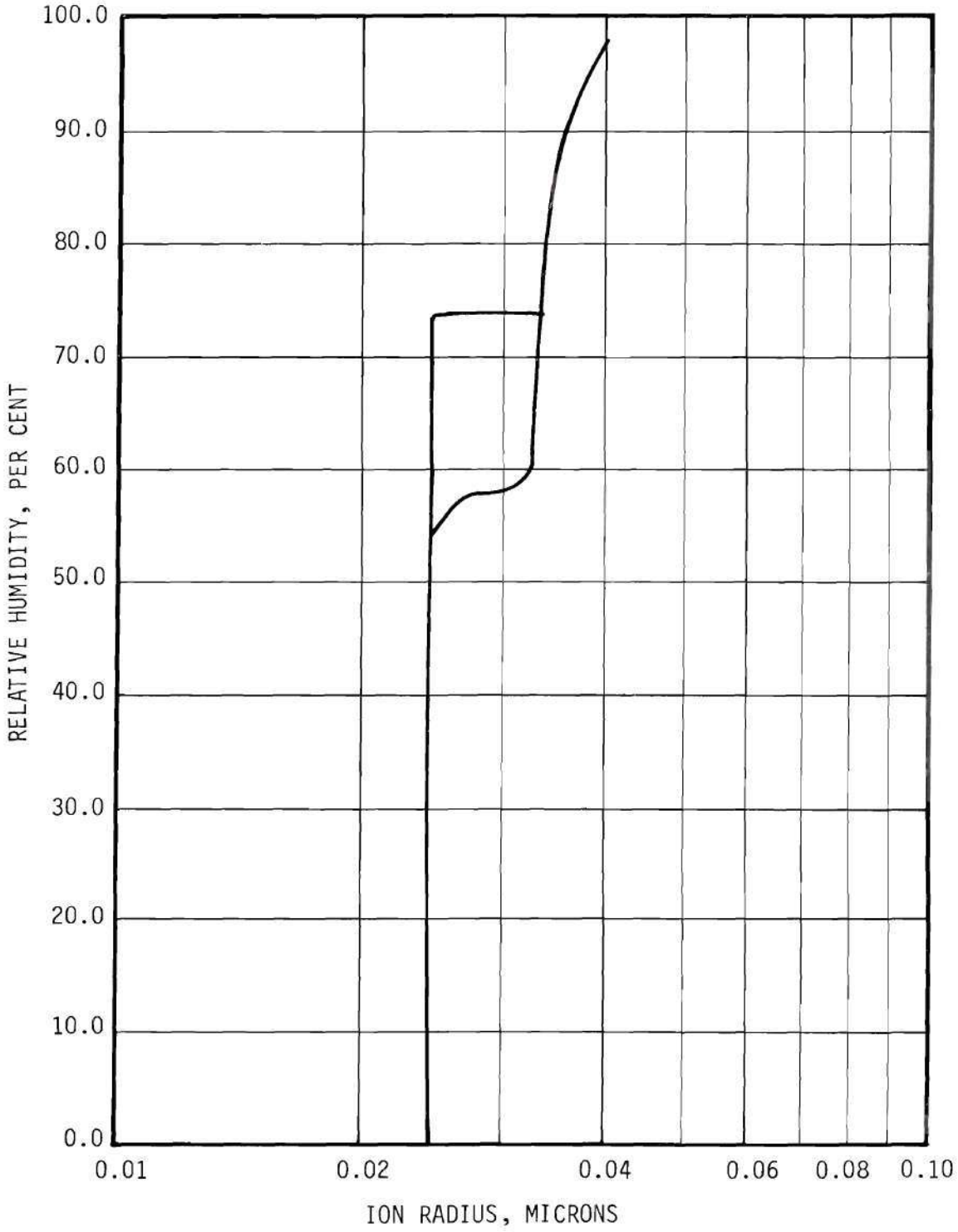

Figure 51. Size Variation of the Mean of the Distribution of a Sodium Chloride Aerosol After a Residence Time of 2.45 Minutes at Equilibrium Relative Humidity.

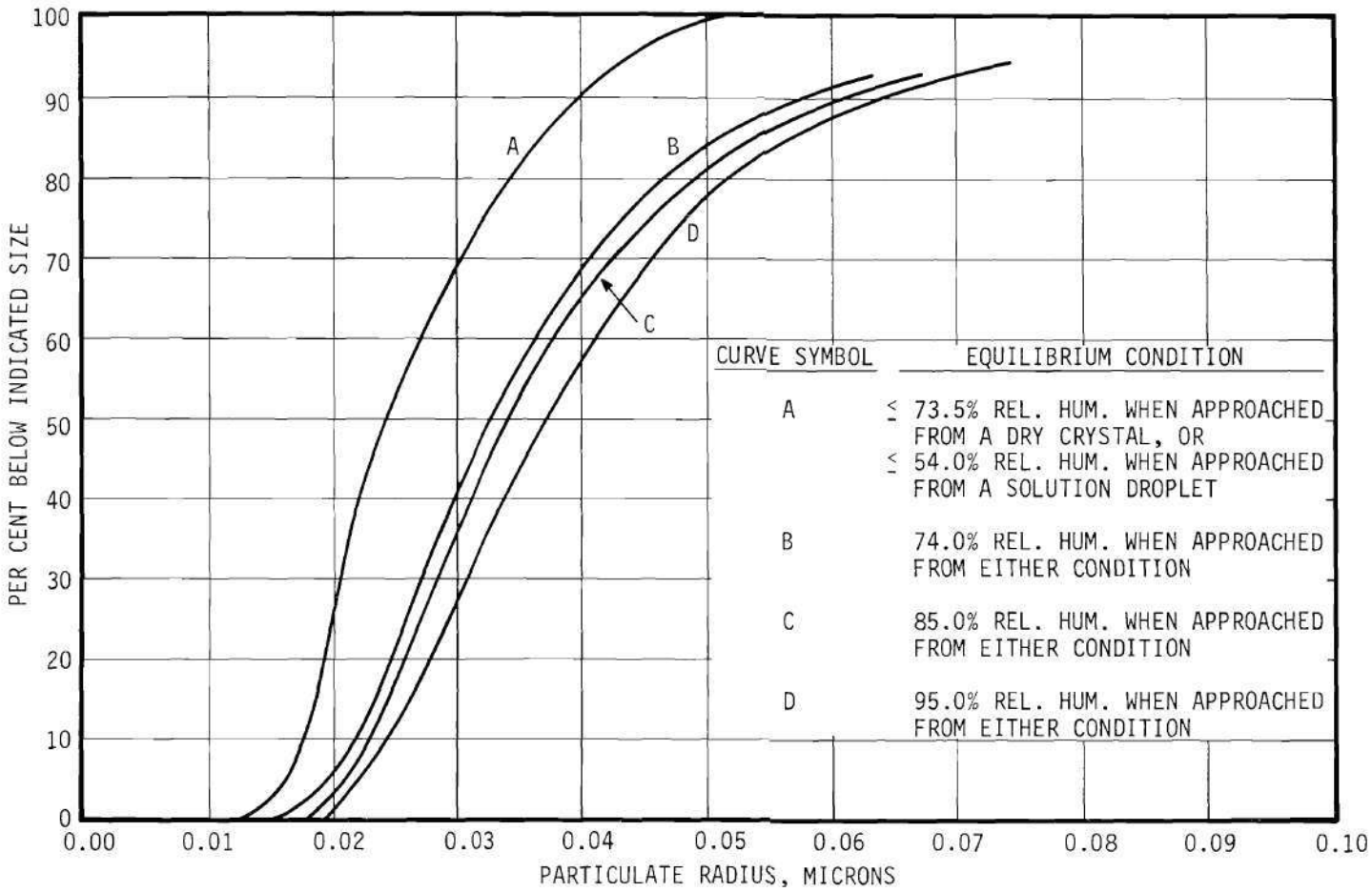

Figure 52. Effect of Decreasing Equilibrium Relative Humidity on the Aerosol Size Distribution After a Residence Time of 2.45 Minutes.

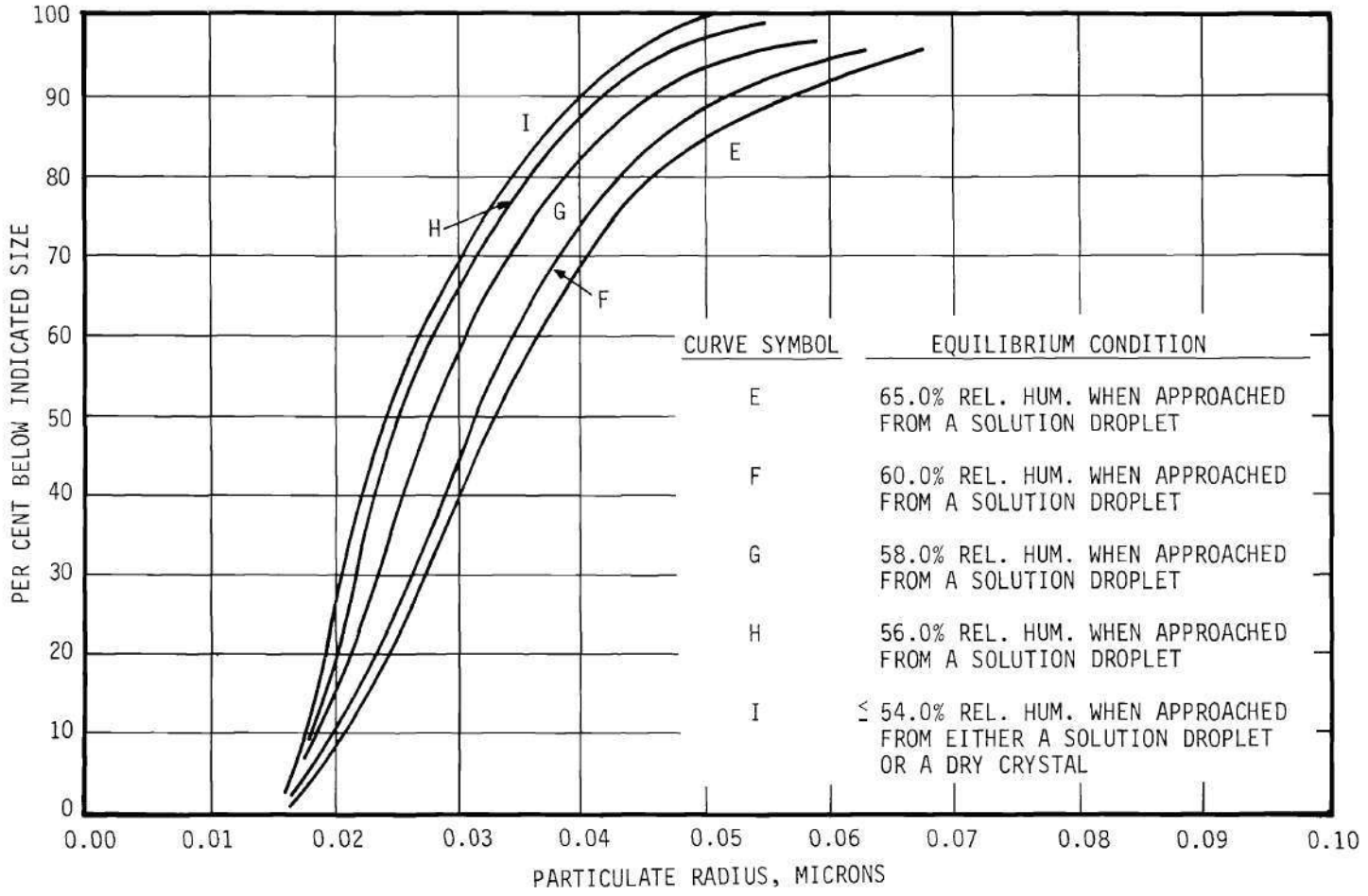

Figure 53. Effect of Decreasing Equilibrium Relative Humidity on the Aerosol Size Distribution After a Residence Time of 2.45 Minutes.

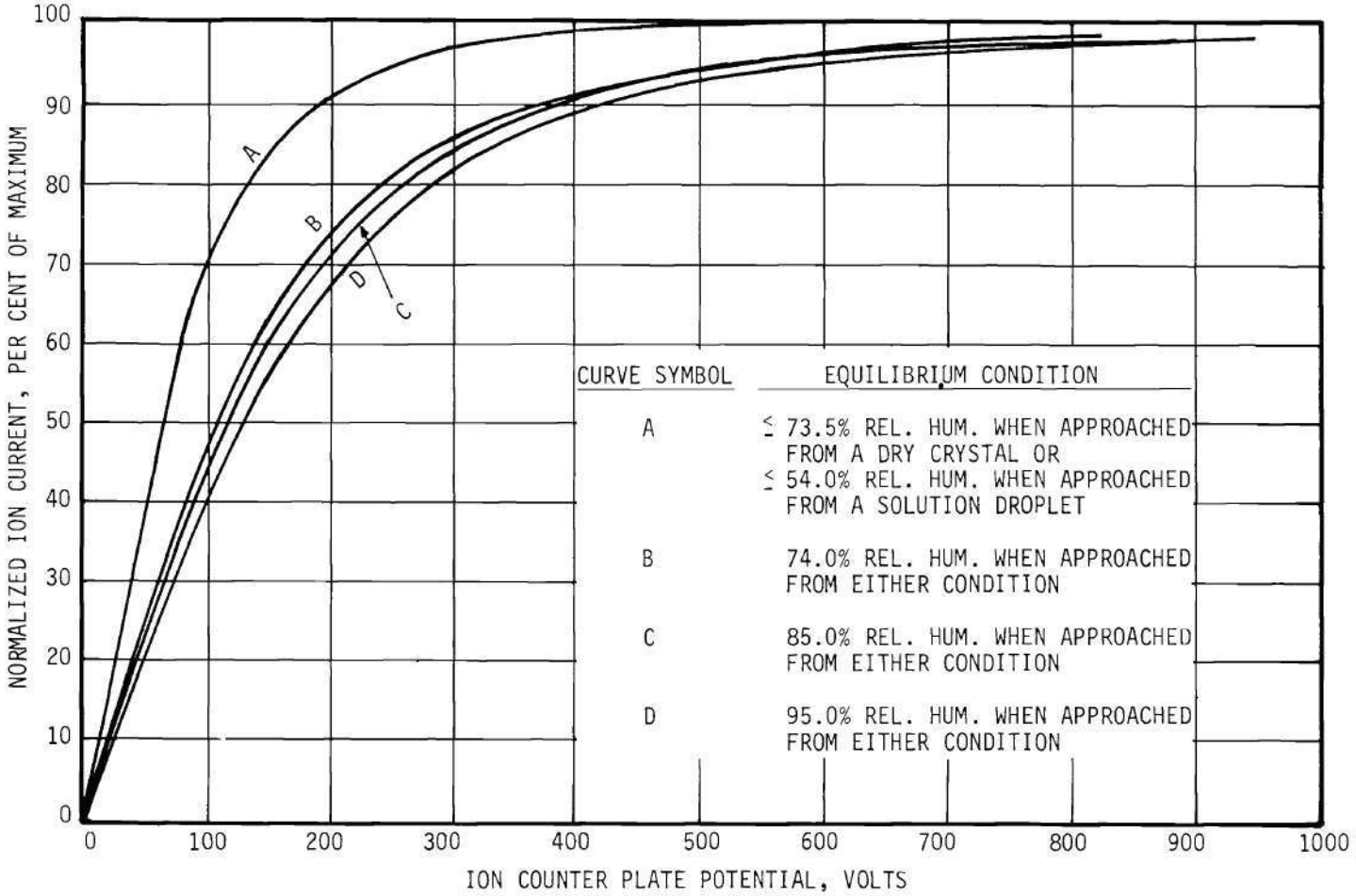

Figure 54. Ion Current Variation with Plate Potential for an Aerosol Residence Time of 2.45 Minutes with Increasing Equilibrium Relative Humidity as Parameter.

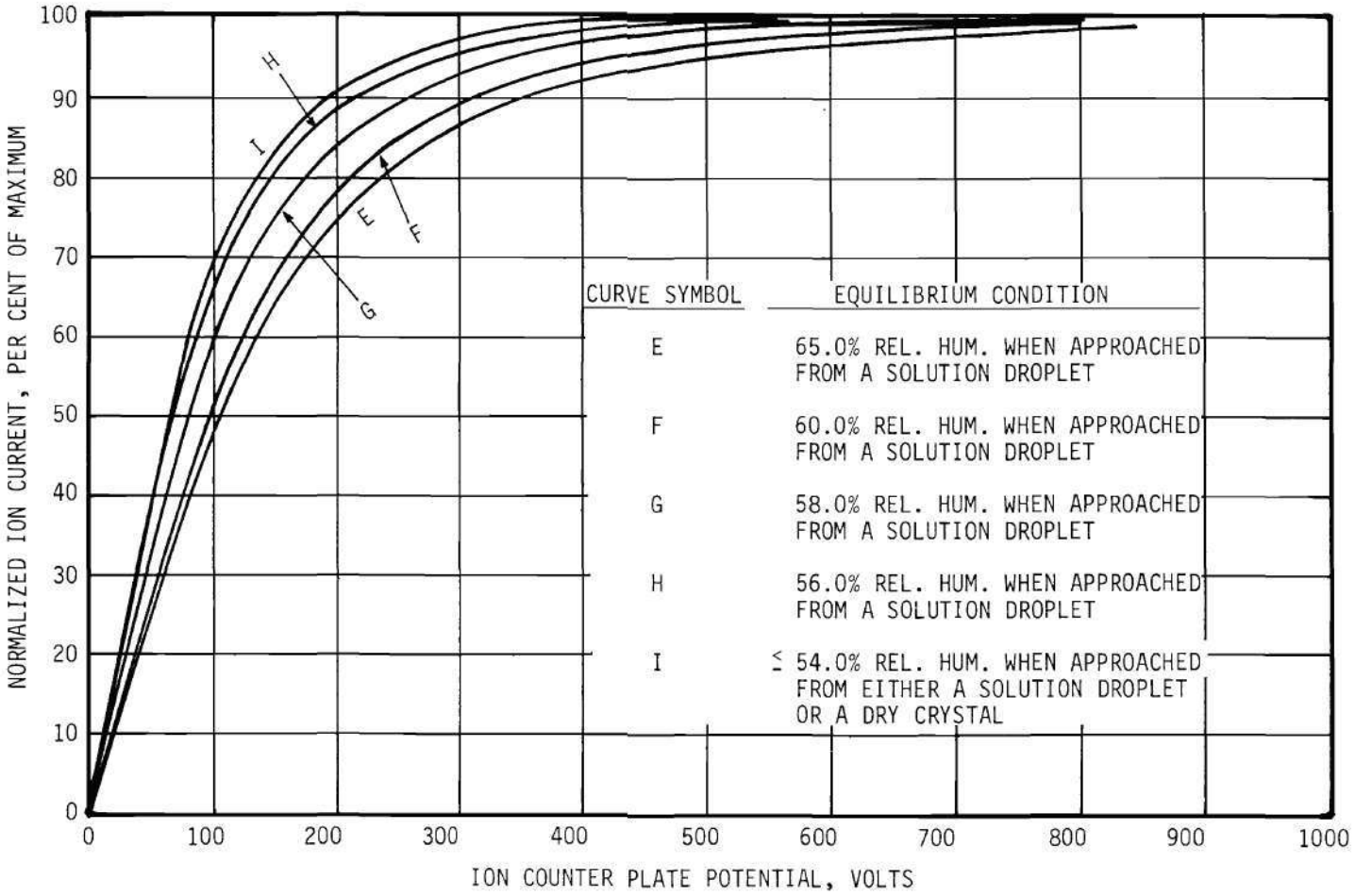

Figure 55. Ion Current Variation with Plate Potential for an Aerosol Residence Time of 2.45 Minutes with Decreasing Equilibrium Relative Humidity as Parameter.

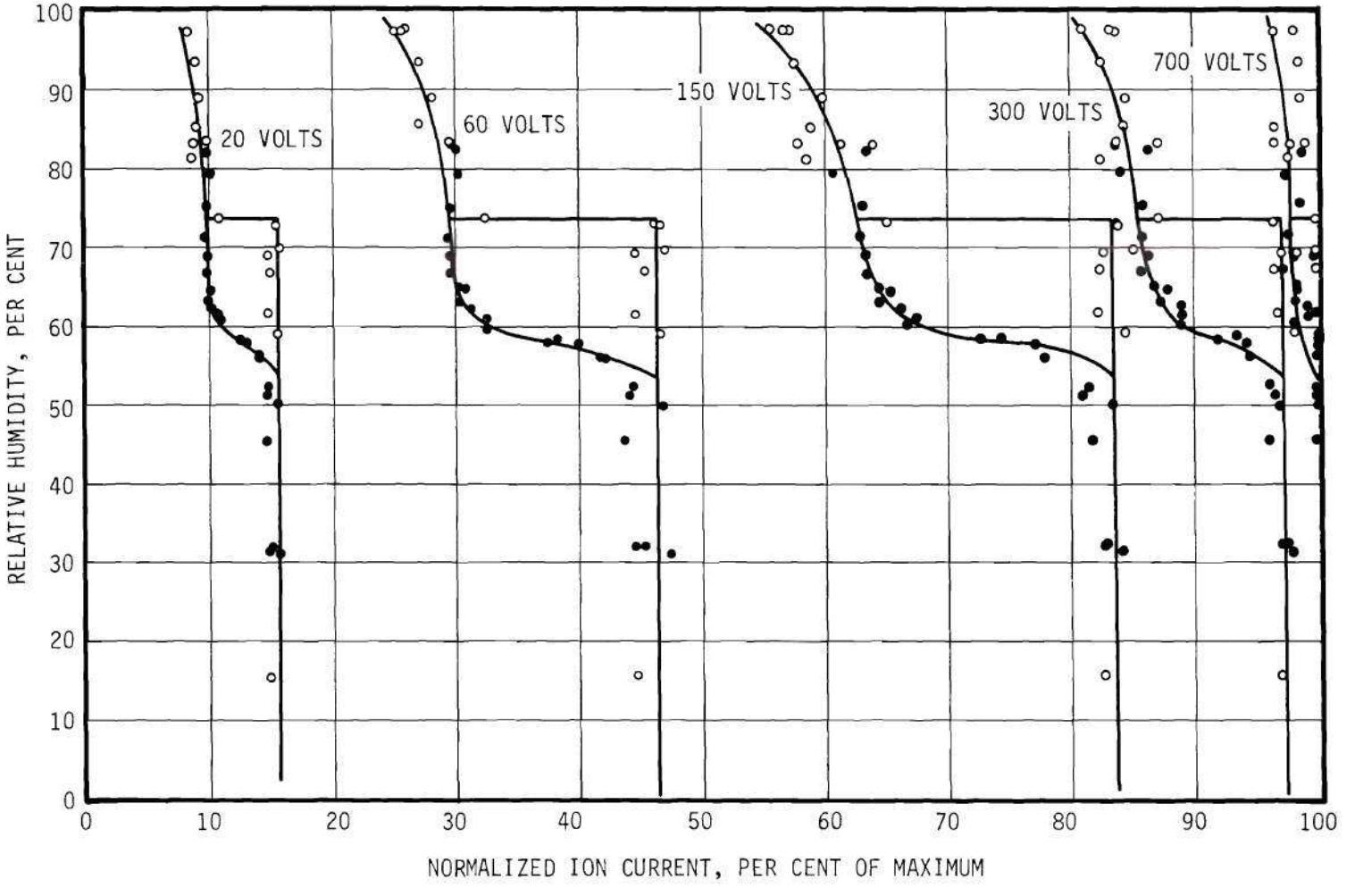

Figure 56. Ion Current Variation with Relative Humidity at a Constant Plate Potential of 20, 60, 150, 300 and 700 Volts for an Aerosol Residence Time of 2.45 Minutes.

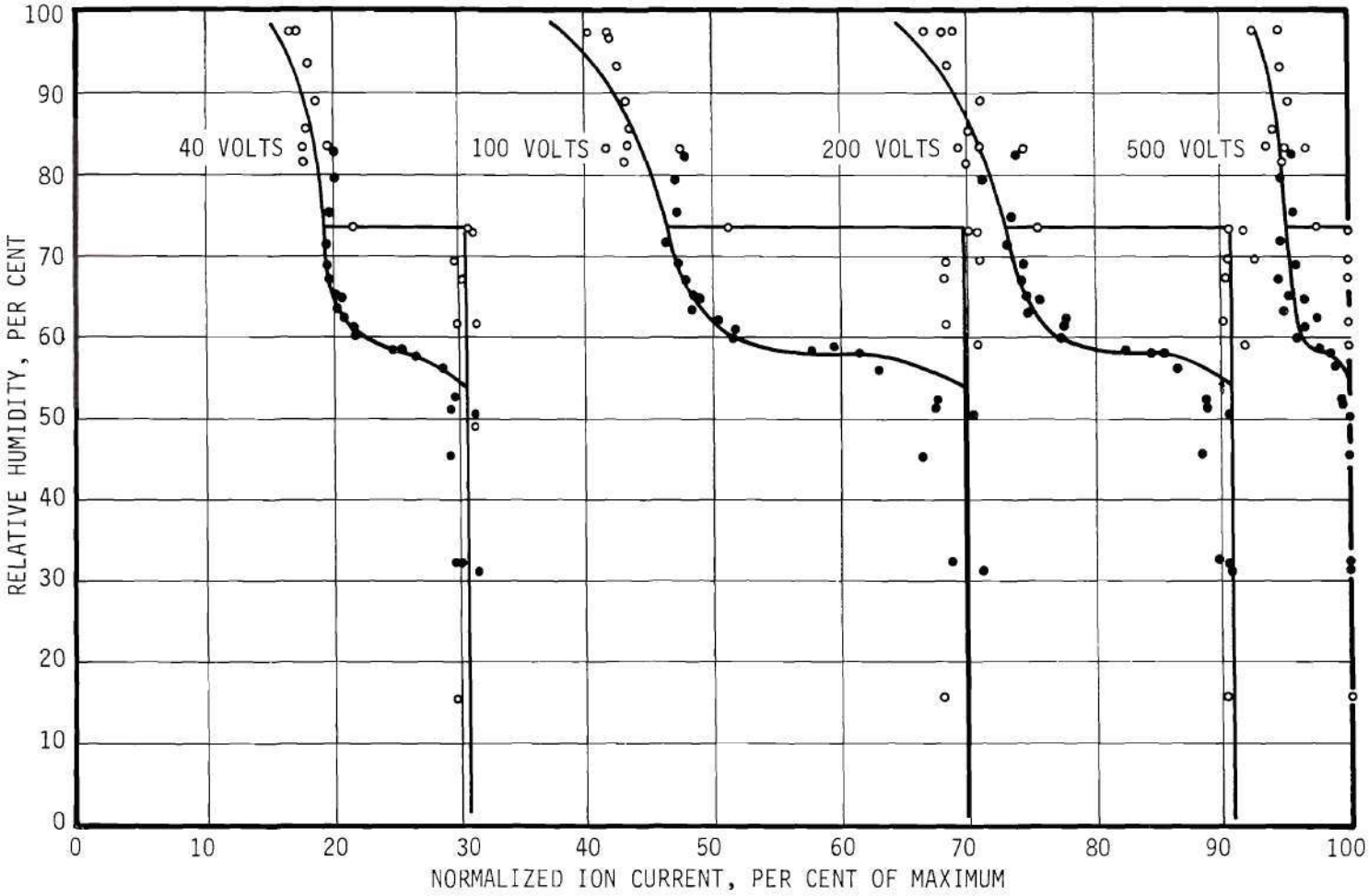

Figure 57. Ion Current Variation with Relative Humidity at a Constant Plate Potential of 40, 100, 200 and 500 Volts for an Aerosol Residence Time of 2.45 Minutes.

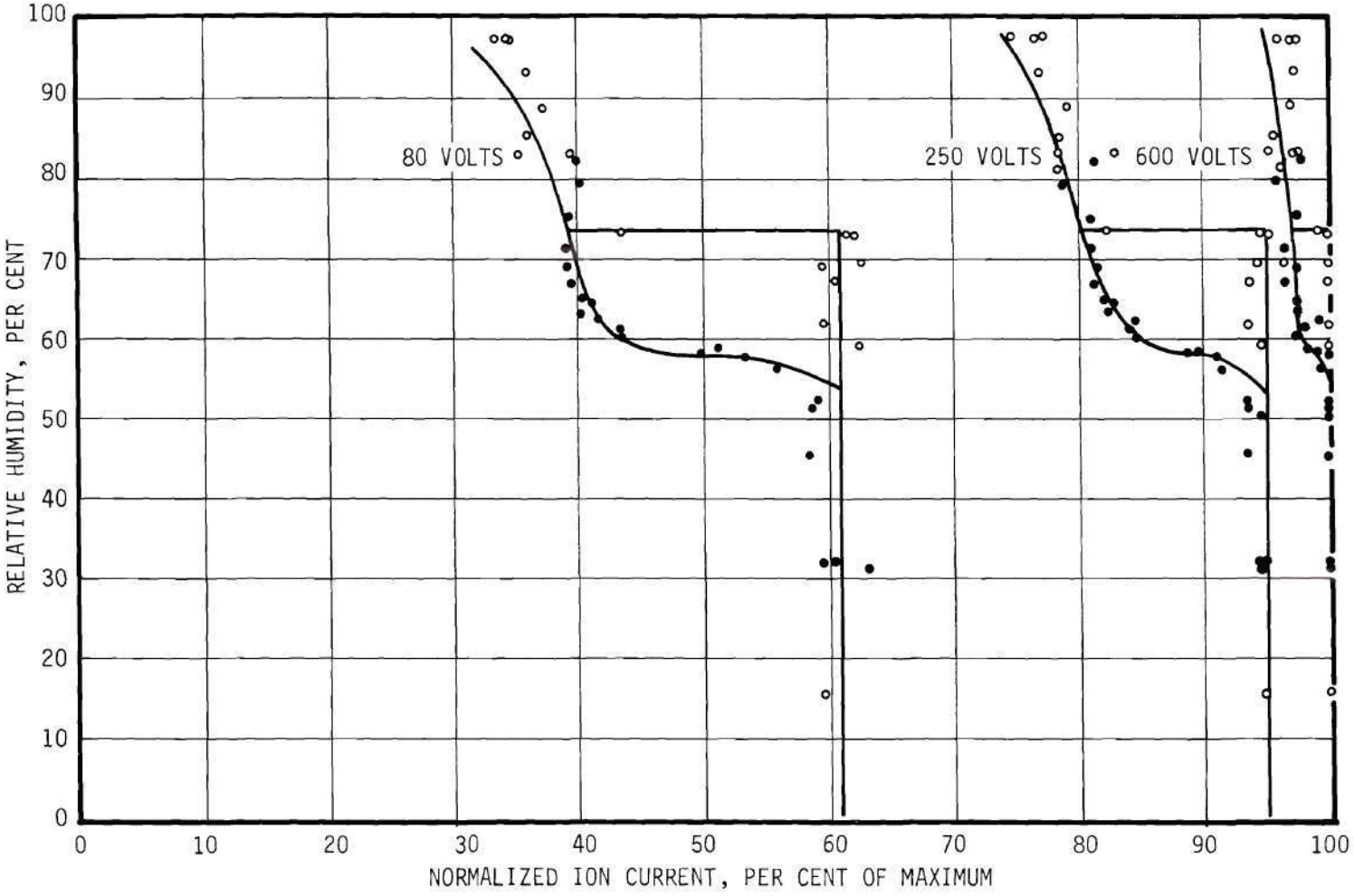

Figure 58. Ion Current Variation with Relative Humidity at a Constant Plate Potential of 80, 250 and 600 Volts for an Aerosol Residence Time of 2.45 Minutes

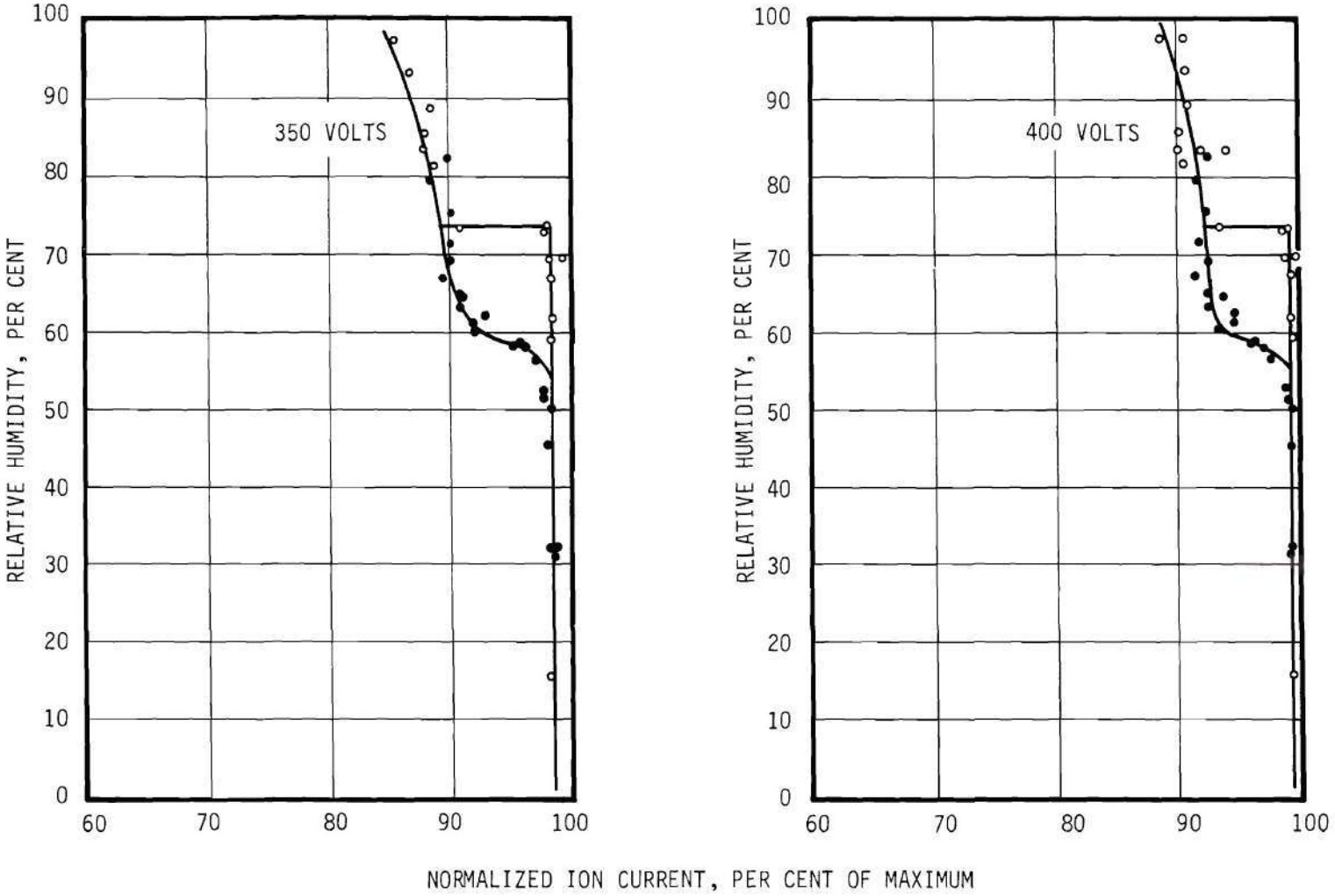

Figure 59. Ion Current Variation with Relative Humidity at a Constant Plate Potential of 350 and 400 Volts for an Aerosol Residence Time of 2.45 Minutes.

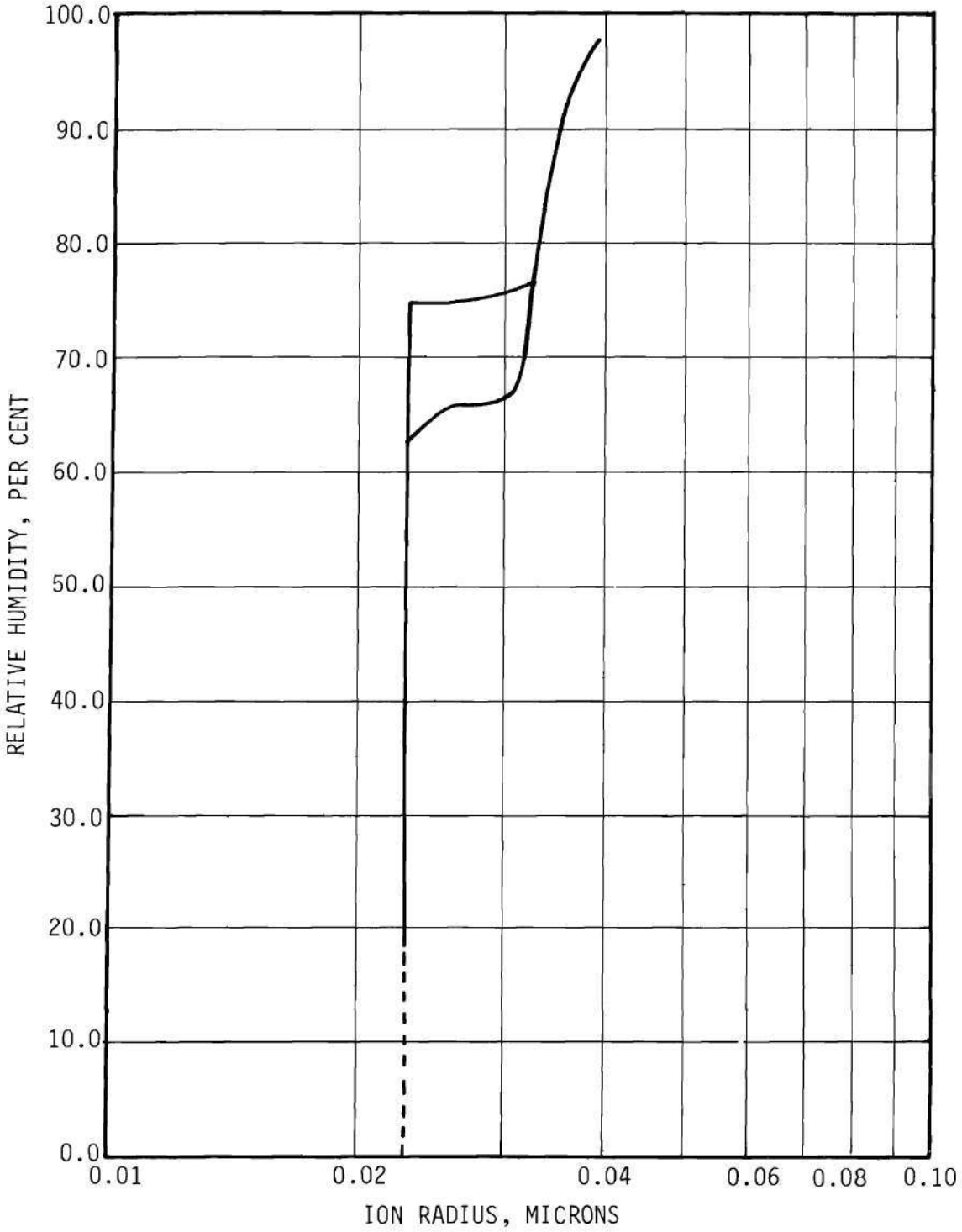

Figure 60. Size Variation of the Mean of the Distribution of a Sodium Chloride Aerosol After a Residence Time of 3.85 Minutes at Equilibrium Relative Humidity.

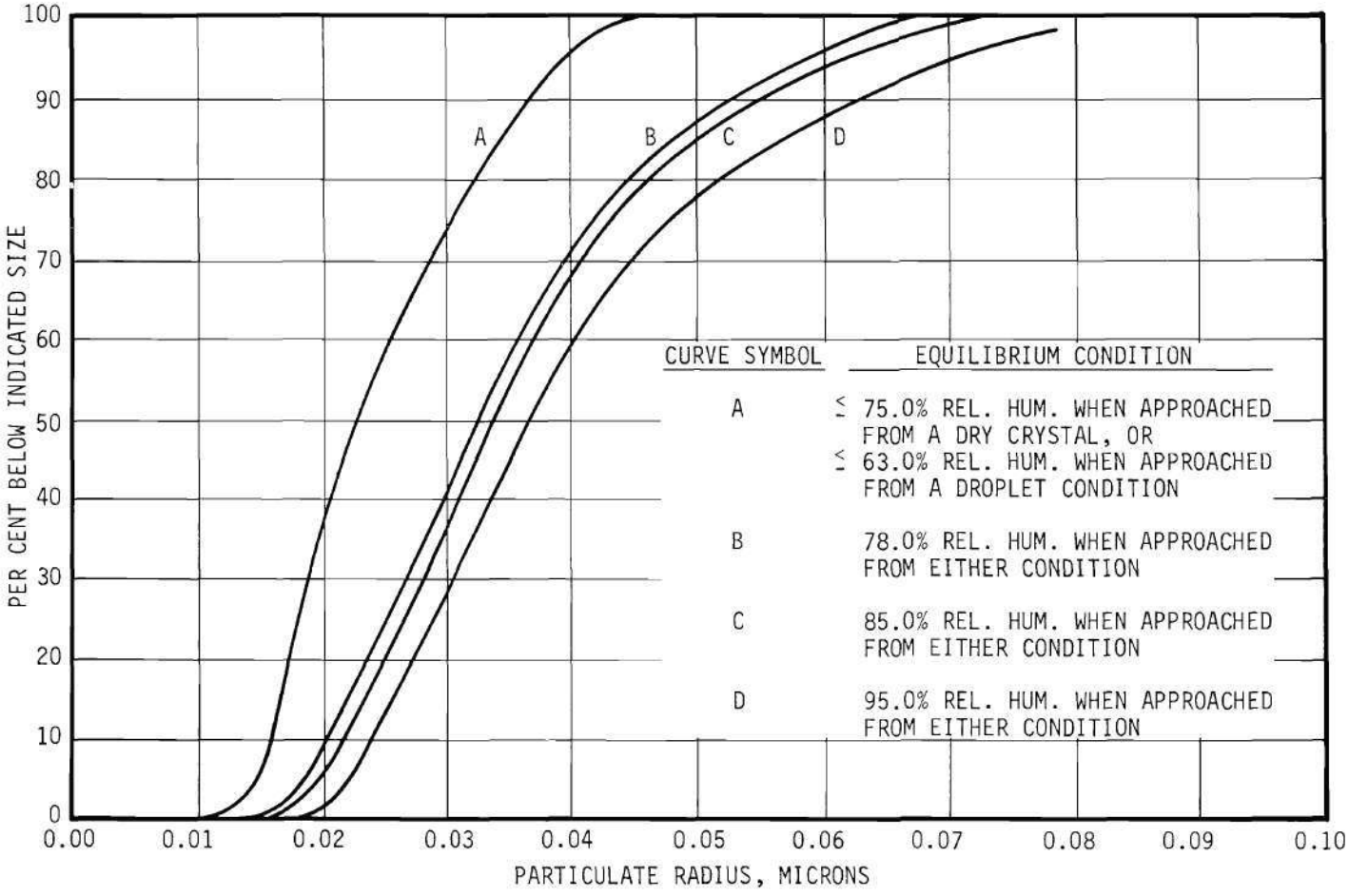

Figure 61. Effect of Increasing Equilibrium Relative Humidity on the Aerosol Size Distribution After a Residence Time of 3.85 Minutes.

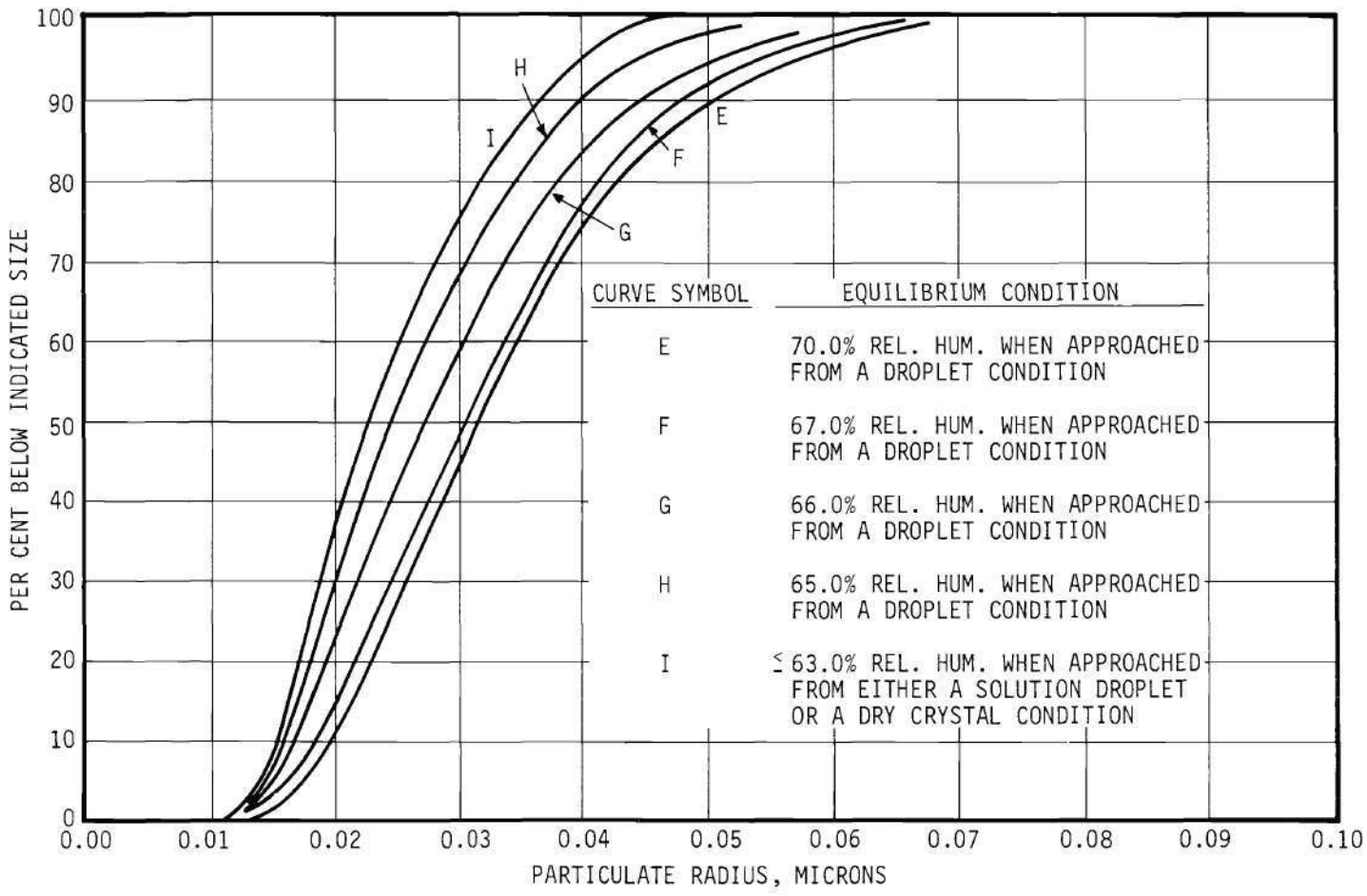

Figure 62. Effect of Decreasing Equilibrium Relative Humidity on the Aerosol Size Distribution After a Residence Time of 3.85 Minutes.

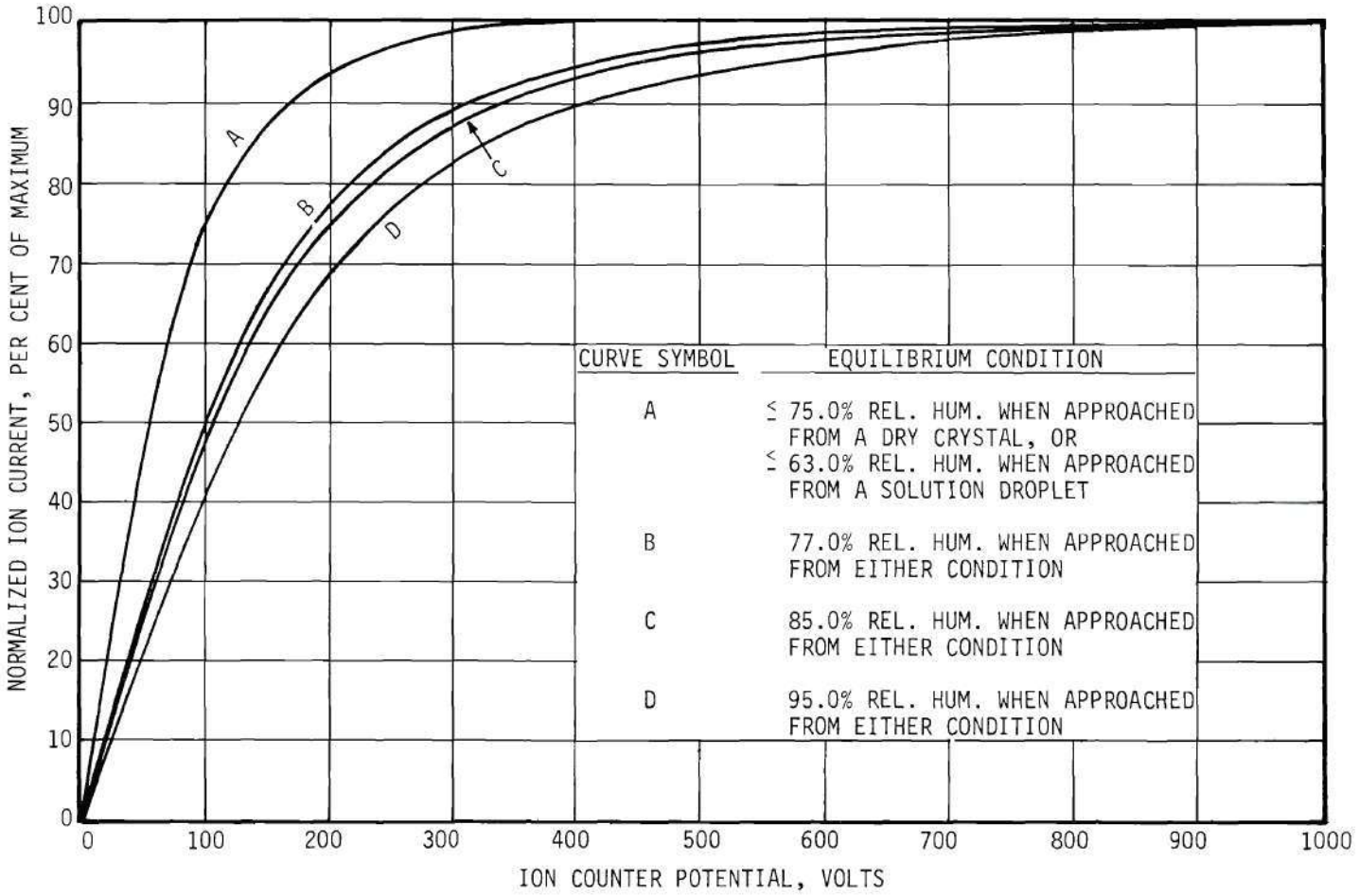

Figure 63. Ion Current Variation with Plate Potential for an Aerosol Residence Time of 3.85 Minutes with Increasing Equilibrium Relative Humidity as Parameter.

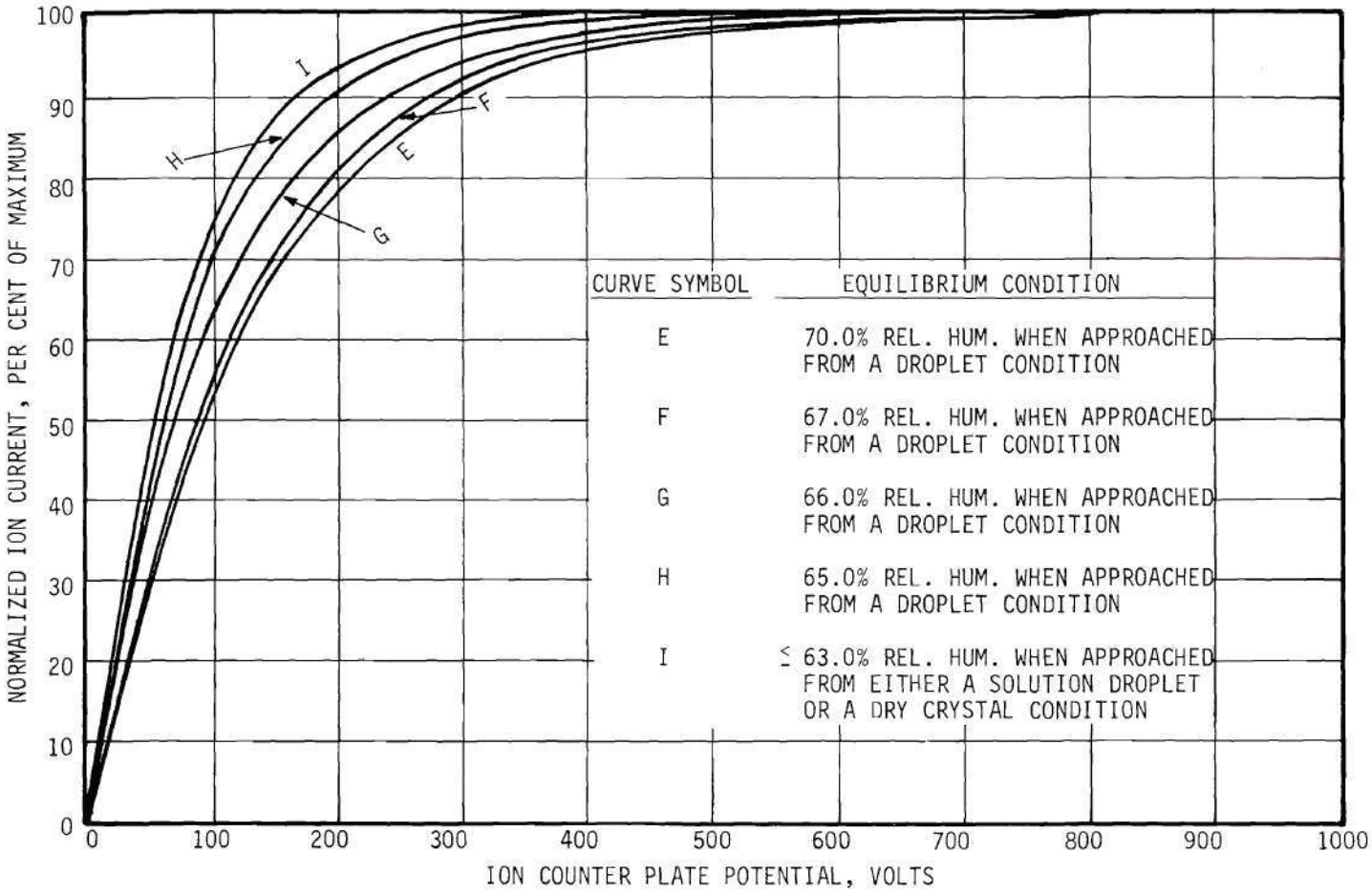

Figure 64. Ion Current Variation with Plate Potential for an Aerosol Residence Time of 3.85 Minutes with Decreasing Equilibrium Relative Humidity as Parameter.

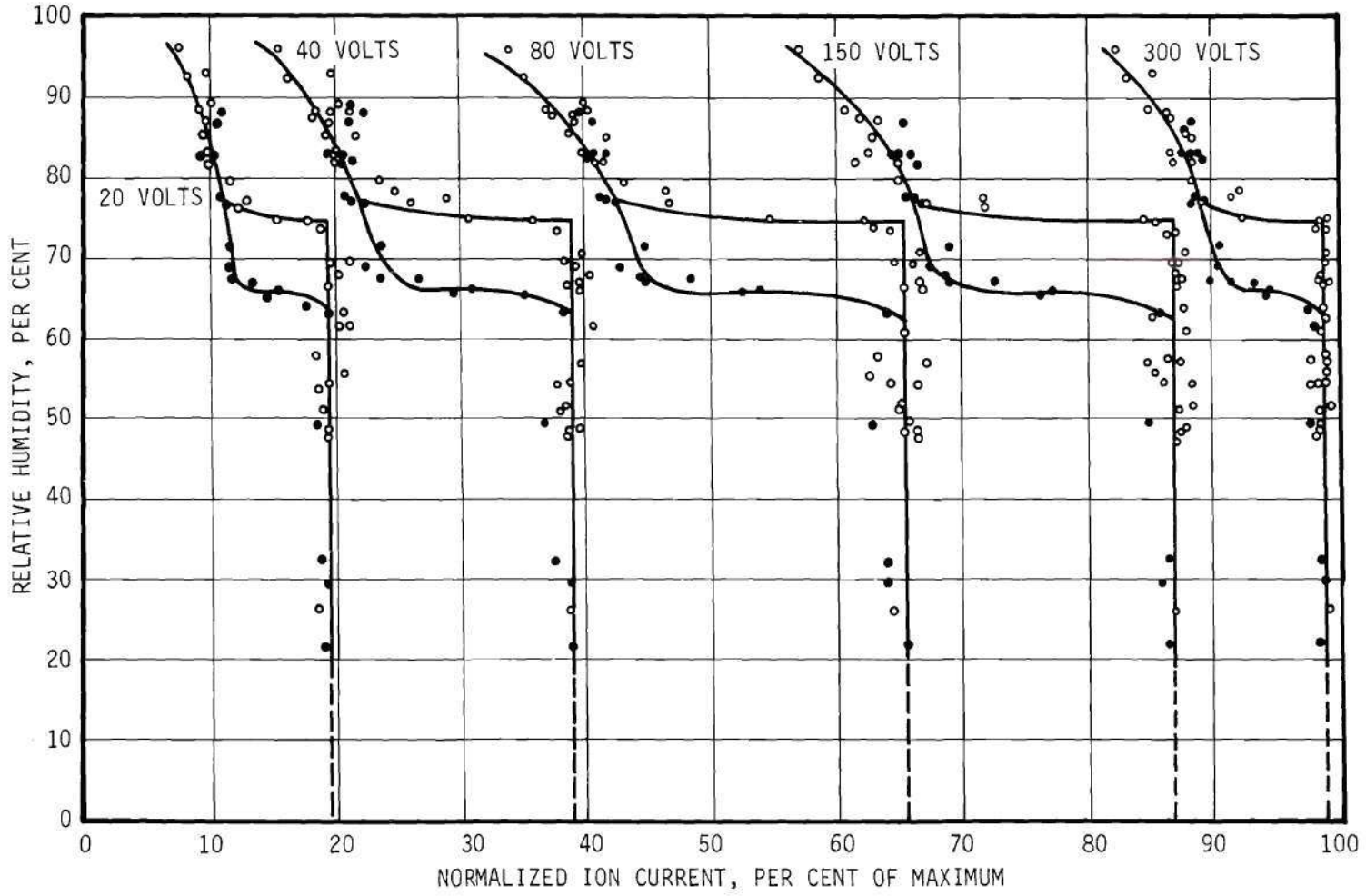

Figure 65. Ion Current Variation with Relative Humidity at a Constant Plate Potential of 20, 40, 80, 150 and 300 Volts for an Aerosol Residence Time of 3.85 Minutes.

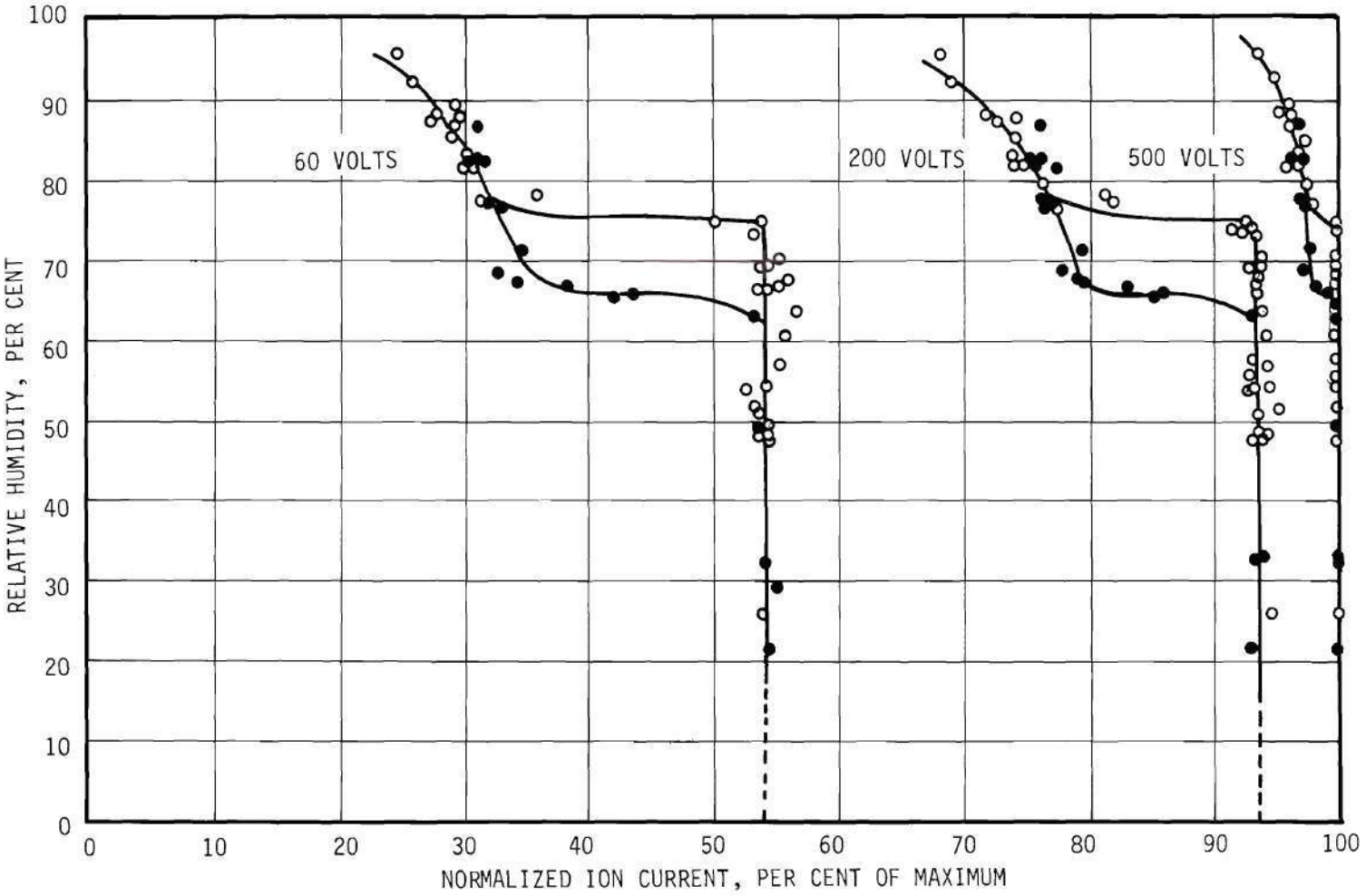

Figure 66. Ion Current Variation with Relative Humidity at a Constant Plate Potential of 60, 200 and 500 Volts for an Aerosol Residence Time of 3.85 Minutes.

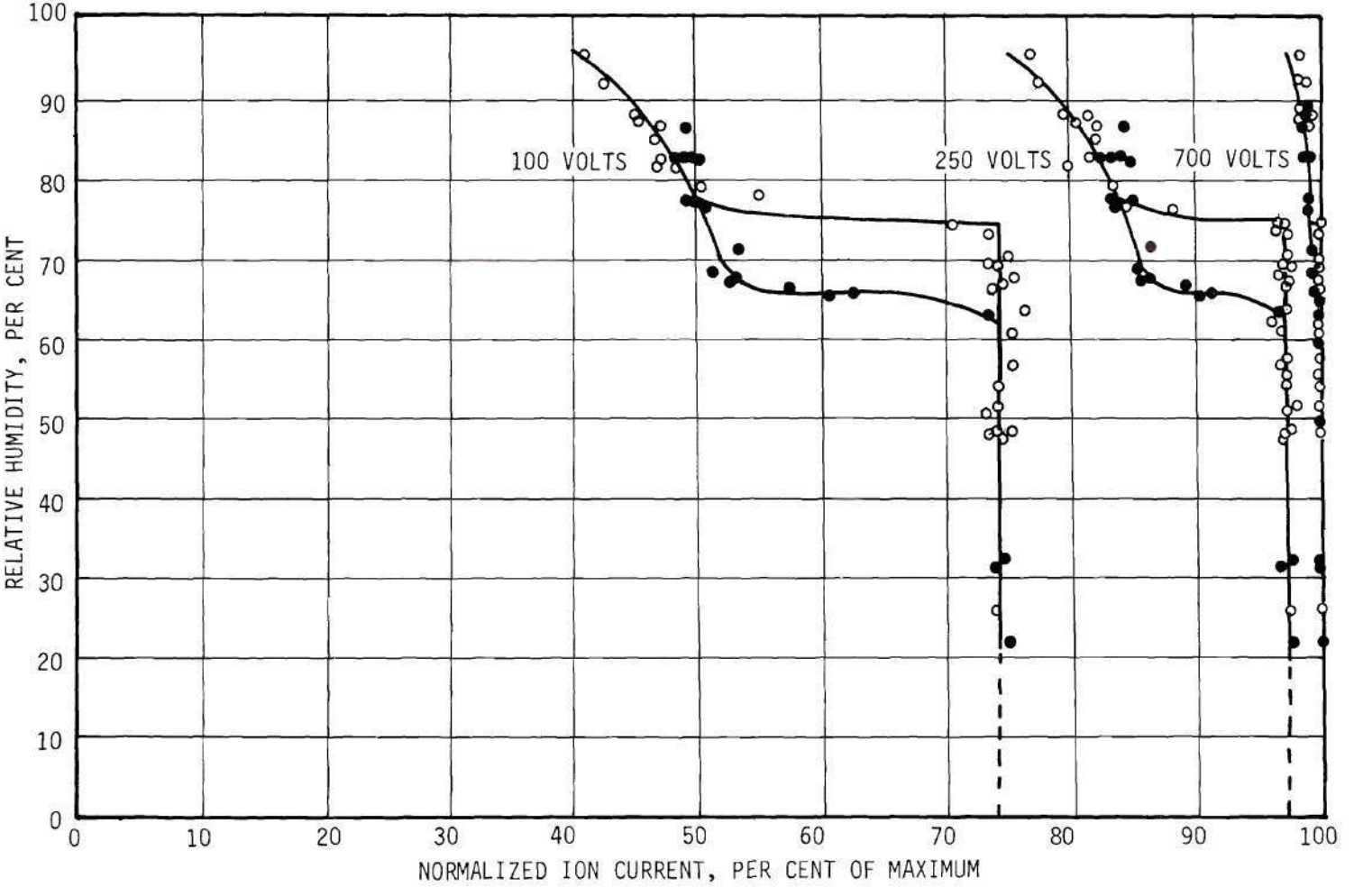

Figure 67. Ion Current Variation with Relative Humidity at a Constant Plate Potential of 100, 250 and 700 Volts for an Aerosol Residence Time of 3.85 Minutes.

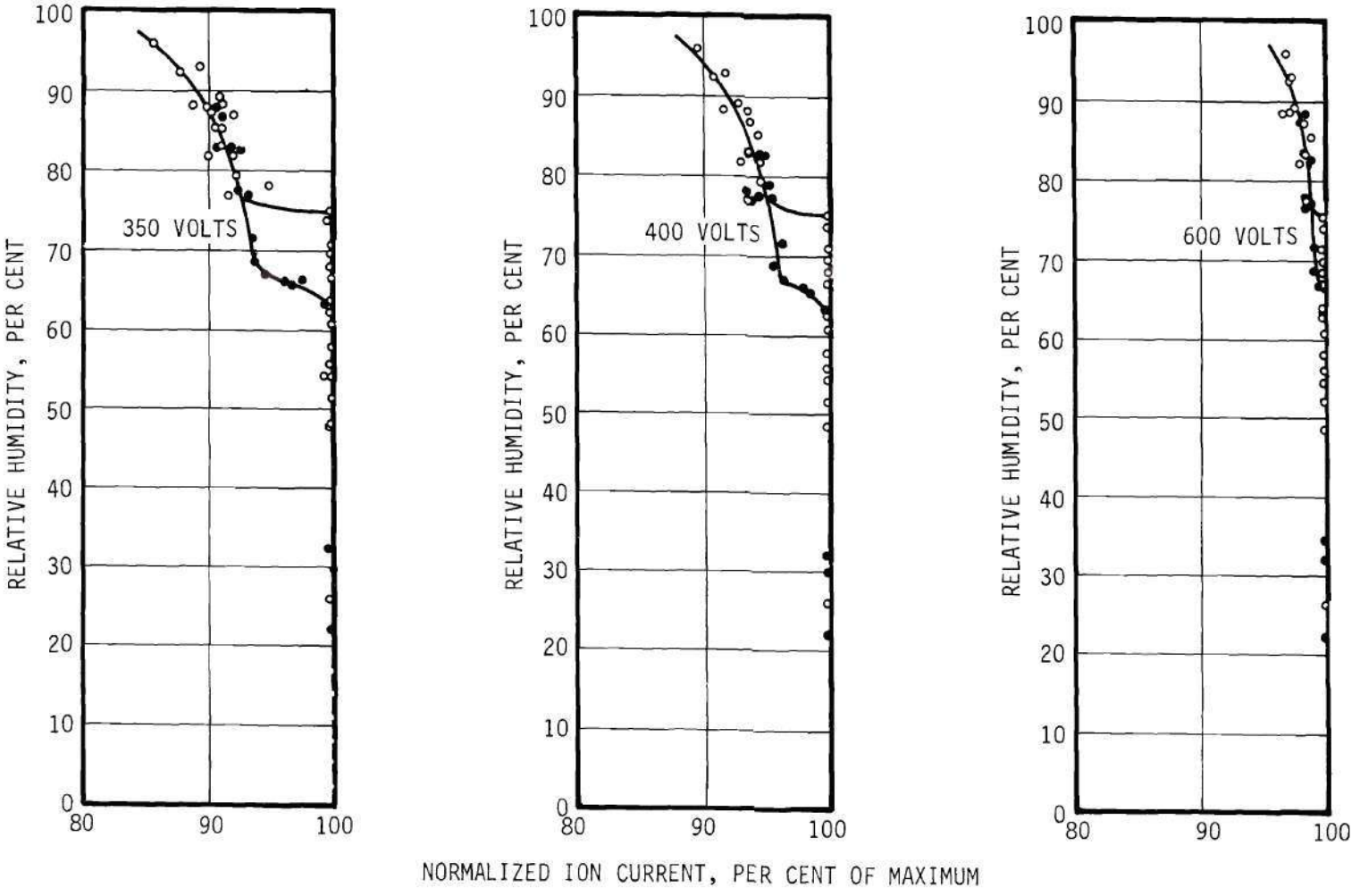

Figure 68. Ion Current Variation with Relative Humidity at a Constant Plate Potential of 350, 400 and 600 Volts for an Aerosol Residence Time of 3.85 Minutes.

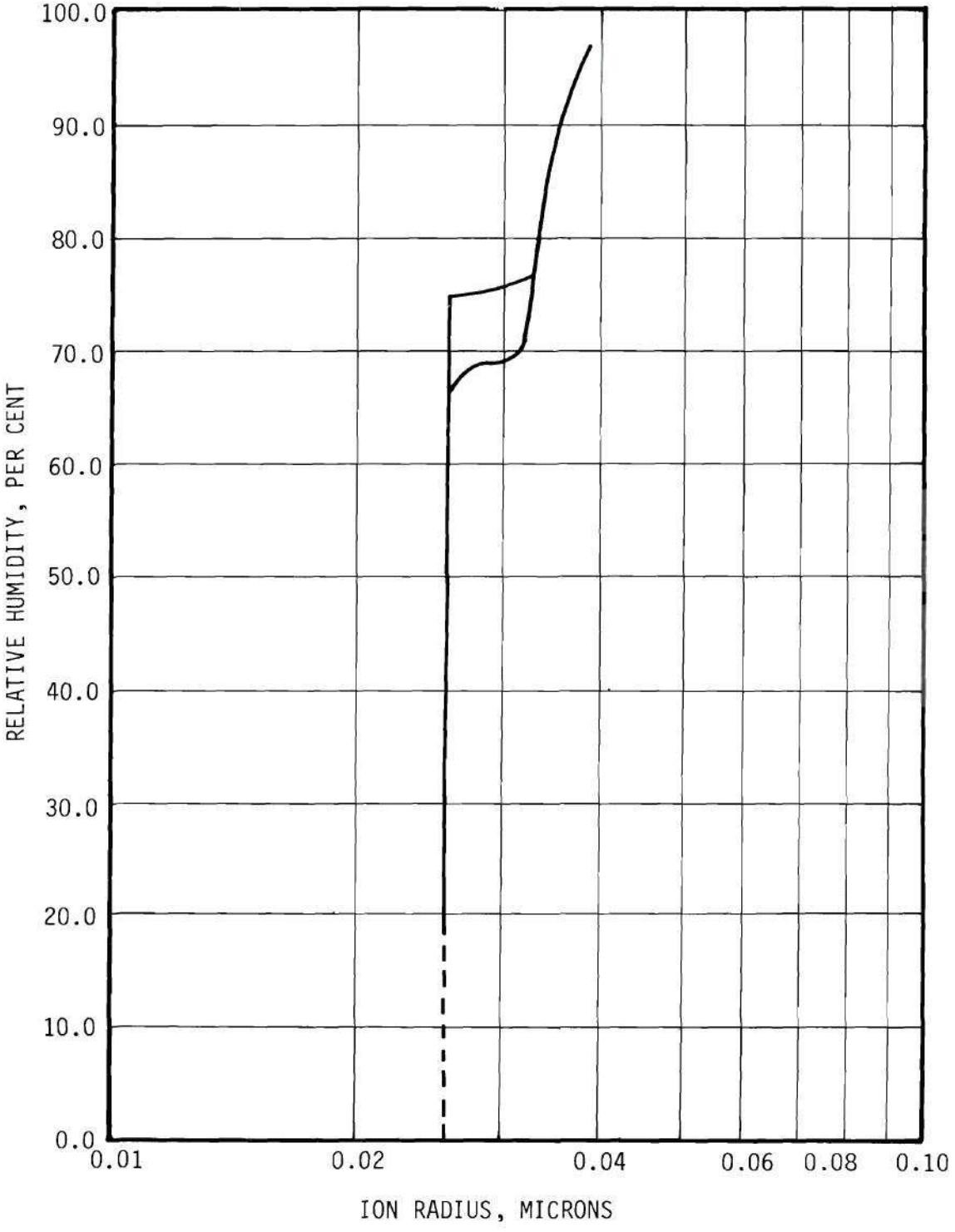

Figure 69. Size Variation of the Mean of the Distribution of a Sodium Chloride Aerosol After a Residence Time of 7.44 Minutes at Equilibrium Relative Humidity.

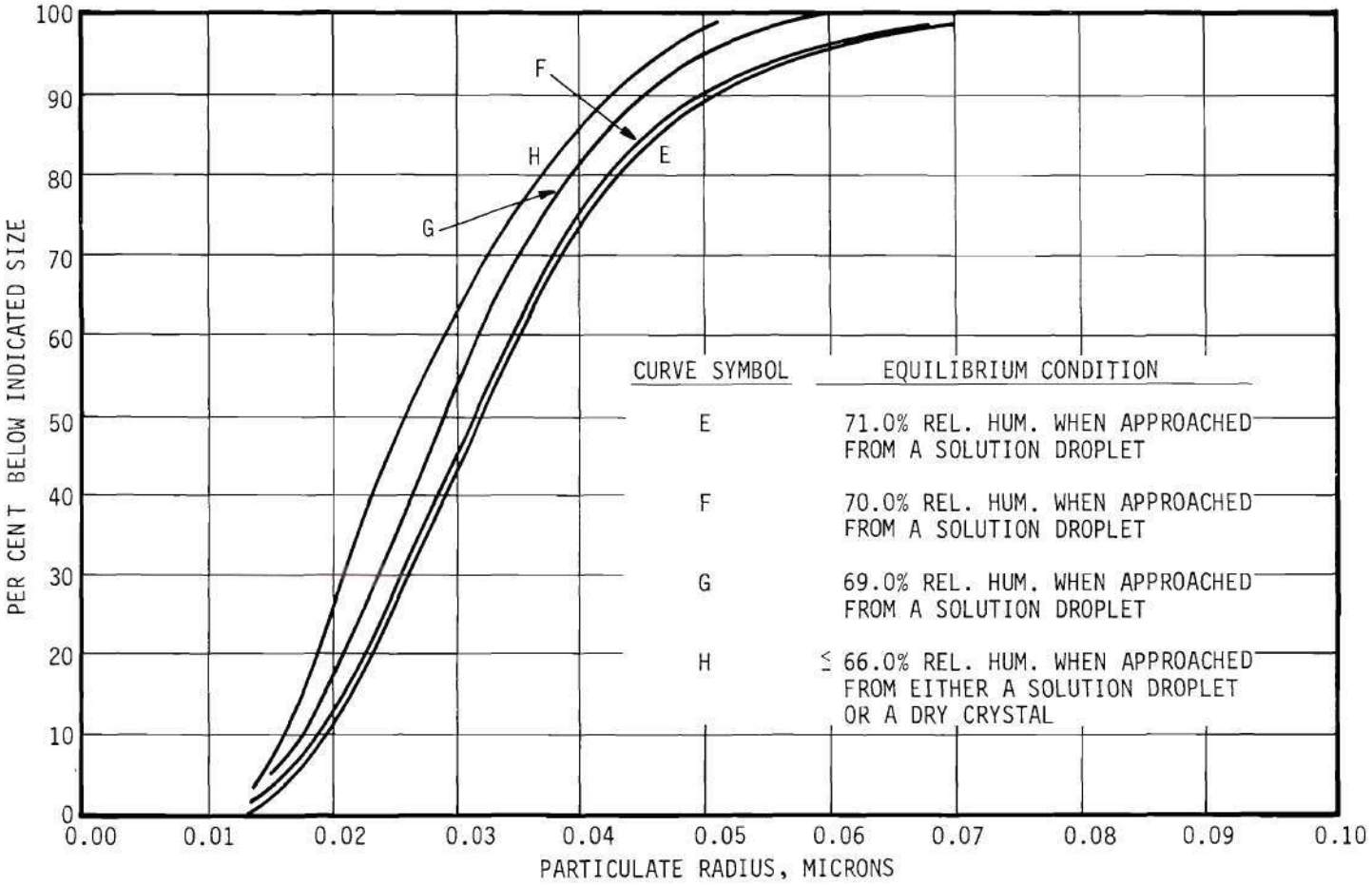

Figure 71. Effect of Decreasing Equilibrium Relative Humidity on the Aerosol Size Distribution After a Residence Time of 7.44 Minutes.

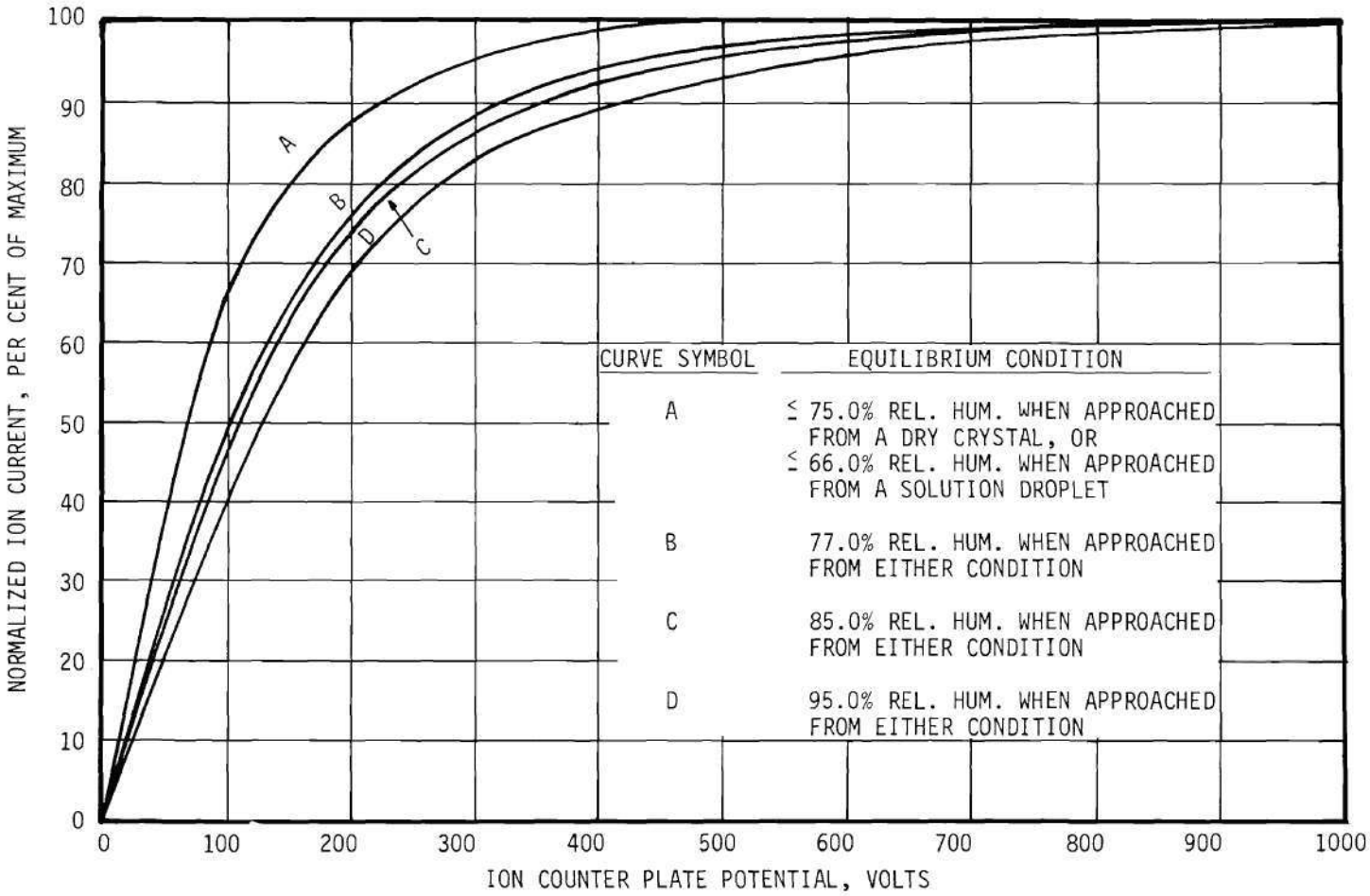

Figure 72. Ion Current Variation with Plate Potential for an Aerosol Residence Time of 7.44 Minutes with Increasing Equilibrium Relative Humidity as Parameter.

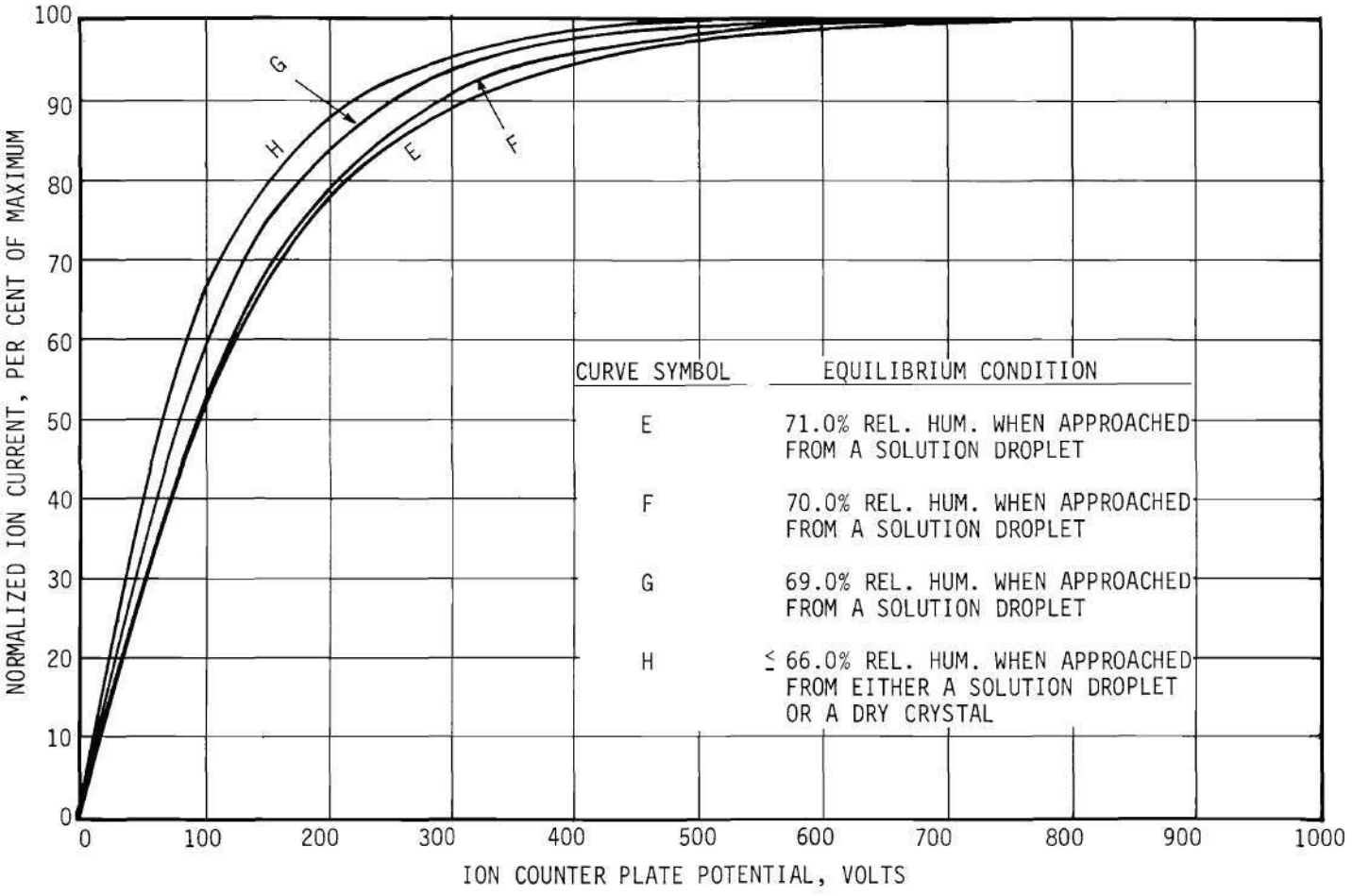

Figure 73. Ion Current Variation with Plate Potential for an Aerosol Residence Time of 7.44 Minutes with Decreasing Equilibrium Relative Humidity as Parameter.

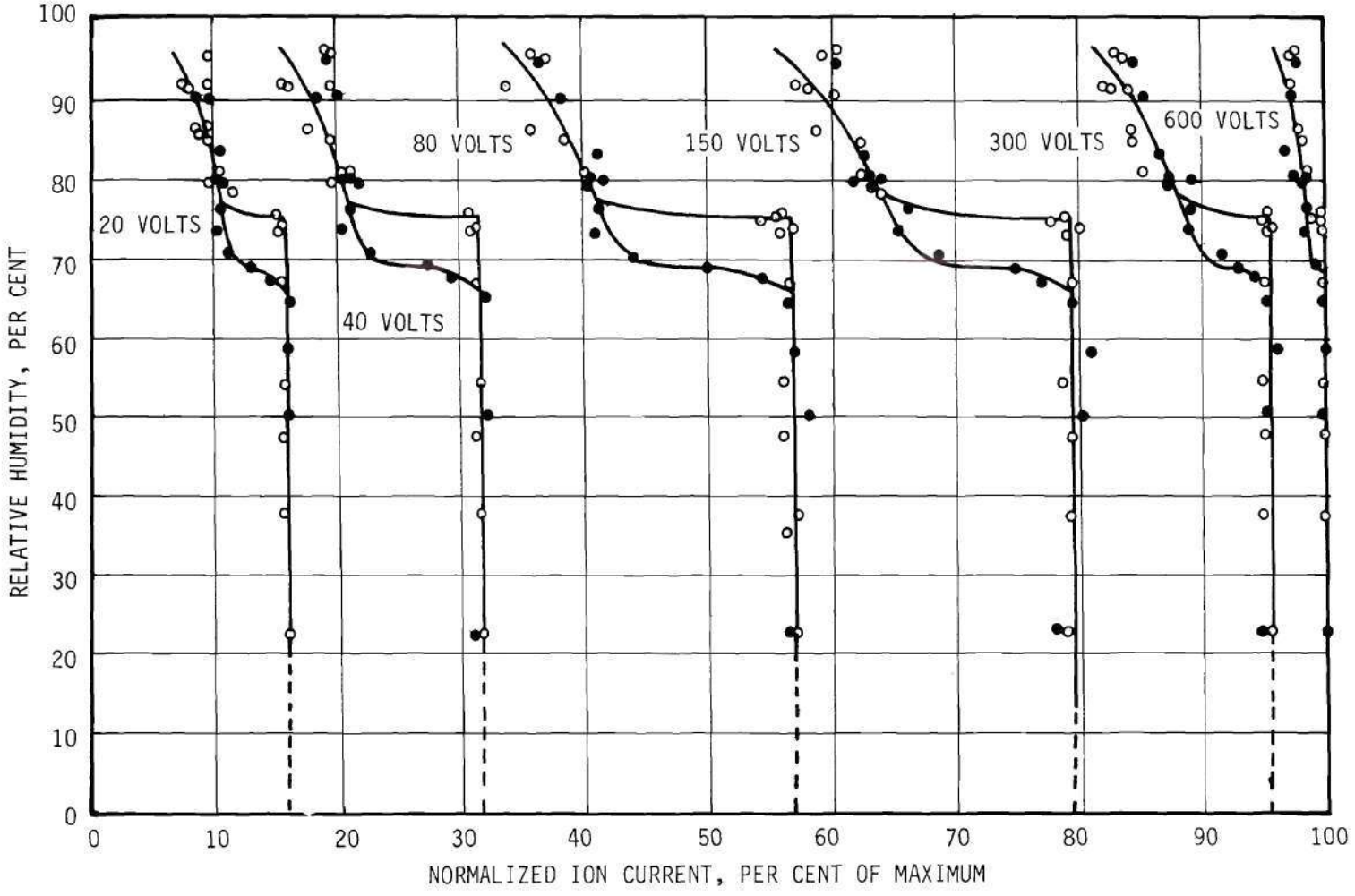

Figure 74. Ion Current Variation with Relative Humidity at a Constant Plate Potential of 20, 40, 80, 150, 300 and 600 Volts for an Aerosol Residence Time of 7.44 Minutes.

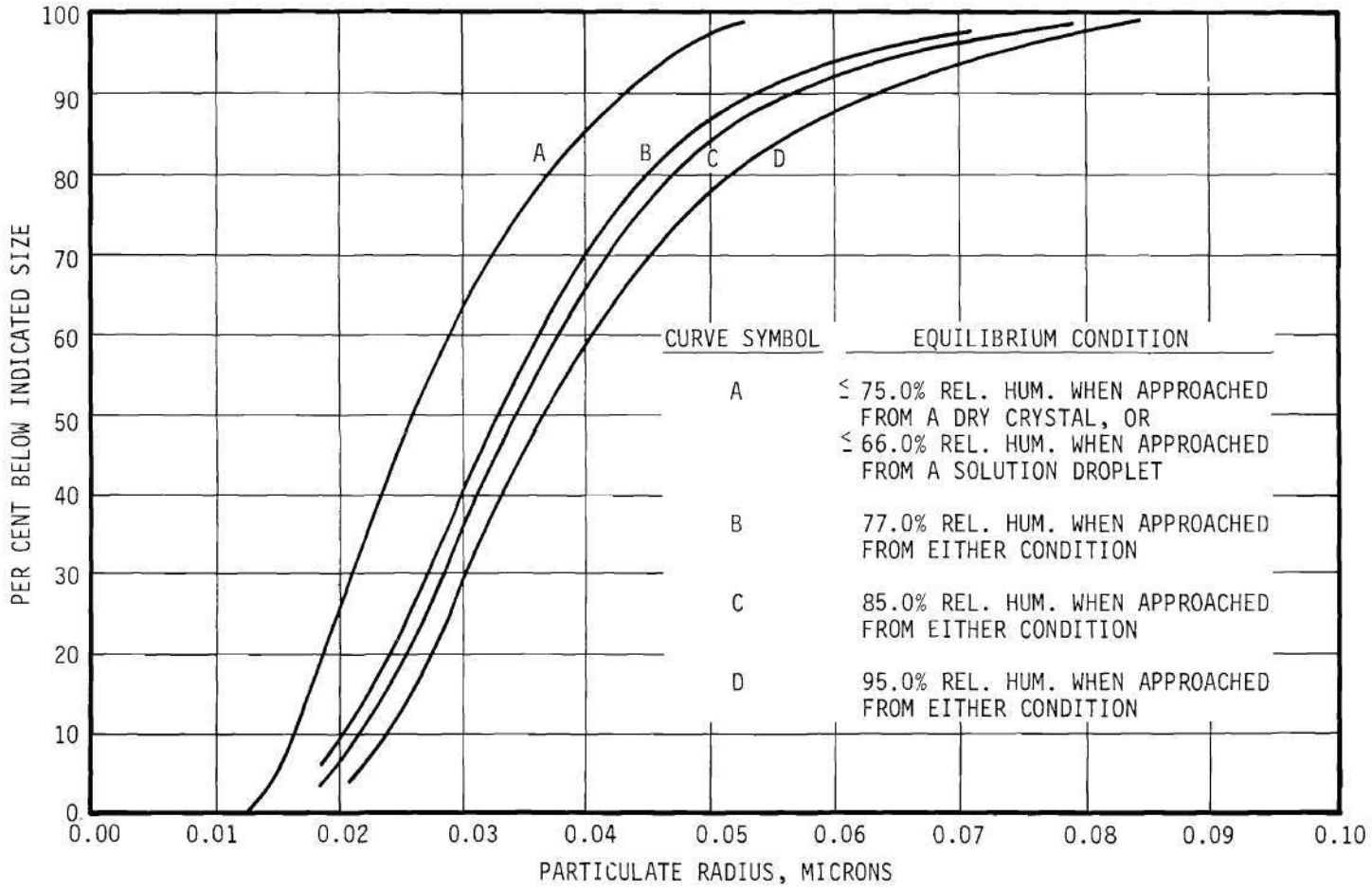

Figure 70. Effect of Increasing Equilibrium Relative Humidity on the Aerosol Size Distribution After a Residence Time of 7.44 Minutes.

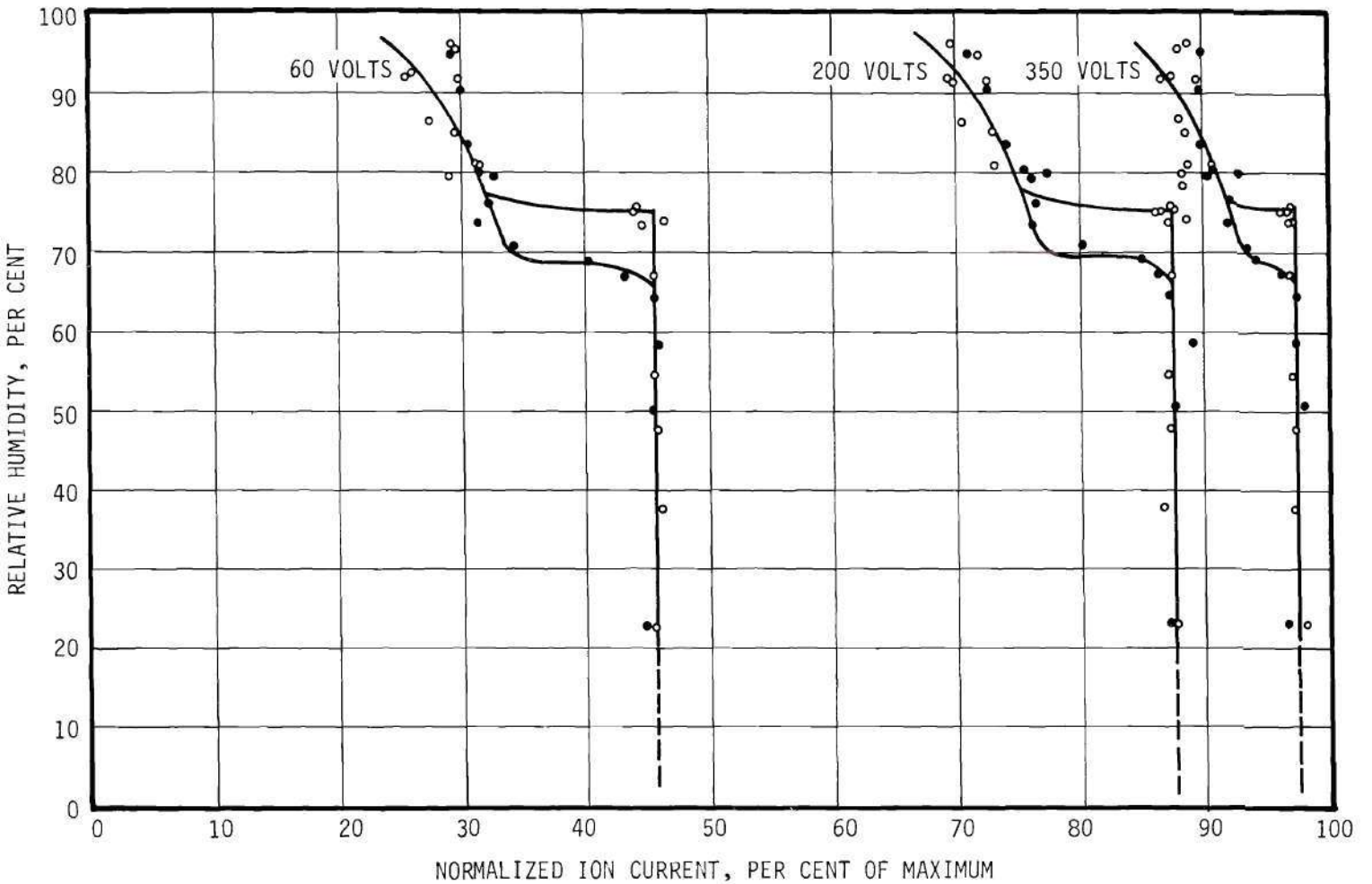

Figure 75. Ion Current Variation with Relative Humidity at a Constant Plate Potential of 60, 200 and 350 Volts for an Aerosol Residence Time of 7.44 Minutes.

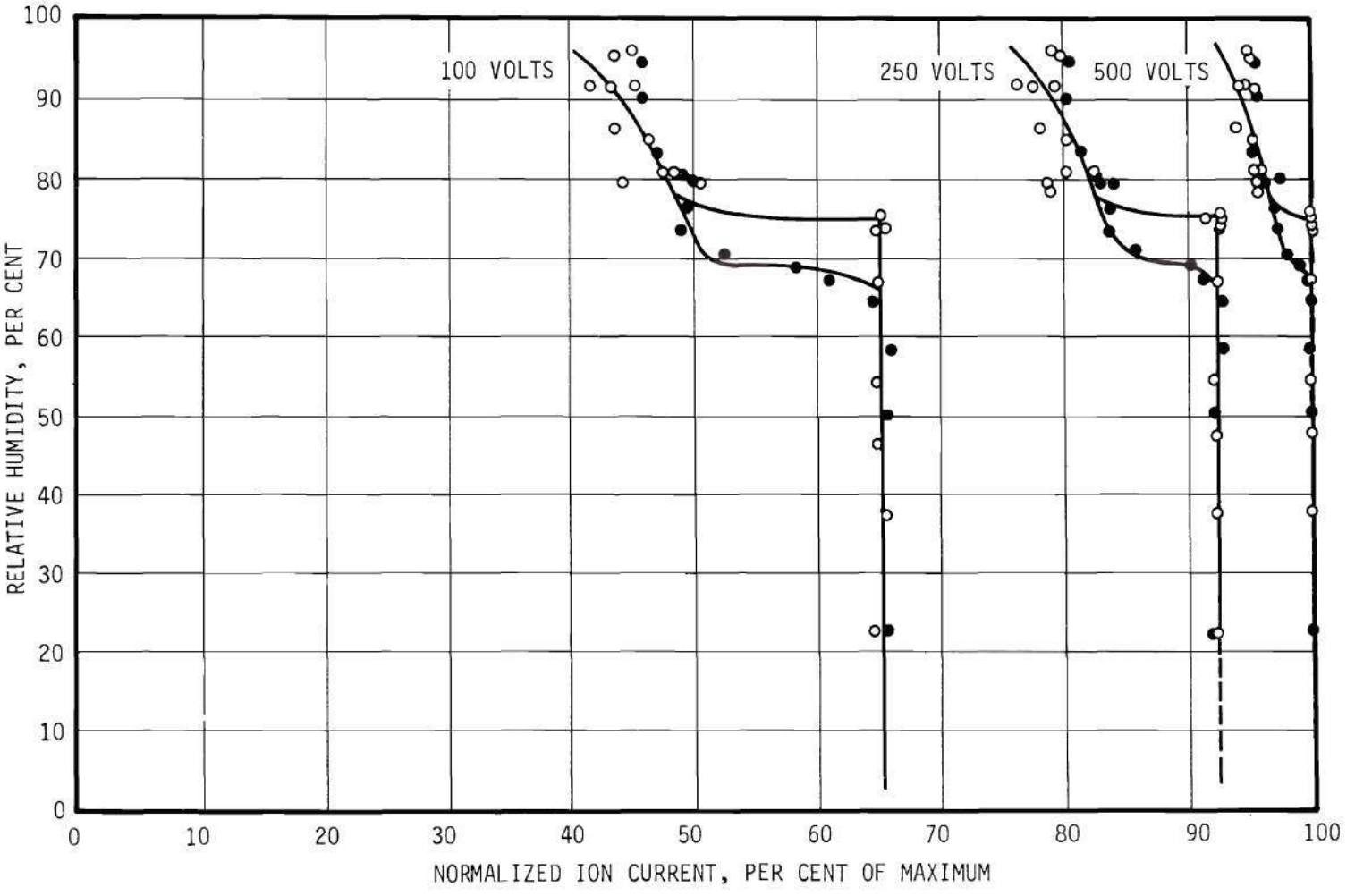

Figure 76. Ion Current Variation with Relative Humidity at a Constant Plate Potential of 100, 250 and 500 Volts for an Aerosol Residence Time of 7.44 Minutes.

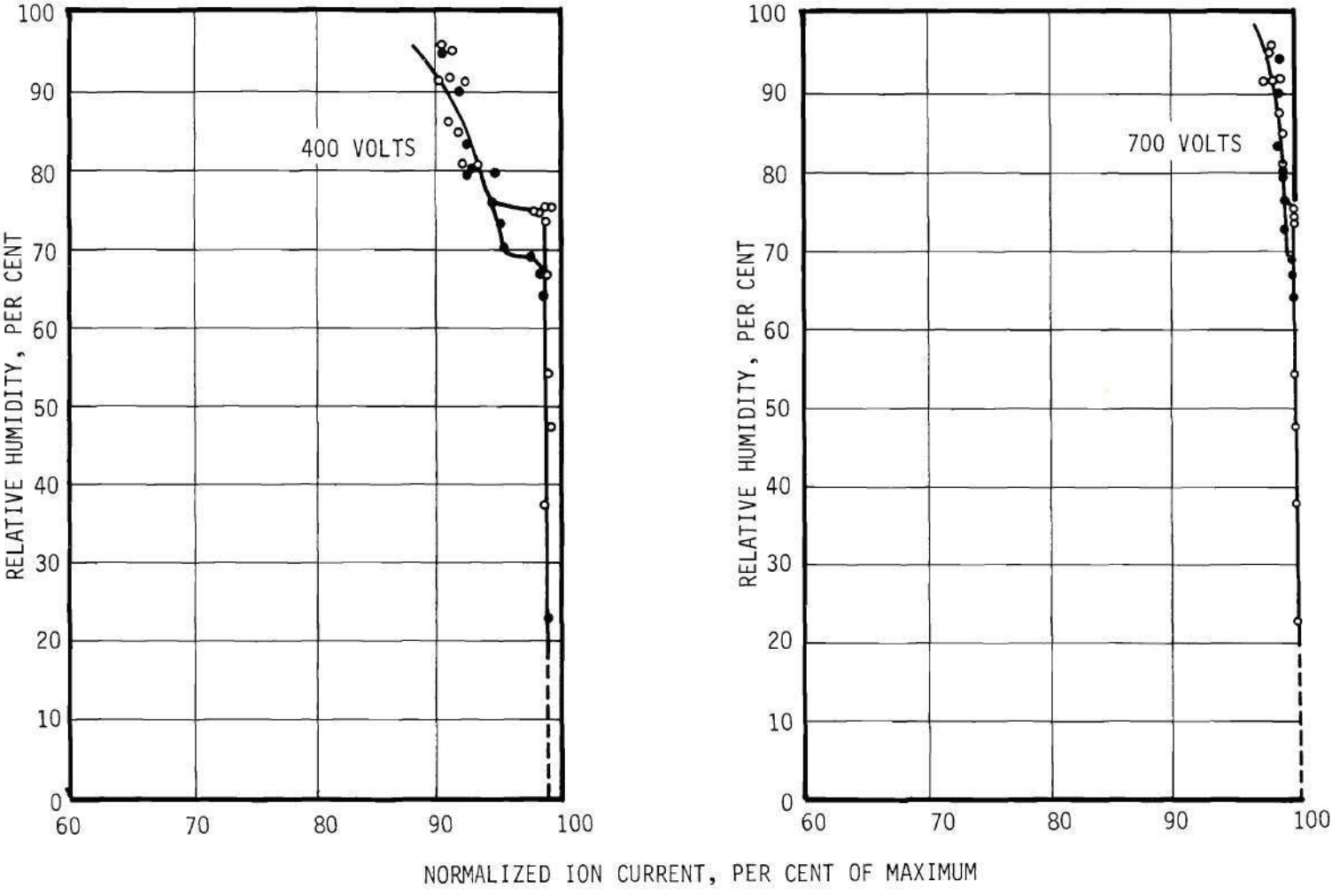

Figure 77. Ion Current Variation with Relative Humidity at a Constant Plate Potential of 400 and 700 Volts for an Aerosol Residence Time of 7.44 Minutes.

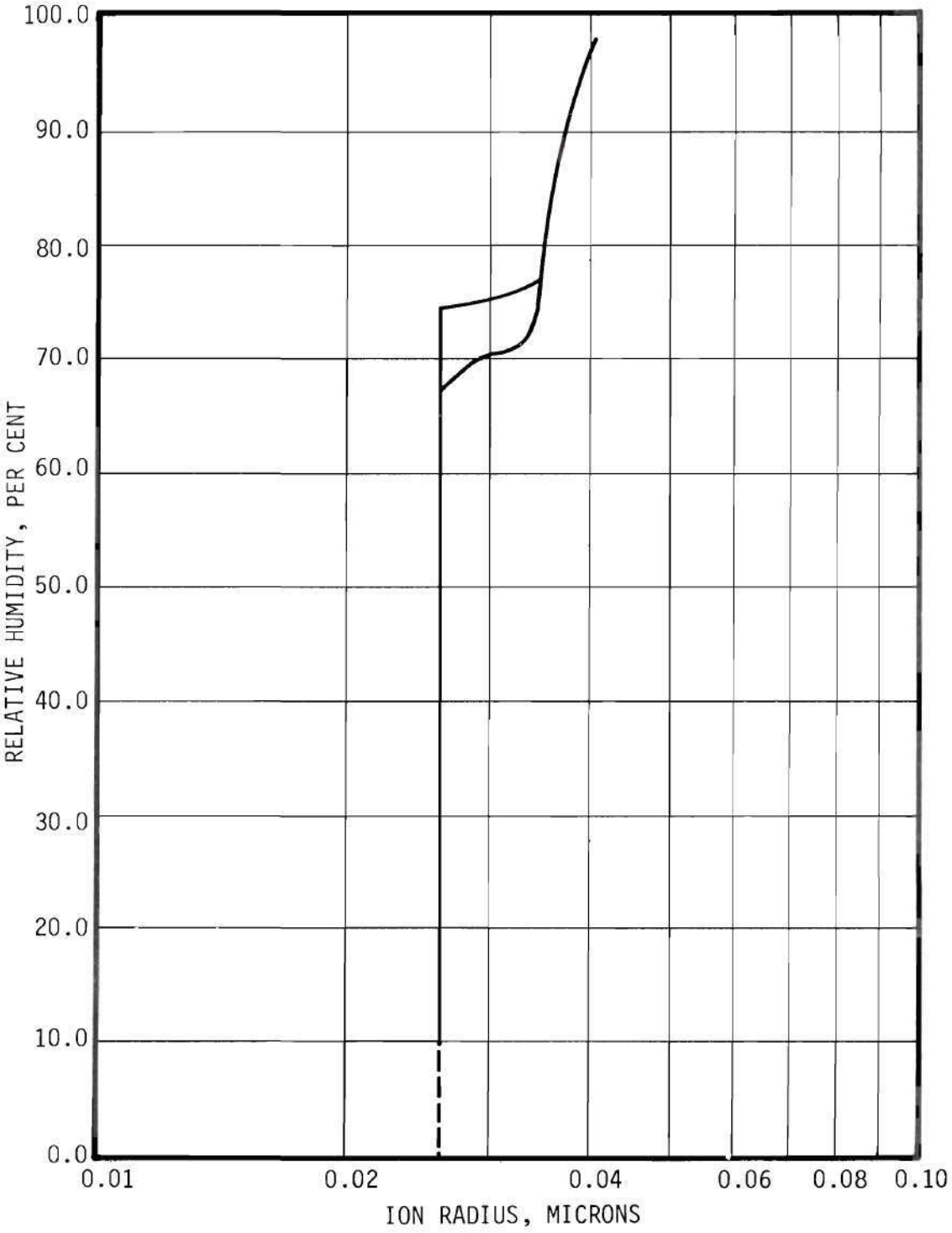

Figure 78. Size Variation of the Mean of the Distribution of a Sodium Chloride Aerosol After a Residence Time of 14.6 Minutes at Equilibrium Relative Humidity.

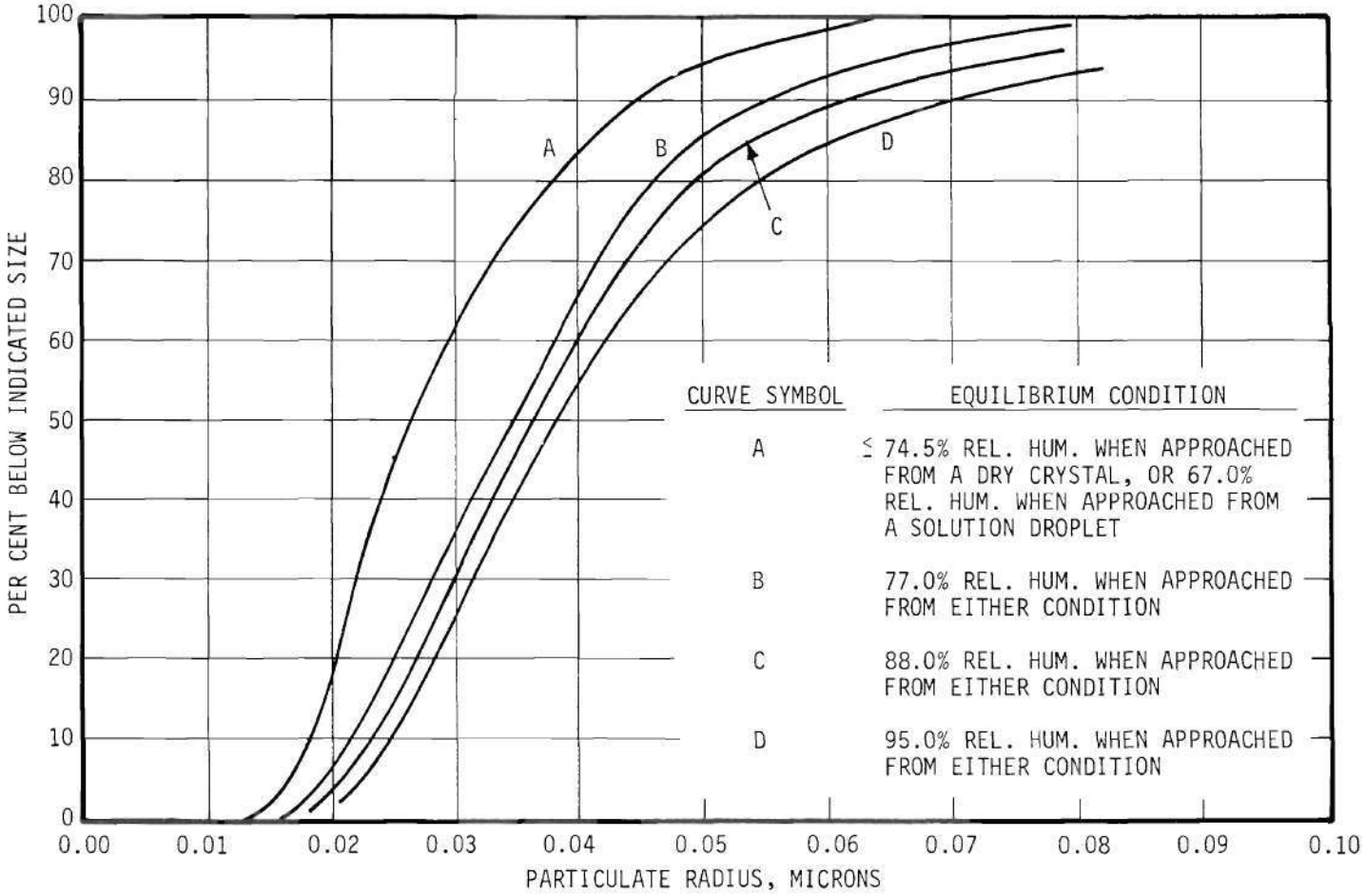

Figure 79. Effect of Increasing Equilibrium Relative Humidity on the Aerosol Size Distribution After a Residence Time of 14.6 Minutes.

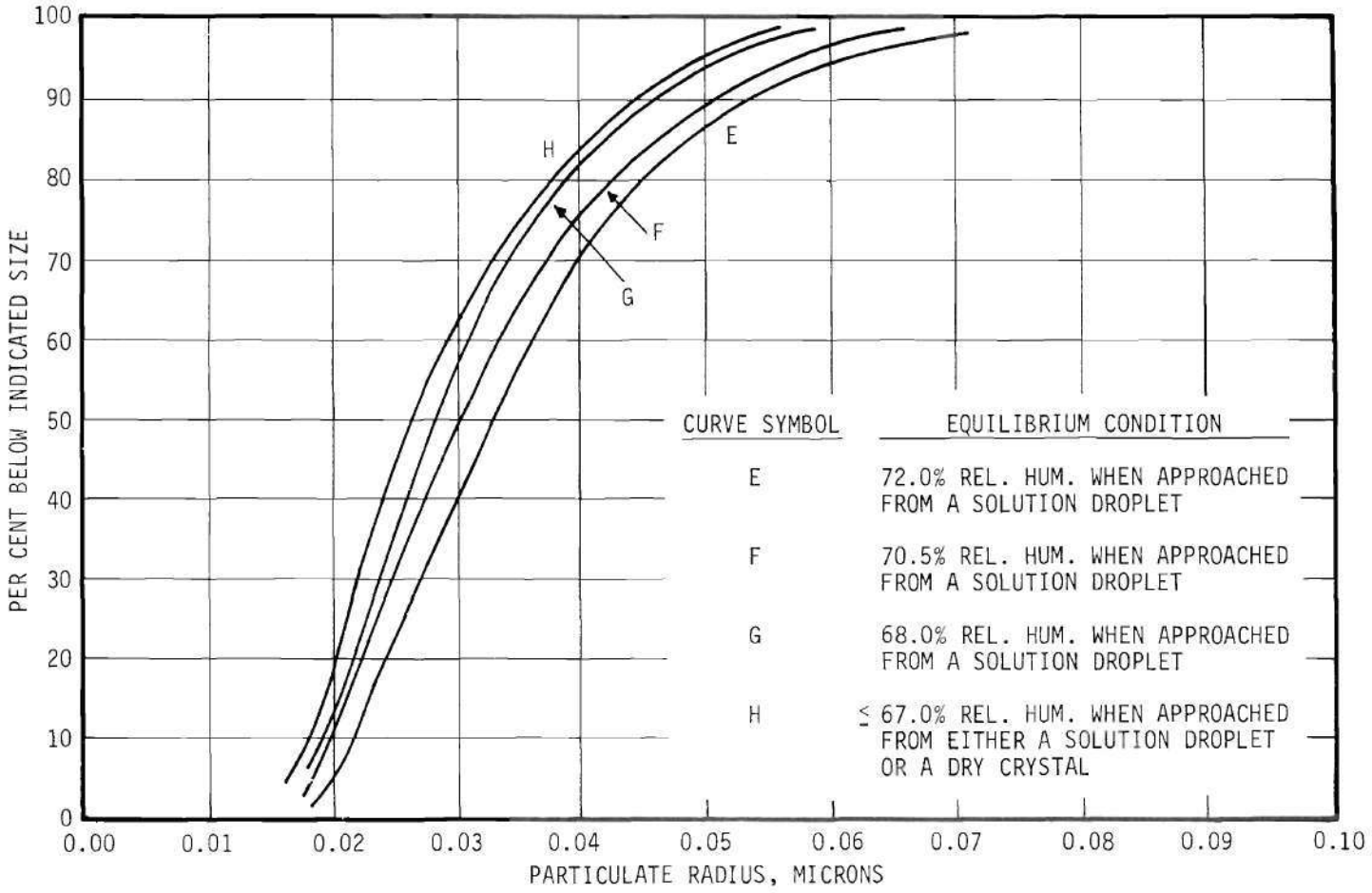

Figure 80. Effect of Decreasing Equilibrium Relative Humidity on the Aerosol Size Distribution After a Residence Time of 14.6 Minutes.

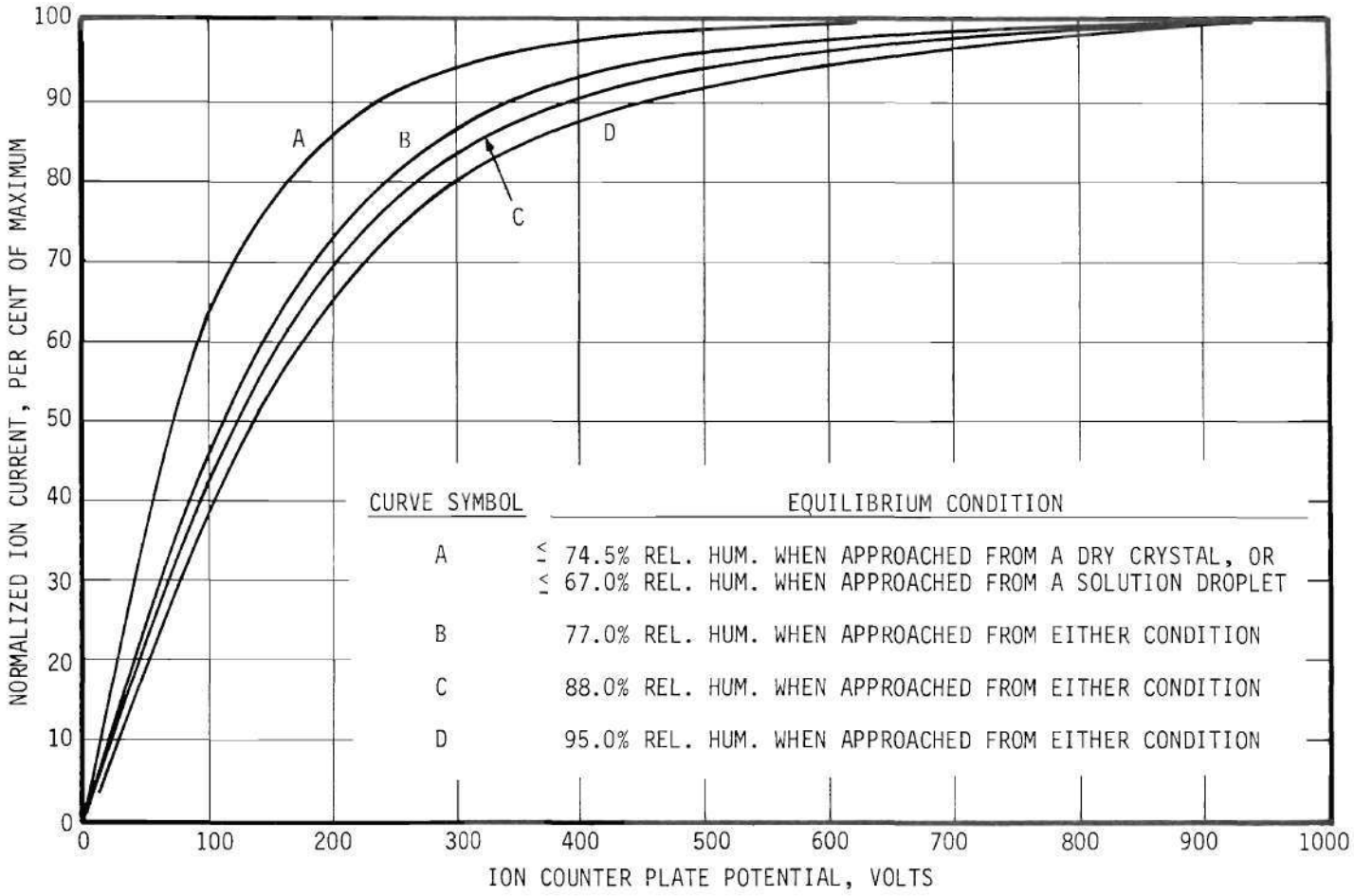

Figure 81. Ion Current Variation with Plate Potential for an Aerosol Residence Time of 14.6 Minutes with Increasing Equilibrium Relative Humidity as Parameter.

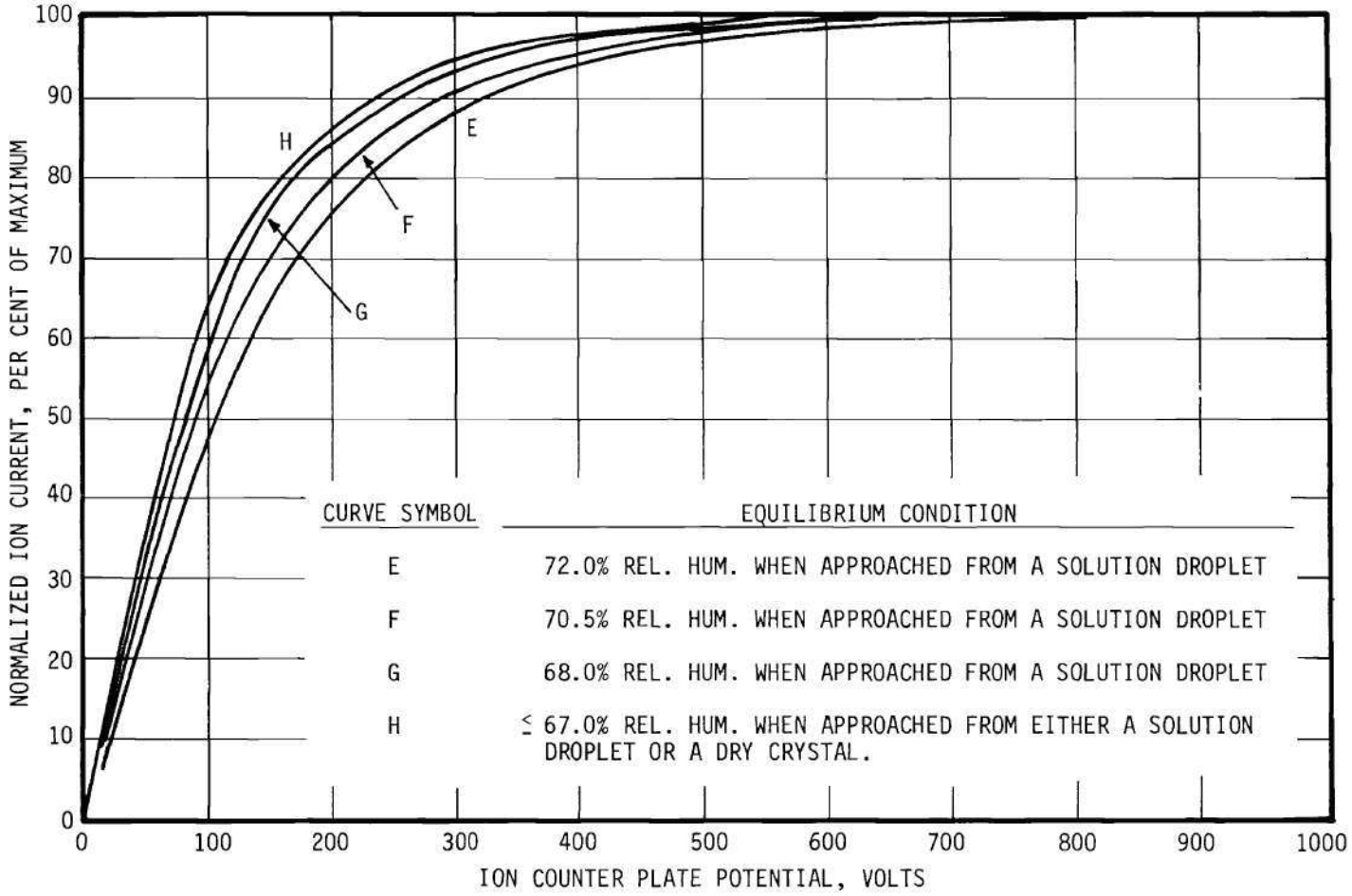

Figure 82. Ion Current Variation with Plate Potential for an Aerosol Residence Time of 14.6 Minutes with Decreasing Equilibrium Relative Humidity as Parameter.

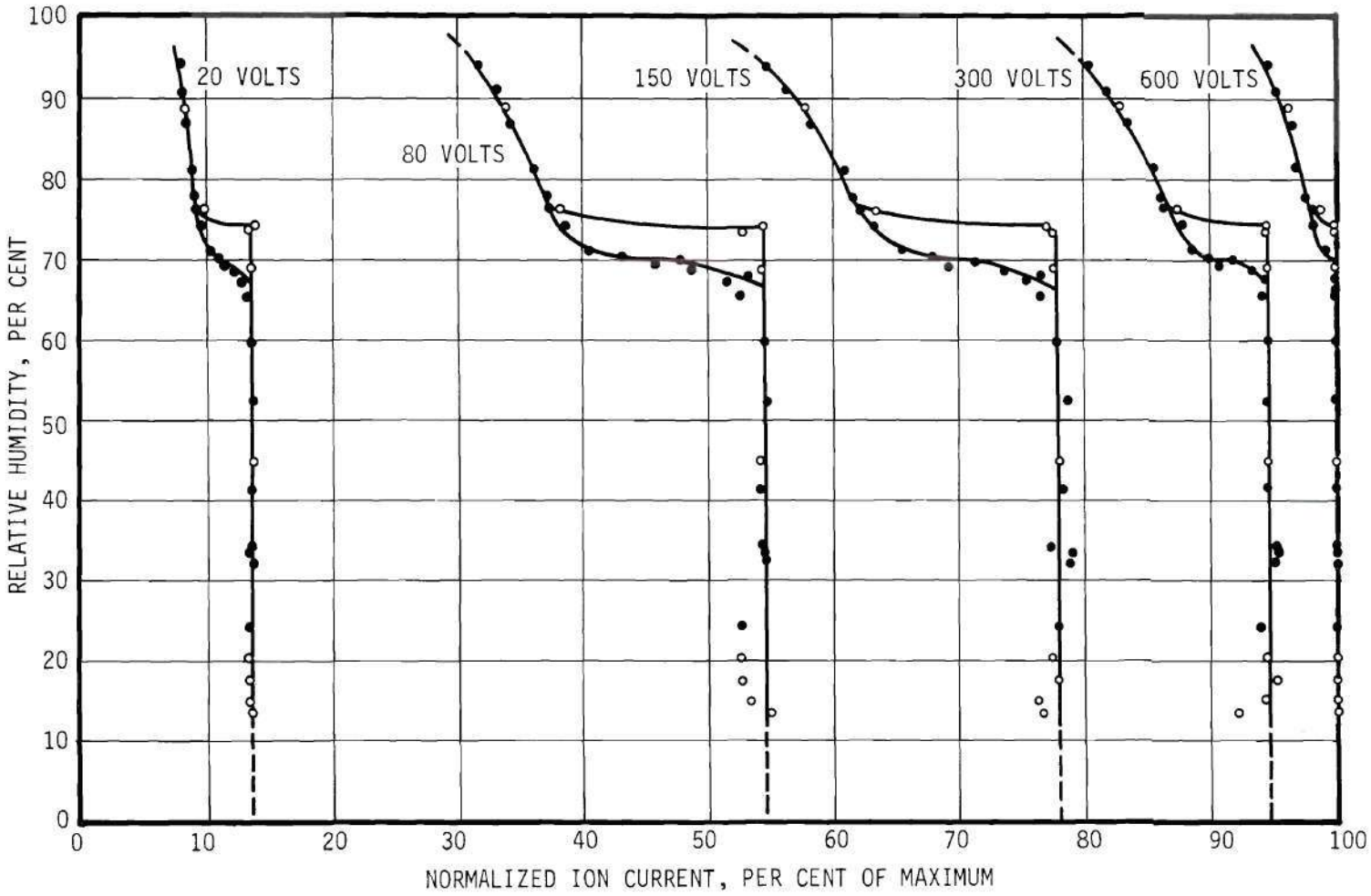

Figure 83. Ion Current Variation with Relative Humidity at a Constant Plate Potential of 20, 80, 150, 300 and 600 Volts for an Aerosol Residence Time of 14.6 Minutes.

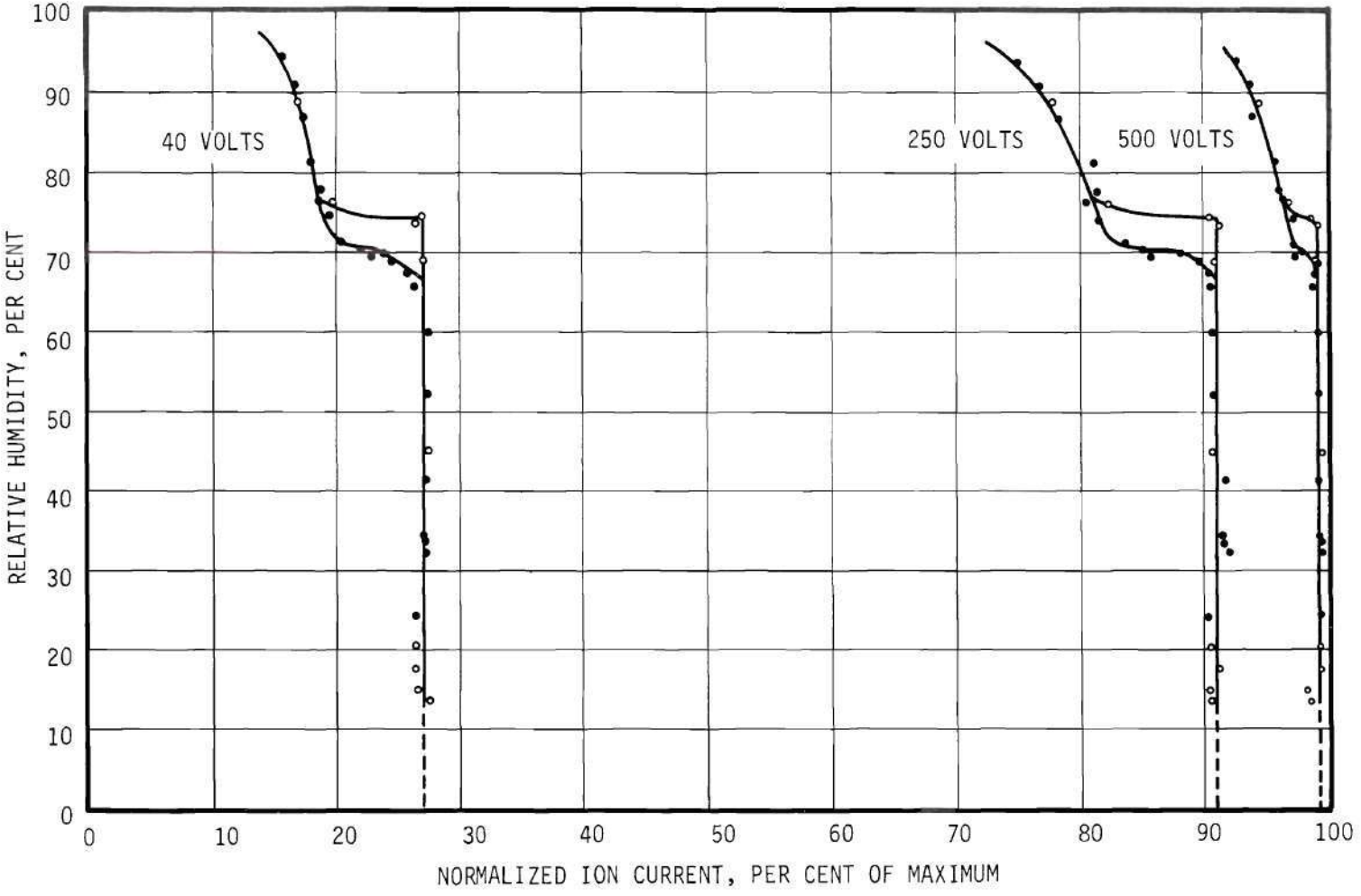

Figure 84. Ion Current Variation with Relative Humidity at a Constant Plate Potential of 40, 250 and 500 Volts for an Aerosol Residence Time of 14.6 Minutes.

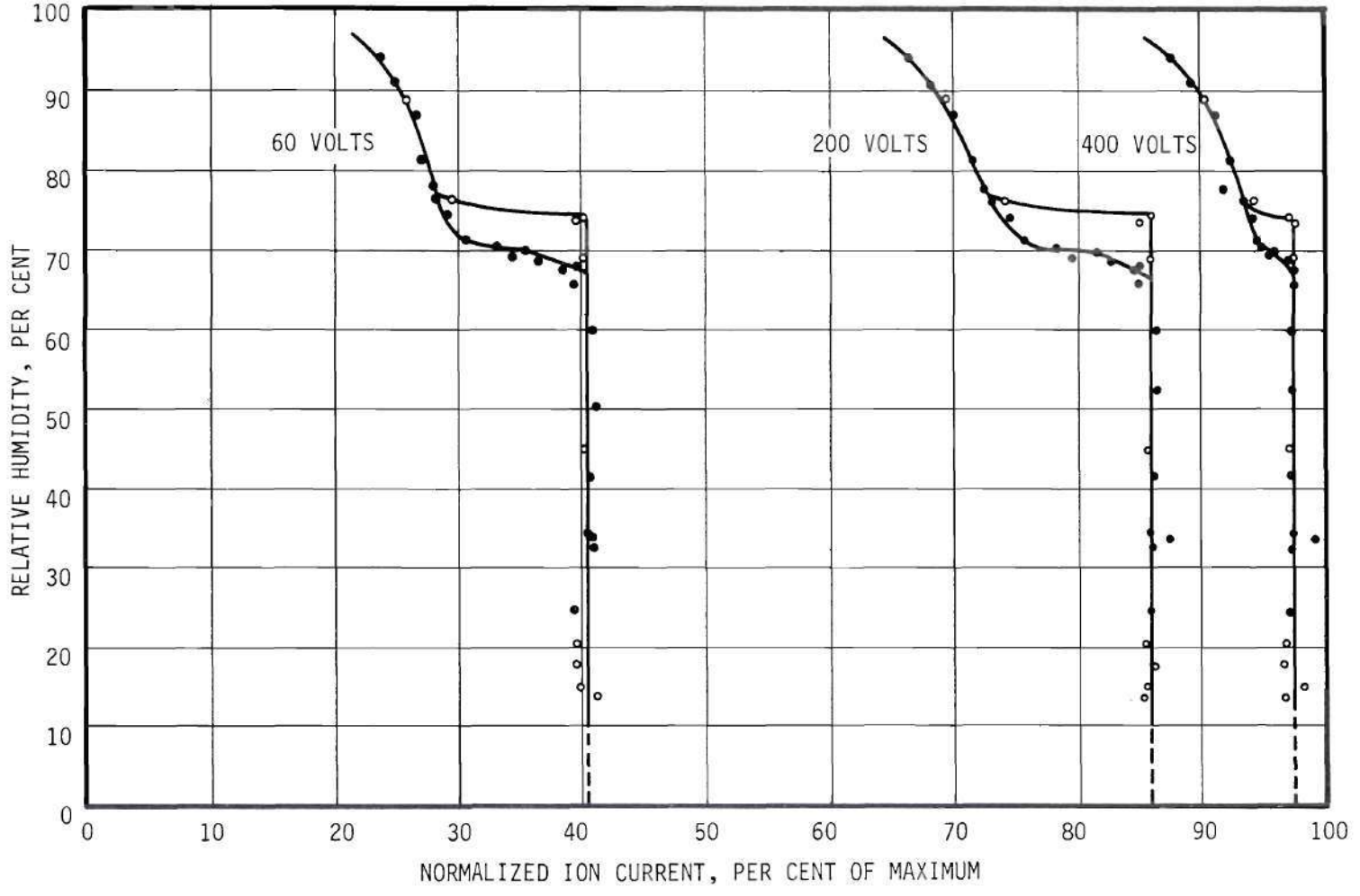

Figure 85. Ion Current Variation with Relative Humidity at a Constant Plate Potential of 60, 200 and 400 Volts for an Aerosol Residence Time of 14.6 Minutes.

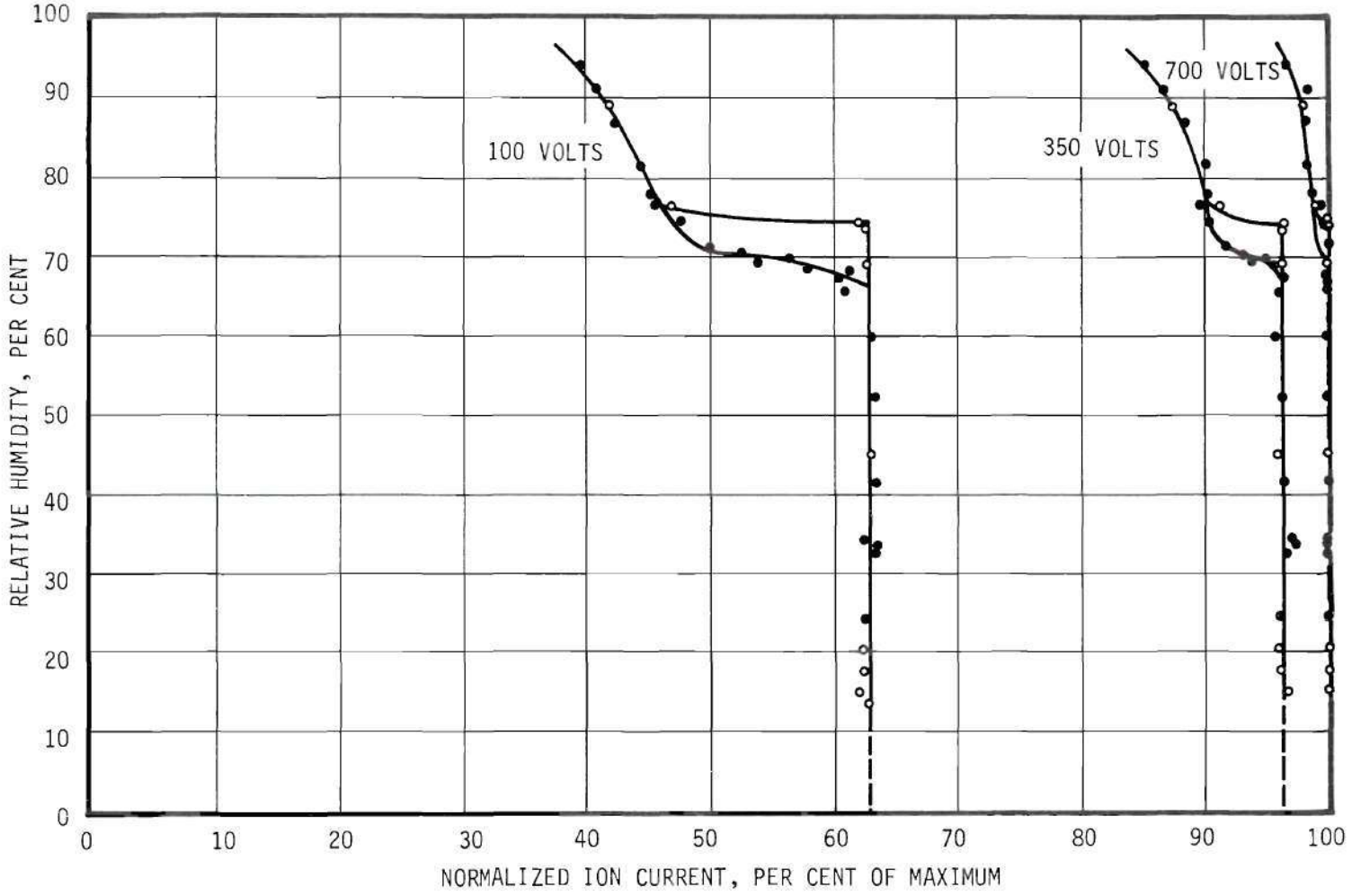

Figure 86. Ion Current Variation with Relative Humidity at a Constant Plate Potential of 100, 350 and 700 Volts for an Aerosol Residence Time of 14.6 Minutes.

APPENDIX F

COMPUTER PROGRAMS

```
2COMMENT PROGRAM NO.  1
2         FROM WEIGHT PER CENT CONCENTRATION VS DENSITY COMPUTES
2         MOLARITY, AND FITS MOLARITY VS DENSITY DATA TO AN M
2         DEGREE POLYNOMIAL THEN PRINTS COEFFICIENTS AND TABULATES
2         WEIGHT PER CENT, MOLARITY AND MOLALITY VS DENSITY                $
2         INTEGER I, J, K, M, N, A  $
2        INTEGER P,Q $
2ARRAY Z(20),S(400),R(20,20),A(15),V(210),U(210)                           $
2INPUT IN(FOR I=(1,1,15)$A(I))                                            $
2INPUT PARAM(N,M,MX)                                                      $
2INPUT DATA(FOR J=(1,1,N)$(U(J),V(J)))                                    $
2OUTPUT ID(FOR I=(1,1,15)$A(I),N,M-1)                                     $
2         OUTPUT OUT( FOR I = (1,1,M)$R(I,P))  $
2         OUTPUT ER( R(P,P))  $
2OUTPUT FIT1(W,NX,X,MOL,Y)                                                $
2OUTPUT FIT2(W,NX,X,MOL,Y,U(I),(U(I)-Y).100/U(I))                          $
2FORMAT HEAD1(15A5,W3,*NUMBER OF POINTS*,I14,B2,*DEGREE OF POLYNOMIAL*,
2              I10,W2)                                                    $
2         FORMAT FMT((6F20.8, W6))  $
2         FORMAT ERFT( *SUM OF SQUARES OF ERROR*, F20.8, W6 )  $
2FORMAT HEAD2(*PER CENT     MOLE FRACTION  MOLARITY (MOLES/ MOLALITY *,
2         *(MOLES/   DENSITY DENS.(DATA) DIFFERENCE*,W0,*BY WEIGHT*,
2         B20,*1000 CC SOLN.)   1000 G WATER)       G/CC*,B7,*G/CC*,
2         B5,*PER CENT*,W2)                                               $
2FORMAT FMT1(B2,X8.5,B5,X8.6,B8,X8.5,B10,X8.5,B7,X8.6,W0)                  $
2FORMAT FMT2(B2,X8.5,B5,X8.6,B8,X8.5,B10,X8.5,B7,X8.6,B1,X8.6,
2         B5,X8.5,W0)                                                     $
2SUBROUTINE FIT                                                           $
2BEGIN
2         Y=R(1,P)+R(2,P).X+R(3,P).X*2+R(4,P).X*3+R(5,P).X*4+
2              R(6,P).X*5+R(7,P).X*6+R(8,P).X*7+R(9,P).X*8+
2              R(10,P).X*9+R(11,P).X*10+R(12,P).X*11+R(13,P).X*12+
2              R(14,P).X*13+R(15,P).X*14+R(16,P).X*15+R(17,P).X*16+
2              R(18,P).X*17+R(19,P).X*18                                  $
2RETURN END FIT                                                           $
2 START..
```

```
2COMMENT PROGRAM NO.  1  (CONTINUED)                                    $
2        READ($$IN)  $     READ($$PARAM)  $
2        IF N EQL 0                  $         STOP                      $
2        READ($$DATA)  $
2COMMENT CONVERSION OF WEIGHT PER CENT TO MOLARITY                       $
2        FOR I=(1,1,N)   $  V(I)=(10.V(I).U(I))/MX                       $
2        P = M + 2  $     Q = M.M  $
2        FOR I = (1,1,M)  $     Z(I) = 0  $
2        FOR I = (1,1,Q)  $   S(I) = 0  $
2        SY = SSY = 0  $
2        FOR K = (1,1,N)  $
2 BEGIN
2        TEMP = 1.0  $
2        X=V(K)                                                          $
2        FOR I = (1,1,Q)  $
2 BEGIN
2        TEMP = TEMP.X  $
2        S(I) = S(I) + TEMP  $
2 END    $
2        TEMP = Y = U(K)                                                 $
2        FOR I = (1,1,M)   $
2 BEGIN
2        TEMP = TEMP.X  $
2        Z(I) = Z(I) + TEMP  $
2 END  $
2        SSY = SSY + Y.Y  $     SY = SY + Y  $
2 END  $
2        M = M + 1  $
2        FOR I = (1,1,M)  $
2        FOR J = (1,1,M)  $
2 BEGIN
2        K = I + J - 2  $
2        IF K NEQ 0  $
2        R(I,J) = S(K)  $
2 END  $
2        R(1,1) = FLOAT(N)  $
```

```
2COMMENT PROGRAM NO.  1  (CONTINUED)                                    $
2        R(1,P) = R(P,1) = SY      $
2        R(P,P) = SSY           $
2        FOR I = (2,1,M)  $
2        R(I,P) = R(P,I) = Z(I-1)  $
2        FOR K = (1,1,M)  $
2 BEGIN
2        FOR J = (K+1,1,P)  $
2        R(K,J) = R(K,J)/R(K,K)  $
2        FOR I = (1,1,K-1),(K+1,1,P)  $
2        FOR J = (K+1,1,P)  $
2        R(I,J) = R(I,J) - R(I,K).R(K,J)  $
2 END  $
2        WRITE($$ID,HEAD1) $
2        WRITE($$OUT,FMT)  $
2        WRITE($$ER,ERFT)  $
2        FOR I=(M+1,1,20)                                               $
2        R(I,P)= 0.0                                                    $
2        WRITE($$HEAD2)                                                 $
2        FOR I=(1,1,N)                                                  $
2BEGIN
2        X=V(I)                                                         $
2ENTER FIT                                                              $
2        W=X.MX/10.Y                                                    $
2        NX=X/( X+(1000Y-X.MX)/18.016)                                  $
2        MOL=1000.NX/18.016(1-  NX)                                     $
2        WRITE($$FIT2,FMT2)                                             $
2END                                                                    $
2        FOR X=(V(N)+0.2,0.2,20.0)                                      $
2BEGIN
2ENTER FIT                                                              $
2        W=X.MX/10.Y                                                    $
2        NX=X/( X+(1000Y-X.MX)/18.016)                                  $
2        MOL=1000.NX/18.016(1-  NX)                                     $
2        WRITE($$FIT1,FMT1)                                             $
2        IF MOL GTR 20.0    $    GO TO START                           $
```

```
2COMMENT PROGRAM NO.  1  (CONTINUED)                                    $
2END                                                                    $
2         GO TO START  $
2         FINISH  $
```

```
2COMMENT PROGRAM NO.  2
2         COMPUTES SOLUTE ACTIVITY VS CONCENTRATION FOR 1.1 ELECTROLYTES
2         GIVEN CONSTANTS FOR SEMI EMPIRICAL EQUATION (12-5-3) IN HARNED
2         AND OWEN AS WELL AS COEFFICIENTS OF M DEGREE POLYNOMIAL FIT OF
2         DENSITY VS SOLUTION MOLARITY                                    $
2INTEGER I,M                                                              $
2REAL C,A,AO,B,D,F,K,R,MX                                                 $
2ARRAY A(15),R(20),NX(210),A2(210),FA2(210)                               $
2INPUT DATA(FOR I=(1,1,15)$A(I))                                          $
2INPUT DATA1(AO,B,D,MX,M)                                                 $
2INPUT DATA2(FOR I=(1,1,M+1)$R(I))                                        $
2OUTPUT IDEN(FOR I=(1,1,15)$A(I))                                         $
2FORMAT FORM1(15A5,W3,B20,W2)                                             $
2FORMAT COLS(*WEIGHT   MOLE     MOLALITY       MOLARITY   MEAN MOLAL  *,
2         * SOLUTE      WATER  SOLUTION     VAN,T   SOLUTION*,W0,*PER *,
2         *   FRACTION   (MOLES/*,B7,*(MOLES/     ACTIVITY   ACTIVITY *,
2         *  ACTIVITY PARTIAL      HOFF    OSMOTIC*,W0,*CENT*,B13,*100*,
2        *0G WATER) 1000CC WATER)  COEFF.*,B24,*PRESS,MM HG  FACTOR  C*,
2         *OEFFICIENT*,W2)                                                $
2OUTPUT COEF(W,NX(I),MOL,C,GI,A2(I),A1,PP,VHF,OC)                         $
2FORMAT FORM2(X6.3,B2,X7.5,B4,X8.5,B5,X8.5,B3,X9.5,B1,F12.5,B1,X8.6,B1,
2         X8.5,B3,X8.4,B2,X8.5,W0)                                        $
2COMMENT COMPUTES DENSITY FROM M DEGREE POLYNOMIAL FIT OF D VS C           $
2SUBROUTINE FIT                                                           $
2BEGIN
2         Y=R(1)+R(2).C+R(3).C*2+R(4).C*3+R(5).C*4+R(6).C*5+
2              R(7).C*6+R(8).C*7+R(9).C*8                                 $
2RETURN END FIT                                                           $
2START.. READ($$DATA)                                                     $
2         READ($$DATA1)                                                   $
2         IF AO EQL 0.0    $    STOP                                      $
2         READ($$DATA2)                                                   $
2         FOR I=(M+2,1,20)  $     R(I)=0.0                               $
2         WRITE($$IDEN,FORM1)                                             $
2         WRITE($$COLS)     $     I=0                  $
2         FOR C=(0.0,0.1,20.0)                                            $
```

```
2COMMENT PROGRAM NO.  2  (CONTINUED)                                    $
2BEGIN                I=I+1                                             $
2         K=(-(1.290**6)(23417*-1.5)((2C)*0.5)/(1+
2              (35.57).(AO)((23417*-0.5))((2.C)*0.5)))+B.C+D.C*2        $
2         F=10*K                                                        $
2         ENTER FIT                                                     $
2         W=C.MX/(10).Y                                                 $
2     NX(I) =C/(C+((1000).Y-C.MX)/18.016)                               $
2         MOL=(1000).(NX(I))/(18.016).(1-(NX(I)))                       $
2         NXI=C /(2.C+((1000).Y-C.MX)/18.016)                           $
2         IF MOL EQL 0.0  $  BEGIN  GI=1.0  $ GO TO FLAG3 $  END        $
2         GI=(1000).F.NXI/MOL.(18.016)                                  $
2FLAG3..  A2(I)=(GI.MOL)*2                                              $
2         IF I EQL 1 $  BEGIN  FA2(I)=0.0   $  GO TO FLAG4  $  END      $
2         FA2(I)=-NX(I)/(1-NX(I)).(A2(I))                               $
2FLAG4..  IF I EQL 1  $  BEGIN  FBAR=SUM=0.0  $  GO TO FLAG1  $  END    $
2         FBAR=(FA2(I)+FA2(I-1))/2                                      $
2         SUM = SUM+(A2(I)-A2(I-1)).FBAR                                $
2FLAG1..  A1=EXP(SUM)                                                   $
2         PP=(23.756).A1                                                $
2         IF A1 EQL 1.0                                                 $
2BEGIN
2         VHF=2.0       $     OC=1.0      $   GO TO FLAG2               $
2END                                                                    $
2         VHF=((1/A1)-1).((1/NX(I))-1)                                  $
2         OC=(LOG(A1))/((-0.036032).MOL)                                $
2FLAG2..  WRITE($$COEF,FORM2)                                           $
2         IF MOL GTR 20.0   $  BEGIN  SUM=0.0  $  GO TO START  $  END   $
2END                                                                    $
2         SUM=0.0      $  GO TO START                                   $
2FINISH                                                                 $
```

```
2COMMENT PROGRAM NO. 3
2        FROM A TABLE OF VALUES OF OSMOTIC COEFFICIENT VS SOLUTION
2        MOLALITY, COMPUTES WATER ACTIVITY, SOLUTION PARTIAL PRESSURE,
2        AND VAN,T HOFF FACTOR. THEN, USING A NUMERICAL INTEGRATION
2        PROCEDURE, COMPUTES SOLUTE ACTIVITY COEFFICIENT AND ACTIVITY  $
2INTEGER I,J,K,M,N,A,P,Q,H,AA                                          $
2ARRAY Z(20),S(400),R(20,20),A(15),V(210),U(210),T(100),AA(2)          $
2INPUT IN1(FOR I=(1,1,2)$AA(I))                                        $
2INPUT IN(FOR I=(1,1,15)$A(I))                                         $
2INPUT PARAM(N,M,MX,E,Y0,G0,X0)                                        $
2INPUT DATA(FOR J=(1,1,N)$(U(J),V(J)))                                 $
2OUTPUT ID1(FOR I=(1,1,2)$AA(I))                                       $
2OUTPUT ID(FOR I=(1,1,15)$A(I))                                        $
2OUTPUT FIT1(K3,PCT,NX,Y1,AC,PP,VHF,G,ACT)                             $
2FORMAT HD1(B36,2A5,W3)                                                $
2FORMAT HEAD1(15A5,W2)                                                 $
2FORMAT HD2(B29,2A5,*(CONTINUED)*,W3)                                  $
2FORMAT HEAD2(*MOLALITY WEIGHT     MOLE     OSMOTIC     WATER   PARTI*,
2        *AL  VAN,T SOLUTE MEAN   SOLUTE*,W0,B9,*PER CENT FRACTION CO*,
2        *EFFICIENT ACTIVITY PRESSURE  HOFF  MOLAL ACTIV. ACTIVITY*,W0,
2        B49,*MM HG   FACTOR COEFFICIENT*,W2)                          $
2FORMAT FMT1(X6.2,B3,X7.3,B2,X7.5,B4,X6.4,B4,X7.5,B2,X7.4,B1,X7.4,B2,
2        X8.4,B1,F11.4,W0)                                             $
2SUBROUTINE FIT                                                        $
2BEGIN
2        FOR H=(2,1,N)                                                 $
2BEGIN
2        IF V(H) GEQ X                                                 $
2BEGIN
2        Y=U(H)-(U(H)-U(H-1))(V(H)-X)/(V(H)-V(H-1))                    $
2        GO TO OUT                                                     $
2END                                                                   $
2END                                                                   $
2OUT..
2RETURN END FIT                                                        $
2SUBROUTINE TRAPZ                                                      $
```

```
2COMMENT PROGRAM NO.  3  (CONTINUED)                                    $
2BEGIN
2         DEL=(K3-X0)/5                                                 $
2         YX=K3-0.00001                                                 $
2         IF X EQL 0.2     $    KX=0.0                                  $
2         J=1     $     T(J) = 0.0                                      $
2FLAG1..  J=J+1     $    SUM = 0.0     $   I=0                         $
2FLAG2..  I=I+1     $     X= X0  + I.DEL                                $
2         ENTER FIT                                                     $
2         K1=(-(1-Y)/X)                                                 $
2         X=X-DEL                                                       $
2         ENTER FIT                                                     $
2         K2=(-(1-Y)/X)                                                 $
2FLAG5..  SUM=SUM+(K1+K2)/2                                             $
2         MM= X0  + I.DEL                                               $
2         X = MM                $
2         IF MM GTR YX                                                  $
2         GO TO FLAG3                                                   $
2         GO TO FLAG2                                                   $
2FLAG3..  T(J)= DEL.SUM                                                 $
2         TT=(T(J)-T(J-1))/T(J)                                         $
2         IF ABS(TT) LSS E                                              $
2         GO TO FLAG4                                                   $
2         DEL = DEL/2                                                   $
2         IF DEL LSS 0.001    $    GO TO START                         $
2         GO TO FLAG1                                                   $
2FLAG4..  G=(G0).EXP(Y1-Y0+T(J)+KX)                                     $
2         KX=T(J)+KX                      $
2         ACT=(G.K3)*2                                                  $
2RETURN END TRAPZ                                                       $
2 START..
2         P=0     $     READ($$IN1)                                     $
2         READ($$IN)   $      READ($$PARAM)   $
2         IF N EQL 0                      $         STOP                $
2         READ($$DATA)  $
2         WRITE($$ID1,HD1)                                              $
```

```
2COMMENT PROGRAM NO.  3  (CONTINUED)                                    $
2        WRITE($$ID,HEAD1) $
2        WRITE($$HEAD2)                                                 $
2        FOR X=(0.2,0.2,2.4),(3.0,0.5,20.0)                             $
2BEGIN
2        VN=V(N)                                                        $
2        IF X GTR VN                                                    $
2        GO TO START                                                    $
2ENTER FIT                                                              $
2        AC=EXP(((-0.036032).Y).X))                                     $
2        PCT=100(X.MX/(1000+X.MX))                                      $
2        NX=X/((1000/18.016)+X)                                         $
2        PP=23.7560.AC                                                  $
2        VHF=((23.7560-PP)/PP).((1/NX)-1)                               $
2        Y1= Y   $   K3=X   $   ENTER TRAPZ                            $
2        WRITE($$FIT1,FMT1)                                             $
2BEGIN   P=P+1                                                          $
2        IF P EQL 29                                                    $
2BEGIN   WRITE($$ID1,HD2)                                               $
2        WRITE($$ID,HEAD1)                                              $
2        WRITE($$HEAD2)                                                 $
2        P=0                                                            $
2END                                                                    $
2END                                                                    $
2        X0 = K3                                                        $
2END                                                                    $
2        GO TO START  $
2        FINISH  $
```

```
2COMMENT PROGRAM NO.  4
2         COMPUTES THE RELATIVE HUMIDITY IN EQUILIBRIUM WITH SUBMICROS
2        COPIC SOLUTION DROPLETS FORMED BY CONDENSATION OF WATER ON
2        HYGROSCOPIC NUCLEI OF ELECTROLYTES USING EQUATION OF MASON
2        AND POLYNOMIAL FITS OF DATA ON SOLUTION DENSITY, SURFACE
2        TENSION AND A TABLE OF DATA ON VAN,T HOFF FACTOR VERSUS
2        SOLUTION CONCENTRATION                                          $
2INTEGER I,M,N,P,K                                                       $
2ARRAY A(15),T(20),Q(20),U(100),V(100)                                   $
2INPUT IDEN(FOR I=(1,1,15)$A(I))                                         $
2INPUT PAR1(MS,DS)                                                       $
2INPUT DATA1(M,FOR I=(1,1,M+1)$T(I))                                     $
2INPUT DATA2(N,FOR I=(1,1,N+1)$Q(I))                                     $
2INPUT DATA3(P,FOR I=(1,1,P)$(U(I),V(I))                                 $
2OUTPUT OUT1(FOR I=(1,1,15)$A(I))                                        $
2FORMAT FORM1(15A5,W3)                                                   $
2OUTPUT OUT2(R0,MO)                                                      $
2FORMAT FORM2(*DRY CRYSTAL RADIUS*,B2,X7.4,B2,*MICRONS*,B6,*DRY CRYST*,
2         *AL MASS*,B2,F12.5,B2,*GRAMS*,W2)                              $
2FORMAT COLS(*DROPLET RADIUS   DROPLET MOLARITY*,B7,*DROPLET MOLALITY*,
2         *   EQUILIBRIUM RELATIVE*,W4,*   MICRONS      (MOLES/1000 CC*,
2         * WATER) (MOLES/1000 G WATER  HUMIDITY, PER CENT*,W2)           $
2OUTPUT OUT3(R,C,MOL,H)                                                  $
2FORMAT FORM3(X9.5,B11,X8.5,B14,X8.5,B16,X8.4,W0)                        $
2SUBROUTINE DENS                                                         $
2BEGIN   D=T(1)+T(2).C+T(3).C*2+T(4).C*3+T(5).C*4+T(6).C*5+T(7).C*6+
2        T(8).C*7+T(9).C*8+T(10).C*9+T(11).C*10                          $
2RETURN END DENS                                                         $
2SUBROUTINE STENS                                                        $
2BEGIN   SIG=Q(1)+Q(2).MOL+Q(3).MOL*2+Q(4).MOL*3+Q(5).MOL*4+Q(6).MOL*5+
2        Q(7).MOL*6+Q(8).MOL*7+Q(9).MOL*8+Q(10).MOL*9+Q(11).MOL*10       $
2RETURN END STENS                                                        $
2SUBROUTINE VANT                                                         $
2BEGIN
2        FOR K=(2,1,P)                                                   $
2BEGIN
```

```
2COMMENT PROGRAM NO.  4  (CONTINUED)                                    $
2        IF V(K) GEQ MOL                                                $
2BEGIN
2        VHF=U(K)-(U(K)-U(K-1))(V(K)-MOL)/(V(K)-V(K-1))                 $
2        GO TO OUT                                                      $
2END                                                                    $
2END                                                                    $
2OUT..
2RETURN END VANT                                                        $
2START.. READ($$IDEN)                                                   $
2        READ($$PAR1)                                                   $
2        IF  MS  EQL  0.0          $        STOP                        $
2        READ($$DATA1)                                                  $
2        READ($$DATA2)                                                  $
2        READ($$DATA3)                                                  $
2        FOR R0=(0.01,0.01,0.05)                                        $
2BEGIN
2        MO=(4/3)(3.14159)((R0)*3)(1**-12)(DS)                          $
2        WRITE($$OUT1,FORM1)                                            $
2        WRITE($$OUT2,FORM2)                                            $
2        WRITE($$COLS)                                                  $
2        FOR R=(0.01,0.001,0.10),(0.2,0.1,1.0)                          $
2BEGIN
2        C=MO(3**15)/4(3.14159)(R*3)(MS)                                $
2        IF  C  GTR 20.0    $      GO TO L1                            $
2        N2=C/(C+((1000).D-C.MS)/(18.016))                              $
2        MOL=(1000).N2/((18.016).(1-N2))                                $
2        ENTER DENS                                                     $
2        ENTER STENS                                                    $
2        ENTER VANT                                                     $
2        IF MOL GTR V(P)                  $
2        GO TO L1                                                       $
2        H=(100).(EXP((1.45282**-9).SIG/(D.R))).(1+
2        (18.016).MO.VHF/(MS.((4/3).(3.14159**-12).(R*3).D-
2        MO)))*(-0.99707/D)                                             $
2        IF H LSS 10.0                                                  $
```

```
2COMMENT PROGRAM NO.  4  (CONTINUED)                                    $
2        GO TO L1                                                       $
2        WRITE($$OUT3,FORM3)                                            $
2L1..    END                                                            $
2END                                                                    $
2        GO TO START                                                    $
2FINISH                                                                 $
```

```
2COMMENT PROGRAM NO.  5
2        COMPUTES ION SIZE VS PLATE VOLTAGE FROM DATA ON AEROSOL
2        FLOW RATE AND ION COUNTER GEOMETRICAL PARAMETERS                $
2REAL F,R1,R2,B2,K,R,S,W,V    $
2INPUT DATA1(F,R1,R2,B2)    $
2OUTPUT OUT1(F,R1,R2,B2)    $
2FORMAT FORM(*ION SIZE VS PLATE VOLTAGE TABULATION*,W3)    $
2FORMAT FORM1(*AEROSOL FLOW RATE =*,X7.1,*ML/MIN*,B2,*R1 =*,X7.4,
2             *IN*,B2,*R2 =*,X7.4,*IN*,B2,*2B =*,X7.4,*IN*,W6)    $
2FORMAT HEAD(*ION SIZE, MICRONS*,B2,*SLIP FACTOR*,B2,*MOBILITY,*,
2             * CM2/VOLT.SEC*,B2,*PLATE VOLTAGE*,W2)    $
2OUTPUT OUT2(R,S,W,V)    $
2FORMAT FORM2(B4,X8.4,B7,X10.6,B10,F11.4,B8,X8.3,W0)    $
2        READ($$DATA1)    $
2        FOR B2=(B2,0.002,0.08)                                          $
2BEGIN
2        WRITE($$FORM)    $
2        K = (7.967).(R2*2-R1*2)/B2    $
2        WRITE($$OUT1,FORM1)    $
2        WRITE($$HEAD)    $
2        FOR R=(0.001,0.001,0.01),(0.012,0.002,0.04),(0.045,0.005,0.1) $
2BEGIN
2        S = 1.0+(0.098/R).(0.882+(0.281).EXP((-16.0).R))    $
2        W = (4.73**-6).S/R    $
2        V = F/(60.0).W.K    $
2        WRITE($$OUT2,FORM2)    $
2END    $
2END                  $
2        STOP        $
2FINISH    $
```

```
2COMMENT PROGRAM NO. 6
2        PROCESSES MICROSCOPE PARTICLE COUNTS INTO SIZE DISTRIBUTIONS  $
2INTEGER I,N,B,A,Z,XX                                                  $
2ARRAY A(15),XX(1250),R(40),B(30),S(30),D(30),X(1250)                  $
2INPUT ID(FOR I=(1,1,15)$A(I))                                         $
2INPUT PARAM(N,Z,C)                                                    $
2INPUT DATA(FOR I=(1,1,N)$XX(I))                                       $
2OUTPUT IDEN(FOR I=(1,1,15)$A(I))                                      $
2FORMAT FMT(15A5,W3,B1,W2)                                             $
2FORMAT COLS(*RANGE OF SIZES    MIDPOINT OF      CUMULATIVE    PER CE*,
2        *NT LESS*,W0,B3,*MICRONS*,B8,*RANGE, MICRONS   FREQUENCY    *,
2        * THAN SIZE*,W2)                                              $
2OUTPUT OUT1(FOR I=(1,1,Z)$(R(I),R(I+1),D(I),B(I),S(I)))               $
2FORMAT FMT1(X7.5,*-*,X7.5,B6,X8.6,B7,I5,B9,X7.3,W0)                   $
2START.. READ($$ID)                                                    $
2        READ($$PARAM)                                                 $
2        IF N EQL 0                                                    $
2        STOP                                                          $
2        READ($$DATA)                                                  $
2        MN=0.0                                                        $
2           MX=C.XX(1)                                                 $
2COMMENT CONVERSION OF DATA INTO SIZE IN MICRONS                       $
2        FOR I=(1,1,N)                                                 $
2BEGIN
2        X(I)=C.XX(I)                                                  $
2        IF X(I) GTR MX                                                $
2BEGIN
2        MX =X(I)                                                      $
2        GO TO L1                                                      $
2END                                                                   $
2L1..
2END                                                                   $
2COMMENT ESTABLISHES RANGES OF SIZE AND COUNT FREQUENCY                $
2        DEL=(MX -MN )/Z                                               $
2        FOR K=(0,1,Z)                                                 $
2        R(K+1)=MN +K.DEL                                              $
```

```
2COMMENT PROGRAM NO. 6 (CONTINUED)                                    $
2        FOR K=(0,1,Z-1)                                              $
2BEGIN
2        FOR I=(1,1,N)                                                $
2BEGIN
2        IF X(I) GEQ R(K+1)                                           $
2BEGIN
2        IF X(I) LEQ R(K+2)                                           $
2BEGIN
2L2..    B(K+1)=B(K+1)+1                                              $
2        GO TO L3                                                     $
2END                                                                  $
2        IF (K+2) EQL (Z+1)                                           $
2BEGIN
2        IF X(I) GEQ (R(K+2)-0.000001)                                $
2        GO TO L2                                                     $
2        GO TO L3                                                     $
2END                                                                  $
2        GO TO L3                                                     $
2END                                                                  $
2L3..
2END                                                                  $
2END                                                                  $
2        FOR I=(1,1,Z)                                                $
2        D(I)=(R(I)+R(I+1))/2                                         $
2COMMENT COMPUTES CUMULATIVE PARTICLE COUNTS FOR EACH SIZE RANGE      $
2        FOR K=(2,1,Z)                                                $
2        B(K)=B(K)+B(K-1)                                             $
2COMMENT COMPUTES PER CENT LESS THAN AVERAGE OF SIZE RANGE            $
2        FOR K=(1,1,Z)                                                $
2        S(K)=100((FLOAT(B(K)))/(FLOAT(B(Z))))                        $
2        WRITE($$IDEN,FMT)                                            $
2        WRITE($$COLS)                                                $
2        WRITE($$OUT1,FMT1)                                           $
2        FOR K=(0,1,Z-1)                                              $
2        B(K+1)=0.0                                                   $
```

```
2COMMENT PROGRAM NO. 6 (CONTINUED)                                    $
2        GO TO START                                                  $
2FINISH                                                               $
```

BIBLIOGRAPHY*

1. Turnbull, D., "The Undercooling of Liquids," Sci. Am., 212, No. 1,38-46 (1965).

2. Wilson, C. T. R., "On the Comparative Efficiency as Condensation Nuclei of Positively and Negatively Charged Ions," Phil. Trans. Roy. Soc. (London), A 193, 289 (1900).

3. Vonnegut, B., "Variation with Temperature of the Nucleation Rate of Supercooled Liquid Tin and Water Drops," J. Colloid Sci., 3, 563 (1948).

4. Aitken, J., Collected Scientific Papers, C. G. Knott, Ed., Cambridge University Press, Cambridge, 1923.

5. Byers, H. R., Elements of Cloud Physics, The University of Chicago Press, Chicago, 1965.

6. Junge, C. E., in Advances in Geophysics, H. Landsberg and J. Van Mieghem, Editors, Academic Press, New York, 4, 1, 1958.

7. Twomey, S., "The Nuclei of Natural Cloud Formation Part I: The Chemical Diffusion Method and its Application to Atmospheric Nuclei", Geofys. Pura e Appl., 43, 227 (1959).

8. Gamble, Jr., A. W., "Indirect Evidence of the Importance of Water Soluble Continentally Derived Aerosols," Tellus, 14, 91 (1962).

9. Strong, C. L., "Venezuela's Peculiar Fog: The Calina," Sci. Am., 205, 172-183 (1961).

10. Dessens, H., "The Use of Spider's Threads in the Study of Condensation Nuclei," Quart. J. Roy. Meteorol. Soc., 75, 23 (1949).

11. Junge, C. E., "Die Konstitution Des Atmosphärischen Aerosols," Ann. Meteorol. (Beiheft), 1952.

12. Orr, Jr., C., F. K. Hurd and W. J. Corbett, "Aerosol Size and Relative Humidity," J. Colloid Sci., 13, No. 5, 472-82 (1958).

---

* Abbreviations for Journals follow the form used by the American Chemical Society in its 1961 List of Periodicals, and in its 1964 and 1965 Supplements.

13. Corbett, W. J. and C. Orr, Jr., "Evaporation of Aerosol Droplets Containing Dissolved Salts," Paper presented at the 138th National Meeting of the American Chemical Society, New York, 1960.

14. Hurd, F. K. and J. C. Mullins, "Aerosol Size Distribution from Ion Mobility," J. Colloid Sci., 17, 91-100 (1962).

15. Volmer, M. and A. Weber, "Keimbildung in Übersättigten Gebilden," Z. Physik. Chem., 119, 277-301 (1926).

16. Becker, R. and W. Doring, "Kinetische Behandlung Der Keimbildung in Übersättigten Dampfen," Ann. Physik., (5), 24, 719-52 (1935).

17. Uhlmann, D. R. and B. Chalmers, "The Energetics of Nucleation," Ind. Eng. Chem., 57, No. 9, 19-31 (1965).

18. Turnbull, D. and Fisher, J. C., "Rate of Nucleation in Condensed Systems," J. Chem. Phys., 17, No.1, 71-3 (1949).

19. Dufour, L., and Defay, R., Thermodynamics of Clouds, Academic Press, New York, p. 195, 1963.

20. Remy, H., "Sorption of Fogs by Liquids," Trans. Faraday Soc., (London), 32, 1185-90 (1936).

21. Orr, Jr., Clyde, F. K. Hurd, W. P. Hendrix and W. J. Corbett, "An Investigation into the Growth of Small Aerosol Particles with Humidity Change," Final Report, Proj. No. A-162, Georgia Institute of Technology, Engineering Experiment Station, Dec. 1956.

22. Mickley, H. S., T. K. Sherwood and C. W. Reed, Applied Mathematics in Chemical Engineering, 2nd. ed., McGraw-Hill Book Co. Inc., New York, pp. 53-59, 1957.

23. The Smithsonian Meteorological Tables, 6th Edition, List, R. J., Editor, The Smithsonian Institution, Washington, D.C., pp. 351-64, 1951.

24. Cambridge Systems Engineering Application Notes, Note 108 N2, p. 3, Jan. 15, 1964.

25. Orr, Jr., Clyde and J. M. Dallavalle, Fine Particle Measurement, The Macmillan Co., New York, p. 33, 1959.

26. Pound, G. M., "Liquid and Crystal Nucleation," Ind. Eng. Chem., 44, No. 6, 1278-83 (1952).

27. Corbett, W. J. "Contributions to the Study of the Surface Energy and Surface Tension of Solids," Ph. D. Thesis, Georgia Institute of Technology, 1964.

28. Preckshot, G. W., and G. G. Brown, "Nucleation of Quiet Supersaturated Potassium Chloride Solutions," Ind. Eng. Chem., 44, 1314-21 (1952).

29. Twomey, S., "The Composition of Hygroscopic Particles in the Atmosphere," J. Meteorol., 11, 334-8 (1954).

30. Whitby, K. T., R. C. Jordan and C. M. Peterson, "Development of a Particle Counter System and Development of a Technique for Studying the Charge on an Evaporating Drop," Progress Report U.S.P.H.S. Grant No. AP-00136-03, University of Minnesota, June 1964.

31. Davies, C. M. "Definitive Equations for the Fluid Resistance of Spheres," Proc. Phys. Soc. (London), 57, 259-70 (1945).

32. International Critical Tables, McGraw Hill Publ. Co., New York, Vol. III, 77-94, 1928.

33. Ibid, Vol. III, p. 327.

34. Ibid, Vol. IV, p. 465.

35. Ibid, Vol. IV, p. 447.

36. Harned, H. S., and B. B. Owen, The Physical Chemistry of Electrolytic Solutions, 3rd Edition, Reinhold Publ. Co., New York, p. 509, 1958.

37. Ibid, p. 161.

38. Ibid, p. 11.

39. Ibid, p. 413.

40. Ibid, p. 13.

41. McDonald, J. E., "Erroneous Cloud-Physics Applications of Raoult's Law," J. Meteorol., 10, 68-70 (1953).

42. Roth, W. A., and K. Scheel, in Physikalisch-Chemisch Tabellen (Landolt-Bornstein), Band 2, Julius Springer, Berlin, p. 1382, 1923.

43. International Critical Tables, McGraw Hill, New York, III, p. 297, 1926.

44. Robinson, R. A. and R. H. Stokes, "Electrolyte Solutions," Academic Press, New York, 1955.

45. Harned, H. S. and B. B. Owen, op. cit., p. 415.

46. Brunauer, S., P. H. Emmett and E. Teller, "The Adsorption of Gases in Multimolecular Layers," J. Am. Chem. Soc., 60, 309-19 (1938).

47. Benson, G. C., H. P. Schreiber and F. Van Zeggeren, "An Experimental Determination of the Surface Enthalpy of Sodium Chloride," Can. J. Chem., 34, 1553-6 (1956).

48. Livingstone, H. K., "The Cross Sectional Areas of Molecules Adsorbed on Solid Surfaces," J. Colloid Sci., 4, 447-58 (1949).

49. Gibbs, J. W., Scientific Papers, Longmans Greens and Co., New York, 1, p. 315, 1906.

50. Dundon, M. L., and E. Mack, Jr., "The Solubility and Surface Energy of Calcium Sulphate," J. Am. Chem. Soc., 45, 2479-85 (1923).

51. Dundon, M. L., "Surface Energy of Several Salts," J. Am. Chem. Soc., 45, 2658-65 (1923).

52. Thomson, Sir William (Lord Kelvin), "On the Equilibrium of Vapor at a Curved Surface of Liquid," Phil. Mag., 42, 448 (1871).

53. Thomson, J. J., Application of Dynamics to Physics and Chemistry, 1st Edition, Cambridge University Press, p. 165, 1888.

54. Wright, H. L., "The Size of Atmospheric Nuclei: Some Deductions from Measurements of the Number of Charged and Uncharged Nuclei at Kew Observatory," Proc. Phys. Soc. (London), 48, 675-89 (1936).

55. Mason, B. J., The Physics of Clouds, Clarendon Press, Oxford, p. 26-7, 1957.

56. Howell, W. E. "The Growth of Cloud Drops in Uniformly Cooled Air," J. Meteorol., 6, 134-49, (1949).

57. Byers, H. R., "Nucleation in the Atmosphere," Ind. Eng. Chem., 57, No. 11, 32-40, (1965).

58. Montgomery, D. W., "New Techniques of Particle Size Analysis," Rubber Age (N.Y.), Feb. 1964.

VITA

Alberto Francisco Hidalgo was born in Habana, Cuba ,on November 11, 1935. He received both his primary and secondary education at Colegio de Belen, a Jesuit private school in Marianao, Habana. There he received his diploma of Bachiller in Science in 1953. That year he entered the Universidad de Vilanova in Marianao, Habana, where he obtained the equivalent of a Bachelor of Chemical Engineering degree and received the highest academic award of the institution. He then joined the Procter and Gamble Company of Cuba where he worked in various responsibilities for a period of two years. Then, he assumed the position of Chemical Supervisor of Industrias Siporex, which he held until 1961 when he came to this country. He entered the Graduate Division of the Georgia Institute of Technology in the summer of 1961. For some time in 1962, he was laboratory instructor in a course in Microbiology in the School of Applied Biology. In July of 1962 he joined the staff of the Engineering Experiment Station as a research assistant. He was awarded the degree of Master of Science in Chemical Engineering in 1963. In 1965 he was promoted to Assistant Research Engineer and in 1966 to Research Engineer. He is the author or co-author of several reports and a member of Sigma Xi.

Mr. Hidalgo was married in 1959 to the former Matilde Gomez-Cortes. They have three daughters and one son.